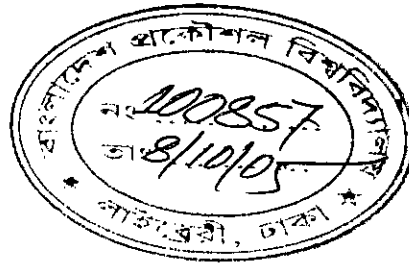


**EVALUATION OF PROPERTIES OF GEOJUTE AND  
ITS ASSESSMENT FOR SHORT TERM AND LONG  
TERM CIVIL ENGINEERING APPLICATIONS**

**M. A. MOHY**



**BANGLADESH UNIVERSITY OF ENGINEERING AND TECHNOLOGY  
DEPARTMENT OF CIVIL ENGINEERING**

**2005**

MASTER OF SCIENCE IN CIVIL ENGINEERING

**Evaluation of Properties of Geojute and Its  
Assessment for Short Term and Long Term Civil  
Engineering Applications**

by

M. A. Mohy

BANGLADESH UNIVERSITY OF ENGINEERING AND TECHNOLOGY



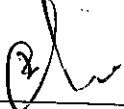
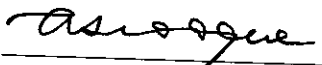
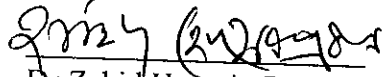
Department of Civil Engineering

2005

## PROJECT REPORT APPROVAL

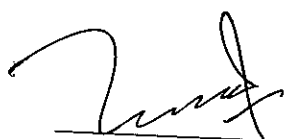
The thesis titled "Evaluation of Properties of Geojute and Its Assessment for Short Term and Long Term Civil Engineering Applications" Submitted by M A. Mohy Roll No: 040304224F, Session: April 2003 has been accepted as satisfactory in partial fulfillment of the requirement for the degree of M.Sc Engineering on 26 April 05.

## BOARD OF EXAMINERS

1.   
 Dr Abdul Jabbar Khan  
 Associate Professor  
 Department of Civil Engineering  
 BUET, Dhaka  
 Chairman
2.   
 Dr Sk. Sekender Ali  
 Professor & Head  
 Department of Civil Engineering  
 BUET, Dhaka  
 Member
3.   
 Dr Md Zoynul Abedin  
 Professor  
 Department of Civil Engineering  
 BUET, Dhaka  
 Member
4.   
 Dr Abu Siddique  
 Professor  
 Department of Civil Engineering  
 BUET, Dhaka  
 Member
5.   
 Dr Zahid Hossain Prodhan  
 Managing Director  
 Arcadia Property Development Ltd.  
 Dhanmondi, Dhaka  
 Member  
 (External)

## CANDIDATE'S DECLARATION

It is hereby declared that this thesis or any part of it has not been submitted elsewhere for the award of any degree or diploma.



---

M. A. Mohy

## **DEDICATION**

*This thesis is dedicated to my parents*

## TABLE OF CONTENT

Title Page	i
Certification Page of Thesis/Project Report Approval	ii
Declaration Page	iii
Dedication	iv
Table of Contents	v
List of Tables	xiv
List of Figures	xvi
List of Abbreviations of Technical Symbols and Terminologies	xxv
Acknowledgements	xxviii
Abstract	xxix
<b>Chapter 1</b>	<b>INTRODUCTION</b>
1.1	General 1
1.2	Background of the Research 5
1.3	Objective of Research 8
1.4	Methodology 8
1.5	Organization of the Thesis 10
<b>Chapter 2</b>	<b>LITERATURE REVIEW</b>
2.1	General 12
2.1.1	Geosynthetic 12
2.1.2	Types of Synthetic Geotextiles 15

2.1.3	Properties of Geotextiles	16
2.2	Geotextile Functions and Applications	16
2.2.1	General	16
2.2.2	Separation	17
2.2.2.1	Definition	17
2.2.2.2	Mechanism	17
2.2.2.3	Applications of Geotextile/Geojute in Separation	18
2.2.2.4	Designing for Separation	18
2.2.2.4.1	Burst Resistance	19
2.2.2.4.2	Tensile Strength Requirement	20
2.2.2.4.3	Puncture Resistance	21
2.2.3	Reinforcement	22
2.2.3.1	Definition	22
2.2.3.2	Mechanism	22
2.2.3.3	Application of Geotextile/Geojute in Reinforcement	22
2.2.3.4	Designing for Reinforcement	23
2.2.4	Filtration	26
2.2.4.1	Definition	26
2.2.4.2	Application of Geotextile/Geojute in Filtration	28
2.2.4.3	Designing for Filtration	29
2.2.5	Drainage	30
2.2.5.1	Definition	30
2.2.5.2	Application of Geotextile/Geojute in Drainage	30
2.2.5.3	Designing for Drainage	30
2.2.6	Miscellaneous	32

2.2.6.1	Reflective Crack Prevention in Bituminous Pavement Overlays	32
2.2.6.2	Railroad Application	33
2.2.6.3	Horizontal Bags and Tubes (aka Geotubes)	34
2.2.6.4	Restoration of Piles (Pile Jacketing)	34
2.2.6.5	Bridge Pier Underpinning	35
2.2.6.6	Uniform Pressure Distribution beneath Caissons	36
2.2.6.7	Erosion-Control Mattresses	36
2.3	Jute Fibre	37
2.3.1	Physical Structure of Jute	38
2.3.2	Physical Properties of Jute	38
2.3.3	Chemical Composition of Jute fibre	40
2.3.3.1	Cellulose	41
2.3.3.2	Hemicellulose	42
2.3.3.3	Lignin	42
2.3.4	Factors Influencing the Quality of Jute	45
2.3.5	Treatment of Jute	46
2.3.5.1	Jute Blended with Cotton/Union Products	46
2.3.5.2	Jute Blended with Coir/Union Products	47
2.3.5.3	Jute Blended with Synthetics Fabrics	47
2.3.5.4	Jute Blended and Treated with Chemicals	50
2.4	Summary	55



<b>Chapter 3</b>	<b>LABORATORY INVESTIGATIONS</b>	
3.1	General	81
3.2	Physical Properties	82
3.2.1	Mass per Unit Area	82
3.2.2	Thickness	83
3.2.3	Specific Gravity	85
3.3	Mechanical Properties	86
3.3.1	Wide-width Strip Tension Test	86
3.3.2	Grab Breaking Load and Elongation Test	87
3.3.3	Trapezoid Tearing Test	88
3.3.4	Puncture Test	89
3.3.4.1	Index Puncture Test	89
3.3.4.2	CBR Puncture Test	91
3.3.5	Burst Strength Test	91
3.3.6	Seam Strength Test	92
3.3.7	General Discussion	93
3.4	Friction Behavior	95
3.5	Pullout Test	98
3.6	Hydraulic Properties	100
3.6.1	Apparent Opening Size (AOS)	100
3.6.2	Permittivity (Cross-Plane Permeability)	102
3.6.3	Transmissivity (In-Plane Permeability)	104
3.7	Endurance Properties	106
3.7.1	Installation Damage	106
3.7.2	Creep under Constant Stress	107

3.7.3	Creep under Confined Stress	109
3.7.4	Abrasion Behavior	109
3.8	Material Selected for Test	111
3.9	Tests Performed	112
<b>Chapter 4</b>	<b>EXPERIMENTAL RESULTS AND DISCUSSION</b>	
4.1	General	145
4.1.1	Mass per Unit Area	145
4.1.2	Nominal Thickness	146
4.1.3	Specific Gravity	147
4.1.4	Wide-Width Tensile Properties	149
4.1.5	Grab Breaking Load and Elongation	151
4.1.6	Trapezoid Tearing Strength	152
4.1.7	Index Puncture Resistance	153
4.1.8	CBR Puncture Resistance	154
4.1.9	Burst Strength Test	154
4.1.10	Apparent Opening Size (AOS)	155
4.1.11	Water Permeability & Permittivity	156
4.1.12	In-plane Flow and Hydraulic Transmissivity	157
4.1.13	Unconfined Tension Creep Behavior	158
4.2	Comparison with Available Geotextile Data	160
4.2.1	Mass per Unit Area	161
4.2.2	Thickness	161
4.2.3	CBR Puncture Strength	161
4.2.4	Grab Tensile Strength	161

4.2.5	Grab Tensile Elongation	162
4.2.6	Wide-width Tensile Strength	162
4.2.7	Wide-width Elongation	162

## **Chapter 5 DESIGNING WITH GEOJUTE AND TECHNICAL ASSESSMENT**

5.1	General	203
5.2	Design Methods	203
5.2.1	Design-by-Cost-and-Availability	204
5.2.2	Design-by-Specification	204
5.2.3	Design by Function	204
5.3	Allowable versus Ultimate Geotextile Properties	205
5.3.1	Strength-Related Problems	206
5.3.2	Flow-Related Problems	207
5.4	Designing for Separation	208
5.4.1	General	208
5.4.2	Problem	208
5.4.3	Solution	209
5.5	Designing for Soil Reinforcement	209
5.5.1	General	209
5.5.2	Problem 1: Geojute Reinforced Walls	210
5.5.3	Solution	210
5.5.3.1	Internal Stability	210
5.5.3.2	External Stability	215
5.5.4	Problem 2: Geojute Reinforced Embankment	218

5.5.4.1	Part I	218
5.5.4.2	Solution	219
5.5.4.3	Part II	220
5.5.4.4	Solution	220
5.6	Designing for Filtration	221
5.6.1	General	221
5.6.2	Problem	221
5.6.3	Solution	222
5.7	Designing for Drainage	225
5.7.1	General	225
5.7.2	Problem I: Gravity Drainage	225
5.7.3	Solution	226
5.7.4	Problem II: Pressure Drainage	227
5.7.5	Solution	228
5.8	Economic Aspects	228
5.8.1	General	228
5.8.2	Need and Considerations for Economic Evaluation	229
5.8.3	Comparative Costs of Geojute and Geotextiles	229
5.9	Economic Benefit of Using Geojute in Different Applications	233
5.9.1	Separation	233
5.9.2	Reinforced Wall	233
5.9.3	Reinforced Embankment	234
5.9.4	Filtration	234
5.9.5	Drainage	234

<b>Chapter 6</b>	<b>CONCLUSIONS AND RECOMMENDATIONS</b>	
6.1	General	236
6.2	Conclusions on Experimental Results	237
6.2.1	Mass per Unit Area	237
6.2.2	Thickness	237
6.2.3	Specific Gravity	237
6.2.4	Wide-width Tensile Test	238
6.2.5	Grab Tensile and Elongation	238
6.2.6	Trapezoid Tearing Strength	238
6.2.7	Index and CBR Puncture	239
6.2.8	Burst Strength	239
6.2.9	Apparent Opening Size (AOS)	239
6.2.10	Permittivity	239
6.2.11	Transmissivity	240
6.2.12	Unconfined Creep Behavior	240
6.3	Conclusions on Designing with Geojute	240
6.3.1	Separation	240
6.3.2	Reinforcement	241
6.3.3	Filtration	241
6.3.4	Drainage	242
	<b>RECOMMENDATIONS FOR FUTURE RESEARCH</b>	243

	xiii
References	244
APPENDIX I	
Typical Ranges of Properties for Currently Available Geotextiles	253
APPENDIX II	
The ASTM & DIN Standards for Determining Design Parameters	254
APPENDIX III	
Data Sheet of Test Results	255

## LIST OF TABLES

<u>Table No</u>	<u>Title</u>	<u>Page</u>
Table 2.1	Important Physical Properties of Jute Fibre	44
Table 2.2	Summary of Jute Blended with Different Materials at BJRI	48
Table 2.3	Summary of Test Results Conducted by Rao et al	49
Table 2.4	Categorization of Jute Based Geotextiles	50
Table 2.5	Thickness and Linear Density of Some Modified Fabrics	51
Table 2.6	Tensile Strength (kN/m) of Some Treated and Blended Fabrics	52
Table 2.7	Bursting Strength (kN/m <sup>2</sup> ) of Some Treated Fabrics	52
Table 2.8	Puncture Test Results (diameter in mm) Some Fabrics	53
Table 2.9	CBR Test Results of Some Fabrics	53
Table 2.10	Water Permeability (lit/m <sup>2</sup> /sec) of Some Treated Fabrics	54
Table 2.11	Pore Size, O <sub>95</sub> (micron) of Some Treated Fabrics	54
Table 2.12	Biodegradability, Durability and Moisture Holding Capacity of Treated and Untreated Jute	55
Table 3.1	Creep Behavior of Polymeric Material	110
Table 3.2	Salient Properties of Samples Selected for Study	113

Table 3.3	Tests Performed in the Research Work	114
Table 4.1	Comparative Properties of Synthetic Geotextile and Geojute	163
Table 5.1	Recommended Reduction Factor Values for Use in Strength-Related Problems	206
Table 5.2	Recommended Reduction Factor Values for Use in Flow-Related Problems	208
Table 5.3	Geojute Length and Spacing	214
Table 5.4	Cost Comparisons between Geojutes	230
Table 5.5	Cost of Woven and Nonwoven Geotextiles	231
Table 5.6	Cost Comparison between Tested Geojute and Nonwoven Geotextile (locally produced)	231
Table 5.7	Price Comparison between Tested Geojute and Nonwoven Geotextile (foreign produced)	231
Table 5.8	Price Comparison between Tested Geojute and Nonwoven Geotextile (foreign produced)	232
Table 5.9	Sources of Geojutes	232
Table 5.10	Summary of Cost of Jute Blended with Different Materials at BJRI	233



## LIST OF FIGURES

<u>Fig No</u>	<u>Title</u>	<u>Page</u>
Fig 2.1a	Geomembrane	59
Fig 2.1b	Geotextile	59
Fig 2.1c	Geonets	59
Fig 2.1d	Geogrids	60
Fig 2.1e	Geocomposites	60
Fig 2.1f	Geo-others (geopipes & geosynthetics clay liners)	60
Fig 2.2	Geotextile classification based on the manufacturing process after Rankilor (1981)	61
Fig 2.3	Photomicrographs of various fabrics used as geotextiles (after Koerner, 1990)	62
Fig 2.4	Geotextiles classification after John (1987)	63
Fig 2.5	Riprap erosion protection	64
Fig 2.6	Geotextile reinforcement	64
Fig 2.7	Schematic representation of separation mechanism (after Koerner, 1997)	64
Fig 2.8	Pressure dissipation through road	65
Fig 2.9	Pavement without separation material	65
Fig 2.10	Pavement with separation material	65
Fig 2.11	Geotextile being forced up into voids of stone base by traffic tire loads (after Koerner, 1997)	65
Fig 2.12	Geotextile being subjected to tensile stress as surface pressure is applied and stone base attempts to spread laterally (after Koerner, 1997)	66

Fig 2.13	Visualization of a stone puncturing a geotextile as pressure is applied from above (after Koerner, 1997)	66
Fig 2.14	Geotextile-reinforced wall	67
Fig 2.15	Geotextile-reinforced embankment	67
Fig 2.16	Earth pressure concepts and theory for geotextile walls (after Koerner, 1997)	67
Fig 2.17	Lateral earth pressure due to a surface load. Left side for line loads and right side for point load (after NAVAC, 1982)	68
Fig 2.18	External stability considerations for geotextile walls	69
Fig 2.19	Conventional aggregate filter system	70
Fig 2.20	Geotextile filter system	70
Fig 2.21	Geotextile cake system	70
Fig 2.22	Various hypothetical mechanisms involved in long-term soil-to-fabric flow compatibility (after Koerner, 1997)	71
Fig 2.23	Various types of retaining walls in which geotextiles can be used as filters (after Koerner, 1997)	72
Fig 2.24	Typical cross sections of underdrain systems with and without perforated pipes (after Koerner, 1997)	73
Fig 2.25	Geotextile placed beneath a rock riprap erosion-control system (after Koerner, 1997)	73
Fig 2.26	Cross section of geotextile silt fence and suggested manner in which system functions (after Koerner, 1997)	74
Fig 2.27	Sketch of drainage of water within geotextile	74
Fig 2.28	Gravity design of drainage (after Koerner, 1997)	75
Fig 2.29	Pressure drainage design (after Koerner, 1997)	75
Fig 2.30	Geotextile in concrete overlay (after U.S. Departments of the Army and the Air force, 1995)	75
Fig 2.31	Geotextile application under railroad (after U.S. Departments of the Army and the Air force, 1995)	76

Fig 2.32	Underpinning of scoured bridge pier using grout-filled geotextile (after Koerner, 1997)	77
Fig 2.33	Prototype for evaluating use of geotextiles as forms for establishing uniform pressure distribution beneath concrete foundations (after Koerner, 1997)	78
Fig 2.34	Typical cross sections and schematics of erosion-control mattresses formed by grout-filled geotextile (after Koerner, 1997)	78
Fig 2.35	Epidermal cell jute plant (after Abdullah, 1999)	79
Fig 2.36	Cross-section stem of jute plant (after Abdullah, 1999)	80
Fig 2.37	Structure of simple woody cell (after Abdullah, 1999)	80
Fig 3.1	Measuring mass per unit area	115
Fig 3.2	Measuring thickness of geojute	115
Fig 3.3	Variation of thickness with time for different applied pressure (after Muhammad, 1993)	116
Fig 3.4	Variation of equivalent single layer thickness with applied pressure for different number of layers (after Muhammad, 1993)	116
Fig 3.5	Determination of specific density	117
Fig 3.6	Variation of specific gravity with soaking time for different types of jute geotextiles (after Muhammad, 1993)	118
Fig 3.7	Variation of specific gravity with time for untwisted loose jute geotextile fibres using vacuum (after Muhammad, 1993)	118
Fig 3.8	Wide width strip tensile test using Autograph Instron machine (after Muhammad, 1993)	119
Fig 3.9	Special jaws with serrated faces for uniaxial wide width strip tensile test(after Muhammad, 1993)	120
Fig 3.10	Tensile test response of various geotextiles manufactured by different process. All are polypropylene fabrics; test specimens were initially 200 mm wide X 100 mm high (after Koerner, 1997)	121

Fig 3.11	Trapezoidal template for trapezoid tearing strength test (after ASTM book of Standard, 2004)	121
Fig 3.12	Test arrangement of index puncture test	122
Fig 3.13	Index test fixture and probe detail (not to scale, after ASTM book of Standard, 2004)	123
Fig 3.14	CBR test fixture and probe	124
Fig 3.15	CBR test fixture fitted with test sample	124
Fig 3.16	Bursting testing machine	125
Fig 3.17 (a)	Test specimen preparation for sewn seam (front view) (after ASTM Book of Standard. 2004)	126
Fig 3.17 (b)	Test specimen preparation for thermally bonded seam (front view) (after ASTM Book of Standard, 2004)	126
Fig 3.18 (a)	Placement of generic seam in clamps for sewn seam (front view) (after ASTM Book of Standard, 2004)	126
Fig 3.18 (b)	Placement of generic seam in clamps for bonded seam (front view) (after ASTM Book of Standard. 2004)	126
Fig 3.19 (a)	Direct shear test device (after Koerner, 1997)	127
Fig 3.19 (b)	Direct shear test data (after Koerner, 1997)	127
Fig 3.19 (c)	Mohr-Coulomb stress space (after Koerner, 1997)	127
Fig 3.20	Direct shear box test apparatus for evaluating friction between jute geotextile and sand (after Muhammand, 1993)	128
Fig 3.21	Schematic pressure diagram for direct shear test (after Muhammand, 1993)	129
Fig 3.22	Direct shearing test for dry sand (after Muhammand, 1993)	129
Fig 3.23	Direct shearing test for saturated sand (after Muhammand, 1993)	130
Fig 3.24	Direct shearing test for friction between saturated sand and jute geotextile $500\text{g/m}^2$ (after Muhammand, 1993)	130

Fig 3.25	Direct shearing test for friction between saturated sand and jute geotextile 600g/m <sup>2</sup> (after Muhammand, 1993)	131
Fig 3.26	Frictional angle for different materials derived from direct shearing tests (after Muhammand, 1993)	131
Fig 3.27	Schematic diagram for modified pullout test apparatus (after Muhammand, 1993)	132
Fig 3.28	Modified pullout test results for interface friction between jute geotextile and wet sand (after Muhammand, 1993)	132
Fig 3.29	Pull out test device (after Muhammand, 1993)	133
Fig 3.30	Test arrangement of Apparent Opening Size (after Muhammand, 1993)	133
Fig 3.31	Constant and falling head permeability apparatus (after ASTM Book of Standard, 2004)	134
Fig 3.32	Sampling pattern for water permeability of geotextiles by permittivity test (after ASTM Book of Standard, 2004)	134
Fig 3.33	Test arrangement of transmissivity	135
Fig 3.34	Schematic drawing of transmissivity test assembly (after ASTM Book of Standard, 2004)	136
Fig 3.35	Schematic drawing of creep test assembly (after ASTM Book of Standard, 2004)	136
Fig 3.36	Schematic drawing of creep test assembly (after Mahaseth, 2002)	137
Fig 3.37	Strain versus time plots from sustained load creep tests	138
Fig 3.38	Series of sustained loadings versus time for deriving strain envelope for elasto-visco-plastic material	139
Fig 3.39	Deriving isochronous load-strain curves for elasto-visco-plastic geosynthetics (after Mahaseth, 2002)	140
Fig 3.40	Results of confined creep tests on various geotextiles (after McGown et al, 1982, 1986)	141
Fig 3.41	Abrasion test results for various geotextiles using the Taber test device model 503 (after Koerner, 1997)	142

Fig 3.42	Untreated geojute samples selected for tests	143
Fig 3.43	Treated geojute samples selected for tests	144
Fig 4.1	Mass per unit area of tested samples	165
Fig 4.2	Schematic arrangement for measurement of equivalent single layer thickness	165
Fig 4.3	Nominal thickness of tested samples	166
Fig 4.4	Variation of thickness of treated geojute with time	166
Fig 4.5	Variation of thickness in percentage within first five minutes of geojute	167
Fig 4.6	Variation of specific gravity with time for untreated geojute	167
Fig 4.7	Variation of specific gravity with time for treated geojute	168
Fig 4.8	Repeated loading universal testing machine	168
Fig 4.9	Wide width strip tensile test using WOLPERT machine	168
Fig 4.10	Grip and jaws of wide width strip tensile machine	169
Fig 4.11	Load versus strain for untreated Jute	170
Fig 4.12	Load versus strain for treated Jute	170
Fig 4.13	Load versus strain for untreated Canvas	171
Fig 4.14	Load versus strain for treated Canvas	171
Fig 4.15	Load versus strain for untreated DW Twill	172
Fig 4.16	Load versus strain for treated DW Twill	172
Fig 4.17	Load versus strain for untreated Hessian	173
Fig 4.18	Average wide-width tensile strength of tested samples	174
Fig 4.19	Average wide-width tensile elongation of tested sample	174
Fig 4.20	Average elongation of tested samples in MD	175

Fig 4.21	Average elongation of tested samples in XMD	175
Fig 4.22	Canvas before wide-width test	176
Fig 4.23	Canvas after wide-width test	176
Fig 4.24	Hessian before wide-width test	176
Fig 4.25	Hessian after wide-width test	176
Fig 4.26	Clamps of grab breaking test	177
Fig 4.27	Clamps of grab breaking test	177
Fig 4.28	Grab breaking load of samples in MD	178
Fig 4.29	Grab breaking load of samples in XMD	178
Fig 4.30	Grab breaking elongations of samples in MD	179
Fig 4.31	Grab breaking elongations of samples in XMD	179
Fig 4.32	Canvas before grab test	180
Fig 4.33	Canvas after grab test	180
Fig 4.34	Hessian before grab test	180
Fig 4.35	Hessian after grab test	180
Fig 4.36	Trapezoid tearing strength of samples in MD	181
Fig 4.37	Trapezoid tearing strength of samples in XMD	181
Fig 4.38	DW Twill sample before trapezoid test	182
Fig 4.39	DW Twill sample after trapezoid test	182
Fig 4.40	Canvas sample before trapezoid test	182
Fig 4.41	Canvas sample after trapezoid test	182
Fig 4.42	Index puncture strength of tested geojute	183
Fig 4.43	Variation in load of individual sample in index puncture test	183
Fig 4.44	CBR strength of samples	184

Fig 4.45	Variation in load of individual sample in CBR puncture test	184
Fig 4.46	Burst strength of untreated samples	185
Fig 4.47	Burst strength of treated samples	185
Fig 4.48	Sieve analysis machine	186
Fig 4.49	Apparent opening size plot of Jute	187
Fig 4.50	Apparent opening size plot of Canvas	187
Fig 4.51	Apparent opening size plot of DW Twill	188
Fig 4.52	Apparent opening size plot of Hessian	188
Fig 4.53	Test arrangement of permittivity	189
Fig 4.54	Permittivity results of samples	190
Fig 4.55	Flow rate per unit width versus normal compressive stress of samples	190
Fig 4.56	Hydraulic transmissivity versus normal compressive stress of samples	191
Fig 4.57	Transmissivity test results for different mass per unit area of nonwoven needle-punched geotextile (after Koerner, 1997)	191
Fig 4.58	Co-efficient of normal permeability versus normal stress (after Rao et al, 1994)	192
Fig 4.59	Co-efficient of in-plane permeability versus normal stress (after Rao et al, 1994)	192
Fig 4.60	Untreated Canvas sample ready for test	193
Fig 4.61	Treated Canvas sample ready for test	193
Fig 4.62	Creep test on progress	194
Fig 4.63	Creep test results of untreated Canvas	195
Fig 4.64	Creep strain versus log time plots for Canvas (after Kabir, 1994)	195



Fig 4.65	Isochronous load versus strain diagrams for untreated Canvas	196
Fig 4.66	Isochronous load versus strain diagrams for Canvas (after Kabir, 1994)	196
Fig 4.67	Creep test results of treated Canvas	197
Fig 4.68	Canvas before creep test	198
Fig 4.69	Ruptured Canvas on 34 <sup>th</sup> day at 40% of ultimate load	198
Fig 4.70	Treated Canvas before creep test	198
Fig 4.71	Ruptured treated Canvas on 23rd Day at 20% of ultimate load	198
Fig 4.72	Mass per unit area of geotextiles, untreated and treated geojute	199
Fig 4.73	Thickness of geotextiles, untreated and treated geojute	199
Fig 7.74	CBR puncture resistance of geotextiles, untreated and treated geojute	200
Fig 4.75	Grab tensile strength of geotextiles, untreated and treated geojute	200
Fig 4.76	Grab tensile elongation of geotextiles, untreated and treated geojute	201
Fig 4.77	Wide-width tensile strength of geotextiles, untreated and treated geojute	201
Fig 4.78	Wide-width elongation of geotextiles, untreated and treated geojute	202
Fig 5.1	Geojute reinforcement layout for retaining wall	212
Fig 5.2	Comparative costs of the tested untreated geojute.	235
Fig 5.3	Comparative costs of treated geojute with geotextiles	235

## LIST OF ABBREVIATIONS OF TECHNICAL SYMBOLS AND TERMINOLOGIES

$\Delta h$	total head lost
AOS	Apparent Opening Size
ASTM	American Society for Testing and Materials
B	width of footing
BJMC	Bangladesh Jute Mills Corporation
BJRI	Bangladesh Jute Research Institute
c	clay cohesion
$c_u$	undrained shear strength of clay
D	depth of footing
DIN	German Standards Committee for Geotextiles
$G_s$	specific gravity of jute geotextile
IJSG	International Jute Study Group
JDPC	Jute Diversification Promotion Centre
$K_a$	coefficient of active pressure
$K_o$	coefficient of earth pressure at rest
$k_p$	in-plane geotextile permeability
L	length of footing
MD	machine direction
N	number of layers of geotextile
N	newton
$N_c$	bearing capacity factors
$N_q$	bearing capacity factors
$N_\gamma$	bearing capacity factors
$\phi$	angle of soil friction (in terms of total stress)
$\phi'$	angle of soil friction (in terms of effective stress)
$O_{90}$	90% of sand retention on geojute

$O_{95}$	95% of sand retention on geojute
$q$	flow rate
$q_f$	ultimate bearing capacity of a footing
$q_o$	Terzaghi's ultimate bearing capacity
$q_u$	surcharge load on the ground surface
$S_v$	vertical spacing of reinforcing element
$t$	time, thickness
$T$	temperature
$T_{avg}$	average thickness of a single layer of geojute
$t_o$	equivalent instantaneous loading time
$T_{total}$	total thickness of a number of layers of geojute
$w$	percentage of water content of clay
$w$	width of the geotextile
$W_{bw}$	weight of flask + distilled water upto the graduation
$W_{bwj}$	weight of flask + geojute + distilled water upto the graduation of the flask
$W_d$	weight of dry solid material of volume $V$
$W_j$	weight of dry jute
$W_w$	weight of water of volume $V$
XMD	cross-machine direction
$\alpha$	shape factor of filling
$\gamma$	soil unit weight (bulk density)
$\gamma'$	submerged density of soil
$\gamma_c$	unit weight of clay slurry
$\gamma_{clay}$	total unit weight of clay slurry
$\gamma'_s$	submerged unit weight of sand
$\gamma_t$	unit weight of soft clay
$\gamma_w$	unit weight of water
$\theta$	angle of inclination of geojute to horizontal clay surface
$\theta$	transmissivity of the geotextile ( $m^2/s$ or $m^3/s-m$ )
$\mu$	coefficient of friction between frictional fills and geojute strip
$\sigma_n$	component of stress normal to a surface of sliding

$\tau_c$	adhesion strength
$\tau_f$	soil shear strength
$\tau_g$	interface adhesion between geojute and clay slurry

## ABSTRACT

This study was undertaken to find out the feasibility of using geojute as an alternative of geotextiles in civil engineering applications. Four types of untreated geojute samples were selected from Bangladesh Jute Mills Corporation (BJMC) and Bangladesh Jute Research Institute (BJRI). Subsequently these were treated by using bitumen. Physical, mechanical, hydraulic, short term and long term tensile tests were performed both on treated and untreated geojute samples. It is appreciated that, neither any standard test method nor any design approach related to geojute are currently available. The ASTM and DIN standard test methods for determining the properties and the design approach commonly employed for geotextiles were adopted.

The application areas for geojute were identified as the filtration in cross plane flow, separation of dissimilar materials, reinforcement of weak soils, and drainage in in-plane flow. These applications, test methods and design approach have been discussed elaborately. The test procedures and results obtained are presented with graphs and charts. An attempt has been made to compare these test results with available geotextile data. Based on these test results some design examples have been presented using the procedures for geotextiles as outlined by Koerner (1997). An economic aspect related to geotextile and geojute is also presented in this study.

It is identified that the range of geojute undertaken in the study may be applied efficiently to perform separation functions between two dissimilar materials for short term to medium term applications. It may also be applied to reinforce weak soils for short term to medium term. The permittivity and apparent opening size of tested geojute allow these to be used in filtration function behind flexible wall systems to allow the backfill soil to be retained in its position. Although, the geojute materials were found to be suitable for pressure drainage applications, these were not found suitable for gravity drainage applications. It is estimated that if geotextiles are replaced with geojute in civil engineering applications as exemplified significant economic benefit can be obtained.

## ACKNOWLEDGEMENT

First, I want to express my deep gratitude to The Almighty and Omnipotent Allah to enable me to perform this research work.

I am extremely delighted to have the opportunity to explicate my cordial gratitude to my supervisor Dr Abdul Jabbar Khan, Associate Professor, Department of Civil Engineering, Bangladesh University of Engineering and Technology (BUET), for his overall supervision, invaluable suggestion and ardent encouragement in every aspect of my thesis work. His constant guidance, persuasion, and above all constructive criticism helped me immensely to complete the work in time. I want to express my indebtedness to him for his superbly technical expertise, impromptu answers and solution to numerous problems.

I want to express my deep gratitude to Dr Zahid Hossain Prodhan, Managing Director, Arcadia Property Development, Dhanmondi, Dhaka for constant support on research materials, inspiration, and guidance to me.

I also want to thank Dr A.B.M. Abdullah, Executive Director and Mr Mohammad Fazlul Huq Bhuiyan, Director (MRP), Jute Diversification Promotion Centre (JDPC) for providing valuable papers on geojute and also Mr Kamal Uddin, Director Technology & Research, Bangladesh Jute Research Institute (BJRI) to provide me untreated and treated Jute samples for the research. I would like to thank Mr M. Mizanur Rahman, Deputy General Manager (Marketing), Bangladesh Jute Mills Corporation (BJMC) for providing huge geojute samples based on which the research is made possible. I must thank Major Sarwar Hossain, Officer Commanding (Administration Company), Prime Minister's Office, Armed Forces Division, Dhaka Cantonment for providing all sorts of vehicular and necessary supports throughout my full study tenure.

I am grateful to technical staff of the geotechnical laboratory of BUET for their continual assistance in laboratory works.

At last, I want to thank my parent, brothers, sisters and spouse who have provided continuous encouragement, inspiration and support to me throughout this research project.

# CHAPTER ONE

## INTRODUCTION



### 1.1 General

The addition of materials to improve the properties of soils was possibly done long before our first historical records. Examples may be the use of tree trunks, small bushes, and the like to stabilize swamps and marshy soils. Such stabilization attempts were undoubtedly continued with the development of a more systematic approach in which timbers of nearly uniform size and length were lashed together to make a matted surface. Such split-log “corduroy” roads over peat bogs date back to 3000 BC (Dewar, 1962). The Archaeological findings in the United Kingdom dating as far back as 2500 BC indicate that some pathways were constructed over logs that were used to stabilize the soft ground (Muhammad, 1993). Chinese used bamboo, wood and straw as soil reinforcement in the construction of portions of the Great Wall of

China more than 2000 years ago (Yamanouchi, 1992). In the days of Ozymandias and Babylon, reed mats were used in wall foundations and as a base for roads and branches of trees were incorporated into walls (Grech, 1995).

The concept of reinforcing poor soils has continued until the present day. Geotextiles were the first to use in erosion control applications and were intended to be an alternative to granular soil filters. Thus, the original and still sometimes used term for geotextiles is 'filter fabrics'. The work originating in the late 1950s using geotextiles behind precast concrete erosion control blocks, beneath large stone riprap, and in other erosion control situations (Barrett, 1966). In the late 1960s, Rhone-Poulenc Textiles in France began working with nonwoven needle-punched fabrics for quite different applications (Koerner, 1997). Emphasis was given on reinforcing unpaved roads, beneath railroad ballast, within embankments and earth dams, and the like. The primary function in many of these applications was that of separation and/or reinforcement. The Dutch and the English can be given credit for early work in the use of geotextiles. ICI Fibres was a major influence in the use of nonwoven, heat-bonded fabrics in a wide variety of uses. Mirafi, Inc. imported the first nonwoven used in the U.S. from ICI Fibres in the late 1970s (Koerner, 1997). Today many manufacturers are involved in the production, sales and distribution of geotextiles. A number of conferences were held exclusively on the subject of geotextiles. More recently, conferences have addressed the entire breadth of geosynthetics, the major ones being those held in 1977, in Las Vegas in 1982, in Vienna in 1986, in Hague in 1990, in Singapore in 1994 and in Atlanta 1998. The culmination of this activity was the formation of the International Geosynthetic Society (IGS). At about this time the synthetic industry had managed to penetrate the jute market.

Synthetic Geotextiles are now being widely used for a number of different geotechnical applications. The functions are mainly filtration in cross plane flow, separation of dissimilar materials, reinforcement of weak soils, drainage in in-plane flow etc (Koerner, 1997). Synthetic materials dominated the field because of its special characteristics like high strength, high thermal insulation, low specific gravity, good resilience, chemical inertness and resistance to moth and bacterial attack (Talukder, et al, 1988). Recently developed woven geotextiles are even ultraviolet



degradation protected. The main feature of geotextile for which it has seen unrivalled growth with a forecast by the United Nations International Trade Centre (UNITC) of 1,400 million m<sup>2</sup> produced by the new millennium is the prolonged design period of 100 to 120 years (Jute Manufactures Development Council, 2004).

As mankind seeks to reduce the conflict between the expanding world population and the limited natural resources available to it on the one hand, and between the daily deterioration of the environment and the exploitation of natural resources for industrialization on the other, it is now realized that the promotion of a fiber other than natural cotton and synthetic cellulose has become very important. It is estimated that the demand for fibres for clothing alone will rise from the current 60 million tons up to 130 million ton per year in the year 2050 (Kozlowski, 1996), not mentioning the fibre consumption for various other purposes. Although the invention of synthetic fibres has brought us uncountable benefits in our everyday life, many of the drawbacks of using synthetics have started to change our attitude toward them.

In view of these developments, jute, a natural fibre has come up to supplement and/or replace synthetics, has been receiving increasing attention from the industry. The past success of jute is due largely to its environment friendly characteristics. Jute fibre is comparable or superior to synthetic fibre in physical and chemical characteristics. Jute is an annually renewable energy source with a high biomass production per unit land area. Jute is biodegradable and its products can be easily disposed without causing environmental hazards. By rotating with other crops, jute improves soil fertility and increases the productivity of other crops. The use of jute as a geotextile will help to; at least partially solves the two biggest environmental problems we are facing today: deforestation and soil erosion (Liu, 2004)

In this connection, two seminars in London and Geneva last year brought together key jute producers with invited researchers, environmental consultants, suppliers, contractors and specifying authorities. Specifications were agreed which geojute would need to meet to satisfy environmental and geotechnical engineers. The obvious uses in erosion control were generally known, but it was interesting to note that composite products involving jute in combination with synthetics, or jute together

with coir, can offer optimum solutions in other areas. Some applications are clearly suited to jute, but the material characteristics need more elaboration.

Besides, a good number of researches and pilot projects have been undertaken in France, England and India under the auspices of United Nations Development Programme (UNDP), United Nations International Trade Centre (UNITC), Jute Manufactures Development Council (JMDC), Agricultural and Environmental Engineering Research, (CEMAGREF), France, Silsoe College, England and Grenoble University, France in order to assess the technical aspects of geojute for civil engineering applications for which geotextiles have been successfully used (Jute Manufactures Development Council, 2004) . The main reason for drawing such attention to geojute materials may be attributed to its low cost compared to synthetic geotextiles in many countries and worlds growing concerns over the ecological imbalance.

The early examples of use of jute are also very rich. To assist in the invasion of Normandy, the British Army developed a machine to lay canvas or fascine rolls to provide roads across beaches and dunes (Thomson, 1988). Jute fabric soaked in bitumen was used in military road construction in Burma front of South East Asia during the Second World War (Kabir et al, 1994). Traditionally soil filled jute bags have been extensively used in military application and in erosion and flood related civil engineering applications. Using jute to protect large areas from erosion, including high-altitude ski-slopes with significant precipitation, has been trialed by Françoise Dinger of CEMAGREF. The ability of jute to absorb five times its own weight of water (3 kg per m<sup>2</sup> of slope) was demonstrated. The retained water firstly attenuates the run-off into the drainage system and is then released gradually to soak into the adjacent soil to nourish the vegetation from severe frosts, so aiding growth. Barbara Lois of SIRAS Company described the extensive environmental works undertaken in France using jute geotextiles, including rehabilitating mine dumps, restoring the Rhone riverbanks and the vegetating high altitude steep slopes at the Winter Olympic ski jump in Savoie. Landscaping of slopes alongside the TGV rail line and along highway cuttings and embankments showed the effectiveness of the geotextiles. Recently, strengthening of a road with geojute in Kakinada port area of

Andhrapradesh, India was effectively done (Rao, 2003). Application of geojute has significantly improved the pavement performance.

## 1.2 Background of the Research

The abundant availability of jute in Bangladesh renders Jute fabrics cost effective for various applications such as temporary roads and yards, repair of permanent roads, drainage application, reclamation works, stabilization of temporary bunds and erosion control. Lee et al (1987), Siew Ann Tan et al (1993), Ramaswamy and Aziz (1989), Lee et al (1989), Rao et al (1994) and Sanyal (1993) have reported on the utilization of Jute fabrics in the construction of haul roads on poor subgrades, land reclamation works, drains for preconsolidating soft clays and for control of erosion. In a study Ramaswamy and Aziz, (1989), Mandal and Murti, (1990), and Karunaratne et al, (1992) have attempted to evaluate physical, mechanical and hydraulic properties of natural geotextiles. In addition, attention is being concentrated on retarding the degradation of natural fibers from microbiological attack. Dastidar (1969) reported use of jute sand wicks in vertical drain application. Kabir et al (1988) presented laboratory studies on repeated loading and filter behavior on some grades of Jute fabrics. Lee et al (1989) reported use of jute fibre drains using coconut coir cores in vertical drain application.

Five grades of jute fabrics were assessed by Kabir et al (1988) to establish their filterability. Pore size and hydraulic conductivity data were produced for each of the grades. Filterability for each of these has been established by using Giroud's (1982) mechanical filter effectiveness criterion and the hydraulic filter effectiveness criterion. Finally, system test results on one of the grades were produced to observe the performance under constant head type flow condition.

Six nonwoven jute based geotextiles consisting of varying proportions of jute and polypropylene fibres were evaluated for their engineering properties by ASTM/BIS standards for geotextiles and related products. The test results, their evaluation and categorization of jute based geotextile fabrics were reported Rao et al (1994). The test results shows that jute based geotextiles were capable of adequately

performing different engineering functions such as, separation, filtration, drainage and reinforcement. The degree to which the fabrics tested fulfill the requirements for the above functions was also brought out.

Venkatappa et al (1994) examined four types of woven jute fabrics embedded in soil for periods up to 2.5 months and submerged in water up to 4 months for changes in stress-strain behavior through narrow strip tensile strength tests. The durability of jute yarns was also assessed by conducting tests with solutions at values of  $p^H$  ranging from 4.5 to 9.0 at room temperature. The studies reveal that the tensile strength of the different fabrics falls to zero within 2.5 months in the biotic environment prevalent in Delhi. However, when jute was fully submerged in water for 4 months, the loss was only 35%. On the other hand, a strength loss up to 50% was observed under conditions of different  $p^H$ , the maximum loss being at  $p^H$ : 5.2.

Kabir et al (1994) tested a number of grades of jute fabrics and fibre drains to establish some of their hydraulic and mechanical behaviour. Test results of four grades of jute fabrics were presented enabling establishment of their hydraulic conductivity and filter behavior. In plane hydraulic conductivity results of two types of jute fibre drains were presented. Static creep behavior of one grade of jute fabric was also presented.

A variety of nonwoven geojute fabrics have been developed by Pandey et al (1994) based on two main functions of geotechnical end uses i.e. soil erosion and road construction. The different two types of nonwoven jute agri-geo-fabs have been developed which can be used for protection of soil erosion. The various jute: polypropylene (PP) blended nonwoven geo-jute fabrics have also been prepared to see the effect of blends with the treatment of urea-formaldehyde (U.F.) resin and its use for road constructions and to protect road damages.

Jane Rickson of Silsoe College, England identified three current main applications for jute: Erosion control and vegetation establishment, agro plant mulching, rural road pavement construction. Testing over 12 years at Silsoe has proved the technical excellence of geojute compared with other natural and synthetic

geotextiles under a range of environmental conditions, showing that vegetation establishment is highly effective when jute is used.

A newly developed wick drain, formed from a jute sleeve packed with coir, showed how combinations of geojute types provide benefits greater than the sum of each. Professor Bob Sarsby of Bolton Institute reported on full-scale trials of soil walls incorporating jute rope reinforcement. This work graphically demonstrated the strength of jute in supporting walls of 4m or more.

In tropical, humid, rainfed and frequently flood-affected countries like Bangladesh quick biodegradability of jute is a disadvantage for its use in geotechnical applications. Recently a wide range of geojute has been developed in the laboratory of Bangladesh Jute Research Institute (BJRI) by blending jute with hydrophobic fibre like coir or by modification with bitumen, latex and wax resinous materials with the collaboration of Bangladesh Jute Mills Corporation (BJMC). This has enabled to produce geojute having designed biodegradability and increased hydrophobicity (Prodhan, 1996).

Geojute was used to protect soil erosion due to flood and long monsoon in Dhaka City Flood Protection Bund in 1993 (Abdullah, 1999). It was also used as pilot scale application for slope protection work on Pakulla-Lawati Road under Tangail district by BJRI and LGED during 2001 as per recommendation proposed by Prodhan (2001). Research on Integrated Geojute Reinforced Earth Structures Design showed that for similar loading and soil conditions, application of Geojute can save up to 50% constructional cost of embankment, dams, rivers, roads, highways, flood controls and similar structures compared to conventional solution (Prodhan, 1994).

Though different researchers, organizations and institutions, have performed many study/research works, a systematic study related to the index & mechanical properties of geojute and their short/long term applicability is yet to be performed for identifying design parameters of these materials for geotechnical applications.

### 1.3 Objective of Research

Based on the problems identified in the above section, the present study is designed to fulfill the following objectives:

- To investigate the physical properties, i.e. mass per unit area, thickness and specific gravity in the geotechnical laboratory of BUET by standard testing method (ASTM/DIN).
- To investigate the mechanical properties; i.e. wide-width strip tension test, grab breaking load and elongation test, trapezoid tearing test, puncture test and burst strength test in the geotechnical laboratory of BUET by standard testing method (ASTM/DIN).
- To investigate the hydraulic properties; i.e. apparent opening size, permittivity (cross-plane permeability) and transmissivity (in-plane permeability) in the geotechnical laboratory of BUET by standard testing method (ASTM/DIN).
- To investigate the endurance properties; creep test of geojute in geotechnical laboratory of BUET by standard testing method (ASTM/DIN).
- To assess the feasibility of using geojute as an alternative of geotextile in civil engineering application.
- To compare the cost between geojute and geotextile.

### 1.4 Methodology

A brief description of the methodology/ experimental design to be followed in conducting the study is given below:

- International Jute Study Group (IJSG), Jute Diversification Promotion Centre (JDPC), Bangladesh Jute Mills Corporation (BJMC) and Bangladesh Jute Research Institute (BJRI) have been contacted for geojute related research papers, documents, information and samples.
- Four grades of geojute have been selected from BJRI and BJMC having varied physical and structural properties, local market availability and potential usefulness in geotechnical applications.

- Three grades of already selected untreated geojute have been treated in BJRI laboratory so that the test results can be compared.
- Test arrangements has been made up and running for the performance of the entire set of tests.
- The physical properties, i.e. mass per unit area, thickness and specific density have been investigated in the geotechnical laboratory of BUET by standard testing method (ASTM).
- The mechanical properties; i.e. wide-width strip tension test, grab breaking load and elongation test, trapezoid-tearing test, puncture test and burst strength have been investigated in the geotechnical laboratory of BUET by standard testing method (ASTM/DIN).
- The hydraulic properties; i.e. apparent opening size, permittivity (cross-plane permeability) and transmissivity (in-plane permeability) have been investigated in the geotechnical laboratory of BUET by standard testing method (ASTM).
- The endurance properties; creep test of geojute have been investigated in geotechnical laboratory of BUET by standard testing method (ASTM).
- A comparative study has been presented on the test results of geojute and geotextile.
- An economic aspect of untreated and treated geojute with synthetic geotextile has been presented.
- An assessment on the feasibility of use of geojute for long and short term geotechnical application has been made
- Some procedures on designing with geojute have been presented.

## 1.5 Organization of the Thesis

The research work conducted for achieving the stated objectives is presented in several chapters of this thesis so that the steps involved in the study may properly delineate the methodology. A brief discussion of the contents of each chapter is as follows:

Chapter Two contains a general description of geotextiles, its different types and properties. The different geotextiles functions and applications are incorporated in this chapter elaborately. Thereafter a review on Jute is presented. Here, discussion on physical and chemical structure, composition and properties of Jute are described. The treatment procedure of Jute, how to improve its strength and quality is covered in this chapter.

The laboratory investigation of physical, mechanical, hydraulic and endurance properties of geotextiles are narrated in Chapter Three as per ASTM and DIN standard. There after, a summary on samples selected for the test is presented. At the end, a brief discussion is made on the tests performed followed by a table.

Chapter Four deals with experimental results and discussion. Here the laboratory test procedures and results of all tests performed are presented with graphs and charts. At the end, a comparison on the test data of available geotextile and tested geojute has been presented.

The designing with geojute and technical assessment is dealt in Chapter Five. Since no standard design method or approach for geojute are available to date, the design methods or approach commonly employed for geotextiles are adopted. Some examples have been illustrated for reinforcement, separation, drainage and filtration using the design procedure outlined by Koerner (1997) for geotextile applications. An economic aspect is presented in this chapter with a cost comparison between geojute and geotextile.



Chapter Six includes the conclusions and recommendations on the basis of the present study and eventually recommendations for the future work are presented.

## ***CHAPTER TWO***

### ***LITERATURE REVIEW***

#### **2.1 General**

Geojute may be envisaged as a potential alternative to geotextiles in many civil engineering applications. In this Chapter, first, the properties and application of geotextiles are presented. Then, the physical properties of a range of geojute are outlined.

##### **2.1.1 Geosynthetic**

All polymers based materials as well as natural products; fiberglass and rubber, which can be used in geotechnical engineering, comprise Geosynthetics family. Geosynthetics can be categorized as follows:

- a. Geomembranes
- b. Geotextiles

- c. Geonets
- d. Geogrids
- e. Geocomposites
- f. Geopipes
- g. Geosynthetic Clay Liners

### **Geomembranes**

These are relatively impermeable materials which are used as a liquid or vapor barrier and made of continuous polymeric flexible sheets. The primary function in containment is as a liquid or vapor barrier. The range of applications is very wide and in addition to the environmental area, applications are rapidly growing in geotechnical, transportation, and hydraulic engineering (Fig 2.1a).

### **Geotextiles**

The term "geotextile" refers to textiles (fabrics) used in geotechnical engineering practice. Geotextiles are thin, flexible, permeable sheets of synthetic material used to stabilize and improve the performance of soil associated with civil engineering works. As per ASTM D 4439-98, a geotextile is defined by as: "any permeable textile material used with foundation, soil, rock, earth, or any other geotechnical (soil and foundation) engineering related material as an integral part of a man made project, structure, or system." Their rise in growth during the past twenty years has been nothing short of awesome (Fig 2.1b).

### **Geonets**

These consist of two sets of coarse, parallel-extruded strands intersecting with a constant angle typically between 60 to 90. Strands of one set are connected to strands of another set by partial melting. The size of strands is typically 1 to 5 mm diameter and the openings are from 5 to 50 mm diameter. Their design function is completely within the drainage area where they have been used to convey liquids of all types (Fig 2.1c)

### **Geogrids**

These are made by heating and pulling a perforated plastic sheet in one or two perpendicular directions and then cooling down for hardening. The small perforated openings become large quasi-rectangular openings, usually 1 to 10 cm in length upon pulling. There are many application areas and they function almost exclusively as reinforcement materials (Fig 2.1d).

### **Geocomposites**

Geocomposites consist of various combinations of geotextiles, geogrids, geonets, geomembrances, and/ or other materials. The application areas are numerous and growing steadily. The major functions encompass the entire range of functions listed for geotextiles (Fig 2.1e).

### **Geopipes**

Geopipes are three-dimensional structures, which form channels in their ribs to allow flow of liquids. This pipe is perhaps the oldest geosynthetic material still available today. They may incorporate filters on the peripheral surfaces (Fig 2.1f).

### **Geosynthetic Clay Liners**

Geosynthetic Clay Liners (or GCLs) are the newest subset within the family of geosynthetic materials. They are rolls of factory-fabricated thin layers of bentonite clay sandwiched between two geotextiles or bonded to a geomembrane. Structural integrity is maintained by needle punching, stitching or physical bonding. They are used as a composite component beneath a geomembrane or by themselves in environmental and containment applications, as well as in transportation, geotechnical, and hydraulic applications (Fig 2.1f).

### 2.1.2 Types of Synthetic Geotextiles

Rankilor (1981) divided synthetic geotextiles into three groups based on the general manufacturing process; these are:

1. Woven
2. Non-woven
3. Knitted

The material properties and details of the manufacturing process may vary between geotextiles in different groups and between geotextiles within the same group. Fig. 2.2 shows a classification of geotextiles based on the manufacturing process after Rankilor (1981). According to Giroud et al (1985) the manufacturing process of a conventional geotextile includes two steps. The first step consists of making linear elements such as filaments, fibers, slit films (tapes) or yarns. Filaments are produced by extruding melted polymer through dies or spinnerets. Fibers (staple fibers) are obtained by cutting filaments to a short length, typically 2 to 10 cm. Slit films are small tapes, typically 1 to 3 mm wide. Yarns are made from filaments, fibers, tapes or in various combinations. The second step consists of combining filaments, fibers, slit films or yarns to make a planar permeable structure called a fabric. Woven geotextiles are manufactured with the use of a weaving loom. The two directions of the loom are termed as warp (lengthwise) and weft or fill (width, perpendicular to the warp). The warp threads are generally thicker than the weft threads because they must withstand tension in the weaving. Properties of woven geotextiles depend on the number of threads per unit length in direction, the weaving pattern and the cross sectional area of the material threads in either direction. Non-woven geotextiles are formed from filaments or fibers arranged at random and bonded together into a planar structure. Depending upon the process on which the filaments or the fibers arranged into a loose web they are bonded together as shown in Fig. 2.3. These are:

1. Chemically bonded non-woven geotextiles: by chemical bonding in which a cementing medium such as synthetic resin is added to bond filaments or fibers together.

2. Heat-bonded non-woven geotextiles: by thermal bonding in which heat causes partial melting of filaments or fibers, which make them adhere together at their intersection points.

3. Needlepunched non-woven geotextiles: by mechanical bonding in which thousands of small barbed needles, set into a board, are punched through the loose web and withdrawn, leaving filaments or fibers entangled.

Fig 2.4 also shows another classification of geotextiles after John (1987). The broad classification between Rankilor and John is more or less same.

### 2.1.3 Properties of Geotextiles

It is essential to note the properties of all commercially available geotextiles for comparison of efficiency in its application in geotechnical engineering. The rapidly changing market and its demands make it difficult to give accurate values, but for typical commercially available geotextiles. Typical range of properties for currently available of geotextiles is shown in Appendix.

## 2.2 Geotextile Functions and Applications

### 2.2.1 General

A geotextile function refers to the specific role played by a geotextile in a soil/geotextile structure. The function is a specific task or capacity that the product is expected to perform within the overall project or installation. For example, in an erosion control application, rock or other riprap material may be placed over a fabric along a stream bank as shown in Fig 2.5. The role of the total system is to prevent erosion of the soil materials along the channel. The geotextile performs the specific function of filtration, allowing water in the soil to pass through the fabric while retaining the soil particles. A geotextile may perform more than one function at a time in a given application. Typically, a single function is determined to be more important and is considered the primary geotextile function with any other concurrent functions considered to be secondary. An example may be a geotextile reinforced soil retaining wall where the fabric is wrapped around the soil to form the wall face as shown in Fig 2.6. The primary function of the geotextile is reinforcement of the retained soil mass.

At the same time, the fabric in the face of the wall may be acting as a filter to permit water within the wall system to escape. In this case, filtration may be considered as a secondary function. Different writers and researchers have developed a number of classifications for geotextile functions ranging in number from as few as four to as many as several dozen. A number of recent writers have used a system which contains six different geotextile functions: separation, filtration, reinforcement, transmission, cushion and barrier. As Koerner (1997) describes, the major functions of geotextiles are separation, filtration, drainage, reinforcement and containment (if geotextile is suitably impregnated). In the subsequent paragraph what this functions means is technically demonstrated with an elaboration on the actual mechanisms embodied within each type of functions.

## **2.2.2 Separation**

### **2.2.2.1 Definition**

Separation is the process of preventing two dissimilar materials from mixing. In this function, a geotextile is most often required to prevent the undesirable mixing of fill and natural soils or two different types of fills. Koerner defines Separation as the placement of a flexible porous textile between dissimilar materials so that the integrity and functioning of both materials can remain intact or be improved. A schematic diagram shown in Fig 2.7 illustrates this mechanism.

### **2.2.2.2 Mechanism**

Geotextiles are commonly used for this function when constructed beneath roadway pavement sections. Roadway pavements are basically structures for taking the high contact pressures from the vehicle tires and reducing that pressure through the depth of the pavement to a level which can be handled by the underlying soil. Pressure dissipation occurs down through the various layers of materials within the pavement as shown in Fig 2.8. Over time, vehicle load applications cause subgrade soils to migrate into the aggregate base of the pavement section. Contamination of the aggregate base by the subgrade results in the reduction of the effective base thickness to less than that which was part of the original design. This concept is illustrated in

Fig 2.9. Reduction of the base thickness results in a decrease in the load carrying capability of the aggregate base and a reduction in the pavement life. As shown in Fig 2.10, geotextiles prevent the subgrade materials from migrating into the aggregate base, thus increasing pavement life.

### **2.2.2.3 Applications of Geotextile/Geojute in Separation**

A geotextile can be placed between a railroad subgrade and track ballast to prevent contamination and resulting strength loss of the ballast by intrusion of the subgrade soil. In construction of roads over soft soil, a geotextile can be placed over the soft subgrade, and then gravel or crushed stone placed on the geotextile. In both the application geotextile may be put for long and short term period.

The geojute may also be put in these applications where geotextile have already been successfully used. A high strength geojute may be placed between a railroad subgrade for short term application. It may also be put in construction of roads over soft soils for long and short term period. The ASTM standards for determining these design parameters are given in Appendix.

### **2.2.2.4 Designing for Separation**

When serving as a separator, the geotextile prevents fines from migrating into the base course and/or prevents base course aggregate from penetrating into the subgrade. The soil retention properties of the geotextile are basically the same as those required for drainage or filtration. Therefore, the retention and permeability criteria required for drainage should be met. In addition, the geotextile should withstand the stresses resulting from the load applied to the pavement. The natures of these stresses depend on the condition of the subgrade, type of construction equipment, and the cover over the subgrade. Since the geotextile serves to prevent aggregate from penetrating the subgrade, it must meet puncture, burst, grab and tear strengths. These requirements are discussed separately below:



### 2.2.2.4.1 Burst Resistance

A geotextile is considered to be laid on a soil subgrade with stone of average particle diameter ( $d_a$ ) placed above it. The voids within the stone will allow the geotextile to enter through it. This entry is resulted by the simultaneous action of the traffic loads being transmitted to the stone, through the geotextile, and into the underlying soil. The stressed soil then tries to push the geotextile up into the voids within the stone. The situation is shown schematically in Fig 2.11. Giroud (1984) provides a formulation for the required geotextile strength that can be adopted for this application.

$$T_{reqd} = \frac{1}{2} p' d_v [f(\epsilon)]$$

where

$T_{reqd}$  = required geotextile burst strength;

$p'$  = stress at the geotextile's surface, which is less than or equal to  $p$ , the tire inflation pressure at the ground surface;

$d_v$  = maximum void diameter of the stone =  $0.33d_a$ ;

$d_a$  = the average stone diameter,

$f(\epsilon)$  = strain function of the deformed geotextile

=  $\frac{1}{4} (2y/b + b/2y)$ , in which

$b$  = width of opening (or void), and

$y$  = deformation into the opening (or void)

The field situation is comparable to the ASTM D 3786 (Mullen) burst test, where the geotextile being stressed into a gradually increasing hemispherical shape until it fails in radial tension. Thus, the adapted form of the previous equation is:

$$T_{ult} = \frac{1}{2} p_{test} d_{test} [f(\epsilon)]$$

$T_{ult}$  = ultimate geotextile strength,

$p_{test}$  = burst test pressure, and

$d_{test}$  = diameter of the burst test device (= 30 mm).

Knowing that  $T_{allow} = T_{ult} / (\text{IIRF})$ , where IIRF = cumulative reduction factors, an expression can be formulated for the FS as follows:

$$\text{FS} = T_{allow} / T_{reqd} = (p_{test} d_{test}) / [( \text{IIRF} ) p' d_v]$$

### 2.2.2.4.2 Tensile Strength Requirement

There is a tendency of geotextile to burst in an out-of-plane mode. This occurs when the geotextile is locked into position by the stone-base aggregate above it and soil subgrade below it. A lateral or in-plane tensile stress in the geotextile is mobilized when an upper piece of aggregate is forced between two lower pieces that lie against the geotextile. This is somewhat similar to grab tensile test as illustrated in Fig 2.12. Here the maximum strain that the geotextile will undergo as the upper stone wedges itself down to the level of the geotextile can be determined. Using the dimensions shown (where  $S \sim d/2$  and  $l_f =$  deformed geotextile length), the maximum strain with no slippage or stone breakage can be calculated.

$$\begin{aligned}\varepsilon &= (l_f - l_o) 100/l \\ &= \frac{[d + 2(d/2)] - 3(d/2)}{3(d/2)} (100) \\ &= \frac{4(d/2) - 3(d/2)}{3(d/2)} (100) \\ &= 33\%\end{aligned}$$

It may be noted that the preceding assumptions result in a strain that is independent of particle size. Thus the strain in the geotextile could be as high as 33% given the idealized (upper-bound) assumptions stated above. The tensile force being mobilized as Giroud (1984) describes:

$$T_{reqd} = p'(d_v)^2 [f(\varepsilon)]$$

Where,

$T_{reqd}$  = required grab tensile force;

$p'$  = applied pressure;

$d_v$  = maximum void diameter  $\approx 0.33 d_a$ , where

$d_a$  = average stone diameter; and

$f(\varepsilon)$  = strain function of the deformed geotextile;

$$= \frac{1}{4} (2y/b + b/2y), \text{ where}$$

b = width of stone void, and  
y = deformation into stone void

### 2.2.2.4.3 Puncture Resistance

Survivability is said to be an important and critical aspect of geotextile not only in separation but also in all other applications. In this regard, sharp stones, tree stumps, roots, miscellaneous debris, and other items, either on the ground surface beneath the geotextile or placed above it, could puncture through the geotextile after backfilling and traffic loads are imposed. The design method suggested by Koerner (1997) for this situation is shown schematically in Fig 2.13. For these conditions, the vertical force exerted on the geotextile is as follows:

$$F_{reqd} = p'd_a^2 S_1 S_2 S_3$$

where

$F_{reqd}$  = required vertical force to be resisted;

$d_a$  = average diameter of the puncturing aggregate or sharp object;

$p'$  = pressure exerted on the geotextile (approximately 100% of tire inflation pressure at the ground surface for thin covering thicknesses);

$S_j$  = protrusion factor =  $h_h/d_a$ ;  $h_h$  = protrusion height  $\leq d_a$

$S_1$  = protrusion factor =  $h_h/d_a$ ;

$h_h$  = protrusion height  $\leq d_a$

$S_2$  = scale factor to adjust the ASTM D 4833 puncture test value (which uses an 8.0 mm diameter puncture probe) to the diameter of the actual puncturing object =  $d_{probe}/d_a$ ;

$S_3$  = shape factor to adjust the ASTM D 4833 flat puncture probe to the actual shape of puncturing object =  $1 - A_p/A_c$ , (values for  $A_p/A_c$  range from 0.8 for rounded sand, to 0.7 for run-of-bank gravel, to 0.4 for crushed rock, to 0.3 for shot rock);

$A_p$  = projected area of puncturing particle;

$A_f$  = area of smallest circumscribed circle around puncturing particle.

### **2.2.3 Reinforcement**

#### **2.2.3.1 Definition**

Reinforcement with geotextiles as described by Koerner (1997) as the synergistic improvement of a total system's strength created by the introduction of a geotextile (that is good in tension) into a soil (that is good in compression but poor in tension) or into other disjointed and separated material. In the most common reinforcement application, the geotextile interacts with soil through frictional or adhesion forces to resist tensile or shear forces. To provide reinforcement, a geotextile must have sufficient strength and embedment length to resist the tensile forces generated, and the strength must be developed at sufficiently small strains (i.e. high modulus) to prevent excessive movement of the reinforced structure.

#### **2.2.3.2 Mechanism**

In the reinforcement function, the geotextile is subjected to a sustained tensile force or load. Soil and rock materials are noted for their ability to withstand compressive forces and their relative low capacity for sustained tensile forces. In much the same way that tensile forces are taken up by steel in a reinforced concrete beam, the geotextile supports tensile forces which cannot be carried by the soil in a soil/geotextile system. As shown in Fig 2.14, in a geotextile-reinforced embankment constructed over soft soils, the geotextile layers are placed across potential rotational failure planes to carry the tensile forces, which cannot be carried by an unreinforced soil mass.

#### **2.2.3.3 Application of Geotextile/Geojute in Reinforcement**

The combined use of soil and a geotextile suggests a number of situations in which geotextile may be used to construct fabric-reinforced walls, reinforced embankments, to stabilize slopes temporarily or permanently, Fig 2.15. The ASTM standards for determining these design parameters are also given in Appendix.

Geojute may also be used to construct short term fabric reinforced earth walls designed to hold backfills. To stabilize slopes for short period it may also be used. Small protection bund may also be constructed with geojute.

#### 2.2.3.4 Designing for Reinforcement

Koerner (1997) reported two different approaches to the design of geotextile walls. One approach used by Broms (1978) and another one used by the US Forest Service, Steward et al and Whitcomd (1979). The latter method is described in this section. This method follows the work that Lee et al (1973) did on reinforced earth with metallic strips and was originally adapted to geotextile walls by Bell et al (1975). The design progresses in parts, as follows:

- Internal stability is first addressed to determine geojute spacing, geojute length and overlap distance.
- External stability against overturning, sliding and foundation failure is investigated and the internal design is verified or modified accordingly.
- Miscellaneous considerations, including wall-facing details, are addressed.

To determine the geotextile layer separation distances, earth pressures are assumed by Koerner (1997) to be linearly distributed using Rankine active *earth pressure* conditions for the soil backfill and *at rest* conditions for the surcharge. Active earth pressure ( $K_a$ ) conditions are used throughout. Another approach would be to use a Coulomb analysis for the earth pressure values. Boussinesq elastic theory for live loads on the soil backfill is used. The earth pressures result as shown in Fig 2.16.

$$\sigma_{hs} = K_a \gamma z$$

$$\sigma_{hq} = K_a q$$

$$\sigma_{hl} = (Px^2z) / R^5$$

$$\sigma_h = \sigma_{hs} + \sigma_{hq} + \sigma_{hl}$$

where,

$\sigma_{hs}$  = lateral pressure due to soil;

$K_a = \tan^2 (45 - \phi/2)$  = coefficient of active earth pressure;

- $\phi$  = angle of shearing resistance of backfill soil;  
 $\gamma$  = unit weight of backfill soil;  
 $z$  = depth from ground surface to layer in question;  
 $\sigma_{hq}$  = lateral pressure due to surcharge load;  
 $q = \gamma_q D$  = surcharge load on ground surface, where  
 $\gamma_q$  = unit weight of surcharge soil, and  
 $D$  = depth of surcharge soil;  
 $\sigma_{hl}$  = lateral pressure due to live load;  
 $P$  = concentrated live load on backfill surface;  
 $x$  = horizontal distance load is away from wall; and  
 $R$  = radial distance from load point on wall where pressure is being calculated.

The calculations of  $\sigma_{hs}$  and  $\sigma_{hq}$  are quite simple, but  $\sigma_{hl}$  presents problems, particularly for multiwheeled truck loads where superposition of each wheel must be performed. In this regard Fig 2.17 greatly aids in such calculations.

By taking a free body at any depth in the total lateral pressure diagram and then summing the forces in the horizontal direction, the following equation for the lift thickness is obtained.

$$\sigma_h S_v = T_{allow} / FS$$

$$S_v = T_{allow} / (\sigma_h FS)$$

where

$S_v$  = vertical spacing (lift thickness),

$T_{allow}$  = allowable stress in the geotextile

$\sigma_h$  = total lateral earth pressure at depth considered, and

FS = factor of safety (use 1.3 to 1.5 when using  $T_{allow}$  as determined above)

The same free-body approach can be taken to obtain the length of embedment of the geotextile layers in the anchorage zone,  $L_e$ . It may be noted that when these values are obtained they must be added to the nonacting lengths ( $L_R$ ) of the geotextile within the active zone for the total geotextile lengths ( $L$ ); that is,

$$L = L_e + L_R$$

where

$$L_R = (h - z) \tan (45 - \phi/2)$$

and

$$\begin{aligned} S_v \sigma_h FS &= 2\tau L_e \\ &= 2(c_a + \sigma_v \tan\delta) L_e \\ &= 2(c_a + \gamma z \tan\delta) L_e \\ L_e &= (S_v \sigma_h FS) / 2(c_a + \gamma z \tan\delta) \end{aligned}$$

where

$\tau$  = shear strength of the soil to the geotextile,

$L_e$  = required embedment length (minimum is 1 m),

$S_v$  = vertical spacing (lift thickness),

$\sigma_h$  = total lateral pressure at depth considered,

FS = factor of safety

$c_a$  = soil adhesion between soil and geotextile (zero if granular soil is used),

$\gamma$  = unit weight of backfill soil,

$z$  = depth from ground surface, and

$\delta$  = angle of shearing friction between soil and geotextile

Finally, the overlap distance  $L_o$  is obtained in a similar way to that above with a few exceptions, namely that the distance  $Z$  should be measured to the middle of the layer and  $\sigma_h$  is not as large as illustrated in Fig 2.16. It is reasonably well-established that the stress in reinforcement elements is maximum near the failure plane and falls off sharply to either side. As an approximation,  $0.5\sigma_h$  will be used, which results in equation

$$L_o = (S_v \sigma_h FS) / 4(c_a + \gamma z \tan\delta)$$

where  $L_o$  is the required overlap length (the minimum is 1 m).

Next, the external stability of the geotextile wall should be considered, which includes overturning, sliding, and foundation failures. These are illustrated in Fig 2.18. These features are common to all wall systems and can be treated in exactly the same way as gravity or crib walls. They are generally site-specific insofar as the calculations are concerned. In the U.S., the Federal Highway Administration has recommended the following: for overturning and foundation-bearing capacity the FS value  $\geq 2.0$  and for sliding the FS value  $\geq 1.5$ .

The miscellaneous considerations that must be addressed are generally the facing details; facing connections (if applicable); seaming methods (if necessary); drainage behind, beneath, in front of the wall; erosion above and in front of the wall, guard posts, light posts, fencing and other appurtenances.

#### **2.2.4 Filtration**

##### **2.2.4.1 Definition**

As Koerner (1997) describes Filtration, "the equilibrium soil-to-geotextile system that allows for adequate liquid flow with limited soil loss across the plane of the geotextile over a service lifetime compatible with the application under consideration". Filtration is the most widely used geotextile function. For centuries, engineers have constructed filter systems using conventional graded aggregates. A geotextile providing a filtration function is serving the same role in soil structures, as were the various gradations of aggregates as shown in Fig 2.19 & 2.20. The filtration function has two concurrent objectives. These are to retain the particles of the filtered soil while permitting water to pass through the plane of the geotextile from the filtered soil. These two parallel roles are the key to filtration design. The filtration function is under continuing study...to determine the exact mechanism, which comes into play. Many researchers speak of a filter cake, which builds up on the face of the geotextile as shown in Fig 2.21. A third factor is also involved, that being a long-term soil-to-geotextile flow compatibility that will not excessively clog during the lifetime of the system. Three particular matter related to filtration i.e. permeability, soil retention and long-term flow compatibility is discussed below:

#### **Permeability**

Geotextile permeability refers to cross-plane permeability when liquid flow is perpendicular to the plane of the fabric. The geotextile used for this purpose are relatively thick and compressible. To define permeability coefficient i.e. *permittivity* thickness is included.

$$\Psi = k \div t$$



$\Psi$  = permittivity,

$k_n$  = cross-plane permeability coefficient (the subscript  $n$  is often omitted), and

$t$  = thickness at a specified normal pressure.

Geotextile permittivity test follows procedure similar to those used for testing soil permeability.

### Soil Retention

It is the process by which geotextile voids are made small enough to retain the soil on the upstream side of the fabric. The coarser soil fraction that must be initially retained is the targeted soil size in the design process. These coarser-sized particles eventually block the finer-sized particles and build up a stable upstream soil structure. For soil-retention design, many formulae are available, most of which use the soil particle size characteristics and compare them to the 95% opening size of the geotextile, defined as  $0_{95}$  of the geotextile. ASTM describes this design method as apparent opening size (AOS) and it is a dry-sieving method. In Europe and Canada, the test method is called filtration opening size (FOS) and it is accomplished by wet and hydrodynamic sieving, respectively. The simplest of the design methods examines the percentage of soil passing a No. 200 sieve, with openings of 0.075 mm. According to Task Force # 25, the following is recommended:

- For soil  $\leq 50$  % passing the No. 200 sieve:

$0_{95} < 0.60$  mm, that is, AOS of the fabric  $\geq$  No. 30 sieve

- For soil  $> 50$  % passing the No. 200 sieve:

$0_{95} < 0.30$  mm that is, AOS of the fabric  $\geq$  No. 50 sieve

Beginning in 1972, a series of direct comparisons of geotextile-opening size ( $0_{95}$ ,  $0_{50}$ , or  $0_{15}$ ) was made in ratio form to some soil particle size to be retained ( $d_{90}$ ,  $d_{85}$ ,  $d_{50}$ , or  $d_{15}$ ). The numeric value of the ratio depends upon the geotextile type, the soil type, the flow regime, and so on. For example, Carroll (1983) recommends the following:

$$0_{95} < (2 \text{ or } 3) d_{85}$$

where  $d_{85}$  is the soil particle size in mm, for which 85% of the total soil is finer.

### **Long-Term Flow Compatibility**

Long-Term Flow Compatibility is determined directly by taking a soil sample and the candidate geotextile(s) and testing them in the laboratory. Either gradient ratio (GR) test (Haliburton et al, 1982) to see that the  $GR \leq 3.0$ , long-term flow (LTF) tests (Raise et al, 1987) to see that the terminal slope of the flow rate versus time curve is adequate for site specific conditions, or a hydraulic conductivity ratio (HCR) test (Williams et al, 198) with resulting HCR values between 0.7 and 0.3 should be performed.

The soil-to-geotextile compatibility assumes the establishment of a set of mechanisms that are in equilibrium with the flow regime being imposed on the system. Koerner (1997) reported there exist a number of possibilities, including upstream soil-filter formation, blocking, arching, partial clogging, and depth filtration. These are shown schematically in Fig 2.22. With respect to how these mechanisms interact, it has been suggested that the geotextile serves as a catalyst to promote the upstream soil, and the now soil-modified geotextile, to generate its own internal filter system. Obviously, a number of phenomena are working together simultaneously, and just what mechanism dominates under what conditions of soil type, geotextile type and flow regime is still an issue that is being investigated. The ASTM standards for determining these design parameters are given in Appendix.

#### **2.2.4.2 Application of Geotextile/Geojute in Filtration**

Geotextile is normally used beneath stone base for paved & unpaved roads and airfields, beneath ballast under railroads. Geojute may be put beneath stone base for unpaved roads for short term. It may also be applied around crushed stone surrounding underdrains and without underdrains, around perforated pipe. Geojute may be put beneath landfills that generate leachate for long term. Both the materials may be used as a silt fence and silt curtain.

### 2.2.4.3 Designing for Filtration

The designs for filtration to follow cover most of the commonly encountered situations. The specific designs to be treated are the following:

- Geotextile filters behind retaining walls (Fig 2.23).
- Geotextile filters wrapped around underdrains (Fig 2.24).
- Geotextile filters used beneath erosion control structures (Fig 2.25)
- Geotextile filters used as silt fences (Fig 2.26)

In this section, Geotextile filters behind retaining walls are discussed and in Chapter Four a design example for this type of system is illustrated. For rest of the three systems, the methods are illustrated with figures.

In order to provide a flow path to allow water to escape from the backfill soil behind conventional reinforced-concrete retaining walls into an underdrain system, it is essential to have a vertical drainage layer typically consisting of granular soil, (Fig 2.23 a) or through weep holes system (Fig 2.23 b). In absence of this drainage layer, hydrostatic pressures will build up and, together with the horizontal soil pressure, could easily cause failure. Again, such hydrostatic pressures, if not dissipated by adequate drainage, can double the pressure against the wall. It must also be considered that the drainage sand must stay free-draining for the lifetime of the wall. If it excessively clogs with backfill soil within this time span, the sand becomes as useless as if it was not there at all. Thus it must be protected by a soil filter or by a geotextile filter. An identical situation, as far as the geotextile is concerned, is in the construction of flexible wall systems that are free-draining in themselves but would, without a soil filter or geotextile filter, allow the backfill soil to move into and through the open spaces. Such walls are illustrated in Fig 2.67c and Fig 2.67d in which the gabion style consists of wire baskets filled with 100 mm and larger stones. To backfill against such walls with no filter medium (soil or geotextile) would be a big mistake. Since the soil filter is difficult to place in a vertical or near-vertical manner and may even require a series of graded filter soils, the geotextile filter becomes very attractive. It is envisaged that geojute may be an eligible candidate material for this type of application. A filter design with geojute is illustrated in Chapter Four.

## **2.2.5 Drainage**

### **2.2.5.1 Definition**

The definition of geotextile drainage is the equilibrium soil-to-geotextile system that allows for an adequate liquid flow with limited soil loss within the plane of the geotextile over a service life-time compatible with the application under consideration. Geotextile drainage occurs in the in-plane direction rather than cross plane as can be seen in Fig 2.27.

### **2.2.5.2 Application of Geotextile/Geojute in Drainage**

Geotextiles may be put as a chimney drain and drainage gallery in an earth dam, as drainage interceptor for horizontal flow, drainage blanket beneath a surcharge fill. It may also be applied as a drain behind a retaining wall, beneath railroad ballast. Sometimes it may be put as a water drain beneath geomembranes and air drain beneath geomembrane.

Geojute may be applied as drainage blanket beneath a surcharge fill for short duration. It may also be applied as a drain behind a retaining wall, beneath railroad ballast for quite long duration.

### **2.2.5.3 Designing for Drainage**

Almost all the geotextiles possess some in-plane drainage capability. Nonwoven needle-punched variety is suitable because it can be made more than 5 mm thick in a cost effective manner. Considering flow capability of geotextile, mainly two general categories of design are being practiced. They are gravity flow and pressure flow. Gravity flow design method is applied in chimney drains and drainage galleries in earth and earth/rock dams pore water dissipaters behind retaining walls, flow interceptors (as in fin drains) beneath a geomembrane-lined reservoir for water drainage or gas conveyance. Pressure drainage design method is applied in vertical drains for rapid soil consolidation, within the soil backfill of reinforced earth walls, within earth embankments and dams, beneath surcharge fills.

The design methods of drainage are similar with filtration except for the direction of flow (in-plane rather than cross-plane). There are three aspects of design: adequate flow capacity, proper soil retention and long-term soil-to-geotextile flow equilibrium. The main design parameter is transmissivity of the geotextile,  $\theta$ .

$$\theta = k_p t$$

Where

$\theta$  = transmissivity

$k_p$  = in-plane geotextile permeability

$t$  = geotextile thickness

In gravity flow design (Fig 2.28) problems, the driving force is mainly the slope at which the geotextile is placd. Using the geometry of the particular situation under consideration, a required transmissivity is calculated by using Darcy's formula. This value is then compared to the allowable transmissivity of the candidate geotextile for calculation of a factor of safety. Depending on the severity of the situation, the factor of safety is determined.

In pressure drainage design method water will flow from locations of higher pressure to locations of lower pressure regardless of the geotextiles orientation. Here flow direction depends on each specific situation. The following equation is formulated for a geotextile placed beneath a surface fill on a fine-grained compressible foundation soil.

$$\theta_{reqd} = k_p t = (B^2 k_s) / (c_v T)^{1/2}$$

where,

$\theta_{reqd}$  = geotextile transmissivity

$k_p t$  = in-plane permeability coefficient of the geotextile

$t$  = thickness of the geotextile

$B$  = width of the surcharge layer

$k_s$  = permeability coefficient of the foundation soil

$c_v$  = vertical coefficient of consolidation of the foundation soil, and

$T$  = time for the surcharge fill to be placed

Fig 2.29 shows an application of pressure drainage design. The ASTM standards for determining these design parameters are given in Appendix.

### **2.2.6 Miscellaneous**

The geotextile may be designed for multiple functions in other applications also. In these cases, a single dominant (primary) function cannot always be identified. Thus, there are primary, secondary, tertiary, and perhaps even quaternary functions that may vary in a particular application. Furthermore, these functions might vary from site to site. Such multiple-function applications are the focus in this section. They should not be taken lightly or be considered of lesser importance than those discussed previously. Some of the major uses of geotextiles are included in this section on multiple-function applications.

#### **2.2.6.1 Reflective Crack Prevention in Bituminous Pavement Overlays**

The resurfacing of existing pavements having excessive cracks in them represents an ongoing and expensive task for the organizations that own and maintain roads (Fig 2.30). Such resurfacing is usually done with bituminous (asphaltic cement) overlays ranging in thickness from 25 to 100 mm. It becomes more irritating to the users and their automobiles when the cracks in the original pavement reflect up through the new overlay earlier than anticipated. To combat this, thicker overlays than desirable are used but at the cost of added expense, lower curb heights, and excessive weight and thickness on the sub-grade system. The use of geotextiles to remedy this has been attempted in a number of ways. In some instances, strips of geotextile have been placed over the crack, spanning it by 150 to 600 mm on each side, and the overlay placed above. Polyester, polypropylene, and fiberglass geotextiles, as well as geogrids, have all been used in this regard. By far the major use, however, has been to place full-width geotextile sheets over the entire pavement surface, which has been waterproofed with asphalt cement or asphalt emulsion, and then overlaid with the final bituminous surfacing. The goal of such a process is to either (a) decrease the

thickness of the overlay while keeping a lifetime equivalent to not using a geotextile, or (b) increase the lifetime of the overlay while using the same thickness as without the use of the geotextile.

A tremendous market has developed for this use, amounting to approximately 70 million m<sup>2</sup> in the U.S. in 1995 (Koerner, 1997). It is interesting to note that users in other countries are not nearly as involved in this application as those in the U.S. This is probably due to better ongoing road maintenance using conventional techniques than that generally practiced in the U.S., but this is not known to be a fact. Finally, it should be noted that this technique is used only for existing bituminous pavements, not for portland-cement concrete pavements. The significantly sharper edges of concrete would generally puncture and tear the lightweight geotextiles customarily used for this application.

#### **2.2.6.2 Railroad Application**

Geotextiles are often used in railroads beneath the stone ballast upon which the wooden or concrete tie system is placed. Here a critical aspect of the design is the depth at which the geotextile is placed beneath the bottom of the tie. It is virtually impossible to identify a unique primary function for geotextile use in railroad applications. Site-specific conditions will vary the primary function among a number of possibilities. Considering the different situations the possible geotextile functions may be the following: (Fig 2.31)

- Separation, in new railroads, between in situ soil and new ballast
- Separation, in rehabilitated railroads, between old contaminated ballast and new clean ballast
- Lateral confinement-type reinforcement in order to contain the overlying ballast stone
- Lateral drainage from water entering from above or below the geotextile within the geotextile
- Filtration of soil pore water rising up from the soil beneath the geotextile, due to rising water conditions or the dynamic pumping action of the individual wheel loads, across the plane of the geotextile

Irrespective of the difficulty of identifying a single function of the geotextile, the acceptance of geotextiles by railroad companies is large and increasing. Newby (1982) reports that as far back as 1882 the Southern Pacific Railroad used geotextiles in over 1600 km of trackage.

### **2.2.6.3 Horizontal Bags and Tubes (aka Geotubes)**

For hundreds of years the use of fabrics to make sandbags has been widely practiced. However, the use of UV-stabilized polymeric fibers has added new life into such installations. With controlled strength and deformation, the bags can be filled with sand, grout or even concrete and can be specially tuned to the particular application at hand. When used for erosion-control work, as they often are, a high-strength woven nylon geotextile sewn together with monochord polyester or Kevlar thread is often used. The bags are placed in a staggered pattern and weigh many tons when filled (Koerner, 1980). It may be noted that both vandalism and UV degradation must be considered when the bags are filled with sand.

### **2.2.6.4 Restoration of Piles (Pile Jacketing)**

All piles in a marine environment suffer deterioration at varying rates. Normal marine exposure, wet-dry cycles, freeze-thaw cycles, and chemical, industrial, and sanitary wastes cause the deterioration. Moreover, each type of pile has its own particular problems. The methods used for the rehabilitation of piles are varied and constantly increasing in number. The oldest technique is to use metal forms, such as corrugated steel in half sections joined together by angles attached to each of the half sections. Dockworkers and divers place, join, and seal the sections, which are used to contain cement grout, which bonds to the deteriorated pile section. This highly labor-intensive operation has led to the development of other, more economical techniques. Rigid plastic forms have been proposed as not only an economical form but as high-strength envelope to prevent further deterioration to the piling system. The annular space between the form and pile can be filled with either concrete grout or a specially formulated epoxy. Another pile-jacketing technique utilizes bituminized-fiber forms. However, all of these systems have a problem with bottom closure and sealing when



they are acting as a form and the pile is not to be jacketed down to the firm subsoils. In addition, complex configurations are all but impossible to form when using rigid enclosures. It should be noted that built-up layers of epoxy or bituminous coatings have also been utilized to protect pilings from deterioration; however, most of these techniques involve hand-placement by divers, and a thorough coating of the piles is difficult and expensive to obtain.

A technique was developed in the 1960s, which utilizes geotextiles as a concrete-forming system (Koerner, 1980). This concept uses as a concrete form a jacket of geotextile, the edges of which are connected by a heavy industrial zipper prefabricated into the geotextile. The ends of the geotextile above and below the deteriorated pile zone are banded to the pile. These flexible geotextile forms possess economic advantages over other concrete-forming systems because of their lightweight, ease of installation, adaptability to any configuration, relatively low cost, and ease of connection onto the piles at any location above the mudline. The geotextile is so designed that when concrete is injected into it, the excess water bleeds through the voids of the geotextile without allowing the cementitious portion to escape. This lowering of the water/cement ratio produces a dense surface of concrete that resists further deterioration of the pile.

#### **2.2.6.5 Bridge Pier Underpinning**

It is very difficult to analysis and design of estimating erosion of shallow foundation bridge piers in rivers and streams (National Academy of Engineering, 1970). Even for bridge piers founded on rock, the rock often deteriorates and is scoured away during floods that are accompanied by high-velocity water. The problem is so severe that divers sometimes find that they can swim beneath the bridge pier itself (Koerner, 1980).

The Ambursen Hydraulic Co. constructed a number of hollow-core, reinforced-concrete slab-and-buttress dams throughout the eastern and midwest U.S. from 1910 to 1940. The dams consisted of flat concrete slabs at 45°, which were supported by vertical buttresses at 3.0 to 4.5 m. Both the slabs and buttresses were relatively thin (e.g., 300 to 600 mm of reinforced concrete). Today, many of these water

reservoir dams are in need of repair, particularly at their buttress footing regions where compressive stresses are the highest.

Using fabrics as flexible forms, some very clever solutions to these difficult problems have been developed. A solution used by Welsh (1977) shown in Fig 2.32 for a number of scoured bridge piers. A geotextile tube is prefabricated to fit around the perimeter of the pier between the top of the stable foundation material and the bottom of the pier foundation. As grout inflation of the geotextile proceeds, pipes are placed to communicate from the outside of the pier to within the enclosure. After the curing of the perimeter tube, an injection of high-strength grout into the inside of the perimeter tube reestablishes the bearing capacity of the pier foundation.

#### **2.2.6.6 Uniform Pressure Distribution beneath Caissons**

When placing prefabricated caissons on uneven bearing strata, stress concentrations can be excessively high. Typically, this occurs in areas where uneven rock is encountered. Use of geotextiles as a form into which high-strength cement grout is placed test case by den Hoedt and Mouw (1978) nicely illustrate (Fig 2.33); Here a prefabricated high-strength geotextile was placed type model concrete caisson and was pumped with grout lifted off the rock foundation and was seen to have the surface. The full-scale project was constructed in a similar

#### **2.2.6.7 Erosion-Control Mattresses**

By taking two sheets of geotextile and joining them at discrete points, a form will result that can be pumped with grout to form a mattress that will conform to essentially any subsoil condition. Internal spacer threads woven into the upper and lower sheets of geotextile control the thickness and geometry. Thicknesses of up to 500 mm have been made with various configurations. Shown in Fig 2.34 are two common styles: a uniform cross-section surface and an undulating surface where filter points are constructed at uniform spacings. These filter points serve to dissipate pore-water pressure trying to escape from the subsoil. They are available in varying

diameters and spacings but are limited in their ability to control large amounts of subsoil seepage.

### 2.3 Jute Fibre

Jute is one of the world's most important long vegetable fibre, being exceeded in quantity only by cotton. It is a bast fibre obtained from the stalks of the dicotyledenous plants that belong to the genus *Corchorus* and the order Tiliaceae. It is collected mainly from two commercially important species, namely, White Jute (*Corchorus capsularis*) and Tossa Jute (*Corchorus olitorius*). The Jute is thought to have originated from Eastern and Southern Africa in prehistoric times. Before traditional industrial use it was used for ropes, twines and 'patta', indigenous cloth locally made from jute, by hand spinning and weaving. These fabrics were used by farmers as apparel or medical value particularly for rheumatism. Leaves and roots of Jute plants were also used as vegetable and medicine in certain areas of Bangladesh and India. It was first used as an industrial raw material for making packaging materials as a replacement for European - grown flax and hemp. Both *capsularis* and *olitorius* are annual plants and similar in general appearance. They have major difference in stem colour, leaf structure, seed pod structure, flower and taste. The plant grows from 152.40 to 406.40 cms. In height and the stalk is from 1.27 to 1.95 cms in diameter.

A temperate, wet and humid climate with alluvial soil structure is conducive for the growth of jute. Jute is a photo-reactive plant and for that long hours of day light are necessary for its rapid growth.

Generally, sowing time starts at the end of February and continues up to the end of May, as there are difference in the sowing time for different varieties and species. After approximately 4 months, harvesting starts. The open network of fibre strands from each plant is extracted by ripping scutching, retting and hackling. Among other processes, retting is one of the most important steps upon which the fibre quality depends to a great extent. In retting, jute plants are exposed to a complex microbiological action for a definite time, preferably in clean slow moving water, during which the fibre bundles are separated from the woody stem, and then washed

and dried and are ready for marketing . If retting is not properly done, hardy, barky, inferior fibrous material is produced and are called "cuttings". Jute stick is another parts of Jute plant that is obtained after retting it has similar composition to that of jute fibre but in different proportion. Jute sticks are one of the main fuels for rural people of Bangladesh. It is also used as fancy and other agronomic, homestead and industrial uses.

Though Bangladesh and India are the leading producers of jute, it is also grown in Nepal, China, Thailand, Indonesia, Burma, Brazil, Vietnam, Taiwan, Cambodia and in some countries of Africa.

### **2.3.1 Physical Structure of Jute**

The stem of the jute plant consist of ring vascular bundles, made up of three distinct regions viz xylem (the innermost woody tissue), the cambium and the phloem, which contains seive tubes, companion cells and bast fibres. Cortex tissue and a layer of epidermal cells (Fig 2.35) surround the vascular bundles.

The lignin component is believed to be located partly in the middle lamella but the maximum lignin (70-80%) is located in secondary as well as primary walls. The primary wall is considered to be the outer sheath of cell wall which is laid down during the period of active elongation of the cell and more fatty materials are found in this layer. The secondary wall is that part which is subsequently deposited on the inside of the primary wall and responsible for the fibre properties of jute. In jute, microfibrils exhibit spiral orientation (angle  $8.1^\circ$ ) round the fibre axis in the Z-form (left to right) in contrast to other bast fibres.

### **2.3.2 Physical Properties of Jute**

Physically jute consists of fibre bundles arranged in several layers between the central hollow woody core and the outer skin. The fibre bundles are associated in wedge shaped groups, the bases of the wedge being towards the core. The fibre bundles branches are united and thus a mesh-work is produced.

Each bundle in the wedges consists of cells or ultimate fibres which are joined together by natural cement. The ultimate fibres are widest at the middle and taper to each end. The diameters of the ultimate fibres are approximately 254  $\mu$  (micron) at the widest part and approximately 15  $\mu$  (micron) at the ends. The length varies between 35-25 mm. Though the ultimate fibres are so short, jute fibres appear to be much longer as the ultimate fibres are joined in a matrix of gummy material. In cross-section (Fig 2.36) the ultimate fibres are more or less polygonal with sharp angles. The lumen or central canal is wide, round or oval in cross-section. The lumen shows constrictions of irregular thickness of cell-wall longitudinally. Towards the end of the fibre, the lumen widens, causing the cell-wall to become thin. Externally, the fibre is smooth and without any transverse markings (joints or nodes).

Each ultimate fibre is composed of a large number of smaller units known as fibrils and these are arranged in right-handed spirals. The fibrils are again made up of molecular chains, closely held together. These are known as micelles. Jute fibre again consists of crystalline, paracrystalline and noncrystalline or amorphous regions. The crystalline part is mostly filled with cellulose whereas; hemicellulose and lignin are present in noncrystalline and para-crystalline parts.

Fibres are found as a secondary growth from the Cambium in contrast to other bast fibres such as flax which are formed directly from primary tissue. Commercial jute fibres consists of strands i.e bast bundles of short individual fibres with ends overlapping so as to produce continuous filaments throughout the length of stalk. As distinct from ultimate fibre this is a net-work built-up of thin polygonal cells. The size of these cells vary widely both in width and length.

The individual fibres are held together by non-cellulosic materials such as lignin, hemicellulose, pectin etc. to form fibre strand. The cell wall of woody material (Fig 2.37) is built up of several layers known as middle lamella (M), primary wall (P), outer layer of the secondary wall (S1), middle layer of the secondary wall (S2), inner layer of the secondary wall (S3) and the lumen (W). The middle lamella is located between the cells and serves the function of binding the cells together. Non-cellulosic constituents in jute especially lignin and hemicellulose are abundant in this region.

The characters usually regarded as constituting jute's quality are color, luster, strength, cleanliness, flexibility, length, proportion of roots and moisture content. A good quality jute fibre should possess good colour. This should be lustrous as more lustrous jute is found to be stronger. The ballistic work of rupture also increases while the carding resistance decreases with the increase in lustre of the fibre. An Indian variety of jute known as "Shamla Daisee" although darkish blue in color is well-known for its high strength, luster and fineness. The fibre should be fine, long and strong. The body of the fibre should be clean. The percentage of roots should be low. Faults, i.e. knots, sticks, specks etc. should not be present. The fibre should be capable of being spun into fine yarns. The moisture content of the fibre must not exceed the standard limit. Important physical properties of jute fibre are listed in Table: 2.2.

A jute fibre is considered to be of good quality when yarns spun having:

- Quality ratio (Q.R) above 90 and
- A low coefficient of variance (C.V)
- Fibre possesses high elasticity and low frictional properties.

Q.R. indicates the strength of the yarns, being expressed as the ratio of breaking strength in lb to the grist of yarn in lb/spindle of 14,400 yards, multiplied by 100. C.V. indicates the irregularity in the weight per unit in a short length of the yarn. Q.R. above 90 and weight C.V. % below 23 indicated fibre of good quality. Q.R. above 80 and C.V. % below 25 indicates fibre of medium quality. Q.R. below 80 and C.V.% above 25 means fibre of poor quality.

### **2.3.3 Chemical Composition of Jute fibre**

Jute is a lignocellulosic fibre composed of cellulose (58-63%), hemicellulose (21-22%), lignin (12-14%), protein (0.8-1.5%), pectin (0.2-0.5%) fat and wax (0.4-0.8%), mineral matter (0.6-1.2%) and traces of tannin and coloring matter. Except for cellulose, all the other components are functioning more or less as cementing materials. In fact, the structure of jute fibre is built up by the three dimensional polymerization of cellulose, hemicellulose and lignin. Stiffness and lower wet strength of jute fibre are closely related to this reinforced resinous structure. It is also

observed that the individual fibres have greater strength and extensibility than the composite fibres.

The physico-chemical properties of jute fibre are predominantly reflected by this complex and peculiar three dimensional structure along with the resultant properties of the individual components like cellulose, hemicellulose and lignin. This clearly indicates that jute fibres although being considered as important natural textile fibres are more woody in nature with a higher lignin content compared with other almost pure cellulosic fibres like cotton. And obviously the chemical reactivity of jute is more akin to wood than it is other textile fibres.

### 2.3.3.1 Cellulose

It has been observed that the molecular weight, fibre length and degree of polymerization of jute cellulose are comparatively smaller than those of cotton. Again jute fibre consists of crystalline, para-crystalline and non-crystalline, amorphous region. Cellulose is the major portion within the crystalline part of jute fibre. The higher moisture regain property of jute fibre compared to most of the other fibres is attributable to these special characteristics of jute fibre.

Chemical composition of cellulose which is the principal structural unit of all cellulosic fibres is identified with that of cotton, comprising of a chain of condensed 1, 4-glucose anhydride residues. Cellulose isolated from jute cannot be distinguished from cotton cellulose by chemical means, but difference in physical properties has been observed. The chain length of cellulose differs from fibre to fibre and cellulose obtained from jute has been found to be much shorter in chain length than cotton cellulose. Jute cellulose, like cotton cellulose gives all the cellulosic reactions with acid, alkali, oxidizing and reducing agents. All cellulose derivatives can be prepared from jute cellulose and can be dissolved in cuprammonium and similar complex solutions.

### 2.3.3.2 Hemicellulose

Although cellulose form the main structural component of jute, the noncellulosic constituents also play an important role in determining its characteristic properties. Jute hemicellulose (21-24%) is divided into two types. (i) Those which are intimately associated with cellulose and (ii) those that are not associated with cellulose. Former group of jute hemicellulose mainly consists of xylan and designated as cellulosan. The second type of hemicellulose again can be divided into two groups, the polyoses which do not contain ureic acid residues and the polyuronide hemicellulose which are composed of ureic acids. Galactose, fructose, glucose, and arabinose etc. are the sugars that have been identified in polyoses in jute. The hemicellulose units of jute are fairly simple and of low molecular weight and susceptible to the action of alkali. They are soluble in dilute alkali and also to some extent in boiling water. Pentosans and hexosans are present in the fibre almost in equal proportions; the latter, however, are the more difficult to dissolve in alkali solutions, even after delignification.

### 2.3.3.3 Lignin

Lignin is the single most important component in jute which is in fact distinguished it from other textile fibre. Some of the peculiar characteristics of the fibre such as yellowing or photo degradation are attributed to its presence. Lignin does not represent one uniform compound but rather is composed of highly polymerized molecules of phenyl propane compound like (i) P-country 1 alcohol (ii) Coniferyl alcohol and (iii) Sinapy alcohol.

The molecular weight of lignin varies from 300 to 140,000 depending on the sources and method of estimation. Regardless of structural uncertainty lignin contains methoxyl, phenolic, hydroxyl groups, ether groups, conjugated carbonyls and double bonded groups. Again carbonyl groups ether groups, methoxyl groups, phenolic hydroxyl groups and conjugated double bonds a -position to benzene rings in lignin structure attribute major chemical properties to jute fibre.



Jute is acidic in nature and its acidity is due to the presence of phenolic hydroxyl groups presents in lignin. There is an ester linkage between phenolic hydroxyl groups in lignin and uronic acid present in jute hemi-cellulose. There is great deal of controversy on the type of chemical bonds that might be present between lignin and polysaccharides in woody material. Many studies have indicated that covalent linkage must exist between lignin and cellulose probably with hemicellulose through glucosidic linkage. In fact physico-chemical properties of jute are the resultant accumulation of all the properties of its constituents.

The contribution of cementing materials (i.e. lignin and hemicellulose) on the tensile properties of jute fibre both in dry and wet conditions is enormous. It has been observed that when jute is treated with the chemical reagents employed in textile pretreatments and bleaching processes, lignin, hemi-cellulose and other encrusting substances are attacked and to some extent removed. The greater the extent of this removal the more the strength of the jute fibre is diminished, particularly when the material is treated in the wet state. This is supposed to be due to breakage of hydrogen bonds.

The photo degradation of textile and polymeric compounds is a long observed phenomenon. This results from a complex sequence of chemical reactions initiated by ultra-violet and visible radiations emitted by the sun. Lignin gives a characteristics ultra-violet absorption spectrum and colour reaction with phenols and aromatic amines. The carbonyl groups and conjugated double bonds to benzene rings in jute lignin are capable of absorbing U.V. radiation present in sunlight and consequently play a vital role in the degradation of jute fibre. It not only causes yellowing of natural and bleached jute fibre but is also associated with colour fading of dyed and printed jute products. This photo-chemically yellowing of jute fibres is also accompanied by strength loss. Again, in common with many other textile fibres, jute is degraded by heat, mildew acids and alkali. Jute burns like other cellulosic fibres but its flammability can be reduced by chemical treatment. Again flavon type of compounds present in jute fibre and iron complexes that are formed at the time of retting are considered as the sources for the natural colour of jute fibre.

**Table: 2.1: Important Physical Properties of Jute Fibre**

1.	Jute cell/ultimate width (Range)	15-204m
2.	Jute cell /ultimate length (Range)	1-6 mm
3.	Jute cell/ultimate width (Average)	184m
4.	Jute cell/ultimate length (Average)	2.5mm
5.	Tenacity	2.7-5.3 g/tex
6.	Specific gravity	1.48
7.	Moisture Regain at 65RH/22° C	13.8%
8.	Fineness (gm/1000m)	1.4-1.65 tex
9.	Breaking elongation	0.8-1.8%
10.	Refractive Index (Parallel)	1.577
11.	Refractive Index (Perpendicular)	1.536
12.	Fluorescence with Corning filter	Bluish white
13.	Phosphorescence	Yellow
14.	Phosphorescence (time)	15 sec
15.	Swelling in water (diameter)	20-21%
16.	Swelling in water (area)	40%
17.	Stiffness (average)	185
18.	Specific heat	0.324 cal/g° C
19.	Water retention	70%
20.	Young's Modulus:	
	a) White	0.86-1.74 (dynes/cm <sup>2</sup> x1000)
	b) Tossa	0.96-1.94 (dynes/cm <sup>2</sup> x1000)
21.	Modulus of Rigidity	
	a) White	(dynes/cm <sup>2</sup> x109)
	b) Tossa	4.42
22.	Linear density	0.94-2.94 tex
23.	Density	1.52-1.59

### 2.3.4 Factors Influencing the Quality of Jute

The factors influencing the quality of jute may be divided into two classes:

- i) Non-controllable factors
- ii) Controllable factors

The non-controllable factors are locality, soil, climate and retting water

High lands often produce fibre of superior quality and low-lying lands generally produce common and low grade fibre. Loamy soil usually produces superior grades while sandy soil often produces coarse fibre. The quality of fibre is affected by excessive and continuous rainfall and heavy floods. These adverse weather conditions often develop a hard periderm on the fibre which is resistant to retting. Retting water is the most important factors influencing the colour and strength of the jute fibre. Retting in muddy water produces fibre of poor colour and luster. Retting in clean slow running water yields the best fibre. Hence the fibre of the Brahmaputra area is usually strong fine, lustrous and white. In those areas where water for retting is plentiful, the fibre is clean and of good colour and luster. Where water for retting is not sufficient, the fibre is usually of dark colour and is often rooty, specky and croppy. The controllable factors influencing the quality of jute include are seed manuring, method of sowing, inter culture, stage of harvest, pests and diseases, retting process and method of extraction of fibre.

Improved strains of seeds produce better quality fibre. Early varieties also produce better fibre. Faster retting produces better fibre and retting of early varieties is weaker, as this is done in the hotter, earlier months. Judicious manuring produces fibre of superior quality. Ununiformity of crop means ununiformity in fibre quality. Weeding and thinning operations are very important as insufficient and untimely weeding and thinning adversely affect the quality of fibre. Harvesting at the pod stage gives the best combination of yield and quality. Harvesting beyond this stage increases the yield but affect the quality. Jute plants affected by pests and diseases produce fibre of inferior quality. These pests and diseases may be controlled by applying insecticides and fungicides. Careful stepping and retting, improve fibre quality. If the retting technique is not correct, faulty fibre is produced. Improper steeping produces croppy and barky jute. Under-retting and uneven retting produces

rooty and specky fibre. Over-retting produces degraded fibre. Single-plant-wise extraction produces better fibre than the bundle-wise extraction.

### 2.3.5 Treatment of Jute

Jute is a biodegradable, photodegradable, thermal degradable, high modulus, less extensible, hygroscopic, coarse fibre. Obviously it has traditionally been used as a raw material for the production of packaging materials. However its versatility is only coming to light now as the world looks on for this natural fibre to take over with the ideal solutions for the modern world. Be it in conserving the soil and the environment or in geotechnical engineering applications. Lately jute and jute products as woven, non-woven, netted, open structure fabrics are being used for different geo-textile materials. In tropical, humid, rainfed and frequently flood affected countries like Bangladesh quick biodegradability of jute is a disadvantage for its use in geotechnical application. To overcome this disadvantage numerous study/research works have been performed by different researchers, organizations and institutions for last few years. Recently a wide range of geojute has been developed in the laboratory of Bangladesh Jute Research Institute (BJRI) by blending jute with hydrophobic fibre like coir or by modification with bitumen, latex and wax resinous materials with the collaboration of Bangladesh Jute Mills Corporation (BJMC). A summary of Jute blended with different materials is shown in Table 2.2. These blending are of different types:

- Jute with natural fibre i.e. jute with cotton, coir, flax etc
- Jute with synthetic fibre like jute blended with polythene, polypropylene, nylon, polyester, polyacrylic etc
- Modification/Treatment of jute with bitumen, latex, wax, resinous material

#### 2.3.5.1 Jute Blended with Cotton/Union Products:

Blending jute with natural fibre like cotton for making furnished and apparel products is a common technology where jute is modified with chemical and softening agents and then cut down into staple length which are then mixed and processed in

cotton system for making yarn and consequently fabrics. On the other hand union fabrics of jute cotton mixture are made by inserting warp and weft thread with different fibres. Both blended and union fabrics are used according to their needs and purposes. For making geotextile materials generally low quality cotton are used in blending and union fabrics. Moreover non-woven materials are also produced with these products. These products further treated with various chemicals, resin, and polymers for improving their strength, duration and other desired properties.

### **2.3.5.2 Jute Blended with Coir/Union Products:**

i) Jute cuttings, low grade jute (SMR) and coir were treated separately with a composite of urea, molasses and wetting agents and all the fibres were then batched passed through teaser card, breaker card and 3 different sliver rolls were made.

ii) Above slivers rolls were then fed to jute finisher card in a ratio of 70:10:20, homogenous mixed sliver from the finisher card passed through the 1st and 2nd finisher drawing and blended yarn of 33.25 lbs/spy yarn was spun through sacking spinning frame of jute. Properties of this jute coir blended yarn are given follows:

- a) Count 23.25 lbs/spy
- b) Tensile strength 1.7 lbs.
- c) Standard deviation 4.25
- d) Co-efficient of variation of strength 24.94%
- e) Quality ratio 51.25%
- f) Twist/inch 2.08
- g) Less hygroscopic/more hydrophobic.
- h) More resistance to water.

### **2.3.5.3 Jute Blended with Synthetics Fabrics**

Blending of jute with synthetic fibres like acryline, polyethylene, polypropylene, polyester and rayon are made by various investigators. Ramaswamy and Aziz ((1989), Mandal and Murti (1990), Karrunaratne et al (1992) attempted to evaluate physical, mechanical and hydraulic properties of natural jute with the

attention being concentrated on retarding the degradation of natural fibres from micro biological attack. Compatibility of two different fibers is the most important properties on which blending of dissimilar fibers are primarily needed. Consequently modification of fibers is necessary for increasing their compatibility through chemical, bio-chemical or mechanical treatment. Sometimes specific machine modification is also necessary. Some blend of jute/rayon, jute/polyester and jute/acrylic of the following proportion: 50:50, 60:40, 65:35, 70:30, 80:20 were made respectively. Rao et al (1994) took six nonwoven jute based geotextiles consisting of varying proportions jute and polypropylene fibres and evaluated for their engineering properties by ASTM/BIS standards. Summary of tests carried on each fabric and the standard adopted is given in Table 2.3.

**Table 2.2 Summary of Jute Blended with Different Materials at BJRI**

Type	Composition	Possible Durability	Biodegradability	Moisture Content	Wt./Unit (gm)	Tensile Strength (lb)
Woven Jute in different structure	Jute	2-6 month	Quick	12-14%	220-800	120-140
Woven Jute in different structure	Jute, Coir	5-12 month	Slow	7-10%	220-800	240-660
Woven Jute but treated composite	Jute Bitumen Carbon	6-48 Month	Long run	3-8%	Var. Wt.	140-700
Non woven	Jute blanket	6-18 month	Slow	8-12%	800	300-800
Woven with different construction	Jute latex	5-20 year	Long run	5-7%	≥ 800	300-800
Non woven	Jute Blanket +Latex	5-20 year	Long run	5-7%	≥ 800	≥ 800

**Table 2.3 Summary of Test Results Conducted by Rao et al**

Properties	Jute based geotextile types					
	JGT1	JGT2	JGT3	JGT4	JGT5	JGT6
<b>Physical properties</b>						
Material Composition	25% J+ 75% PP	50% J+ 50% PP	75% J+ 25% PP	75% J+ 25% PP	75% J+ 25% PP	75% J+ 25% PP
Role idth , length (m)	05, 10	05, 10	05, 10	05, 10	05, 10	05, 10
Weight (gsm)	282	270	272	220	353	500
Thickness (mm)	2.6	3.8	2.1	2.6	4.3	4.9
<b>Mechanical properties</b>						
Tensile Strength (kn/m)	6.7	2.65	8.43	0.25	2.65	4.2
Percentage Elongation at maximum load (%)	21.6	98.7	29	83	89	95.8
<b>Survivability Properties</b>						
Puncture resistance Falling Cone Method (mm)	9.5	2.0	9.5	1.0	0.5	0.5
Elongation (mm)	-	70	-	100	60	60
CBR resistance (kN)	1.54	0.42	1.92	0.07	0.24	1.49
CBR Elongation (mm)	48	92	42	68	80	60
Index Puncture (kN)	0.34	0.18	0.45	0.036	0.13	0.50
Index Elongation (mm)	14	28	14	29	31	22
<b>Hydraulic Properties</b>						
Permittivity (mm/sec)	0.1	2.59	0.03	1.8	3.9	2.0

After Rao et al (1994)

Based on the results presented above summarized in Table 2.3, Rao et al attempted to categorize the jute based geotextiles fabrics as to their suitability for various geotechnical functions presented in Table 2.4.

**Table 2.4 Categorization of Jute Based Geotextiles**

Fabric Type	Typical function			
	Separation	Filtration	Drainage	Reinforcement
JGT 1	Y	Y	Y	Y
JGT 2	Y	Y	Y	N
JGT 3	Y	Y	N	Y
JGT 4	N	Y	Y	N
JGT 5	Y	Y	Y	N
JGT 6	Y	Y	Y	Y

Y: can be used; N: cannot be used

### 2.3.5.4 Jute Blended and Treated with Different Chemicals

#### a) Jute Treated with Bitumen

Carbon black to be prepared with required quantity of volatile oil and then bitumen emulsion to be added with paste and stirred. After mixing homogenously, the emulsion to be laminated on the jute fabrics by brush manually and dried in sunlight or open area at normal temperature and pressure (NTP). Jute, Canvas and DW Twill samples were treated applying this method at BJRI laboratory. These three types of samples were tested for this study.

#### b) Jute Treated with Silicate of Specific Viscosity

Silicate solution is prepared by adding hot water and stirred according to need and then used on the modified bitumen treated samples manually and dried at NTP.

#### c) Jute Treated with Ca-based Grease Composite

Ca-based grease is added with required amount of carbon black and a paste is prepared by adding volatile oil. The composite paste is then rubbed haphazardly by hand on the jute fabrics and finally rubbing is completed by brush. Once the rubbing is completed, a small amount of carbon black is sprayed over the located area or full sample, and then again, paste is rubbed by brush.

#### d) Jute Treated with Sodium Carbonate

Sodium Carbonate and Sulphate of Copper is mixed with water and sprayed manually over jute fabrics. The treated fabrics to be dried on sunlight at NTP.

e) Jute covered (sandwiched) with polypropylene.

f) Jute blended with 3% polypropylene and then thermally bonded.

g) Jute treated with 15% acrylic emulsion.

h) Jute blended with 3% polypropylene.

i) Jute treated with 15% urea formaldehyde.



Non-woven jute fabric weight  $350 \text{ g/m}^2$  treated with different chemicals were tested as regard to their resistance to microbial attack as well as strength and their geotechnical properties like tensile strength, thickness, bursting, punched, CBR, water permeability, and pore size distribution. The results are shown in the Tables: 2.5, 2.6, 2.7, 2.8, 2.9, 2.10 and 2.11.

**Table 2.5: Thickness and Linear Density of Some Modified Fabrics**

Sample	Thickness (mm)	Linear Density ( $\text{g/m}^2$ )
Untreated	3.05	350.93
Binder+Copper nepthenate	2.85	455.50
Binder+ CCA	2.90	437.25
Coal Pitch Anthraescene oil	2.75	787.50

CCA: Copper Chromium Arsenic

**Table 2.6: Tensile Strength (kN/m) of Some Treated and Blended Fabrics**

Sample Code	0 days		15 days		30 days		45 days	
	MD	XMD	MD	XMD	MD	XMD	MD	XMD
UJ <sub>1</sub>	0.82	1.62	0.65	1.25	0.36	0.82	-	-
UJ <sub>2</sub>	0.95	1.75	0.46	0.95	0.32	0.66	-	-
UJ <sub>3</sub>	0.72	1.07	0.35	0.80	0.25	0.62	-	-
PCN <sub>1</sub>	4.56	8.56	4.14	7.07	3.57	6.21	2.93	6.21
PCN <sub>2</sub>	4.25	8.32	3.82	8.00	2.57	7.07	2.26	6.27
PCN <sub>3</sub>	4.02	8.12	3.76	7.85	2.19	7.12	1.82	6.02
HCCA <sub>1</sub>	9.65	16.24	8.13	16.07	5.62	10.27	4.85	9.92
HCCA <sub>2</sub>	8.25	12.93	7.95	11.75	6.29	9.92	5.20	8.77
HCCA <sub>3</sub>	8.12	13.63	7.78	11.20	6.78	10.29	5.51	8.20
CA <sub>1</sub>	20.15	32.62	20.09	32.52	20.16	32.53	20.12	32.50
CA <sub>2</sub>	19.17	32.12	19.18	32.08	19.07	32.05	18.27	32.07
CA <sub>3</sub>	19.86	31.25	19.57	31.02	19.26	31.09	19.09	31.07

**Table 2.7: Bursting Strength (kN/m<sup>2</sup>) of Some Treated Fabrics**

Sample code	0 days	15 days	30 days	45 days
UJ <sub>1</sub>	245.0	150.0	90.1	-
UJ <sub>2</sub>	225.4	160.7	89.2	-
UJ <sub>3</sub>	205.8	140.6	50.7	-
PCN <sub>1</sub>	313.6	265.6	190.2	100.1
PCN <sub>2</sub>	303.8	260.6	185.7	101.2
PCN <sub>3</sub>	300.0	254.5	175.6	98.3
HCCA <sub>1</sub>	340.8	280.7	262.9	180.7
HCCA <sub>2</sub>	340.2	275.6	261.2	120.7
HCCA <sub>3</sub>	335.2	269.3	259.2	111.7
CA <sub>1</sub>	280.8	269.8	265.7	270.9
CA <sub>2</sub>	275.2	270.6	272.6	270.0
CA <sub>3</sub>	260.7	255.8	250.2	260.0

**Table 2.8: Puncture Test (diameter in mm)**

Sample code	0 days	15 days	30 days	45 days
UJ <sub>1</sub>	-	-	-	-
UJ <sub>2</sub>	-	-	-	-
UJ <sub>3</sub>	-	-	-	-
PCN <sub>1</sub>	32	38	45	-
PCN <sub>2</sub>	38	40	48	-
PCN <sub>3</sub>	36	39	45	-
HCCA <sub>1</sub>	23	29	35	42
HCCA <sub>2</sub>	23	29	32	43
HCCA <sub>3</sub>	23	28	36	45
CA <sub>1</sub>	19	20	22	25
CA <sub>2</sub>	20	21	25	28
CA <sub>3</sub>	22	22	25	30

**Table 2.9: CBR Test Results of Some Fabrics**

Sample Code	Plunger Penetration (mm)	with GT (C <sub>1</sub> )	without GT (C <sub>2</sub> )	(C <sub>1</sub> /C <sub>2</sub> )
UJ <sub>1</sub>	2.5	6.15	6.27	0.98
	5.0	7.24	7.99	0.90
	7.5	7.36	7.82	0.94
PCN <sub>1</sub>	2.5	7.52	7.24	1.20
	5.0	7.76	6.79	1.14
	7.5	7.24	5.75	1.26
HCCA <sub>1</sub>	2.5	6.58	6.14	1.10
	5.0	9.56	7.54	1.27
	7.5	6.62	6.28	1.37
CA <sub>1</sub>	2.5	8.92	6.69	1.30
	5.0	11.37	7.79	1.43
	7.5	12.48	7.81	1.60

**Table 2.10: Water Permeability (lit/m<sup>2</sup>/sec) of Some Treated Fabrics**

Sample code	0	15 days	30 days	45 days
UJ <sub>1</sub>	94.3	100.7	120.7	-
UJ <sub>2</sub>	90.3	124.6	130.2	-
UJ <sub>3</sub>	92.1	120.7	130.6	-
PCN <sub>1</sub>	47.2	52.6	52.7	60.2
PCN <sub>2</sub>	46.2	53.7	55.6	65.6
PCN <sub>3</sub>	48.9	54.9	57.9	65.7
HCCA <sub>1</sub>	21.2	26.7	30.1	42.4
HCCA <sub>2</sub>	20.2	27.8	33.9	42.4
HCCA <sub>3</sub>	21.5	26.9	32.6	45.6
CA <sub>1</sub>	4.24	4.34	4.52	3.36
CA <sub>2</sub>	4.30	4.60	4.70	4.80
CA <sub>3</sub>	4.30	4.52	4.56	4.67

**Table 2.11: Pore Size, O<sub>95</sub> (micron) of Some Treated Fabrics**

Sample code	0 days	15 days	30 days	45 days
UJ <sub>1</sub>	41	72	-	-
UJ <sub>2</sub>	44	74	-	-
UJ <sub>3</sub>	45	76	-	-
PCN <sub>1</sub>	36	45	68	-
PCN <sub>2</sub>	39	47	70	-
PCN <sub>3</sub>	40	49	72	-
HCCA <sub>1</sub>	33	37	61	77
HCCA <sub>2</sub>	34	38	62	78
HCCA <sub>3</sub>	35	39	64	80

UJ = Untreated Jute fabric

PCN<sub>j</sub> = Acrylic binder + Copper naphthenate

HCCA<sub>j</sub> = Acrylic binder + Copper Chromium Arsenic (CCA)

CA<sub>j</sub> = Coal pitch + Anthracene oil

NDP = Needles Penetration Depth

It is observed that untreated jute fabrics are susceptible to microbial attract and undergo degradation in properties during accelerated soil burial test. Untreated jute non woven fabrics do not withstand punctured resistance. On the other hand, copper naphthenate plus acrylic and CCA+Acrylic binder treated fabrics give better performance then that of untreated fabric for same duration. These fabrics can be used as filter and separator. Most promising results are obtained from jute fabrics treated with coal tar and Anthracene oil.

Jute Geotextiles undergo designed biodegradation in soil; the decomposition of fibres takes place within ecological cycle, climatic conditions and soil properties. A few types of jute geotextiles treated with various chemical compositions designated by treatment I, treatment - II, Treatment - III, Treatment - IV respectively and then tested their biodegradability, durability, moisture holding capacity in a standard laboratory test. Results of above treated geotextiles are shown in the Table: 2.12.

**Table 2.12: Biodegradability, Durability and Moisture Holding Capacity of Treated and Untreated Jute**

Type of product	Biodegradability		Durability	Moisture holding capacity
	Time in month	Weight loss (%)	Time in year	
Light weight Hessian	3	30	0.25-0.80	(%)
Treatment I	12	15	0.50-1.25	9-10
Treatment II	12	10	2.0-5	6-8
Treatment III	12	5	>10	5.6
Treatment IV	12	1-3	>20	3-4

#### 2.4 Summary

1. All polymer based materials as well as natural products; fiberglass and rubber, which can be used in geotechnical engineering, comprise geosynthetics family. A geotextile is defined as any permeable textile material used with foundation, soil, rock, earth, or any other geotechnical engineering related material as an integral part of a man made project, structure, or system. It is divided into woven, non-woven and knitted groups based on the general manufacturing process.

2. Geotextile function refers to the specific role played by a geotextile in a soil/geotextile structure. It may perform more than one function at a time in a given application. Koerner (1997) describes, the major functions of geotextiles are separation, filtration, drainage, reinforcement and containment (if geotextile is suitably impregnated).

3. Separation is the process of preventing two dissimilar materials from mixing. In this function, a geotextile is most often required to prevent the undesirable mixing of fill and natural soils or two different types of fills so that the integrity and functioning of both materials can remain intact or be improved.

4. Geotextile can be placed between a railroad subgrade and track ballast to prevent contamination and resulting strength loss of the ballast by intrusion of the subgrade soil. In construction of roads over soft soil, a geotextile can be placed over the soft subgrade, and then gravel or crushed stone placed on the geotextile. The geojute may also be put in these applications where geotextile have already been successfully used. Since the geotextile serves to prevent aggregate from penetrating the subgrade, it must meet puncture, burst, grab and tear strengths.

5. Reinforcement with geotextiles as described by Koerner (1997) as the synergistic improvement of a total system's strength created by the introduction of a geotextile (that is good in tension) into a soil (that is good in compression but poor in tension) or into other disjointed and separated material. In the most common reinforcement application, the geotextile interacts with soil through frictional or adhesion forces to resist tensile or shear forces. To provide reinforcement, a geotextile must have sufficient strength and embedment length to resist the tensile forces generated, and the strength must be developed at sufficiently small strains (i.e. high modulus) to prevent excessive movement of the reinforced structure.

6. The combined use of soil and a geotextile suggests a number of situations in which geotextile may be used to construct fabric-reinforced walls, reinforced embankments, to stabilize slopes temporarily or permanently. Geojute may also be used to construct short term fabric reinforced earth walls designed to hold backfills. To stabilize slopes for short period it may also be used. Small protection bund may also be constructed with geojute.

7. Filtration is the equilibrium soil-to-geotextile system that allows for adequate liquid flow with limited soil loss across the plane of the geotextile over a service lifetime compatible with the application under consideration. It is the most widely used geotextile function. The filtration function has two concurrent objectives. These are to retain the particles of the filtered soil while permitting water to pass through the plane of the geotextile from the filtered soil. These two parallel roles are the key to filtration design.

8. Geotextile is normally used beneath stone base for paved & unpaved roads and airfields, beneath ballast under railroads. Geojute may be put beneath stone base for unpaved roads for short term. It may also be applied around crushed stone surrounding underdrains and without underdrains, around perforated pipe. Geojute may be put beneath landfills that generate leachate for long term. Both the materials may be used as a silt fence and silt curtain.
9. The definition of geotextile drainage is the equilibrium soil-to-geotextile system that allows for an adequate liquid flow with limited soil loss within the plane of the geotextile over a service life-time compatible with the application under consideration. Geotextile drainage occurs in the in-plane direction rather than cross plane.
10. Geotextiles may be put as a chimney drain and drainage gallery in an earth dam, as drainage interceptor for horizontal flow, drainage blanket beneath a surcharge fill. It may also be applied as a drain behind a retaining wall, beneath railroad ballast. Geojute may be applied as drainage blanket beneath a surcharge fill for short duration. It may also be applied as a drain behind a retaining wall, beneath railroad ballast for quite long duration.
11. The geotextile may be designed for multiple functions in other applications also. In these cases, a single dominant (primary) function cannot always be identified. Thus, there are primary, secondary, tertiary, and perhaps even quaternary functions that may vary in a particular application. Furthermore, these functions might vary from site to site. Such multiple-function applications are the focus in this section. They should not be taken lightly or be considered of lesser importance than those discussed previously. Some of the major uses of geotextiles are: reflective crack prevention in bituminous pavement overlays, railroad application, horizontal bags and tubes, restoration of piles, bridge pier underpinning, uniform pressure distribution beneath caissons and erosion-control mattresses.
12. Jute is one of the oldest surviving agro-industries in Bangladesh and has been traditionally in use for flexible packaging, especially sacks. The special physical attributes of jute have opened up new avenues for diversification promoted mostly as

a result of global concerns for environment. Geojute is one such diversified product of jute with designed biodegradability and increased hydrophobicity which has proved to be highly effective in addressing a number of soil-related problems in civil engineering. Functionally, Geojute does not have much dissimilarity with man-made Geotextiles.

13. Jute is a biodegradable, photodegradable, thermal degradable, high modulus, less extensible, hygroscopic, coarse fibre. In tropical, humid, rainfed and frequently flood affected countries like Bangladesh quick biodegradability of jute is a disadvantage for its use in geotechnical application. To overcome this disadvantage numerous study/research works have been performed by different researchers, organizations and institutions for last few years. Recently a wide range of geojute has been developed in the laboratory of Bangladesh Jute Research Institute (BJRI) by blending jute with hydrophobic fibre like coir or by modification with bitumen, latex and wax resinous materials with the collaboration of Bangladesh Jute Mills Corporation (BJMC).



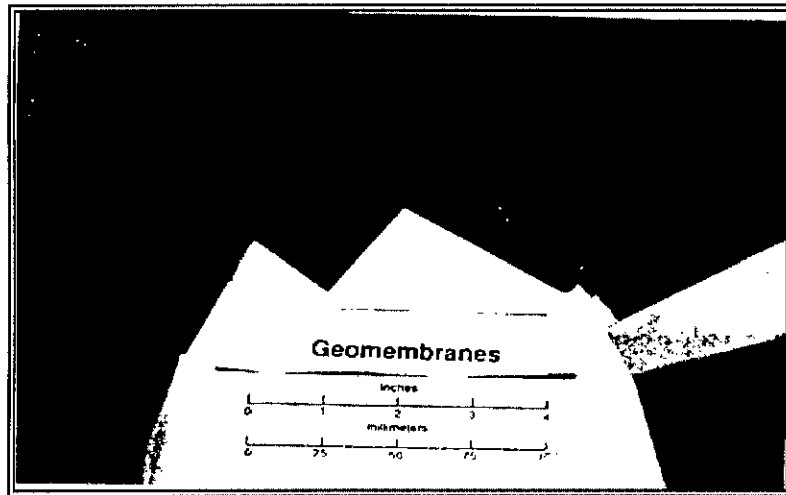


Fig 2.1a Geomembrane

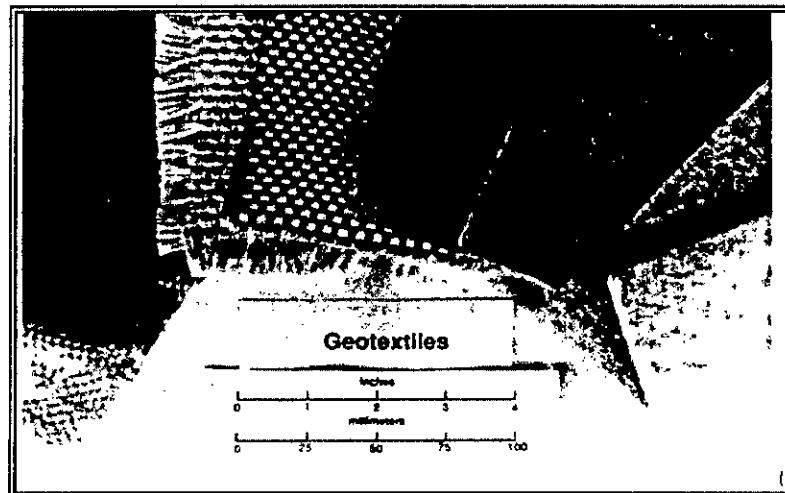


Fig 2.1b Geotextile

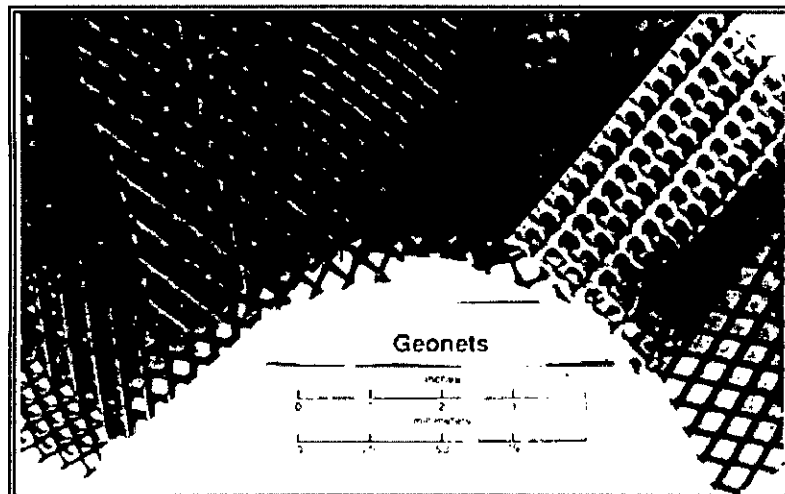


Fig 2.1c Geonets

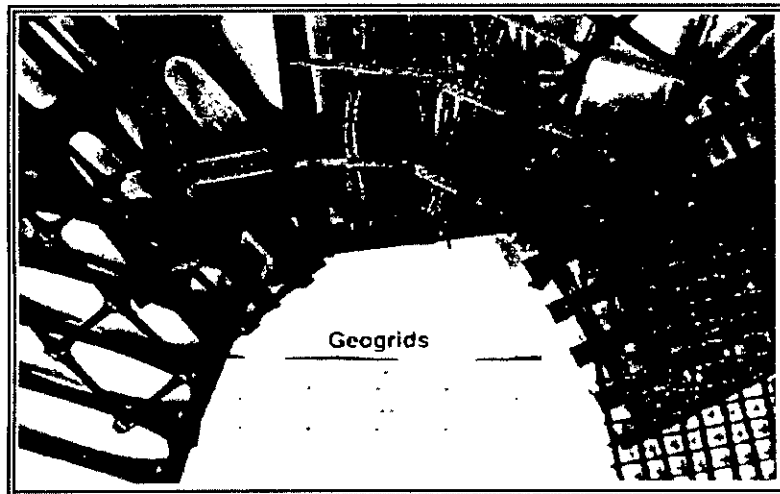


Fig 2.1d Geogrids

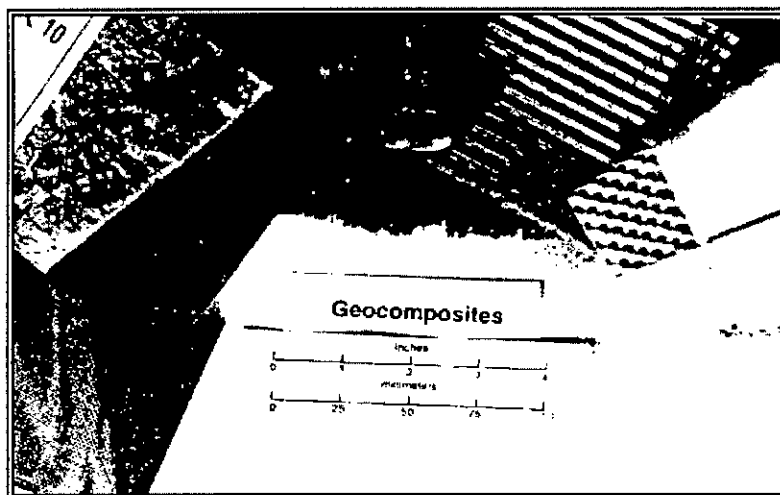


Fig 2.1e Geocomposites

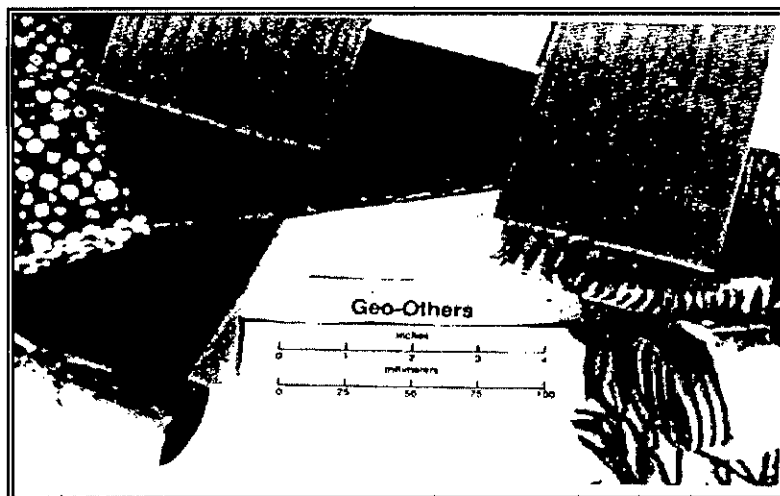


Fig 2.1f Geo-others (geopipes & geosynthetic clay liners)

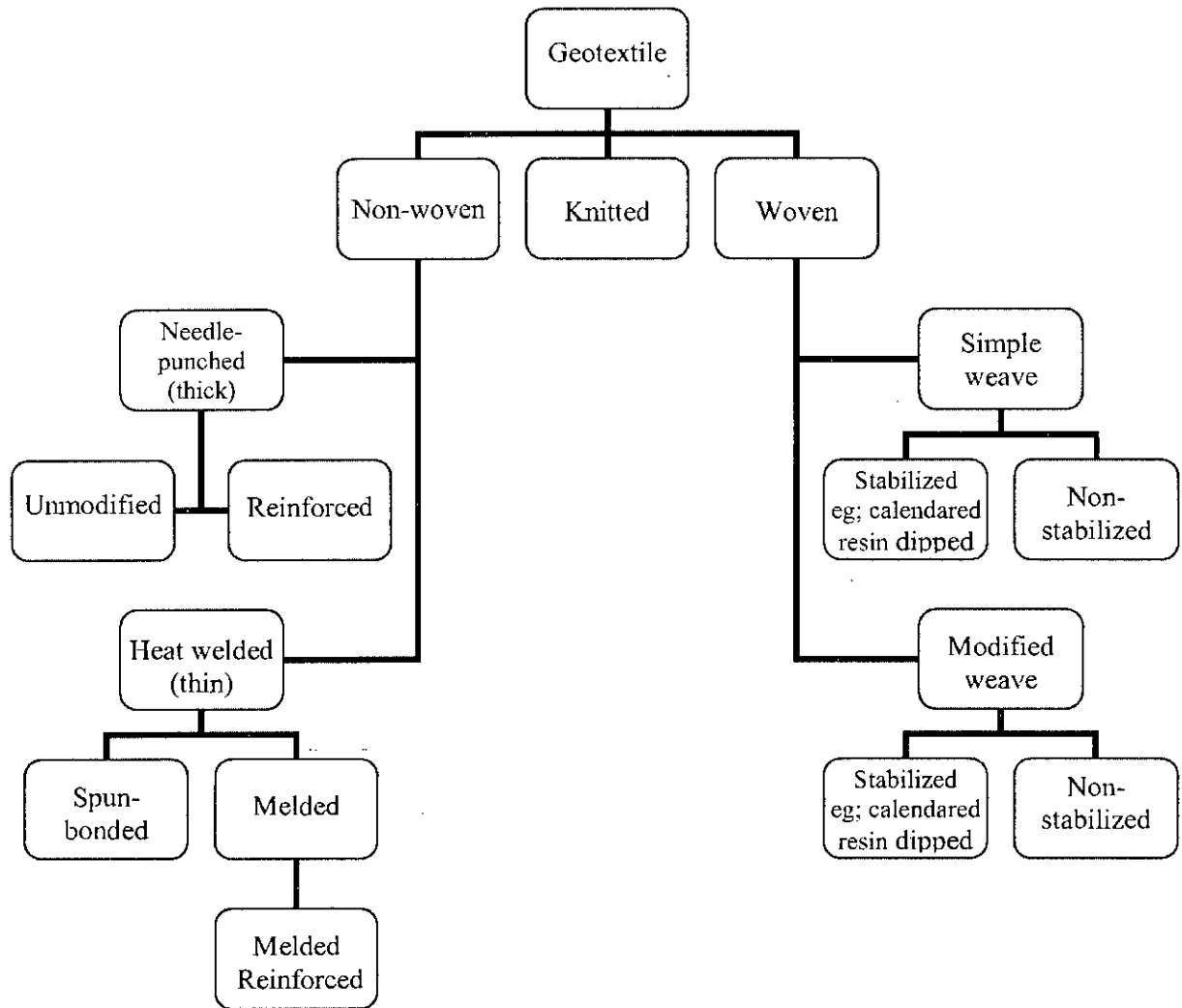


Fig. 2.2 Geotextile classification based on the manufacturing process (after Rankilor, 1981)

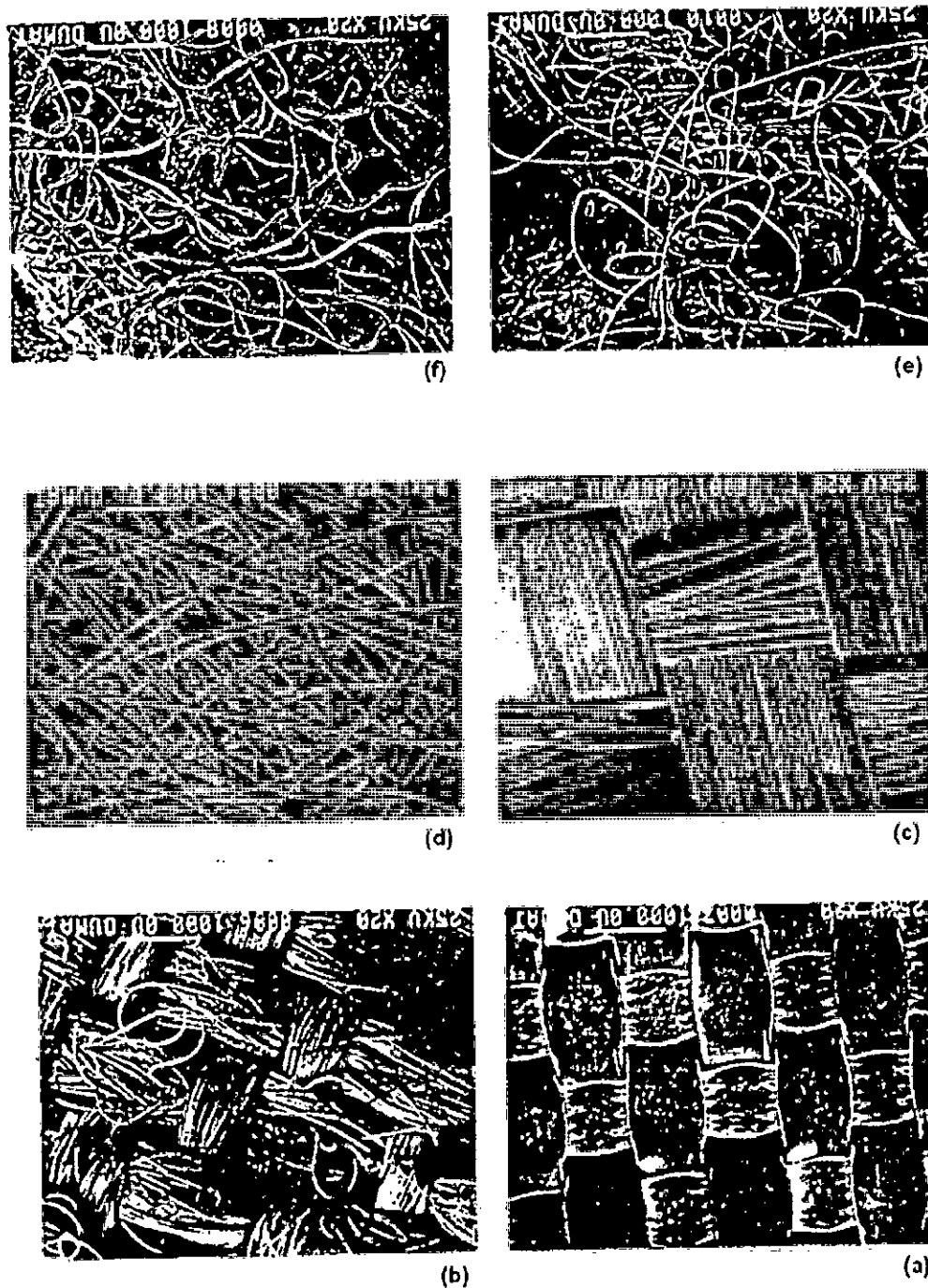


Fig 2.3 Photomicrographs of various fabrics used as geotextiles: (a) Woven monofilament (b) Woven multifilament (c) Woven slit (split) film (d) Nonwoven heat-bonded (e) nonwoven needle-punched (f) Nonwoven resin (chemically) bonded (after Koerner, 1990)

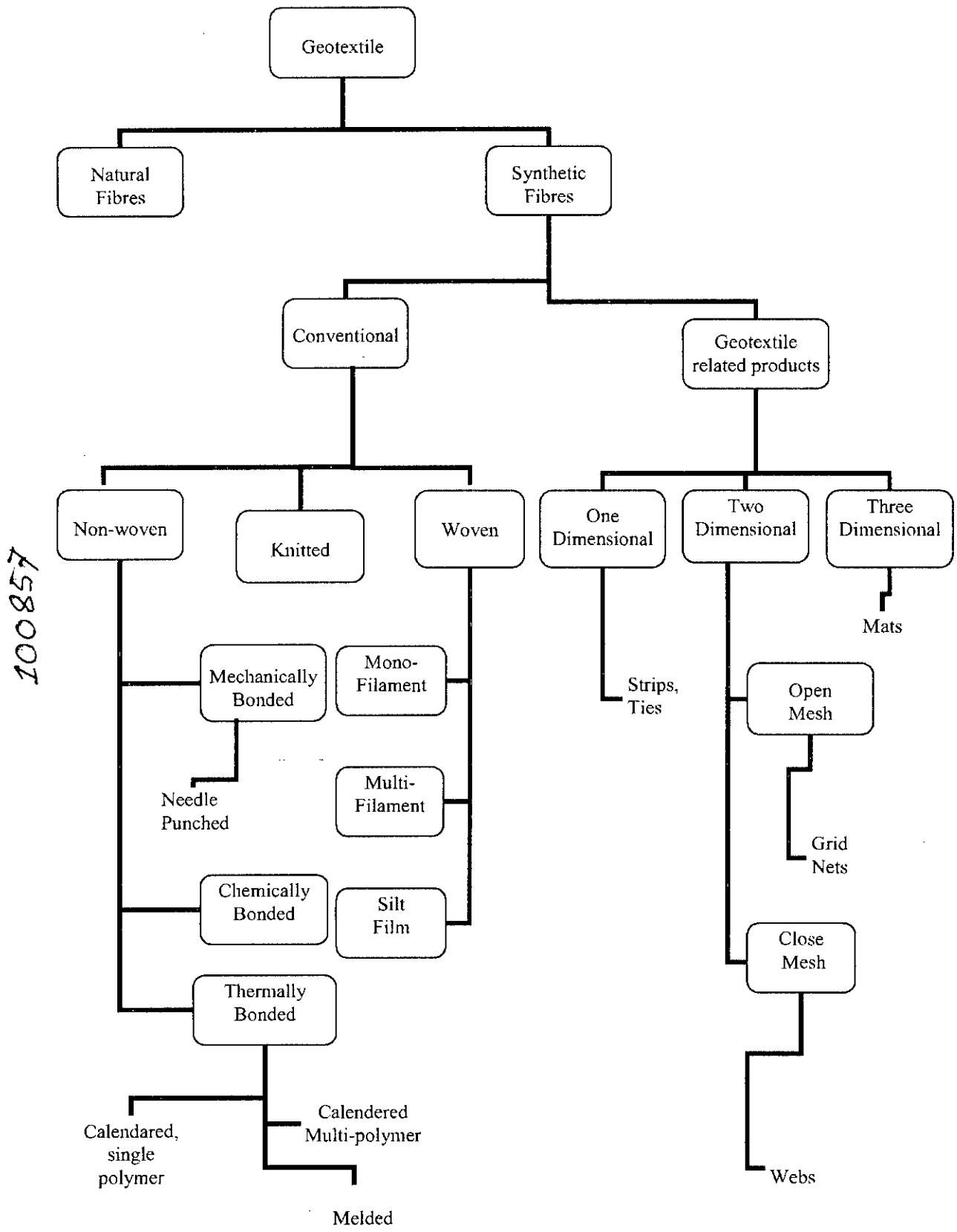


Fig 2.4 Geotextiles classification after John (1987)

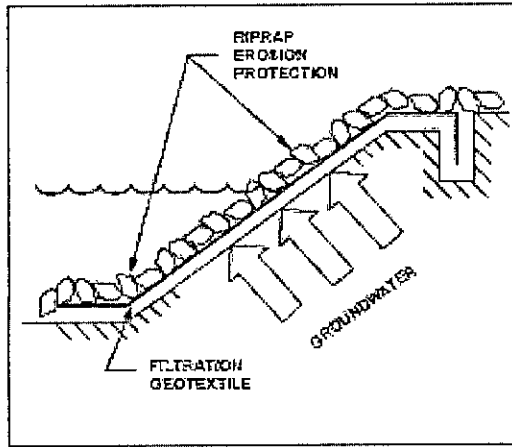


Fig 2.5 Riprap erosion protection

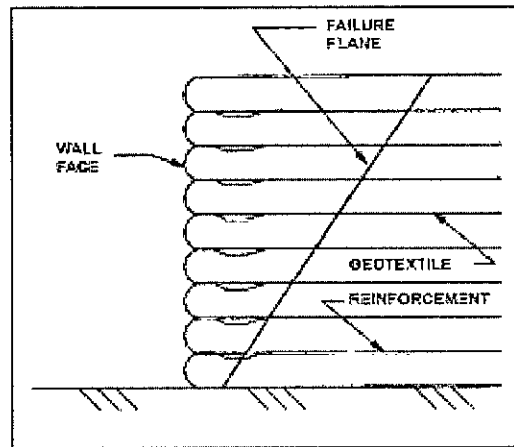


Fig 2.6 Geotextile reinforcement



Without Geojute



With Geojute

(a) Mechanism of soil fines pumping into stone aggregate voids and prevention using geojute



Without Geojute



With Geojute

(b) Mechanism of stone aggregate intrusion into soil subgrade and prevention using geojute

Fig 2.7 Schematic representation of separation mechanism (after Koerner, 1997)

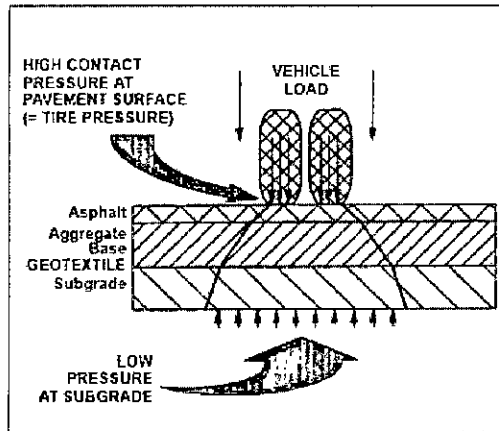


Fig 2.8 Pressure dissipation through road

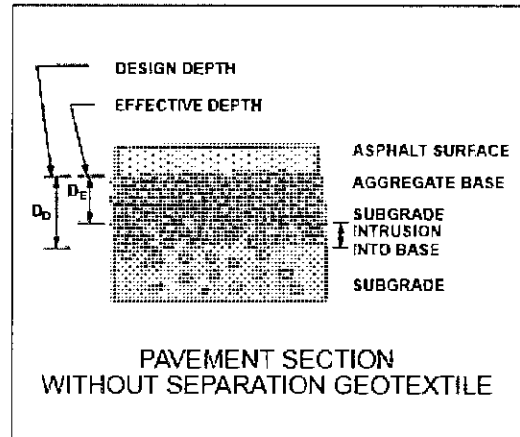


Fig 2.9 Pavement without separation material

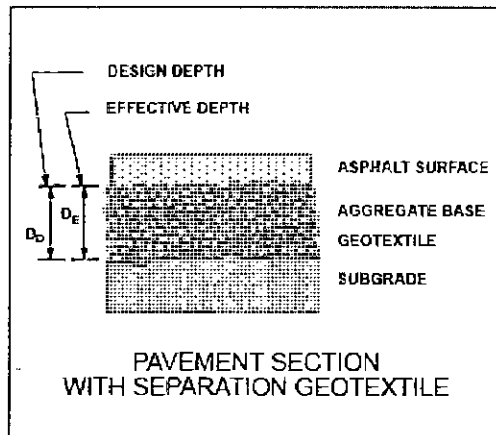


Fig 2.10 Pavement with separation material

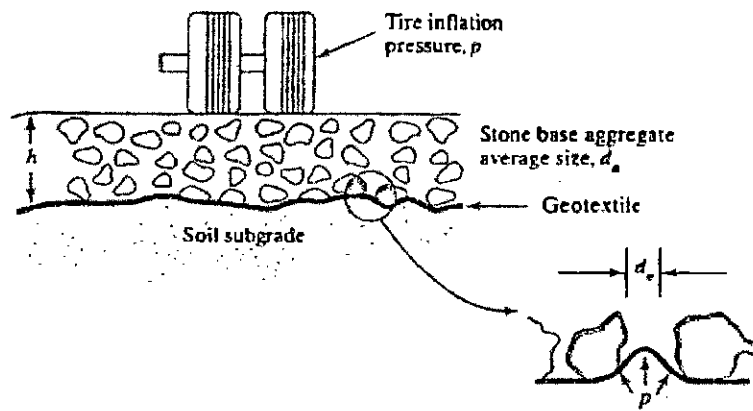
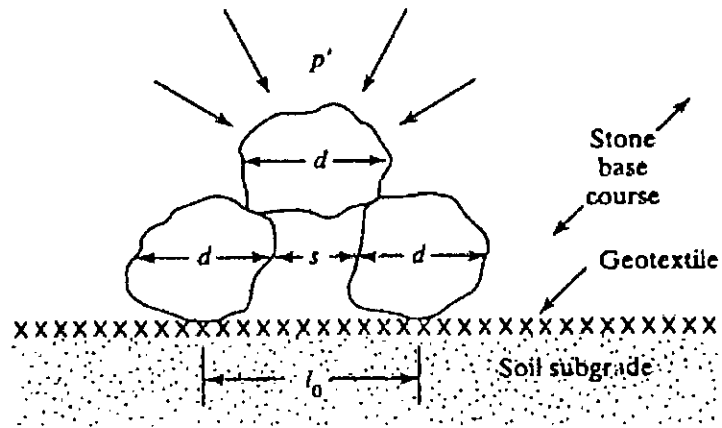
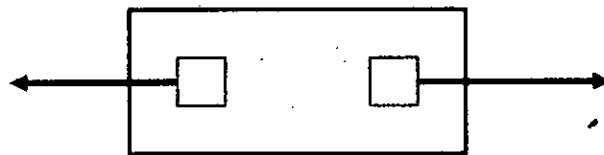


Fig 2.11 Geotextile being forced up into voids of stone base by traffic tire loads  
(after Koerner, 1997)



(a) Actual situation



(b) Analogous grab tension test

Fig 2.12 Geotextile being subjected to tensile stress as surface pressure is applied and stone base attempts to spread laterally (after Koerner, 1997)

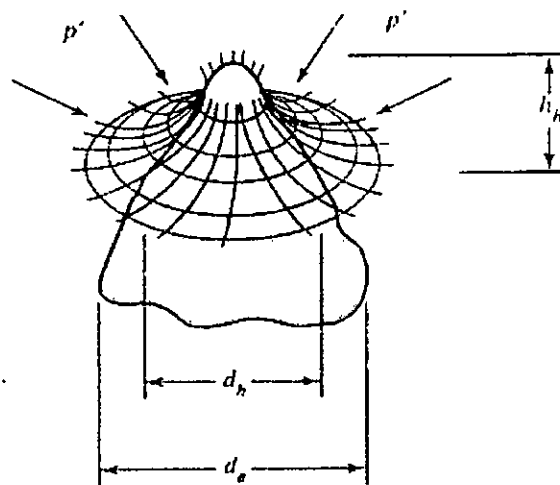


Fig 2.13 Visualization of a stone puncturing a geotextile as pressure is applied from above (after Koerner, 1997)



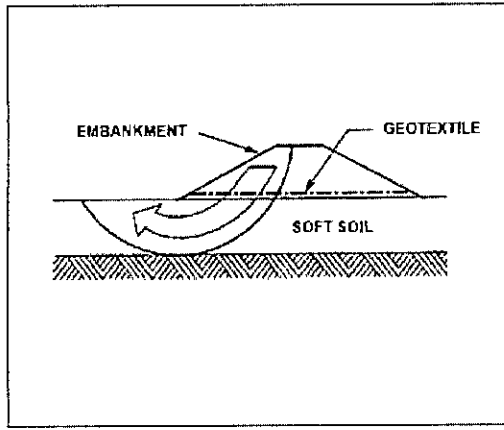


Fig 2.14 Geotextile-reinforced embankment

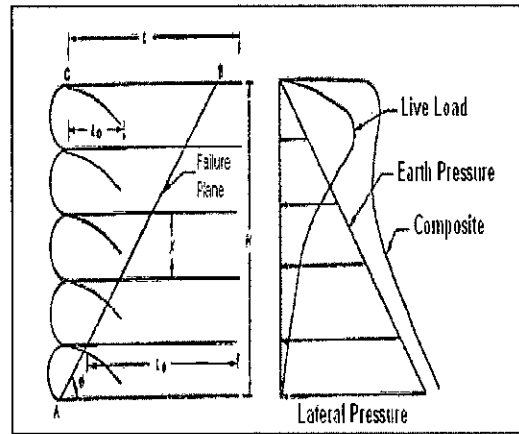


Fig 2.15 Geotextile-reinforced wall

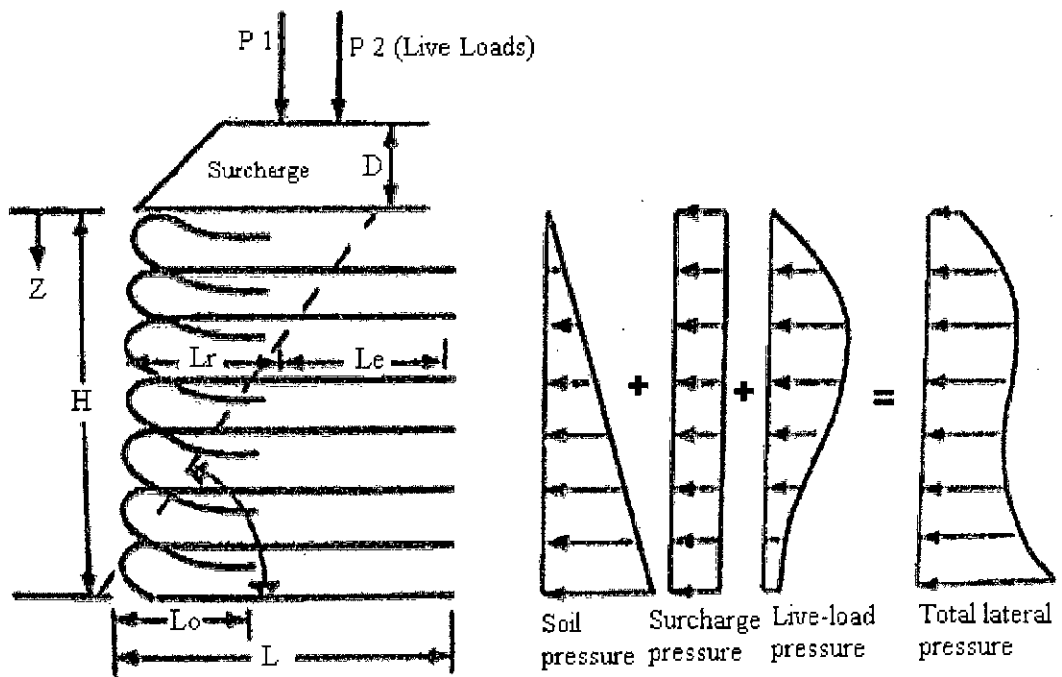


Fig 2.16 Earth pressure concepts and theory for geotextile walls (after Koerner, 1997)

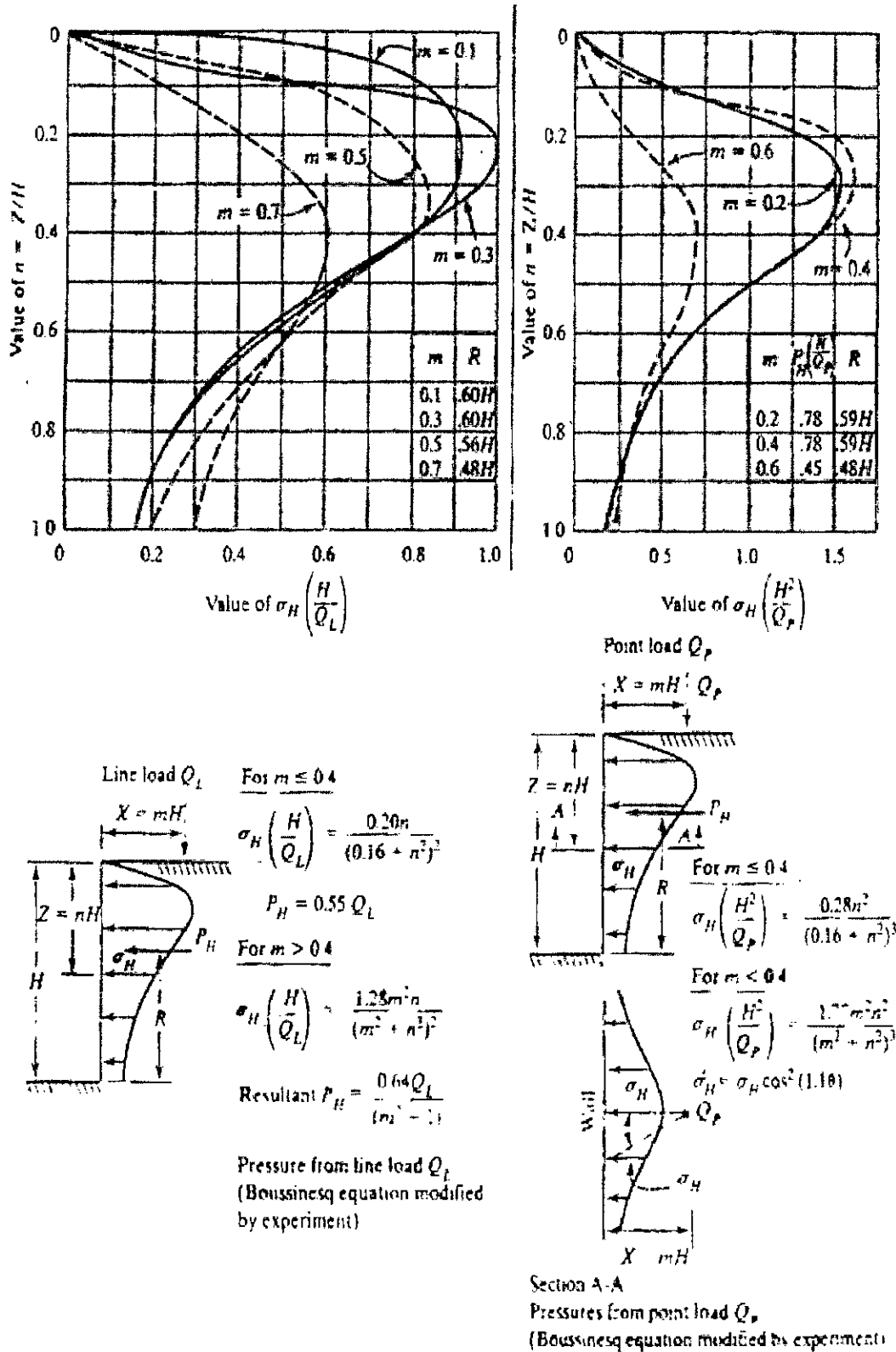
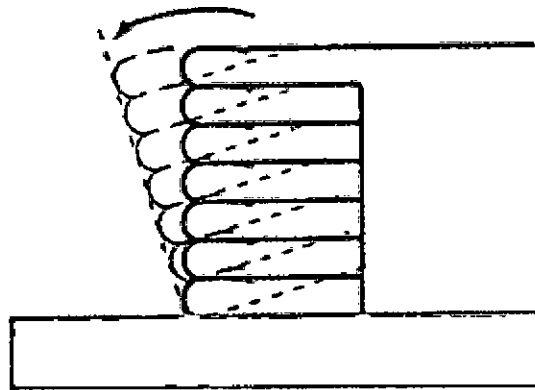
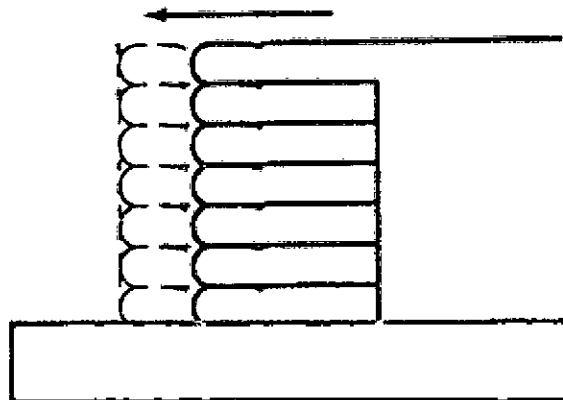


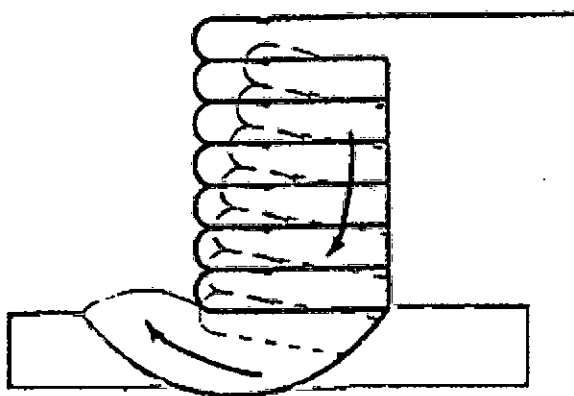
Fig 2.17 Lateral earth pressure due to a surface load. Left side for line loads and right side for point load (after NAVAC, 1982)



(a) Overturning considerations



(b) Sliding considerations



(c) Foundation considerations

Fig 2.18 External stability considerations for geotextile walls

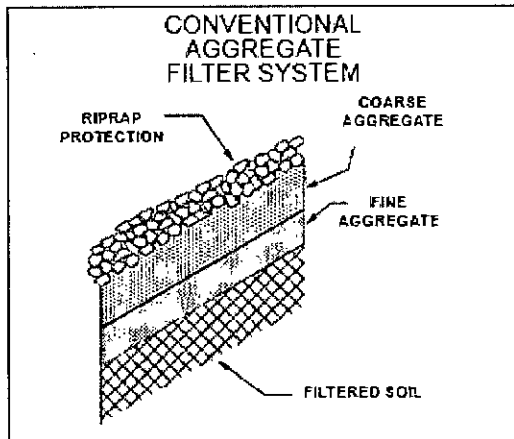


Fig 2.19 Conventional aggregate filter system

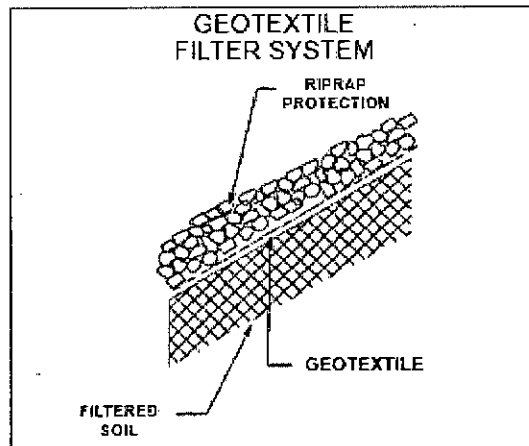


Fig 2.20 Geotextile filter system

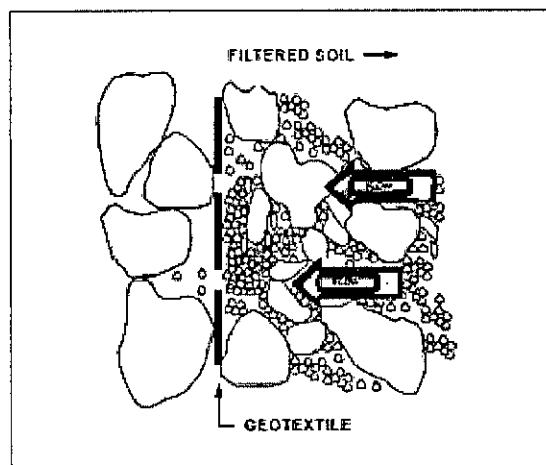
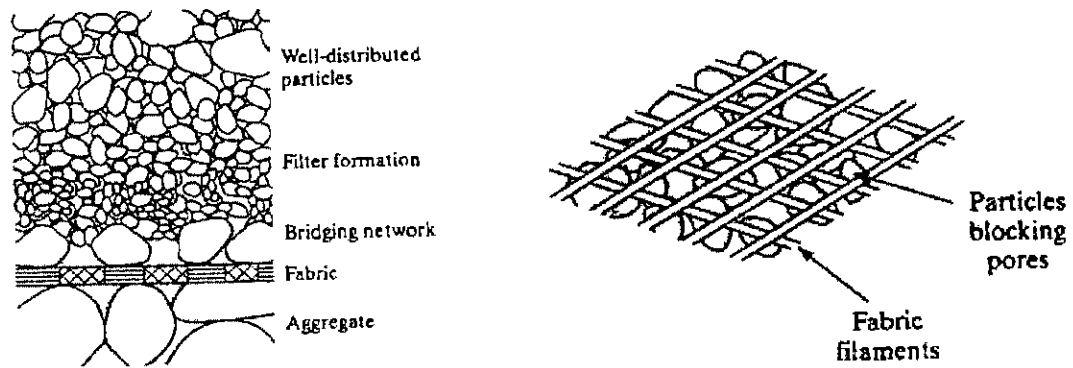
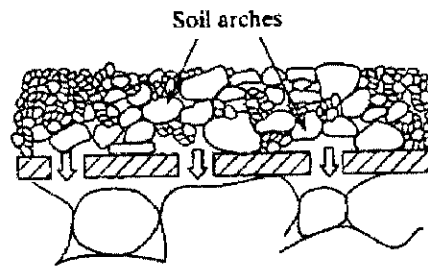


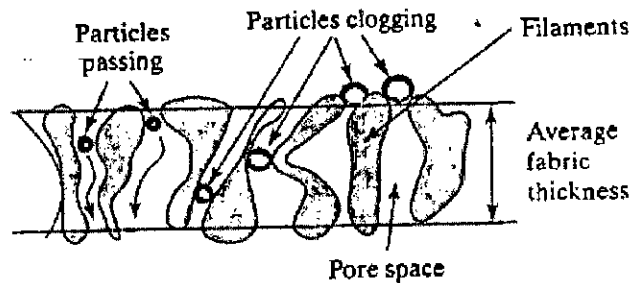
Fig 2.21 Geotextile cake system



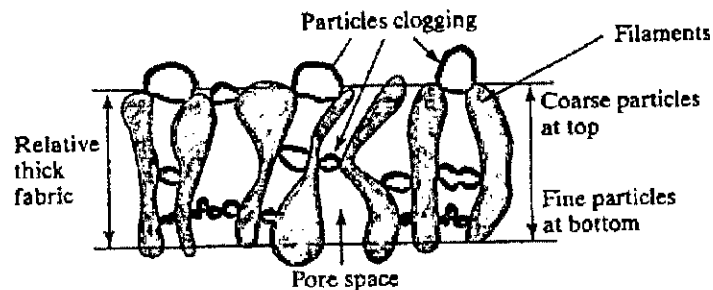
(a) Formation of an upstream soil filter (b) Upstream particles blocking geotextile opening



(c) Upstream particles arching over geotextile opening

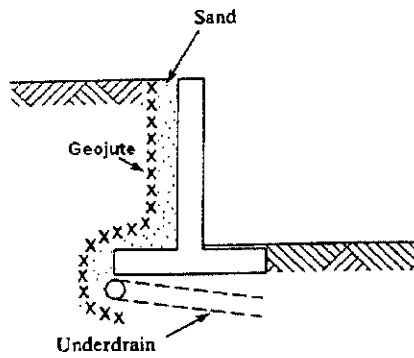


(d) Soil particles clogged within geotextile structure

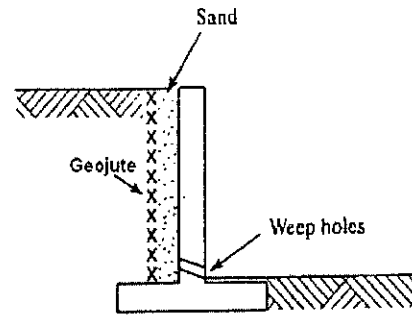


(e) Depth filtration concept using thick geotextile

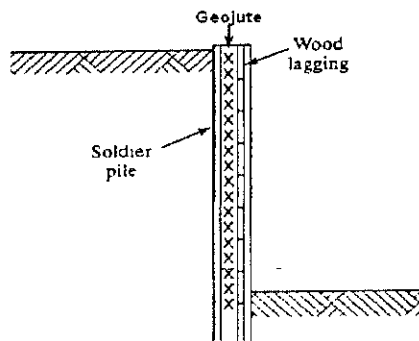
Fig 2.22 Various hypothetical mechanisms involved in long-term soil-to-fabric flow compatibility (after Koerner, 1997)



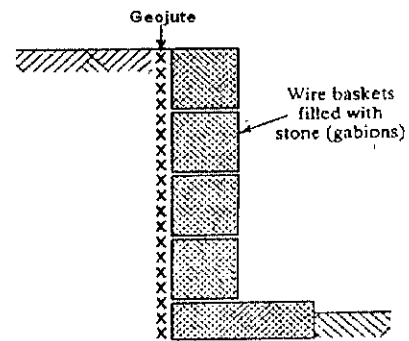
(a) Rigid retaining wall with underdrains



(b) Rigid retaining wall with weep holes



(c) Temporary retaining wall with open sheeting



(d) Flexible retaining wall made from gabions

Fig 2.23 Various types of retaining walls in which geotextiles can be used as filters (after Koerner, 1997)

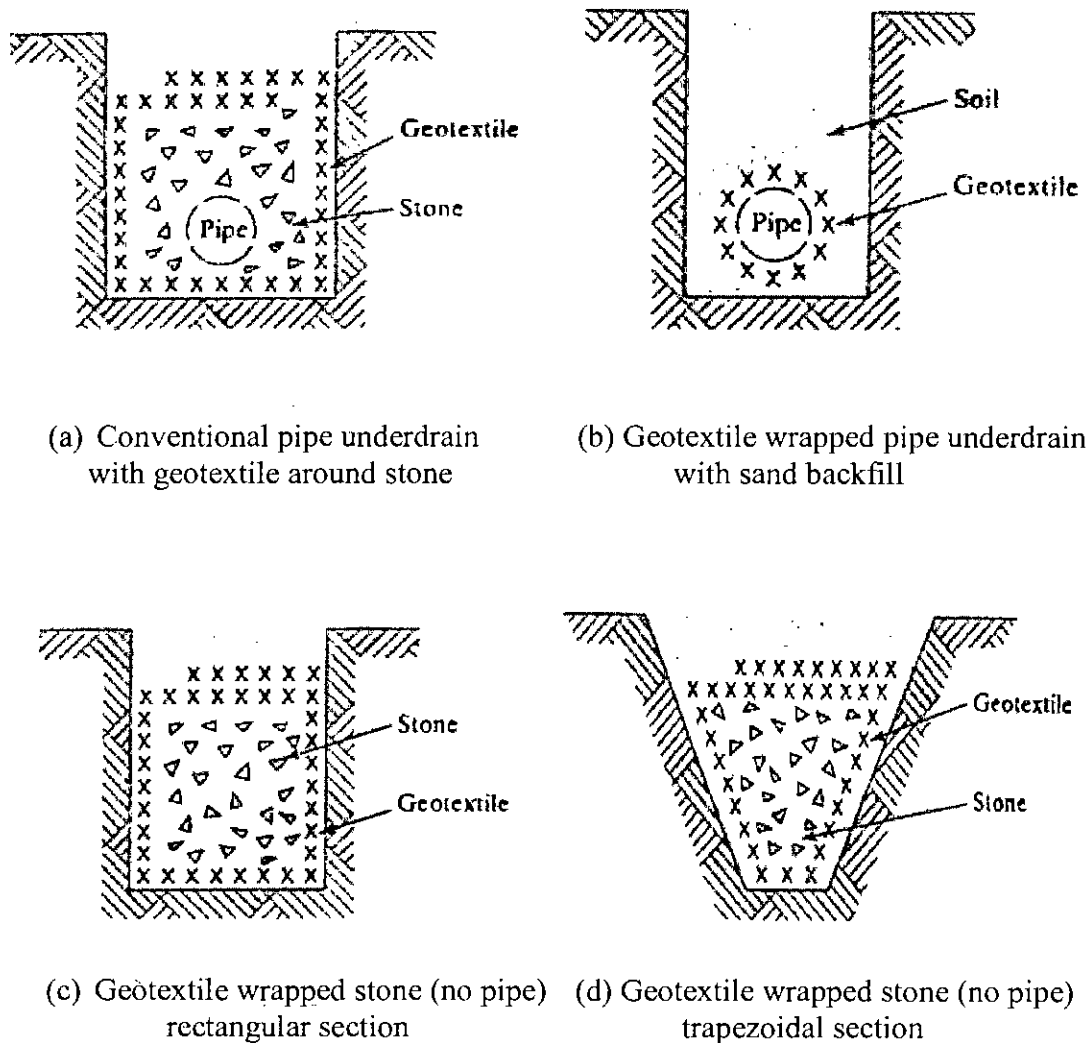


Fig 2.24 Typical cross sections of underdrain systems with and without perforated pipes (after Koerner, 1997)

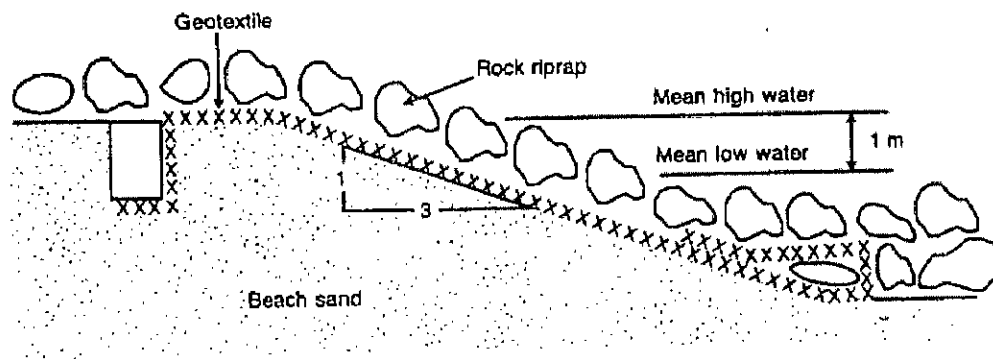


Fig 2.25 Geotextile placed beneath a rock riprap erosion-control system (after Koerner, 1997)

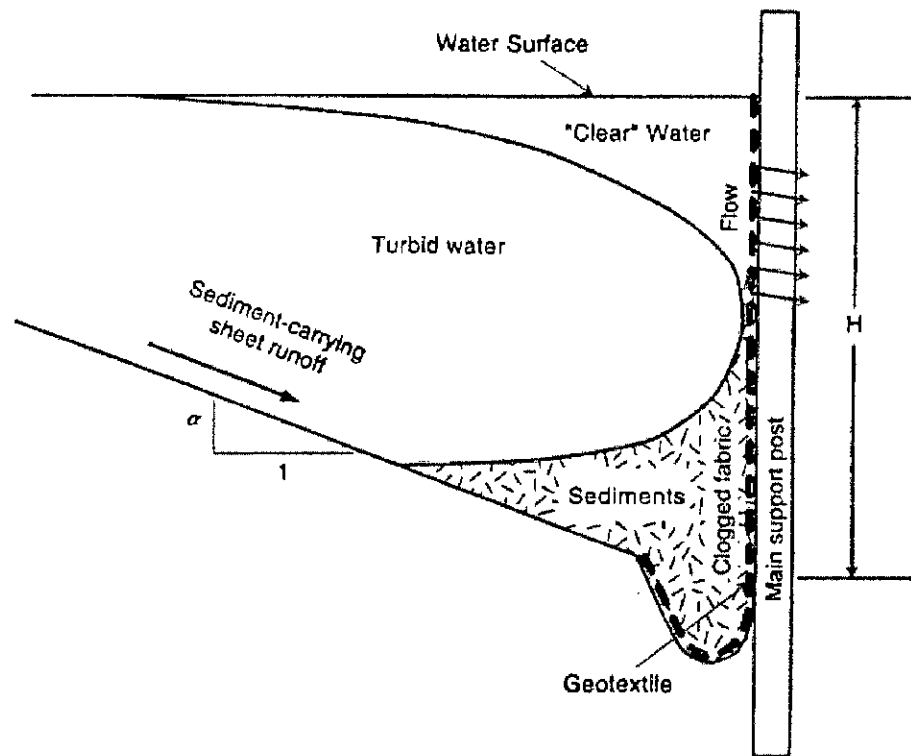


Fig 2.26 Cross section of geotextile silt fence and suggested manner in which system functions (after Koerner, 1997)

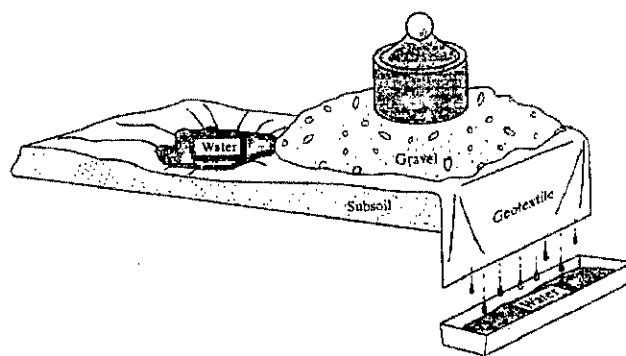


Fig 2.27 Sketch of drainage of water within geotextile

6 7



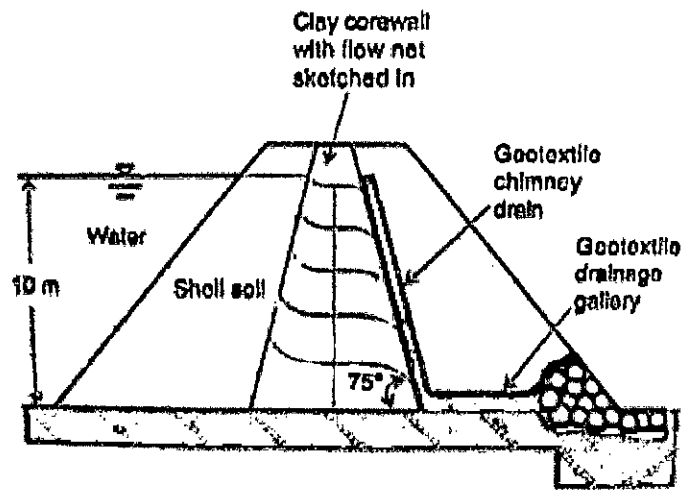


Fig 2.28 Gravity design of drainage (after Koerner, 1997)

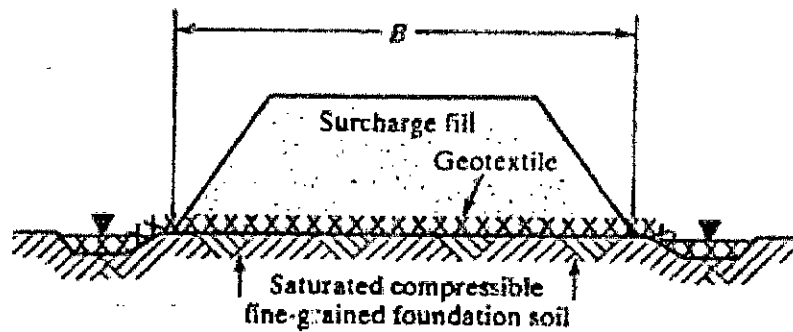


Fig 2.29 Pressure drainage design (after Koerner, 1997)

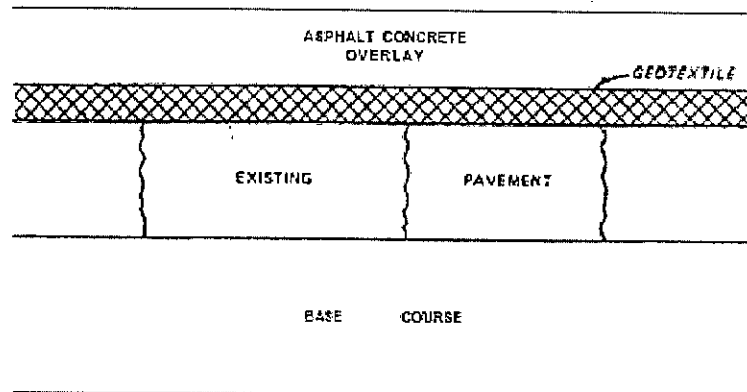
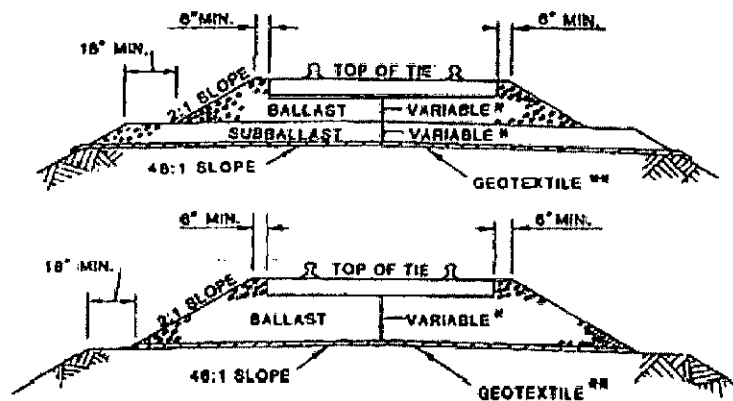
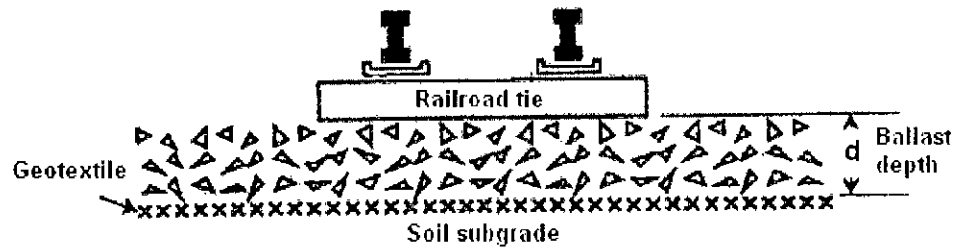


Fig 2.30 Geotextile in concrete overlay (after U.S. Departments of the Army and the Air force, 1995)



<sup>\*\*</sup> MINIMUM REQUIREMENTS:  
 WITHOUT GEOTEXTILE: BALLAST: 12" MINIMUM  
 SUBBALLAST: 6" MINIMUM  
 WITH GEOTEXTILE: TOTAL DEPTH BALLAST/SUBBALLAST  
 BETWEEN BOTTOM OF TIE AND GEOTEXTILE: 12" MINIMUM  
<sup>\*\*</sup> PROTECTIVE SAND LAYER ABOVE, BELOW, OR BOTH ABOVE  
 AND BELOW IS OPTIONAL.  
 IF USED, MINIMUM LAYER THICKNESS IS 2"

Fig 2.31 Geotextile application under railroad (after U.S. Departments of the Army and the Air force, 1995)

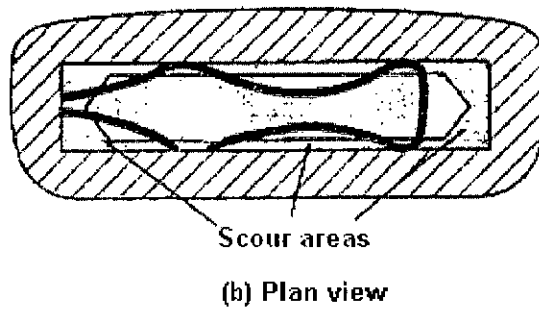
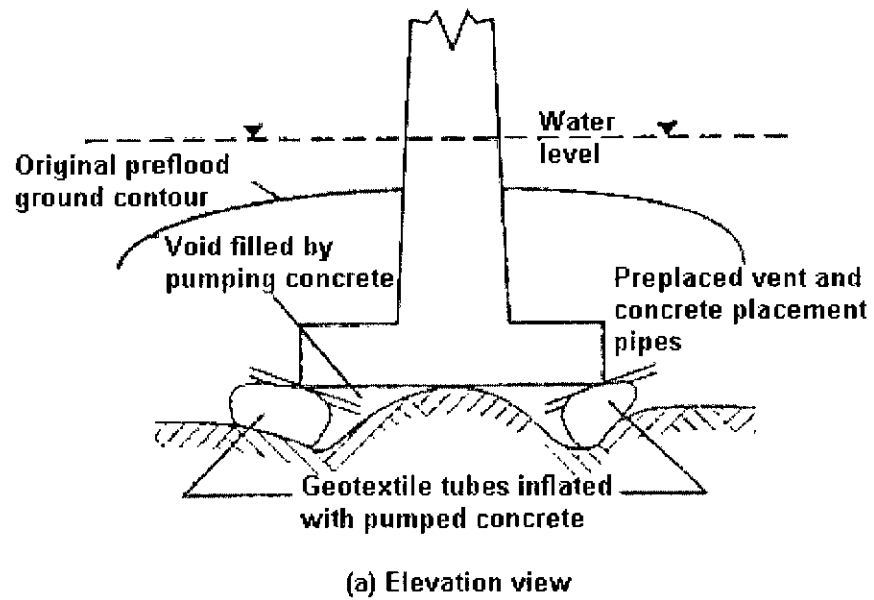


Fig 2.32 Underpinning of scoured bridge pier using grout-filled geotextile (after Koerner, 1997)

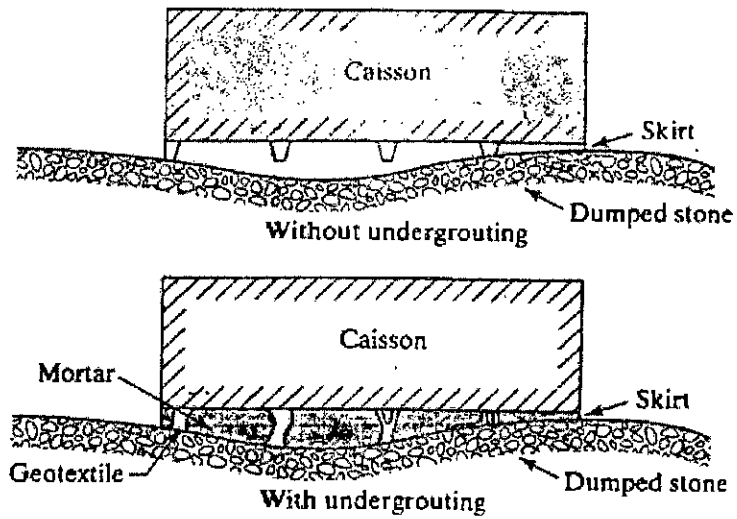


Fig 2.33 Prototype for evaluating use of geotextiles as forms for establishing uniform pressure distribution beneath concrete foundations (after Koerner, 1997)

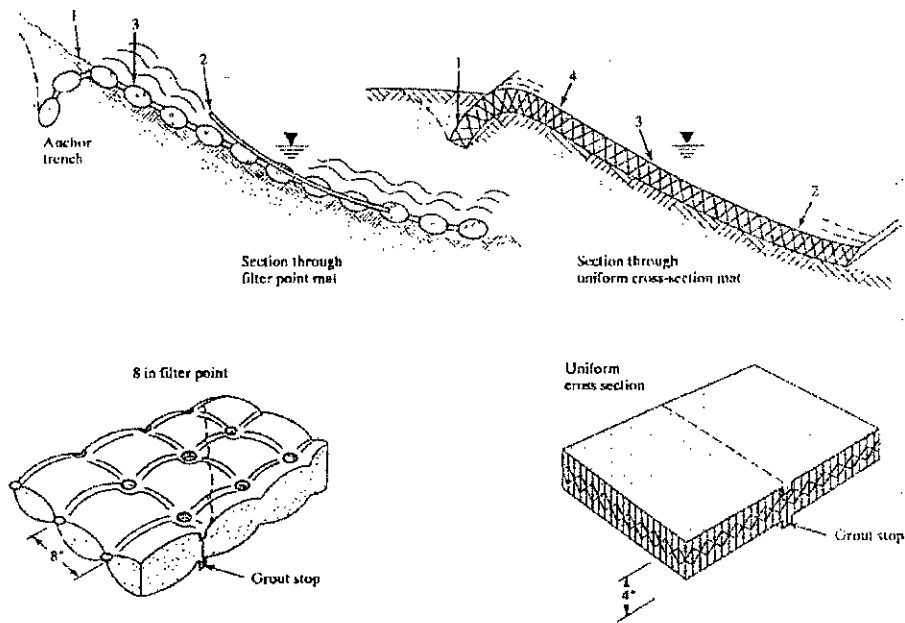


Fig 2.34 Typical cross sections and schematics of erosion-control mattresses formed by grout-filled geotextile (after Koerner, 1997)

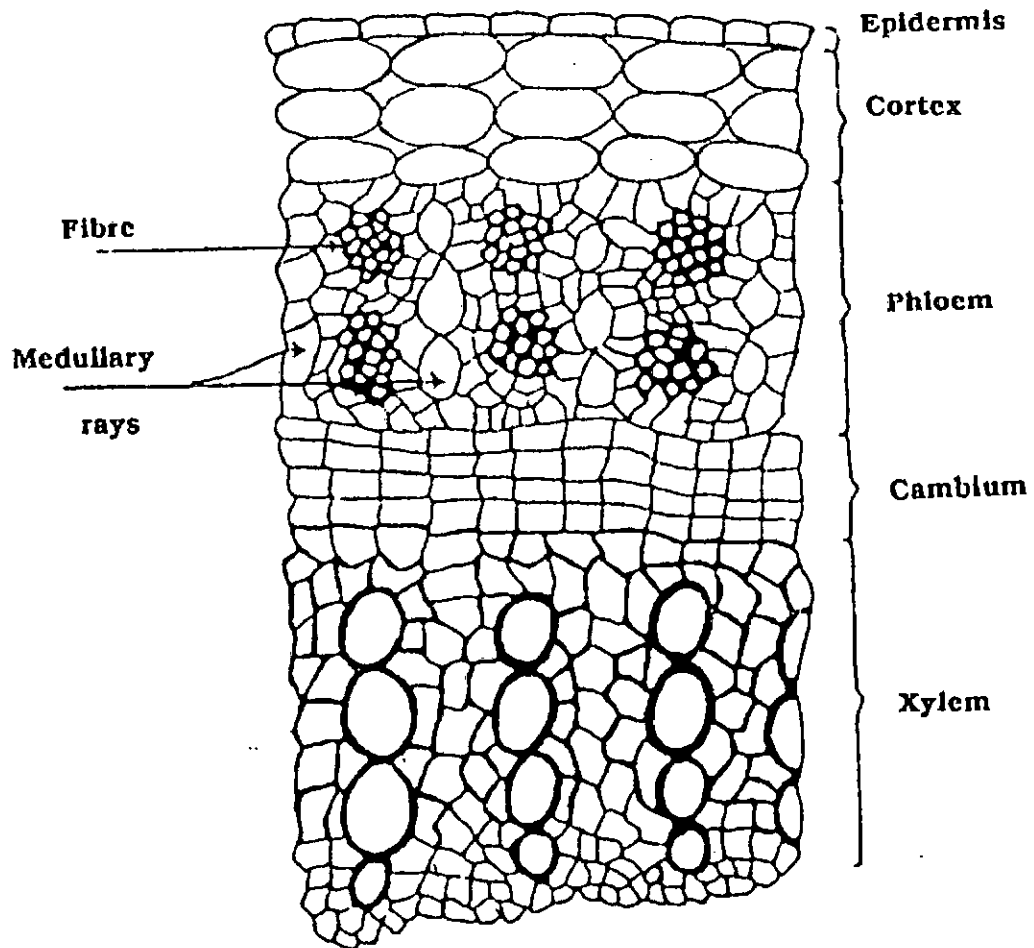


Fig 2.35 Epidermal cell of jute plant (after Abdullah, 1999)

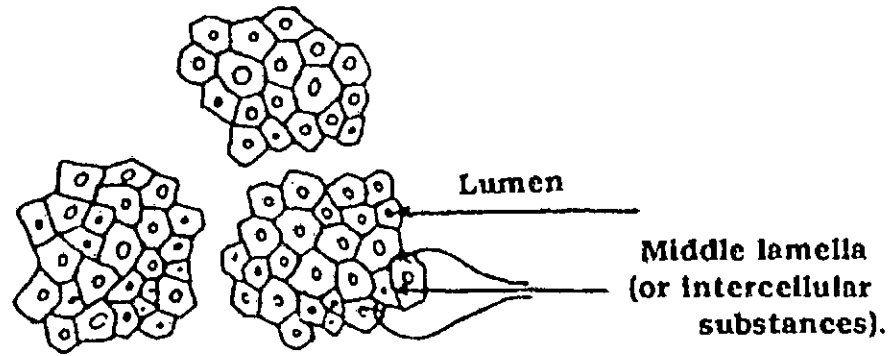


Fig 2.36 Cross-section Stem of jute plant (after Abdullah, 1999)

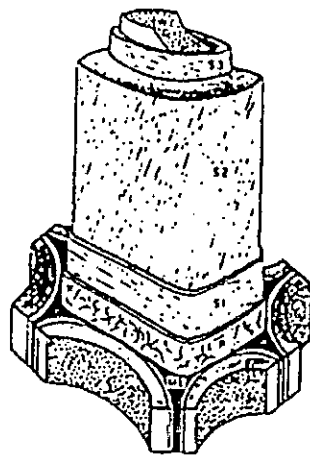


Fig 2.37 Structure of simple woody cell (after Abdullah, 1999)

## **CHAPTER THREE**

# **LABORATORY INVESTIGATIONS**

### **3.1 General**

Being a growing industry, the geotextile currently does not yet have a completely unified set of worldwide standards and test methods. Yet the activity toward such an ultimate goal is very intense (Koerner, 1997). As observed by Koerner, many of the test methods are not fully standardized as far as their test procedures are concerned. In the U.S. the ASTM has a standards committee specifically organized for geosynthetics (D35); however, there are also worldwide organizations. Few of them are: International Organization for Standards (ISO), German Standards Committee for Geotextiles (DIN), British Standards Institution (UK) etc. Geotextiles tests can be divided into two categories: Index tests and Design tests. Index tests are relatively simple to perform and provide basic properties primarily for purpose of quality control. Such properties are also of value for

classifying geotextiles, however, and in some cases they have been empirically related to engineering behavior. Design tests attempt to model the anticipated field conditions and frequently involve a combination of the geotextiles and the proposed fill material in an appropriate manner. Such tests generally employ relatively complex apparatus and are often both expensive and time-consuming.

It may be noted that since no standard test methods for determining engineering properties of geotextiles are available to date, the methods commonly employed for geotextiles may be adopted. Muhammad (1993), Rao et al (1994), Kabir et al (1994) adopted the same procedure. A brief description on each test based on ASTM & DIN is appended below:

### **3.2 Physical Properties**

#### **3.2.1 Mass per Unit Area**

Mass per unit area is the proper term by which the weight of geotextile is meant. Geotextiles mass per unit area is given in grams per square meter ( $\text{g/m}^2$ ) and rounded to the nearest  $0.1 \text{ g/m}^2$ . The mass per unit area of a geotextile is determined by weighing test specimens of known dimensions, cut from various locations over the full width of the laboratory sample (Fig 3.1). The calculated values are then averaged to obtain the mean mass per unit area of the laboratory sample.

This test method is used to determine if the geotextile material meets specifications for mass per unit area. This test method can be used for quality control to determine specimen conformance. This measurement allows for a simple control of the delivered material by a comparison of the mass per unit area of the delivered material and the specified mass per unit area.

As per ASTM D 5261-92 a minimum five test specimen is cut such that they are representative of the entire roll width and with a combined total minimum area of  $100,000 \text{ mm}^2$  ( $155 \text{ in}^2$ ). Each test specimen should be equal to an area not less than  $10,000 \text{ mm}^2$  ( $15.5 \text{ in}^2$ ). The mass (or weight) is measured to the nearest 0.01% of the total specimen mass: length and width is measured under zero geotextile tension. Since fabric cost is directly related to mass per unit area, it is an important property.



Calculation of the mass per unit area of each of the specimen to be done as follows:

$$m = M_s \times 1\,000\,000/A$$

where:

$m$  = mass per unit area rounded to the nearest  $0.1 \text{ g/m}^2$

$M_s$  = mass of the specimen, g, and

$A$  = area of the specimen,  $\text{mm}^2$

After calculating individual mass per unit area, the averages of all five specimens are to be found out.

### 3.2.2 Thickness

Thickness is one of the basic physical properties of a geotextile used to control the quality of many geotextiles and geomembranes. It is more of a descriptive property than design-oriented property. In certain industrial applications, the thickness may be rigidly controlled within specified limits. Bulk and warmth properties of jute products are often estimated based on their thickness measured before and after abrasion or shrinkage. Thickness values are required in calculation of some geotextile and geomembrane parameters such as permeability coefficients, tensile stress (index), and the like thickness is not indicative of field performance and therefore is not recommended for specifications.

The thickness of a geotextile is the distance between the upper and lower surface when measured under a specified pressure. The thickness of geotextiles and geomembranes may vary considerably depending on the magnitude and the duration of pressure applied. Where observed changes occur, thickness decreases when applied pressure is increased. To minimize variation, specific sample size and applied pressure are indicated in ASTM D 5199-98 to ensure all results are comparable. As per this test method, the thickness testing instrument should have the thickness gage having a base (or anvil) and a free moving presser foot plate whose planar faces are parallel to each other to  $<0.01 \text{ mm}$  (Fig 3.2). A gage with a 56.4 mm (2.22 in) diameter presser foot, the base should extend at least 10 mm in all directions further than the edge of the  $2500 \text{ mm}^2$  circular pressor foot, should be used for

measurements of geotextiles. This instrument must be capable of measuring a maximum thickness of at least 10 mm to an accuracy of at least  $\pm 0.02$  mm. The gages should be constructed to permit gradual application of pressure to a specific force of  $2 \pm 0.02$  kPa ( $0.29 \pm 0.003$  psi) for geotextiles.

As per this test, a pressure of 2 kPa is recommended as a standard for the determination of the nominal thickness of geotextiles. Test specimens are removed from laboratory sample in a randomly distributed pattern across the width with no specimen taken nearer than 100 mm (4 in) from the selvage or roll edge. From each unit in the laboratory sample, test specimens are cut such that the edge of the specimens should extend beyond the edge of the pressor foot by 10 mm (0.39 in) in all directions. Normally 10 (ten) specimens are taken for each test.

An important consideration is to check whether the strain gauges have truly come into equilibrium under each load increment. The introduction of a weight would induce compression of the fabric. Thus, it is important to read the gauges as quickly as possible once the presser plate is deemed to have come to equilibrium at the standardized time duration. The thickness of jute fabric continues to decrease under pressure for considerable time because of the compressibility. Muhammad (1993) studied the effect of time on thickness of jute matting under different pressure. Fig.3.3 indicates that, at the end of two minutes, the plate can be considered to have effectively reached the equilibrium. Thus for the thickness tests, the time interval to record readings from strain gauges may be standardized to 5 minutes while the suggested time interval by ASTM is only 5 sec. Another important finding can be observed that around 98% of compressibility is reached after 5 minutes of applied load. Muhammed (1993) has also tested different numbers of layers under a wide range of pressure. The average thickness,  $T_{avg}$  was calculated from the total thickness,  $T_{total}$ , and the number of layers tested,  $N$ , by

$$T_{avg} = T_{total}/N$$

The total thickness of jute under uniform applied load in field condition can be estimated by multiplying the number of sheets used and the average single layer thickness at that particular load as shown in Fig 3.4. From this fig, it is possible to

calculate the thickness of any number of layers of geojute under any applied pressure. The plotted graphs can be extrapolated for higher pressure and higher number of layers of geojute sheets.

### 3.2.3 Specific Density

Specific gravity is one of the important properties of geotextiles which can determine the flexibility to work on and under water and other types of liquid. The specific gravity of geotextile is a useful classification property which is indirectly related to durability, strength and filtration.

According to ASTM D-123, Specific gravity,  $G_s$  is the ratio of the weight of equal volume of water at 4<sup>0</sup> C and is expressed by

$$G_s = \frac{\frac{W_d}{V}}{\frac{W_w}{V}} = \frac{W_d}{W_w}$$

Where  $W_d$  is the weight of dry solid material of volume  $V$  and  $W_w$  is the weight of water of equal volume at 4<sup>0</sup>C. For different room temperature conditions a correction factor is required to accommodate temperature variations. This correction factor is also applicable in determining the specific gravity of geotextile materials by water displacement method.

ASTM D 1117-80 has suggested different test methods for determining Absorbency time and Absorptive capacity of non-woven fabrics. However, there is no test method to determine the specific gravity of geotextile fabrics. A laboratory procedure suggested by Muhammad (1993) is followed in this research work for determining specific gravity (Fig 3.5). In this test, three types of jute geotextiles matting having unit weights of 400, 500 and 600 g/m<sup>2</sup> were used. Fig.3.6 shows the increase in specific gravity of the jute geotextile with soaking time under laboratory conditions without vacuum application. It is reported that after 70 to 80 hours of soaking all the jute fabrics reached a maximum specific gravity of 1.42 from initial

value of 0.7 to 0.9 depending upon the jute type. It is also found out from this test that the geotextiles with a lower unit weight ( $\text{g/m}^2$ ) reaches the maximum specific gravity within a shorter time than that with a higher unit weight. Fig 3.7 shows variation of specific gravity with time for untwisted loose jute geotextile fibres using vacuum.

### 3.3 Mechanical Properties

The mechanical properties indicate the geotextile's resistance to tensile stresses mobilized from applied loads and/or installation conditions. The properties are determined by two types of tests. Some are performed with the geotextiles by itself and called index or in-isolation tests, while others are associated with a standard soil or with the site-specific soil called performance tests. The mechanical tests performed in this study are:

- Wide-width Strip Tension Test
- Grab Breaking Load and Elongation Test
- Trapezoid Tearing Test
- Puncture Test
- Burst Strength Test
- Seam Strength Test
- Friction Behavior
- Pullout Test

#### 3.3.1 Wide-width Strip Tension Test

The most common wide-width test is ASTM D 4595 and ISO 10319. In this test a relatively wide specimen is gripped across its entire width in the clamps of a constant rate of extension (CRE) type tensile testing machine operated at a prescribed rate extension, applying a longitudinal force to the specimen until the specimen ruptures. Tensile strength, elongation, initial and secant modulus and breaking toughness of the test specimen can be calculated from machine scales, dials, recording charts, or an interfaced computer. The equipment to be used in this test must be a constant rate of extension (CRE) type that should conform to the Specification D 76.

Fig 3.8 shows a standard tensile testing machine (Autograph Instron) with a maximum capacity of 1000 kN. It has automatic load and elongation recorders and special jaws with serrated faces as shown in Fig 3.9 to firmly grip on the specimen to prevent slippage. These special jaws are capable of testing up to 300 mm wide specimens and permit no rotation about the grips.

Typical responses of geotextiles made from different manufacturing processes are given in Fig 3.10. It may be noted here that the vertical axis is in force per unit width of fabric (i.e., kN/m), which is not a bona fide stress unit. To obtain stress units, this value is divided by the geotextile's thickness, but this is not conventionally done, since the thickness varies greatly under load and during the extension process.

The strain rate commonly used in this test should be given careful consideration. Haliburton *et al.*, (1978) has suggested using 150 mm wide X 300 mm long specimens at a strain rate of 2%/min while Andrawes *et al.*, (1984) recommended 200 mm wide X 100 mm long specimens to be tested at the same rate. ASTM wide strip standard test uses a 200 mm wide X 100 mm long specimen at a strain rate of 10%/min. The difference in specimen size and strain rate adopted by various researchers raises the question as to what effect the specimen size and strain rate will have on the results.

The determination of the wide-width strip force-elongation properties of geotextiles provides design parameters for reinforcement type applications, for example design of reinforced embankments over soft subgrades, reinforcement of slopes. When strength is not necessarily a design consideration, an alternative test method may be used for acceptance testing. Most geotextiles can be tested by this method. This test method is applicable for testing geotextiles either wet or dry. It is used with a constant rate of extension type tension apparatus.

### 3.3.2 Grab Breaking Load and Elongation Test

In grab Breaking Load and Elongation test, a continually increasing load is applied longitudinally to the specimen and the test is carried to rupture. Values for the breaking load and elongation of the test specimen are obtained from machine scales or

dials, autographic recording charts, or interfaced computers. The grab method is applicable whenever it is desired to determine the "effective strength" of the fabric in use, that is, the strength of the material in a specific width, together with the additional strength contributed by adjacent material. There is no simple relationship between grab tests and strip tests since the amount of fabric assistance depends on the construction of the fabric. It is useful as a quality control or acceptance test.

ASTM D 4632 describes the test procedures for Grab breaking and elongation. The test specimen for grab test is rectangular in shape and is cut 4 in by 8 in. Cut specimens are used for grab tests in the machine direction with the longer dimension parallel to the machine direction and the specimen in the cross-machine direction with the longer dimension parallel to the cross-machine direction. Normally 10 (ten) specimens are tested in each direction. The distance between the clamps at the start of the test is set at  $75 \pm 1$  mm ( $3 \pm 0.05$  in). The load range of the testing machine is set such that the maximum load occurs between 10 and 90% of full-scale load. Machine is operated at a speed of  $300 \pm 10$  mm/min ( $12 \pm 0.5$  in/min).

### 3.3.3 Trapezoid Tearing Test

During installation, geotextiles are subjected to tearing stresses. A test simulating such situations is important. The methods developed for such test to date can vary widely. There are three tear tests commonly used: trapezoidal, tongue and Elmendorf. Trapezoid tearing load is the force required to break individual yarns in a fabric. ASTM D 4533-91 describes this test. As per this test, an outline of an isosceles trapezoid is marked on a rectangular specimen cut for the determination of tearing strength as shown in Fig 3.11, and nonparallel sides of the trapezoid marked on the specimen are clamped in parallel jaws of a tensile testing machine. The separation of the jaws is continuously increased so that tear propagates across the specimen. At the same time, the force developed is recorded. The tearing strength, which is the maximum value of the tearing force, is obtained from the autographic force-extension curve. The trapezoid tear method produces tension along a reasonably defined course such that the tear propagates across the width of the specimen. The trapezoid tearing strength for woven fabrics is determined primarily by the properties of the yarns that

are gripped in the clamps. In nonwoven fabrics, because the individual fibres are more or less randomly oriented and capable of some reorientation in the direction of the applied load, the maximum trapezoid tearing strength is reached when the required to rupture one or more fibres simultaneously.

The trapezoid tearing strength method is useful for estimating the relative tear resistance of different fabrics or different directions in the same fabric. In this test the rectangular specimen is cut 76.2 by 201.6 mm (3 by 8 in). For the measurement of the tearing strength in the machine (or warp yarns) and cross-machine direction (or filling yarns), the specimens are cut so that the longer dimension parallel to the machine direction and cross machine direction respectively. Each specimen is marked with an isosceles trapezoid template. A preliminary cut 15.9 mm (0.625 in) long at the centre of the 25.4 mm (1 in) edge is made. The distances between the clamps are set at  $25 \pm 1$  mm ( $1 \pm 0.05$  in). The load range of the testing machine is selected such that the maximum load occurs between 15 and 85% of full scale of load. Machine is set to operate at a speed of  $300 \pm 10$  mm/min ( $12 \pm 0.5$  in/min). Ten specimens are tested for each machine and cross-machine direction.

### **3.3.4 Puncture Test**

#### **3.3.4.1 Index Puncture Test**

There is a need for an assessment of geotextile resistance to objects such as stones and stumps under quasi-static conditions. Such a test is described under ASTM D 4833. As per this method, a test specimen is clamped without tension between circular plates of a ring clamp attachment secured in a tensile testing machine; a force is exerted against the center of the unsupported portion of the test specimen by a solid steel rod attached to the load indicator until rupture of the specimen occurs. The maximum force recorded is the value of puncture resistance of the specimen. This test method is an index test for determining the puncture resistance of geotextiles, geomembranes and related products. The use of this test method is to establish an index value by providing standard criteria and a basis for uniform reporting.

The Tensile/Compression Testing Machine to be used for this test must be a constant-rate-of extension (CRE) type, with autographic recorder conforming to the

requirements of Specification D 76 (Fig 3.12). The ring clamp attachment, consisting of concentric plates with an open internal diameter of  $45 \pm 0.025$  mm ( $1.772 \pm 0.001$  in.), capable of clamping the test specimen without slippage. The suggested clamping arrangement as per ASTM D 4833 is shown in Fig 3.13. The external diameter is suggested to be  $100+0.025$  mm ( $3.937 \pm 0.001$  in.). The diameter of the six holes used for securing the ring clamp assembly is suggested to be 8 mm (0.135 in.) and equally spaced at a radius of 37 mm (2.95 in.). The surfaces of these plates can consist of grooves with O-rings or coarse sandpaper bonded onto opposing surfaces. A solid steel rod, with a diameter of  $8 \pm 0.01$  mm ( $0.35 \pm 0.005$  in.) having a fiat end with a  $45^\circ = 0.8$  mm (0.315 in.) chamfered edge contacting the test specimen's surface.

For performing the test, a laboratory sample to be taken from a swatch extending the full width of the geotextile. The sample so taken should exclude material from the outer wrap and inner wrap around the cores unless the sample is taken at the production site. The test specimen to be cut of a diameter 100 mm (4 in) to facilitate clamping. No specimen to be taken nearer the selvage or edge of the geotextile sample than  $1/10$  the width of the geotextile sample. Total 15 specimens to be tested for each type of geotextile. The machine speed to be set  $300+10$  mm (12 in+ $1/2$  in)/min until the puncture rod completely ruptures the test specimen.

This test is a popular one due to its simplicity and its ability to be automated. It is important to note the exact shape of the end of the metal rod. Three types are in current use: hemispherical, flat and beveled flat. The interrelationships and differences between these types have not been identified. The last type, with a 0.8 mm  $45^\circ$  bevel around its circumference is specified in D 4833 as can be seen in. The small size of the device is also of concern. For example, a lightweight nonwoven geotextile can selectively be chosen in a low-density fibre region or in a high-density fibre region. The differences in puncture resistance will be vary large and vary largely. With such a concern in mind, Koerner et al (1986) have developed a large-size puncture test.



### 3.3.4.2 CBR Puncture Test

This test is formalized as ISO/DIS 12236 and in Germany as DIN 54307. It uses a conventional soil-testing CBR plunger and mold as shown in Fig 3.14 and Fig 3.15. As per this test, the penetrating steel rod to be 50 mm in diameter and the geotextile is firmly clamped in an empty mold with a 150 mm inside diameter. The circumference of the plunger should be beveled 0.80 mm on a 45° angle so as not to cut the yarns at the edge of the rod. The laboratory sample to be taken from a swatch extending the full width of the geotextile. The sample so taken should exclude material from the outer wrap and inner wrap around the cores. The test specimen to be cut of a diameter 250mm to facilitate clamping. No specimen to be taken nearer the selvage or edge of the geotextile sample than 1/10 the width of the geotextile sample. Total six specimens to be tested for each type of geotextile. The machine speed to be set 300+10 mm (12 in+1/2 in)/min until the puncture rod completely ruptures the test specimen.

Considering these two types of test, i.e. index puncture and CBR puncture Koerner (1997) opined that the CBR test for puncture strength or as a form of axisymmetric tensile strength has considerable merit.

### 3.3.5 Burst Strength Test

As per ASTM D 3786-79, the burst strength is defined as the force or pressure required to rupture a textile by distending it with a force, applied at right angles to the plane of the fabric, and under specified conditions. There are two test methods which stress geotextiles out of plane, thereby mobilizing tension until failure occurs. The most common is the Mullen burst test (Fig 3.16), which is covered in ASTM D 3786. In this test, an inflatable rubber membrane is used to distort the geotextile into the shape of a hemisphere of 30 mm diameter. The diaphragm is expanded by fluid pressure to the point of specimen rupture. Bursting of the geotextile occurs when no further deformation is possible. The test is widely used for quality control.

The other one uses a large rectangular test specimen and deforms it by an underlying rubber membrane. In this test the geotextile remains very close to plane

strain conditions. As such, the pressure-versus-strain response yields a very accurate modulus. It is a difficult test to setup and perform.

Ten specimens are to be tested for each type of samples. The samples should be at least 5 in (125 mm) square, or circles 5 in (125 mm) in diameter. Specimen need not be cut for testing. It is to be avoided for taking two or more specimens from areas that include the same wale or course yarns, from knitted fabrics.

### 3.3.6 Seam Strength Test

The ends or sides of the geotextiles rolls are joined together for transferring tensile stress. It may be joined by sewing, stapling, heat welding, tying, and gluing. The most common method is by sewing. Where two sections are joined and must withstand tensile stress or where the security of the connection is of prime importance, sewing is the most reliable joining method. Various styles of sewn seams practiced, but whatever the type, they must be laboratory-evaluated for their load-transfer capability from one geotextile roll to another. The ASTM D 4884 describes the details of the test. The comparable ISO test is ISO 10321.

As per ASTM D 4884, a seam, 200 mm (8 in) wide is gripped across the entire width in the clamps of a tensile testing machine, operated at a prescribed rate of extension, applying a longitudinal (perpendicular) force to the specimen until the seam or geotextile ruptures. The results achieved in this test method can more accurately correlate to the seam strength values anticipated in the field and may also be used for acceptance testing of commercial shipments of geotextile.

A constant-rate-of-extension (CRE) type, conforming to Specifications D 76 must be used. The machine must be set to a rate of extension of  $10 \pm 3$  %/min. The clamps shall be wide enough to grip the entire width of the specimen and have the appropriate clamping power to hold the test specimen in place without crushing (damaging) the machine direction and cross-machine direction yarns. At least six specimen to be tested from the laboratory samples. Each specimen should be approximately 250 mm (10 in) wide with a stitch line in the centre for sewn seams or approximately 200 mm (8 in) wide with the seam weld in the centre for thermally

bonded seams running parallel to either the machine direction or cross-machine directions as shown in Fig 3.17 (a) and Fig 3.17 (b) for sewn seams and thermally bonded seams respectively. This wider specimen to be cut for sewn seams to achieve a final test specimen width of 200 mm (8 in). When removing the shaded area from a specimen as shown in the Fig 3.17 (a) & (b), the angles between the 25 mm extensions which are parallel to the seam and that section of the specimen having a finished width of 200 mm is 90°.

Insertion of specimen in the clamps is an important matter for the test. The seam specimen to be mounted centrally in the clamps facing in the open front position. This has to be done by having the two lines, that were previously drawn as close as possible to the inside edges of the lower and upper jaw with the seam centred. The seam and gage lines must be parallel to the clamps as shown in Fig 3.18 (a) and Fig 3.18 (b).

### 3.3.7 General Discussion

Grab tensile strength method was selected as the standard procedure to provide a qualitative assessment of geotextile strength. Since the conventional grab tension tests call for narrow strips with aspect ratios (ratio of clamped width to gage length) less than one this test method is found to be inappropriate to produce representative stress strain behavior of geotextiles. The wide width strip tension test with a specimen aspect ratio of 2:1 appears to provide a more realistic measure of tensile strength and related stress strain behavior for most geotextiles. Normally, the puncture tests are recommended for a wide variety of fabrics to evaluate the bursting strength of the knitted geotextiles. It is not recommended for woven geotextiles. ASTM D 3787-89 method for puncture test is considered satisfactory for an acceptance testing of commercial shipments of knitted geotextiles for bursting strength since the method is used extensively in the trade for acceptance testing. Efforts had been given to correlate between different tensile tests and the plunger puncture test by Moritz and Murray, (1982). The trapezoid tearing load is a tension test in which the strength is determined by the fibers of composite structure, and their

bonding or interlocking. It is also useful for estimating relative ease of tearing of non-woven geotextiles.

The concept of tension testing in geotextiles is closely linked to the use of geotextiles, as an element in soil reinforcement and the perception of "strength" must be broader than a simple stress-strain diagram. Simplicity of procedure and clarity of concept are indispensable if a geotextile tension test is to gain wide acceptance throughout the industry. Tensile test data may be used for various purposes, such as quality control in manufacture, on-site construction controls and in project design.

Various test methods are devised (Andrawes et al. 1984) and suggested for laboratory evaluation of tensile strength of geotextiles. These test methods are designed to simulate the in-situ load and strain conditions of geotextiles; however, all are too complex for routine laboratory use. The load-extension behavior of geotextiles is normally determined by uniaxial testing. There are, however, several types of uniaxial tests.

The importance of the aspect ratio of the test specimen has been demonstrated by McGown et al., (1982). As specified in ASTM D4595-86 (Reapproved 1994), a specimen with an aspect ratio of 2:1 appears to provide a more reproducible measurement of tensile strength and related stress-strain behavior for geotextiles. Essentially the dimensions of the test specimen should be large enough to account for local variability of the geotextile fibers and distribution and reduce the wasting to an acceptable level. The larger specimen size, uniformity of load distribution across the width of the specimen and strain rates with this test seem to comply with many geotechnical applications. A minimum length of 100 mm in the direction of testing is considered satisfactory to account for most Jute geotextiles.

A meaningful laboratory test is required under known boundary conditions to duplicate the in-situ conditions. It must be remembered that the laboratory tensile tests described here relate to geotextiles in isolation, whereas in practice nearly all geotextiles are encapsulated within a confined soil mass. Simulated in situ testing of the geotextiles was performed by McGown et al (1982) where soil was placed vertically with geotextile sheet with the help of two pressure bellows. In many

geotechnical applications the geotextiles are stressed in plane-strain conditions. It is very important to know the boundary conditions of the geotextile specimen before the tensile tests. In a uniaxial test a material may show a brittle and stiff behavior under plane strain while the same material may show a ductile and extensible behavior under plane stress conditions.

Myles and Carswell (1986) used three types of clamping systems for tensile testing. These gripping devices are very expensive and involve large amount of laboratory space. Because of the simplicity associated with the mounting of the specimen roller grips they are used in geotextile's laboratory tests for the determination of different tensile strength characteristics. A significant amount slippage occurs in the geotextile specimen as the applied tensile load increases through the roller grips. Leshchinsky and Fowler (1990) introduced a new technique involving strain gauge attachment on the geotextile specimen to measure the tensile strength of high strength geotextiles. The purpose of this test was to eliminate the edge effect of the wide-width test to represent plane strain conditions. Attachment of strain gauges onto the geotextiles is not simple and requires high skill and proper attention. Using super glue or silicone adhesive onto the natural fibre for cementing the strain gauges is not very effective as was used by Leshchinsky and Fowler (1990).

### **3.4 Friction Behavior**

It is essential to know the soil-to-geotextile friction behavior in many design problems. The coefficient of friction between a geotextile and soil, or between any geotextile combinations selected by the user, is determined by placing the geotextile and one or more contact surfaces, such as soil, within a direct shear box. As Ingold (1982), reported the most common method is the direct shear test used in geotechnical engineering. In this test, a constant normal compressive stress is applied to the specimen (3.19 a), and a tangential (shear) force is applied to the apparatus so that one section of the box moves in relation to the other section. The shear force is recorded as a function of the horizontal displacement of the moving section of the shear box. The test is performed for a minimum of three different normal stresses, selected by the user, to model appropriate field conditions. When the test is repeated at different

normal stresses, the data is plotted, a trend is established, as shown in Fig 3.19 (b), and the parameters of the Mohr-Coulomb failure criterion are obtained. From a comparison of the geotextile-to-soil response versus the soil-to-soil response, the shear strength efficiencies on the soil's cohesion and friction angle can be obtained. It may be noted that the soil's shear-strength parameters are the upper limit, that is, an efficiency of 1.0. Conversely, some interfaces may result in a drop from peak strength to a lower residual strength. This requires the plotting of a second curve (Fig 3.19 c) that will define the residual shear-strength parameters.

Depending upon the type of geotextiles and purpose different sizes of shear boxes are used (Lydick and Zagorski, 1991), (Kokkalis and Papacharisis, 1989). It was found by Dembicki and Jermolowicz (1991) that the friction between soil and geotextile in shear box test depends on various soil and geotextile properties such as dimensions of pores between fibers, their irregularity, normal stress density and gradation coefficient of granular soil, etc. The other type of measuring friction uses inclined plane box where the interface frictional angle was found to be lower than the angle determined from the conventional direct shear box test for the same geotextile specimen (Girard *et al.*, 1990). The ASTM D 5321 direct shear test calls for a shear box of 300 mm X 300 mm in size. Koerner (1997) opined that such a large test box is appropriate for geonets, geogrids and many geocomposites and considers being excessive for geotextiles. Standard geotechnical engineering laboratory shear boxes (e.g., 100 mm X 100 mm), are satisfactory for geotextile testing and focus should be on more relevant shear-strength testing parameters, such as the following than on the box size.

- Use of site-specific soil types
- Control of density and moisture content of the as-placed soil
- Geotextile fixity conditions
- Saturation conditions during consolidation and shear testing
- Actual type of saturation fluid (e.g., leachate)
- Use of field anticipated strain rates
- Adequate shear box deformation to achieve residual shear strength

It was suggested that the high normal stress applied in the direct shear box test causes the soil particles embedded in the geotextile pores causing high value of friction angle. This was contradicted by Koutsourais *et al.* (1991) and suggested that under low normal stresses, dense cohesionless soil with geosynthetics exhibited a higher interface friction angle than higher normal stresses. Clay slurry with very high moisture content cannot be used either in direct shear box or in the inclined plane box.

Muhammad (1993) conducted a study to determine frictional behavior of jute geotextile using a direct shear box. A general view of the test apparatus is shown in Fig 3.20, and its schematic arrangement in Fig 3.21. The shear box was composed of two parts, the upper half that is immovable and the lower half that is capable of sliding. The lower half of the box has its sliding system on ball bearings placed on a special track on a supporting frame, which enabled sliding strictly in one direction. The inside dimensions of the box were 6 cm in length, 6 cm in width and 2 cm in depth. After placing a dummy hard perspex block in the lower half, the jute sheet specimen was firmly wrapped over the box through its bottom. The upper half was then placed over the jute sheet on the bottom half. With sand in the upper half, the shear force could be applied via a variable speed motorized device. The sand was tested in both air-dried and saturated condition during the investigation.

The test was performed by pouring the sand sample into the upper half of the shear box is compacted by placing a 6 cm X 6 cm X 2.5 cm metal block and imparting 20 blows from a 0.75 kg mallet to achieve a dry density of  $1.74 \text{ g/cm}^3$ . The loading plate (platen) was then placed and a normal pressure was then applied. The shearing force was applied through the variable speed motor at a horizontal displacement rate of 1 mm/min until the shear failure occurred. This was indicated by the decrease in peak shear force as registered in the proving ring. The same procedure continued for different magnitudes of normal loads to obtain a well-defined shear stress-normal stress plot. Direct shear tests have been performed for both dry and saturated sand ( $\rho_d = 1.86 \text{ g/cm}^3$ ) by conventional ASTM direct shear method which is applicable for soil.

Wide ranges of normal stresses were applied to obtain the friction between jute geotextile and sand particles. Firstly, the direct shear tests were conducted to

evaluate the friction angle of dry and saturated sand, the stress-strain curves of which are shown in the Fig 3.22 and Fig 3.23 respectively. The shear stresses against shear displacement for saturated sand and with jute of 500 g/m<sup>2</sup> and 600 g/m<sup>2</sup> for varying normal stresses are shown in the Fig 3.24 and Fig 3.25 respectively. Fig 3.26 shows the normal stress versus shear stress for sand and jute geotextiles from which the friction angle can be obtained by measuring the slope.

It was clear that insertion of the geotextile causes a reduction in friction angle. For saturated sand and jute 500 g/m<sup>2</sup> the reduction is 3% while for saturated sand and jute 600 g/m<sup>2</sup> is 7.3%. The internal friction angle for dry sand and saturated sand are found to be 38.4° and 36.9° respectively. The lower value for saturated sand is probably due to the moisture film between saturated sand particles. The reduction in value for friction between jute geotextiles and saturated sand may be due to the smoothness of the geotextile fibers, which are exposed to the sand particles.

### 3.5 Pullout Test

Within the reinforcement function, Geotextiles may be used to provide anchorage for many applications. In this test, geotextiles are laid horizontally between the soil of the lower and upper case of shear test apparatus. The shear boxes are immovable and the geotextile is stretched by pulling one end externally. By measuring, the pull out stress at different applied normal stress the angle of friction can be determined. It was found by Rao and Pandey (1988) that the friction values obtained by pull out tests were much higher than that obtained by direct shear test. The strain required to mobilize full friction is observed to be much more in the case of pull out test than that in the direct shear test. During the pull out test the geotextile is pulled against the stationary soil mass, therefore a considerable amount of total strain is used to cause extension in the geotextile strip and the rest of strain is used to mobilize interface friction. Hence, the total strain is a combination of the tensile strain and the strain required for mobilizing friction. This indicates that a larger portion of applied pull stress is used up by the geotextile itself causing higher value of interface friction. The above-mentioned conventional procedures to measure the interface friction between geotextile and soil, which are dependant on a number of factors, are



only applicable for granular soil and geotextile interface. Measuring interface friction between clay slurry of very high water content and natural geotextile is somewhat a new idea in the field of geotextile application. Muhammad (1993) conducted two different techniques in a research. Details of the test procedure and various parameters involved are discussed in subsequent paragraph.

Schematic diagram of the pull out test apparatus is shown in Fig 3.27 and a general view of the prototype-testing device is shown in Fig 3.29. In this test, the geotextile specimen is held with a 6 cm diameter and 1 cm thick circular lightweight perspex disc on which the normal loads are applied. A 6 cm diameter hole with 2 cm deep is grooved on a rectangular perspex box. A nylon smooth thread is connected to the circular perspex disc, which can be pulled over a frictionless pulley by a set of weights. This low friction pulley is inserted into a vertical stand which is fixed at the top of the device where the pulley can be adjusted up or down. Firstly, the saturated sand is poured into the hole in such a way that the depth of the sand specimen is higher than the depth of the hole and to achieve the same dry density of sand as that of direct shear box test. The circular Perspex disc wrapped with the jute geotextile is then placed on the saturated sand. The connected thread is passed over the smooth pulley with its weight pan on the other side. A low magnitude of normal weight is then placed on the circular disc. Weights are placed on the pan to pull the circular disc horizontally. These are then increased gradually to record down the exact shearing force, which will cause the geotextile slip or fail against the sand particles. This process is continued for different normal loads to obtain the corresponding shearing loads. Graphs for shearing stress versus normal stress were plotted to obtain the friction between jute geotextiles and sand particles.

Two different jute geotextiles are used with dry and saturated sand. The results of the pull out tests are shown in the Fig 3.28. It is found that the frictional values for jute 500 g/m<sup>2</sup> and jute 600 g/m<sup>2</sup> are 34.3° and 31.7° respectively, which are lower than the values obtained from the direct shear tests. This may be due to less shearing stress developed in the pull out test and low magnitude of applied normal pressure.

Test results by Collios et al. [36] show a relationship of pullout test results to shear test results with some notable exceptions. For pullout testing, if the soil particles

are smaller than the geotextile openings, efficiencies are high; if not, they can be low. In all cases, however, pullout test resistances are less than the sum of the direct shear test resistances. This is due to the fact that the geotextile is taut in the pullout test and exhibits large deformations. This, in turn, causes the soil particles to reorient themselves into a reduced shear strength mode at the soil-to-geotextile interfaces, resulting in lower pullout resistance. The stress state mobilized in this test is a very complex one requiring additional research.

### **3.6 Hydraulic Properties**

Hydraulic tests on geotextiles involve new and original tests concepts, methods, devices, interpretation and databases. The hydraulic tests are necessary and tremendously important. It has both geotextile tests in-isolation and with soil. The tests which will be discussed are:

1. Apparent Opening Size
2. Permittivity (Cross-Plane Permeability)
3. Transmissivity (In-Plane Permeability)

#### **3.6.1 Apparent Opening Size (AOS)**

Opening pore size of the fabric controls the filtration performance of a geotextile. Pore size of the fabric should therefore determine the retention ability of soil grains and permeability of water. The ideal retention criteria for fabrics should specify an appropriate fabric pore structure in order to provide adequate seepage and to prevent piping in the soil and clogging in the fabric. Fabric pore size distribution is the key parameter that controls a fabric's ability to retain the soil grains. Different effective pore sizes have been described by Ogink (1975). A term "Steepness factor" defined as  $O_{50}/O_{98}$ , where  $O_{50}$  and  $O_{98}$  are 50% and 98% opening sizes respectively, is used for determining retention criteria. A high steepness factor of 0.8 to 0.9 is considered as typically favorable while a value of 0.3 to 0.4 is unsuitable for soil retention.

Calhoun (1972) developed a test for equivalent opening size (EOS) to characterize the soil particle retention ability of various fabrics. The test involved in the determination of the size of the rounded sand particles which when sieved through the fabric will pass only 5% or less by weight. The EOS was defined as the "retention on" size of that fraction expressed as a U.S. standard sieve number. The EOS test only provides a method for determining the relative size of the largest straight through openings in a fabric. Two fabrics may have similar EOS values but dramatically different pore structures and porosities, for example, those found in woven versus non-woven fabrics.

Apparent Opening Size (AOS),  $O_{95}$  is a property of geotextile, which indicates the approximate largest particle that would effectively pass through the geotextile. A test for measuring the apparent opening size was developed by the U.S. Army Corps of Engineers to evaluate woven geotextiles. The test has since been extended to cover all geotextiles, including the nonwoven types. The AOS or equivalent opening size (EOS) is essentially same. The equivalent ASTM test is designed D 4751. The test uses known diameter glass beads and determines the  $O_{95}$  size by standard dry sieving. Sieving is done using beads of successively larger diameters until the weight of beads passing through the test specimen is 5%. This defines the  $O_{95}$  size of the geotextiles' opening in millimeters. It may be noted here that the  $O_{95}$  value only defines the one particular void size of the geotextile and not the total pore size distribution. AOS, EOS and  $O_{95}$  all refer to the same specific pore size, the difference being that AOS and EOS are sieve numbers, while  $O_{95}$  is the corresponding sieve-opening size in millimeters.

In the ASTM sieving method, a geotextile specimen is placed in a sieve frame (Fig 3.30), then standard glass beads are placed on the geotextile surface, a mechanical sieve Shaker shakes the geotextile and frame laterally. It imparts lateral and vertical motion to sieve, causing the particles thereon to bounce and turn so as to present different orientations to the sieving surface. The procedure is repeated on a new specimen of the same type of geotextile with other various sizes of glass beads until its equivalent or apparent opening size is determined. AOS is that bead size for which 5% or less of the beads pass through the fabric. The ASTM committee D-35 suggests using "static masters" to eliminate the build up of static electricity and to

soak the fabric in water to remove the surface coating which may act to clog some of the openings. As a laboratory sample for acceptance testing, a full width swatch 1 m (1 yd) long from the end of each roll of fabrics is taken in the lot sample, after first discarding a minimum of 1 m (1 yd) of fabric from the very outside of the roll. Five specimens from each swatch in the laboratory sample is cut to fit the appropriate sieve pan.

The AOS test is a poor test. This technique is very time consuming and tedious. Many geotextiles do not have surface films and in general natural geotextiles may not build up much static electricity during shaking. In order to subject all fabrics to the same simple procedure for pore-size measurement, a modified method is developed using a dry sieve analysis, which aims at establishing a characterization of a fabric with respect to size and uniformity. According to ASTM for AOS test, the geotextile has to be changed after using a particular uniform size of glass beads to maintain the jute fabric opening at each time of testing. The proposed method uses only one specimen to get the value of AOS.

Using a geotextile as a medium to retain soil particles necessitates compatibility between it and the adjacent soil. This test method is used to indicate the apparent opening size in a geotextile, which reflects the approximate largest opening dimension available for soil to pass through. Test Method D 4751 for the determination of opening size of geotextiles is acceptable for testing of commercial shipments of geotextiles.

### **3.6.2 Permittivity (Cross-Plane Permeability)**

One of the major functions that geotextiles perform is filtration. In filtration, the liquid flows perpendicularly through the geotextile into crushed stone, a perforated pipe, or some other drainage system. It is important that the geotextile allow this flow to occur without being impeded. The geotextile's cross-plane permeability is defined with the term Permittivity ( $\Psi$ ). Permittivity is an indicator of the quantity of water that can pass through a geotextile in an isolated condition. As per ASTM D 4439-98 Permittivity, ( $\Psi$ ), (T-1), of geotextiles is defined as the

volumetric flow rate of water per unit cross sectional area per unit head under laminar flow conditions, in the normal direction through a geotextile.

$$\Psi = \frac{k_n}{t}$$

Where

$\Psi$  = permittivity ( $s^{-1}$ )

$k_n$  = permeability (properly called hydraulic conductivity) normal to the geotextile (m/s), and

$t$  = thickness of the geotextile (m)

The ASTM D 4431-98 uses a device as shown in Fig 3.31 to measure the permittivity of geotextile test specimens. It is similar to ISO/DIS 11058. By this method either Constant head or Falling head can be used, although the standard is written around the constant head test at a head of 50 mm. The important test consideration for this test are preconditioning of the fabric, temperature and the use of de-aired water. ASTM D4491 requires a dissolved oxygen content of less than 6.0 mg/l. Tap water is allowed unless dispute arise, in which case de-ionized water should be used.

In Constant head test, a head of 50 mm (2 in) of water is maintained on the geotextile throughout the test. The quantity of flow is measured versus time. The constant head test is used when the flow rate of water through the geotextile is so large that it is difficult to obtain readings of head change versus time in the falling head test. In Falling head test a column of water is allowed to flow through the geotextile and readings of head changes versus time are taken. The flow rate of water through the geotextile must be slow enough to obtain accurate readings.

In order to obtain a representative value of permittivity, a specimen of 1-m<sup>2</sup> (1-yd<sup>2</sup>) is taken. As per Fig 3.32 four specimens, A, B, C, and D are selected. Specimen A is taken from the centre of the sample, B is taken at one corner (centre located 200 mm (8 in) from the corner), C is taken from midway between A and B, and D is taken from the same distance from A as C, located on a line with A, B and C. The diameters of the cut specimen are considered as 73 mm (2.87 in) so that it fits the

testing apparatus. The specimen is conditioned by soaking in a closed container of deaired water, at room conditions, for a period of 2 hour. The minimum specimen diameter is to be 25 mm (1 in).

The permittivity test described so long, has the geotextile test specimen under zero normal stress, a situation rarely encountered in the field. To make the test more performance-oriented, numerous attempts to construct a permittivity-under-load device have been made. Generally a number of layers of geotextile (from 2 to 5 layers) are placed upon one another with an open-mesh stainless steel grid on top and bottom. This assembly is placed inside a permeameter and loaded normally via ceramic balls of approximately 12 mm diameter. Thus normal stress is imposed on the geotextile, but flow is only nominally restricted. Loading by soil it self (which would definitely affect flow) is completely avoided. The test has been standardized by ASTM D 5493.

### 3.6.3 Transmissivity (In-Plane Permeability)

For the flow of water within the plane of the geotextile (e.g., in the utilization of the drainage function), the variation in geotextile thickness (its compressibility under load) is again a major issue. Thus transmissivity ( $\theta$ ) was introduced.

$$q = k_p i A = k_p i (W \times t)$$

$$k_p t = \theta = q/iW$$

Where

$\theta$  = transmissivity of the geotextile ( $m^2/s$  or  $m^3/s\cdot m$ )

$k_p$  = permeability (hydraulic conductivity) in the plane of the geotextile (m/s)

$t$  = thickness of the geotextile (m)

$q$  = flow rate ( $m^3/s$ )

$W$  = width of the geotextile (dimensionless) =  $\Delta h/L$

$\Delta h$  = total head lost (m) and  $L$  = length of the geotextile (m)

As per ASTM D 4716-95, Hydraulic Transmissivity, ( $\theta$ ), for a geosynthetic is the volumetric flow rate per unit width of specimen per unit gradient in a direction parallel to the plane of the specimen. A number of test devices are configured to

model the above formulation, where liquid (usually water) flows in the plane of the geotextile (of dimensions  $L \times W \times t$ ) in a parallel flow trajectory; ASTM D 4716 and ISO/DIS 12958 use such a device (Fig 3.33).

The flow rate per unit width is determined by measuring the quantity of water that passes through a test specimen in a specific time interval under a specific normal stress and a specific hydraulic gradient. The hydraulic gradient ( $s$ ) and specimen contact surfaces are selected by the user either as an index test or as a performance test to model a given set of field parameters closely as possible. Measurements may be repeated under increasing normal stresses selected by the user. Hydraulic transmissivity should be determined only for tests or for specific regions of tests that exhibit a linear flow rate per unit width versus gradient relationship, that is, laminar flow.

This test method is intended either as an index test or as a performance test used to determine and compare the flow rate per unit width of one or several candidate geosynthetics under specific conditions. This test method may be used as an index test for acceptance testing of commercial shipments of geosynthetics but caution is advised since information on between-laboratory precision of this test method is incomplete.

A schematic drawing of an assembly is shown in Fig 3.34. It consists of a base and a reservoir. The sturdy metal base has smooth flat bottom and sides are capable of holding a test specimen of sufficient area and thickness. The reservoir is a clear plastic or glass extending the full width of the base. The height of the reservoir is at least equal to the total length of the specimen. A catch trough extending the entire width of the base is provided for collection and measurement of the outflow from the specimen.

Three specimens are removed from each laboratory sample that is spaced along a diagonal extending across the swatch. Specimens are cut such that the longer dimension is parallel to the geotextile direction to be tested. The specimen width and length is kept as 300 mm (12 in) and 350 mm (14 in) respectively, or the length to allow the specimen to extend into the reservoir and weir a distance of 25 mm (1 in) whichever is greater. Normally three gradients are selected from 0.05, 0.10, 0.25,

0.50, and 1.0. The flow rate testing is performed using a minimum of three applied normal stresses selected from the following values: 10, 25, 50, 100, 250 and 500 kPa.

### **3.7 Endurance Properties**

The physical, mechanical and hydraulic properties determine the short-term material behavior of the as-manufactured fabrics. The behavior during service conditions over the design lifetime of the system is determined by the endurance properties.

#### **3.7.1 Installation Damage**

Harsh installation stresses can cause geotextile damage. These stresses sometimes might become more severe than actual design stresses for which geotextile is intended. There are a number of studies available, but most involve the removal of the geotextile after a considerable time, usually years. A survey conducted by Koerner and Koerner (1990) in order to assess the installation damage of geotextiles involving hundred field sites. Geotextiles were evaluated by removing approximately 1.0 m<sup>2</sup> within hours after placement. Most of the geotextiles were used for highway base separation, but some were for embankments, walls, underdrains, erosion control, staging areas, access ways, and so on. The entire exhumed sample was brought into the laboratory along with an equal size of the unused and uninstalled geotextile for comparison purposes. Test specimens were taken from both the exhumed and unused geotextiles, and were tested. A percent strength reduction was calculated. The mechanical tests those were performed are, grab tensile, puncture resistance, trapezoidal-tear resistance, burst resistance, wide-width strength in machine direction and wide-width strength in cross-machine direction.

From the whole assessment of the exhumed geotextiles Koerner and Koerner (1990) suggests that no geotextile less than 270 g/m<sup>2</sup> should be used unless special precautions are taken, such as a sand cushioning layer along with lightweight construction equipment, to avoid installation damage.



### 3.7.2 Creep under Constant Stress

Creep is commonly defined as the time-dependent increase accumulative strain in a material resulting from an applied constant force. The most undesirable property of polymer is the tendency to creep. It is an important property to evaluate on polymers because it is considered as creep sensitive material. The test specimens are considered of the wide-width variety and are usually stressed by means of stationary hanging weighs. Since the test duration is long, a number of tests are often conducted simultaneously by cascading the test specimens and their respective loads. The setup can also be horizontal with a number of specimens connected to one another. The schematic diagram of the test arrangement for geotextile and geogrid are shown in Fig 3.35 and Fig 3.36 respectively.

ASTM D 5262-97 describes the detail of this test. Selection of the load in creep test is important and is usually based on a percentage of the geotextile's strength as determined from a conventional test such as Wide-width tensile test etc. Considering the maximum tensile strength as 100%, creep test stresses 10%, 20%, 40%, and 60% are sometimes evaluated. Stresses are commonly applied for 1,000 to 10,000 hours and readings are taken at progressively longer time increments from the beginning of the test (e.g. 1, 2, 5, 10 and 30 minutes; then 1, 2, 5, 10, 30, 100, 200, 500 and 1000 hours. For creep tests longer than 1000 hours readings every 500 hr are usually adequate. The elongation or percent strain versus time is plotted for each stress increment. The qualitative plots are shown in Fig 3.37. From this plot isochronous curves are then developed.

Isochronous curves are the plots of load versus strain at the same temperature from different loading tests. In order to obtain isochronous (load-strain) curves materials (specimen) are subjected to a series of loads  $P_1$ ,  $P_2$  and  $P_3$  at time  $t_0$  and sustained as shown in the Fig 3.38, which is a plot of load versus time. The plots of total strain against time for the above loadings are constructed as shown in the Fig 3.39 (a) for elasto-visco-plastic materials following the procedure described below. For any time  $t_1$ , total strain values corresponding to the loads  $P_1$ ,  $P_2$  and  $P_3$  are scaled off from the figures (a) of total strain-time plots. In the same manner for any time  $t_2$  and  $t_3$ , corresponding strain values to the loads are obtained from the same figures and

marked on the plots of load versus strain. These points corresponding to different time's  $t_1$ ,  $t_2$  and  $t_3$  respectively, are joined to produce curves for  $t_1$ ,  $t_2$  and  $t_3$  respectively. Thus a family of curves is obtained. The typical isochronous curves for elasto-visco-plastic materials are shown in the Fig 3.39 (b).

Each of the test methodologies involves different form of data presentation and for a particular test; several forms of data presentation can be used. The most widely applicable form of presenting these data is in the form of isochronous Load-Strain curves at a constant temperature. Commonly, these are produced from sustained load (creep) test data. However, they can also be produced from most test procedures, for example CRS test. It should be noted that the areas under the Isochronous Load-Strain curves represent the absorbed Strain Energy at the specific time and limiting strain and may be termed as the Isochronous Strain Energy.

This test method should be used to characterize geosynthetics intended for use in applications in which creep is of concern. The plane strain condition imposed during testing must be considered when using the test results for design. The basic distinctions between this test method and other test methods for measuring tension creep behavior are the width of the specimens tested and the measurement of total elongation from the time or specimen of loading. The greater widths of the specimens specified in this test methods minimize the contraction edge effect (necking) that occurs in many geosynthetic materials and provides a closer relationship to actual material behavior in plane strain tension condition.

Different researchers, organizations and institutions have performed numerous studies/research on creep behavior. Table 2.1 lists various investigations to study creep behavior of polymeric material. Creep is a function of stress level, temperature and material type. It is generally recognized that thermal contraction and expansion, associated with small temperature changes during the test, may produce changes in the apparent creep rate, especially near the transition temperature.

### 3.7.3 Creep under Confined Stress

McGown et al performed confined creep test with the confined wide-width tensile test device. Fig 3.40 shows the general tendency of the creep behavior of geotextiles which improve with soil confinement. This test reveals that the major improvement occurs with nonwoven needle-punched geotextiles, followed by other nonwovens, and then by woven geotextiles. This test is time consuming to perform but very important to set realistic creep-reduction factors.

### 3.7.4 Abrasion Behavior

When in service, the abrasion of geotextiles can be the cause of the failure of soil-geotextile systems. ASTM D1175 describes the test methods for abrasion resistance of textile fabrics and cover six procedures: inflated diaphragm; flexing and abrasion; oscillatory cylinder; rotary platform, double head; uniform abrasion; and impeller tumble. In all cases, abrasion is defined as "the wearing away of any part of a material by rubbing against another surface." There are, however, a large number of variables to be considered in such a test. Results are reported as the percent weight lost or strength/elongation retained under the specified test and its particular conditions.

Koerner (1997) describes one of the tests for evaluating the abrasion resistance of geotextiles. It uses a rotary platform, double head method. In the test, both heads are fitted with 1000 g weights and vitrified abrasion wheels. The test specimen is disk-shaped with a 90 mm outer diameter and a 60 mm inner diameter. The specimen is placed on a rubber base on the platform, which is rotated and abraded by the stationary abrasion wheels for up to 1000 cycles. Two strip tensile specimens are cut from the abraded geotextile and tested for their tensile strengths. The average value is then compared to the tensile strength of the nonabraded geotextile and the results are reported as a percentage of strength retained by the geotextile after abrasion. The percentage of elongation retained after abrasion is reported in Fig 3.41, gives the results for different types of geotextiles, all of which are approximately 200 g/m<sup>2</sup>.

Table 3.1 Creep Behavior of Polymeric Material

Ser no	Author/ Investigator	Year	Material Tested	Creep Mechanism
1	Holtz, Broms	1977	Polyester Fabric	$b = 0.14$ to $0.1 B$
2	Finnigan	1977	a. Polyester b. Polyamide c. Polypropylene	0.14 to 0.18 $b = 0.22$ to $0.36$ 1.44 (worst)
3	Van Leevnen J.H.	1977	a. Polyester b. Poly amide c. Polypropylene	0.14 to 0.22 $b = 0.22$ to $0.36$ 1.44
4	Haliburton Anglin and Lawmssteir	1978	High tensile strength fabric	$b$ is zero to moderate and high. Test is useful to identify whether fabric is susceptible to creep or not
5	Shrestha, Bell	1980	-	The creep mechanism is complex and needs considerable research.
6	McGown et al	1982	a. Bidim u 24 - Polyester b. Terram 1000 Polypropylene (100%) & Polyethylene (33%)	Creep tests done in (i) Unconfined & in-isolation, and (ii) confined in-soil conditions. Substantial reductions in strain are observed when confined in-soil, the initial strain were less. Unconfined in-isolation creep test over estimates long-term operational strains.
7.	National Highway institute FHA	1985		Creep potential $p_c$ , i.e. Ratio of time dependent elongation to initial elongation for unconfined and confined conditions has been reported. Use of unconfined tensile creep to develop design has been advocated.
8.	P.R. Ranfcolor (Bidim Published literature)	19B1	a. Spun bound Polypropylene Bidim U64,U44, U23, U34  b. Polyester, Polyaramid & Woven PP Needle-punched PP	Creep behavior under a load of 20% of breaking strength was studied. Polyester rapidly achieved stability while polypropylene was deformed and finally reached breaking point.  Polyester and polyaramid showed similar behavior while polypropylene has high creep coefficient and finally reached breaking point.
9.	Green Wood JH Era Technology Limited (ICI UK)	1986	a. Polyester  b. Polypropy	The creep behavior of yarn and fabric were studied. The creep coefficient was of similar order for both as obtained by Finnigan (1977). Creep of woven fabric is considerably higher than that for the yarn.  Creep behavior of yarn depended upon stress. It is non-linear. Creep is very high at 60% of breaking load. Creep of woven and nonwoven fabrics showed concave behavior and it reached breaking point within 1000 hours.

(after Desai et al, 1988)

Presently ASTM and ISO tests are, though many devices are commercially available to perform it. The descriptions for this test are available I ASTM D 4886 and ISO 13427 respectively. Koerner opined that all of these tests, however, are questionable simulators of field abrasion conditions. In many cases it would be better to use some sort of tumble test, such as the German Test Standard DIN 5385, which is a large test using basalt-stone aggregate abrading a geotextile test specimen within a 1.0 m diameter rotating drum.

### **3.8 Materials Selected for Test**

A careful thought has been given in selecting the samples for the research. For collecting samples, International Jute Study Group (IJSG), Jute Diversification Promotion Centre (JDPC) Bangladesh Jute Mills Corporation (BJMC) and Bangladesh Jute Research Institute (BJRI) were contacted.

The International Jute Study Group is an intergovernmental body set up under the aegis of UNCTAD to function as the International Commodity Body (ICB) for Jute, Kenaf and other Allied Fibres. The IJSG is the legal successor to the erstwhile International Jute Organization (IJO), was established on 27 April 2002, to administer the provisions and supervise the operations of the Agreement establishing the Terms of Reference of the International Jute Study Group, 2001. The organization is the outcome of a series of meetings and UNCTAD conferences, which commenced in March 2000 in Geneva and concluded in April 2001 in Geneva. The head office of this organization is situated in Manipurpara, Dhaka. Jute Diversification Promotion Centre (JDPC) was set up by the Ministry of Jute, Government of Bangladesh through an Office Memorandum on 31 October 2002. The JDPC has been created with the vision of reviving the past glory of jute as "Golden Fibre" through extension of uses of jute by vertical and horizontal diversification and thereby improving the socio-economic conditions of the all section of people involved directly and indirectly with the Jute Sector. The Bangladesh Jute Mills Corporation (BJMC) was established on 1972 in order to overall operation, management, maintenance and future development agenda of all the jute mills of Bangladesh, considered as the world's largest state owned manufacturer and exporter of jute products. Bangladesh Jute

Research Institute is regarded as the countries oldest and only jute research organization, established on 1951 in order to regulate, control and promote agricultural, technological and economic research on jute and allied fibres and their manufactures and dissemination of results thereof.

Considering the climatic condition, BJRI has developed as many as fifty types of jute products by blending jute with hydrophobic fibre like coir or by modification with bitumen, latex, wax resinous materials with the collaboration of BJMC and other governmental and non-governmental organizations since its inception of technological research on jute since 1963. Four untreated samples were selected from BJRI and BJMC (Fig 3.42). Amongst them three samples were treated with bitumen (Fig 3.43) by BJRI as per the procedure described in para 2.3.5.4 (a). The treated samples selected so that the test results can be compared with untreated one. The salient properties of the samples are presented in Table 3.2.

It may be mentioned that none of these samples were manufactured for the purpose of geotechnical engineering application. These samples are selected for this study for inclusion of materials having varied physical and structural properties and also local market availability. The Jute is a densely woven fabric by using relatively flat type of yarn. It is manufactured in BJRI sample producing factory mainly for research purpose. The Canvas is a very densely woven fabric, woven by round twisted yarns. Canvas used to mainly produced in ABC Mill of Adamjee Jute Mills. After the layoff of Adamjee Jute Mills, all the machines were transferred to Latif Bawany Jute Mills situated at Demra of Dhaka. The Canvas is the least porous out of the four and is now produced in Latif Bawany Jute Mills. The Twill is also woven by using relatively flat type yarns like Jute. It is manufactured in many jute mills of Bangladesh. The Hessian is the most porous amongst four and produced in all the jute mills of Bangladesh. It is used extensively in different works.

### **3.9 Tests Performed**

It is mentioned in chapter 2 that since there are no specific standard test methods for determining or evaluating physical, mechanical and hydraulic properties of geojute, which are fast becoming attractive in the field of geotechnical engineering

because of its ecological, economical and aesthetical advantages to date, the methods commonly employed for geotextiles are adopted.

To determine the physical properties of geojute three tests have been performed. Six tests were performed to determine the mechanical properties. To determine the hydraulic properties three tests were performed. Creep test has been performed to determine long term tensile strength. As a whole total thirteen tests were performed. Twelve tests have been performed as per ASTM test standards and one test has been performed as per DIN (Germany) standard. An overview of tests performed is shown in Table 3.3.

**Table 3.2: Salient Properties of Samples**

Trade Name	Source	Condition	Commercial Characteristics			
			Width (inch)	Wt. (oz/yd <sup>2</sup> )	Colour	Packing (yds/bale)
Jute	BJRI	Treated & Untreated	40-50	18-35	black & natural	500
Canvas	BJMC	Treated & Untreated	36-45	14-20	black & natural	1000
DW (Double Works) Twill	BJMC	Treated & Untreated	20-30	11-24	black & natural	500/1000
Hessian	BJMC	Treated	22-80	5-14	natural	700/2000

Source: Bangladesh Jute Mills Corporation Handout, 2003

**Table 3.3 Tests Performed in the Research Work**

SL	ASTM/ DIN No	ASTM/DIN Test Name	Properties to be determined
1	D 5261	Standard Test Method for Measuring Mass per Unit Area of Geotextiles	Physical Properties
2	D 5199	Standard Test Method for Measuring the Nominal Thickness of Geosynthetics	Physical Properties
3	D 1117	Standard Test Method for Determining Absorbency Time and Absorptive Capacity of Non-oven Fabrics	Physical Properties
4	D 4595	Standard Test Method for Tensile Properties of Geotextiles by the Wide-Width Strip Method	Mechanical Properties
5	D 4632	Standard Test Method for Grab Breaking Load and Elongation of Geotextiles	Mechanical Properties
6	D4533	Standard Test Method for Trapezoid Tearing Strength of Geotextiles	Mechanical Properties
7	D 4833	Standard Test Method for Index Puncture Resistance of Geotextiles	Mechanical Properties
8	DIN 54307	CBR Puncture Resistance	Mechanical Properties
9	D 3786	Standard Test Method for Hydraulic Bursting Strength of Knitted Goods and Nonwoven Fabrics	Mechanical Properties
10	D 4751	Standard Test Method for Determining Apparent Opening Size of a Geotextile	Hydraulic Properties
11	D 4491	Standard Test Methods for Water Permeability of Geotextiles by Permittivity	Hydraulic
12	D 4716	Test Method for Determining the (In-plane) Flow Rate per Unit Width and Hydraulic Transmissivity	Properties
13	D 5262	Standard Test Method for Evaluating Unconfined Tension Creep Behavior of Geosynthetics	Long term tensile strength



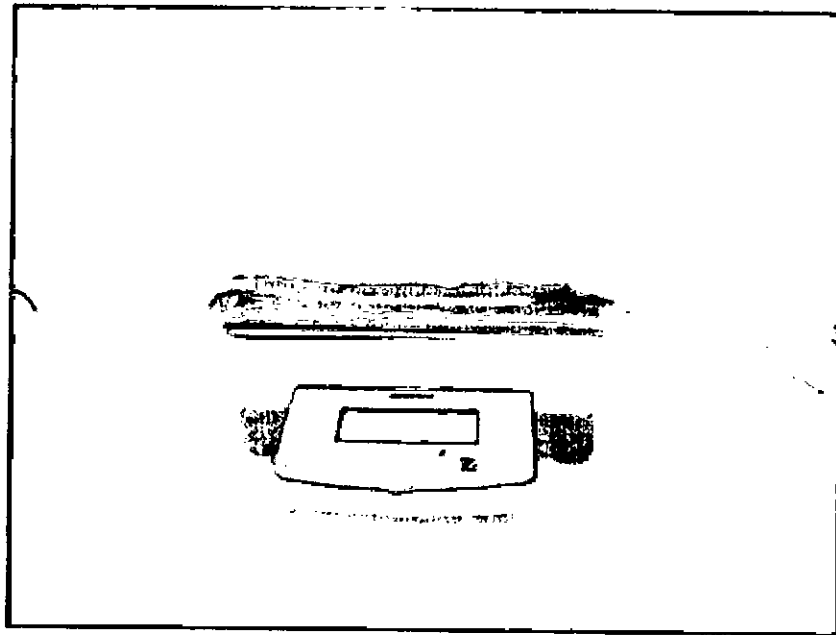


Fig 3.1 Measuring mass per unit area

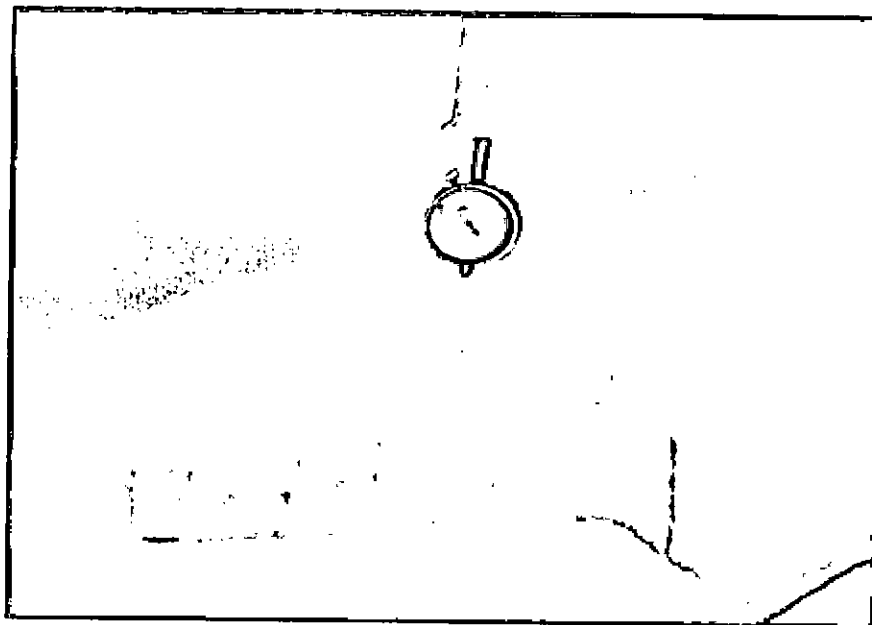


Fig 3.2 Measuring thickness of Geojute

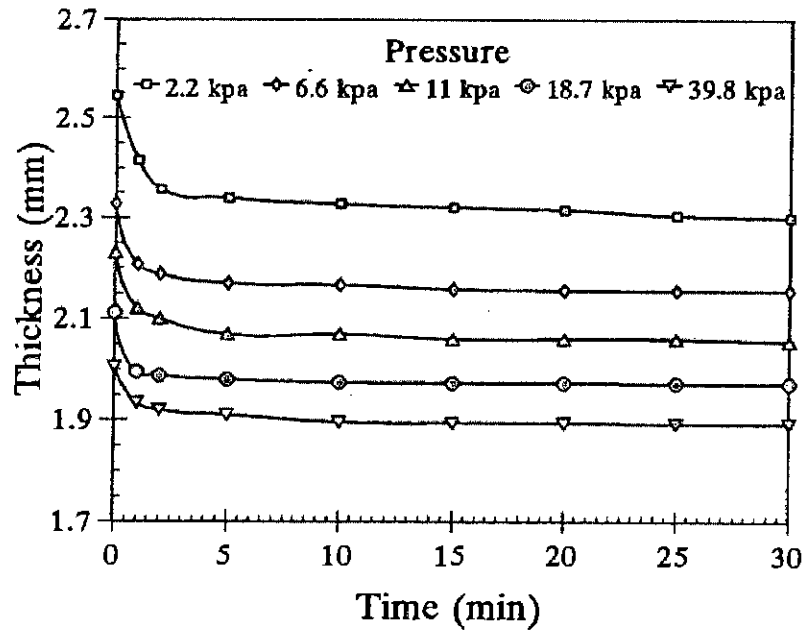


Fig 3.3 Variation of thickness with time for different applied pressure (after Muhammad, 1993)

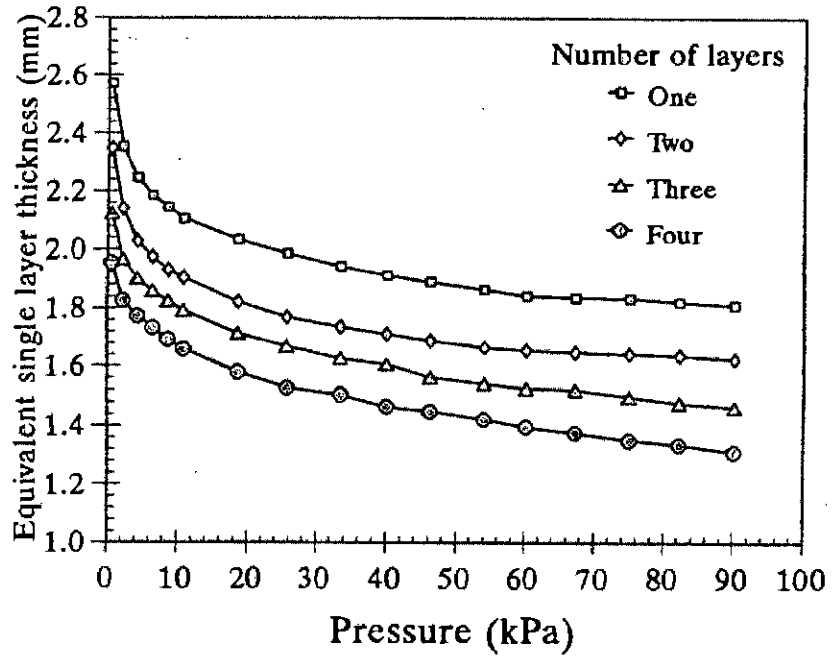


Fig 3.4 Variation of equivalent single layer thickness with applied pressure for different number of layers (after Muhammad, 1993)

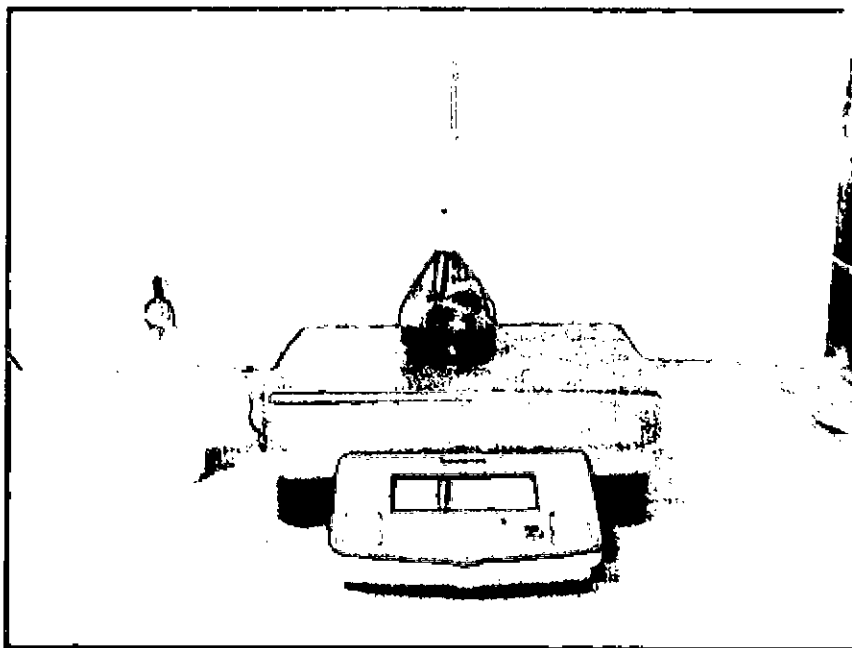


Fig 3.5 Determination of specific density

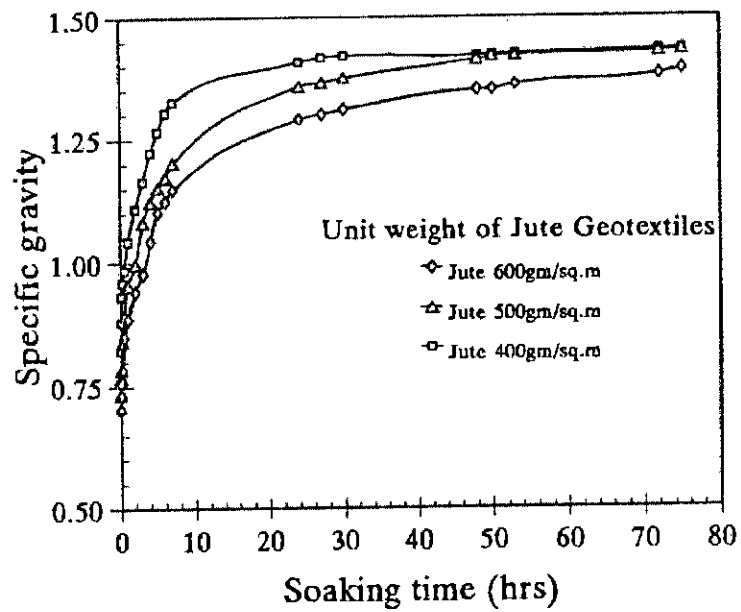


Fig 3.6 Variation of specific gravity with soaking time for different types of jute geotextiles (after Muhammad, 1993)

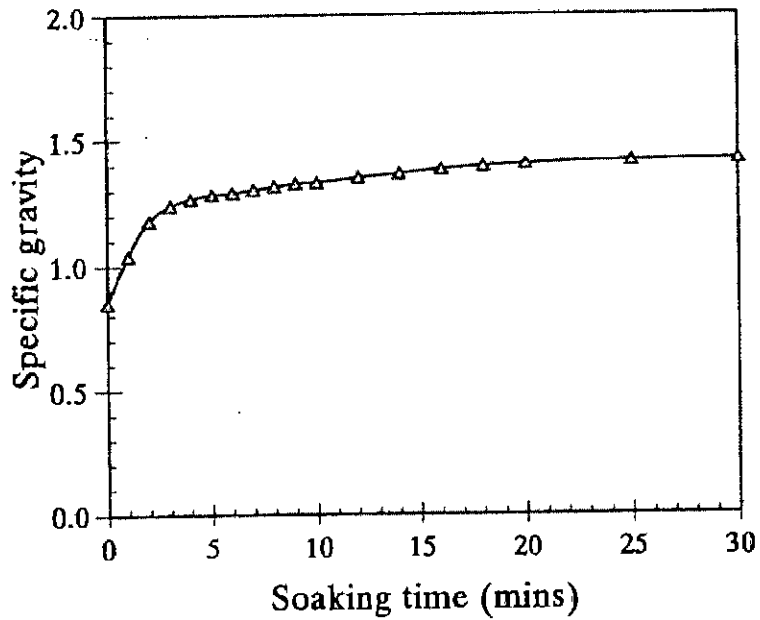


Fig 3.7 Variation of specific gravity with time for untwisted loose jute geotextile fibres using vacuum (after Muhammad, 1993)

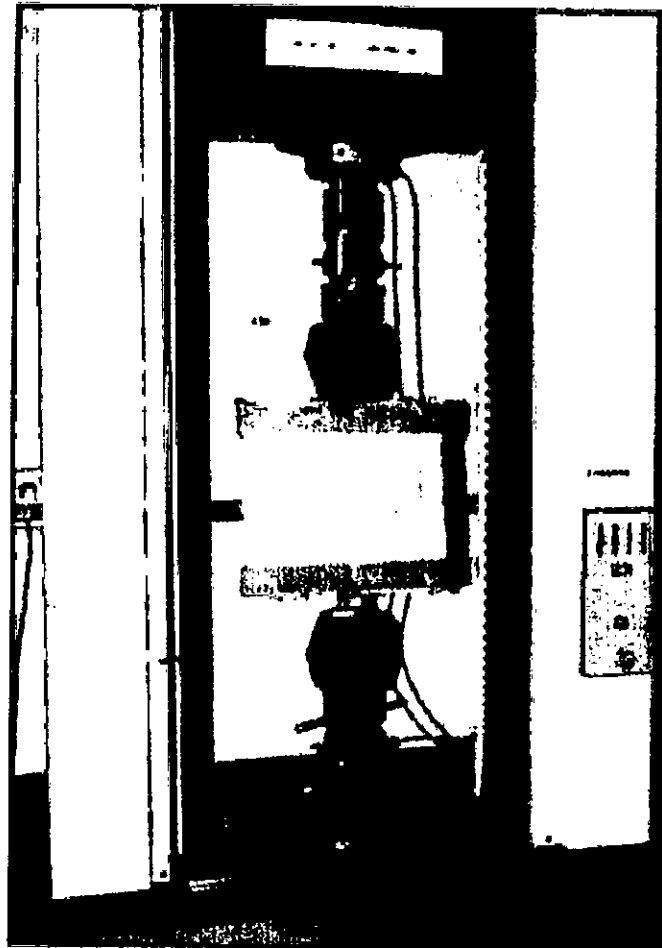


Fig 3.8 Wide width strip tensile test using Autograph Instron machine (after Muhammad, 1993)

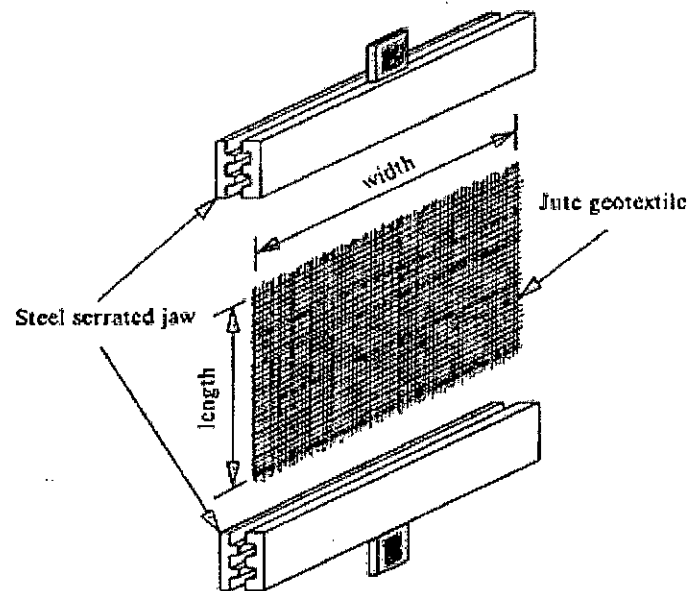


Fig 3.9 Special jaws with serrated faces for uniaxial wide width strip tensile test (after Muhammad, 1993)

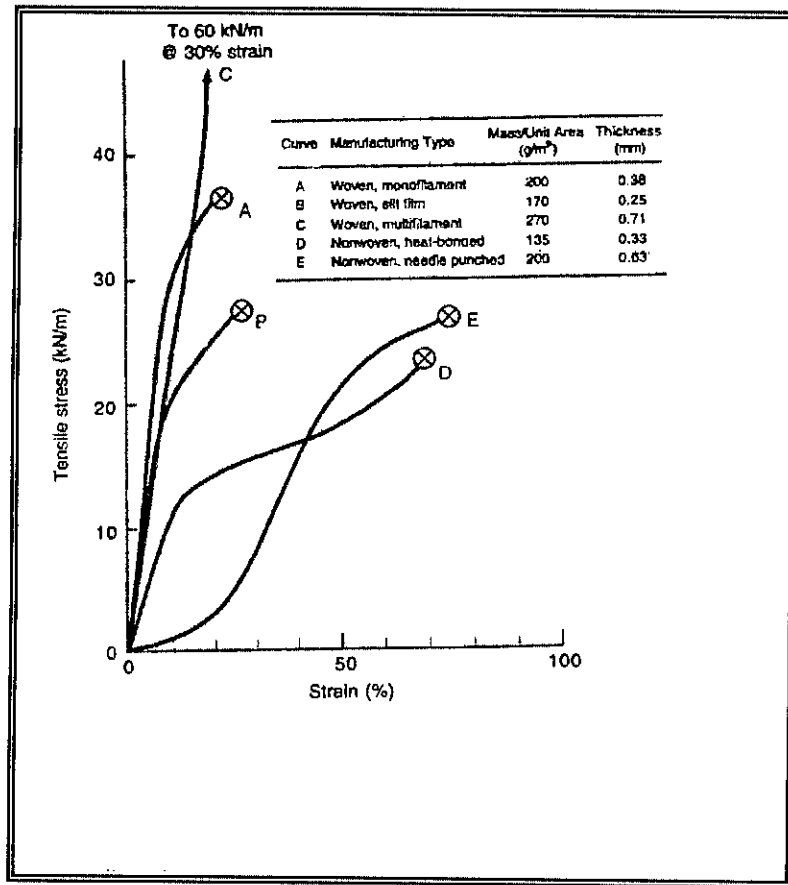


Fig 3.10 Tensile test response of various geotextiles manufactured by different process. All are polypropylene fabrics; test specimens were initially 200 mm wide X 100 mm high (after Koerner, 1997)

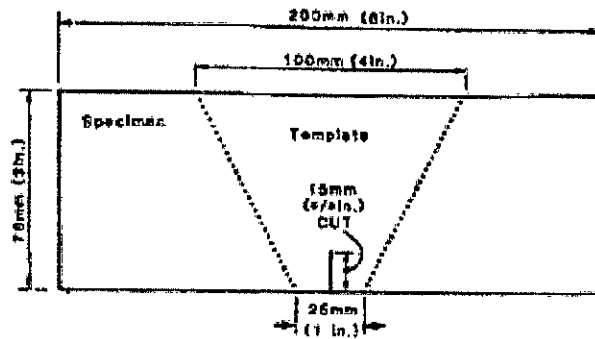


Fig 3.11 Trapezoidal template for trapezoid tearing strength test (after ASTM book of Standard, 2004)

9.57

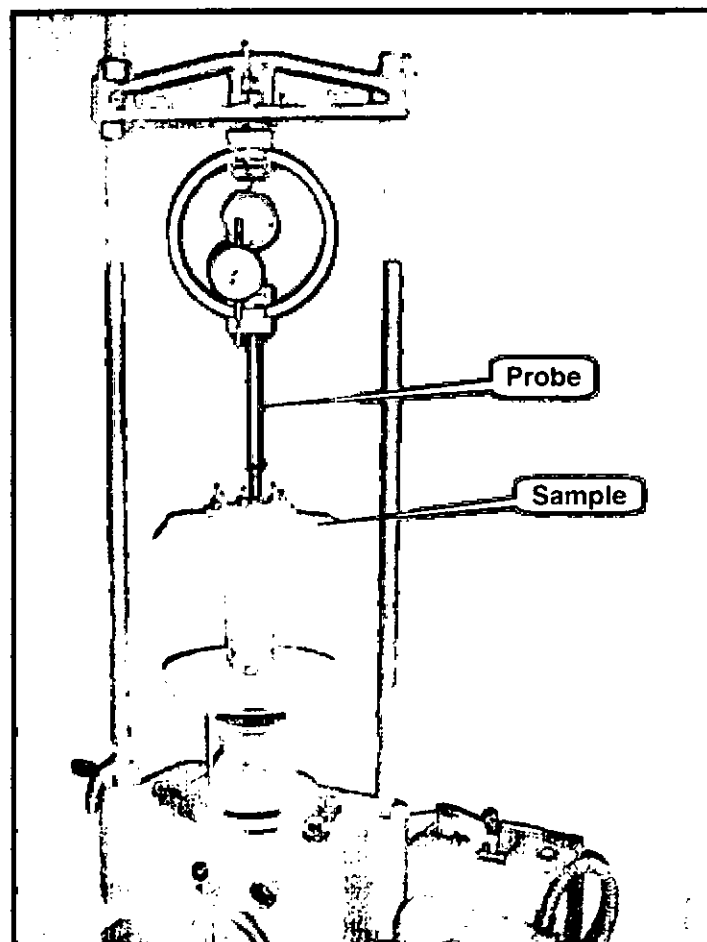


Fig 3.12 Test arrangement of index puncture test



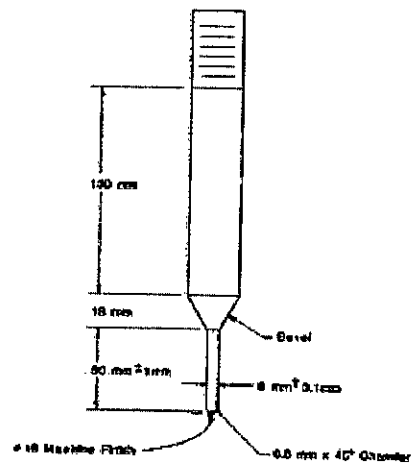
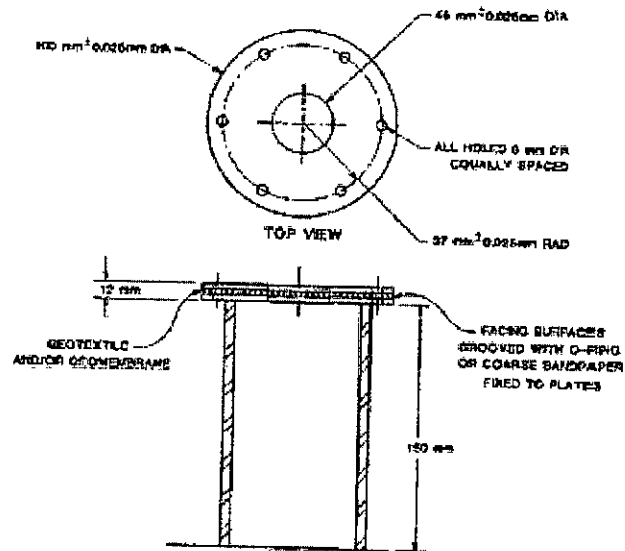


Fig 3.13 Index test fixture and probe detail (not to scale, after ASTM book of Standard, 2004)

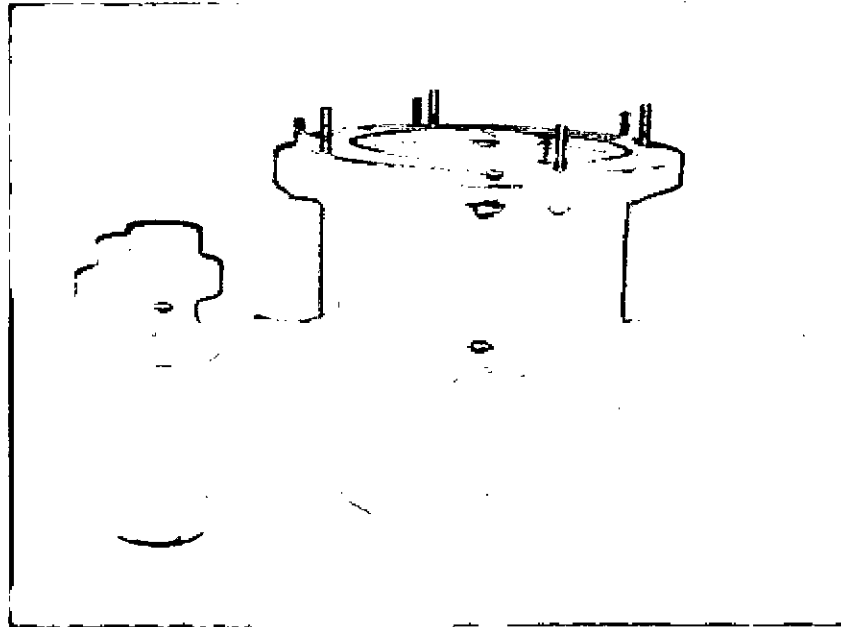


Fig 3.14 CBR test fixture and probe

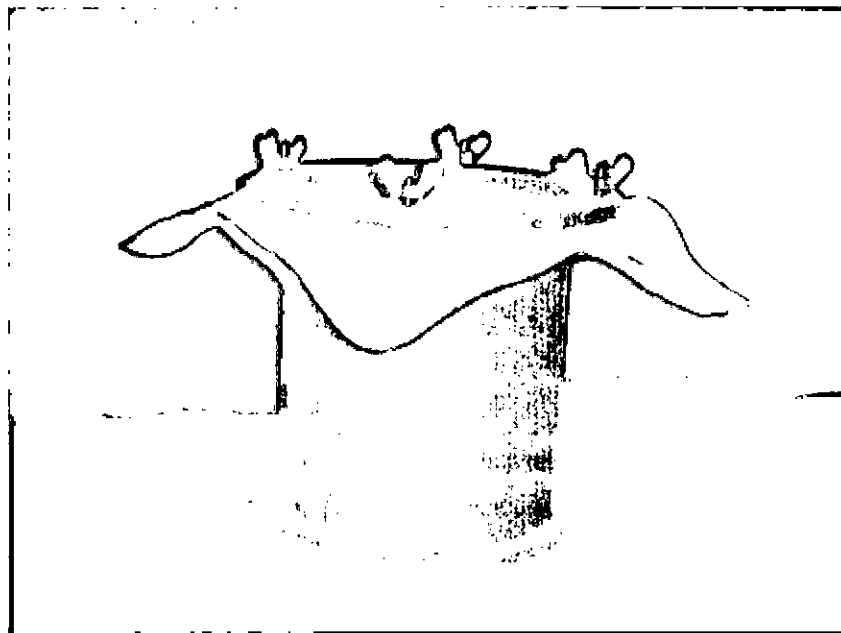


Fig 3.15 CBR test fixture fitted with test sample

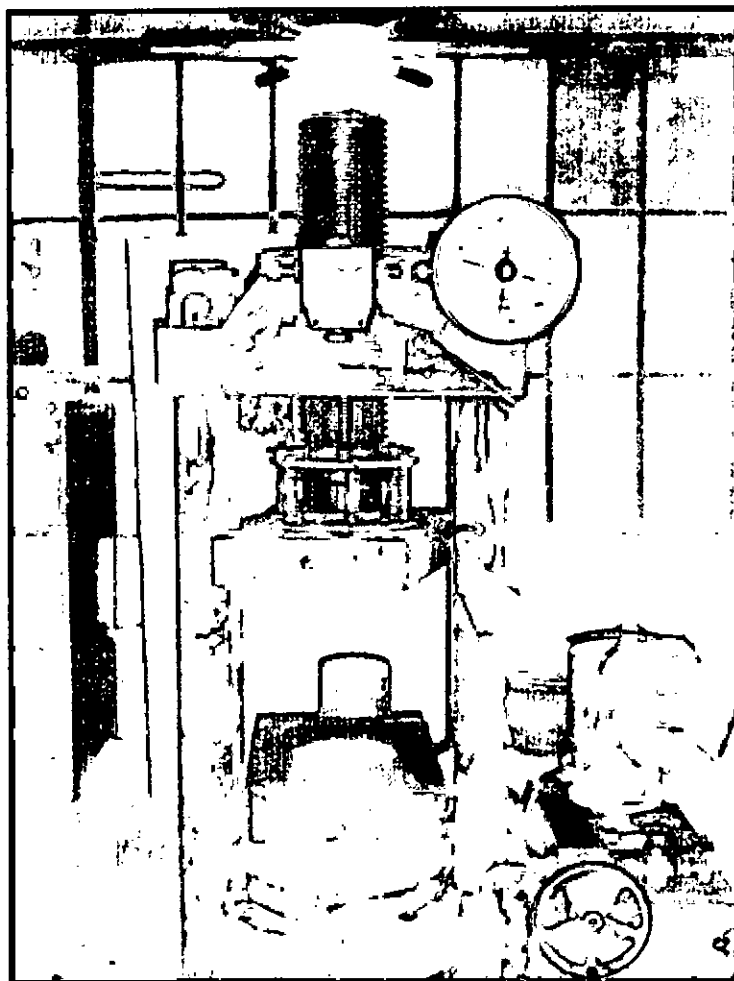


Fig 3.16 Bursting testing machine

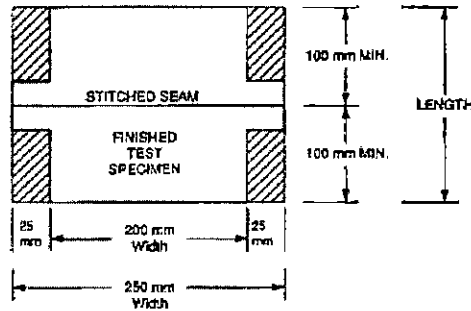


Fig 3.17 (a) Test specimen preparation for sewn seam (front view) (after ASTM Book of Standard, 2004)

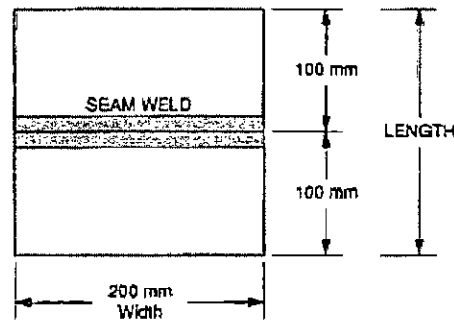


Fig 3.17 (b) Test specimen preparations for thermally bonded seam (front view) (after ASTM Book of Standard, 2004)

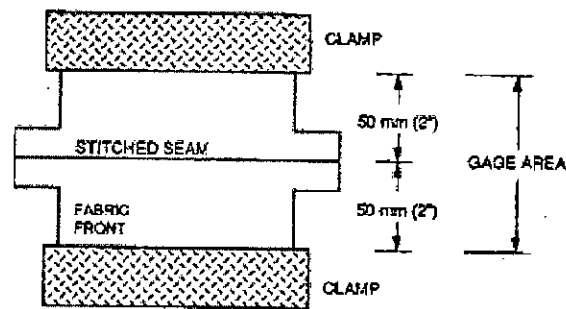


Fig 3.18 (a) Placement of generic seam in clamps for sewn seam (front view) (after ASTM Book of Standard, 2004)

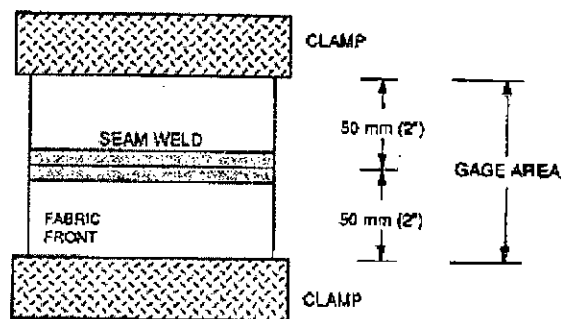


Fig 3.18 (b) Placement of generic seam in clamps for bonded seam (front view) (after ASTM Book of Standard, 2004)

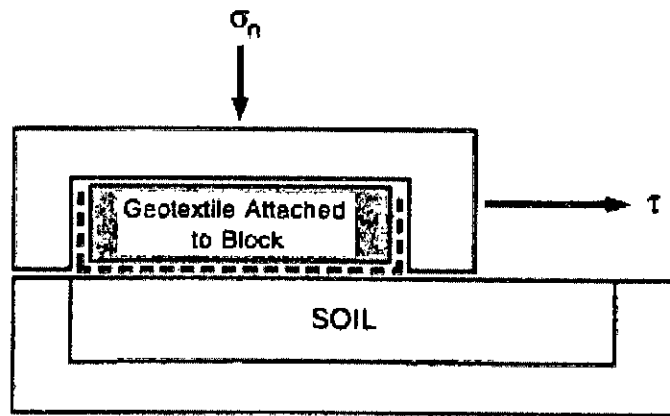


Fig 3.19 (a) Direct shear test device (after Koerner, 1997)

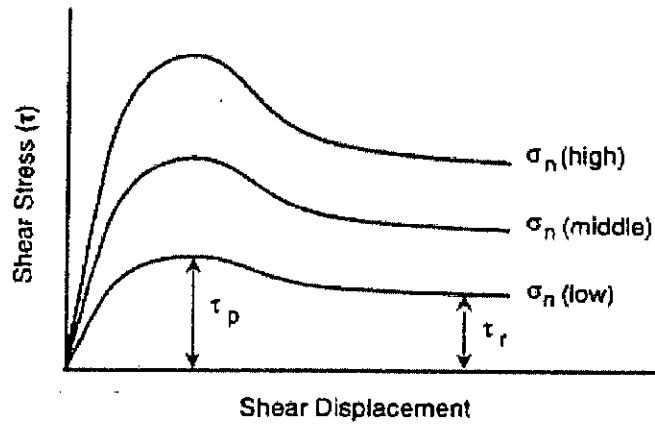


Fig 3.19 (b) Direct shear test data (after Koerner, 1997)

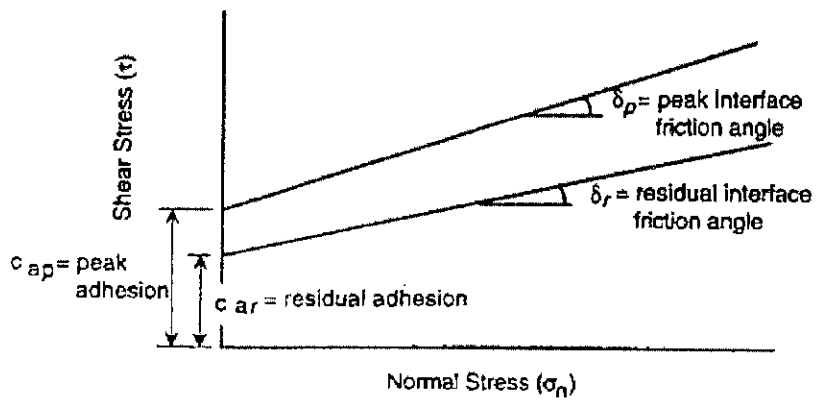


Fig 3.19 (c) Mohr-Coulomb stress space (after Koerner, 1997)

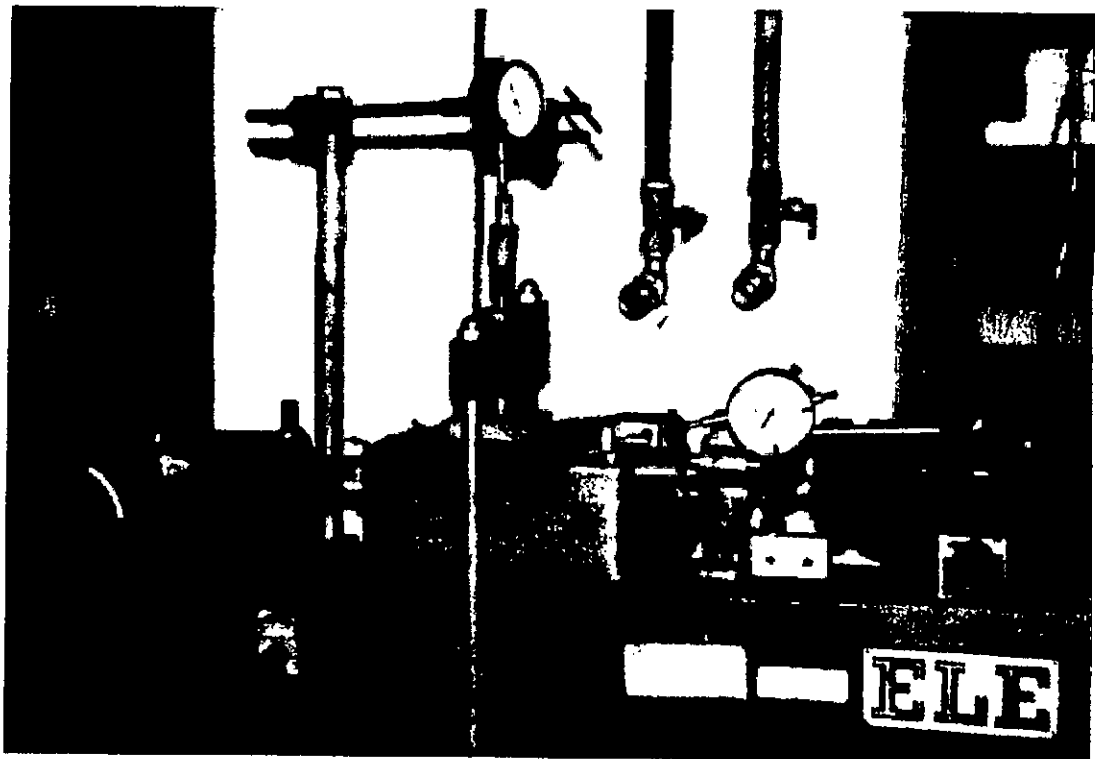


Fig 3.20 Direct shear box test apparatus for evaluating friction between jute geotextile and sand (after Muhammand, 1993)

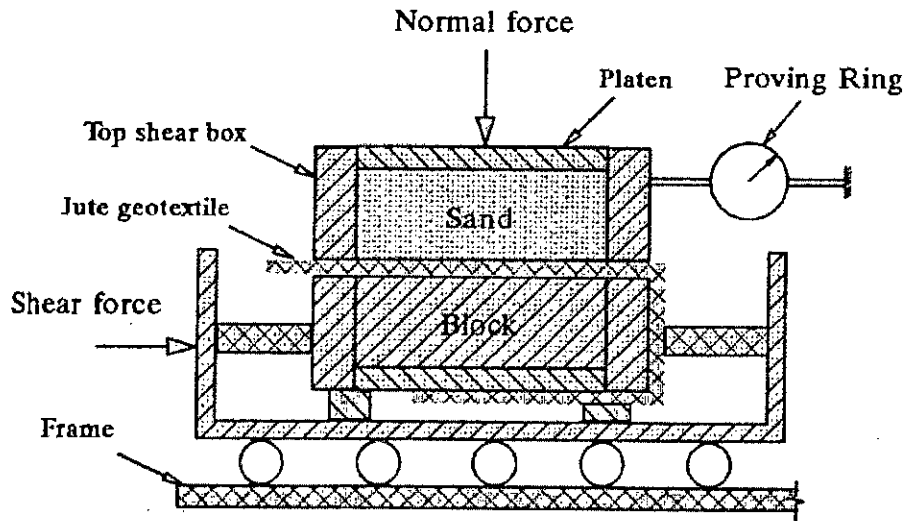


Fig 3.21 Schematic pressure diagram for direct shear test (after Muhammand, 1993)

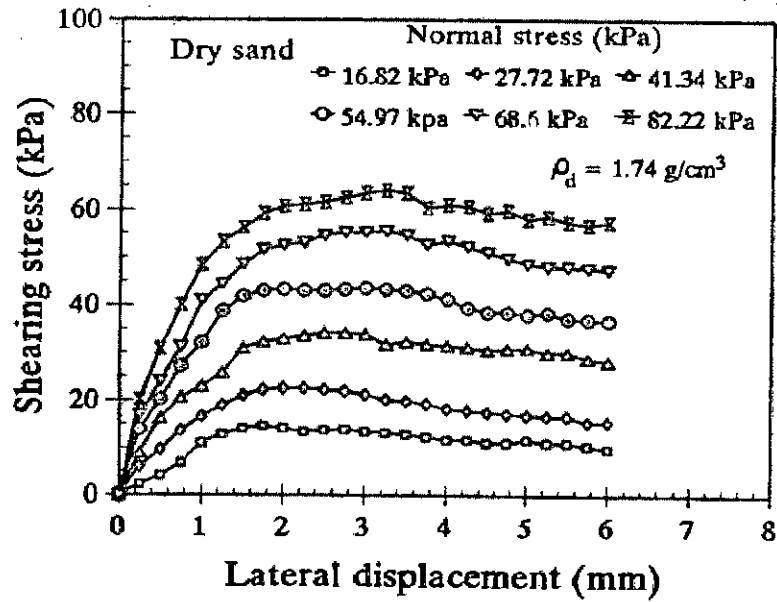


Fig 3.22 Direct shearing test for dry sand (after Muhammand, 1993)

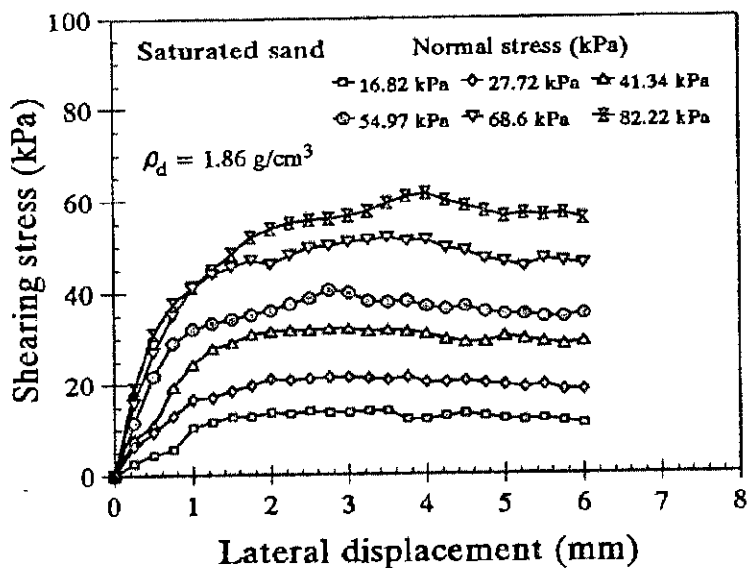


Fig 3.23 Direct shearing test for saturated sand (after Muhammad, 1993)

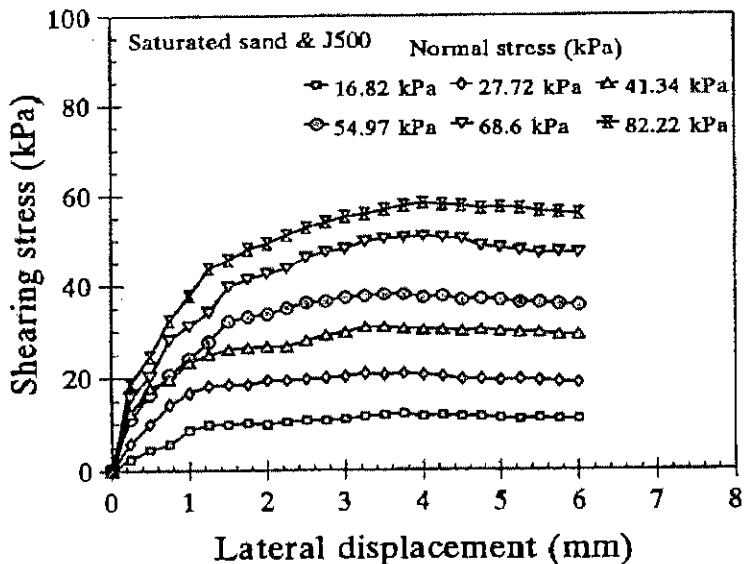


Fig 3.24 Direct shearing test for friction between saturated sand and jute geotextile 500g/m<sup>2</sup> (after Muhammad, 1993)



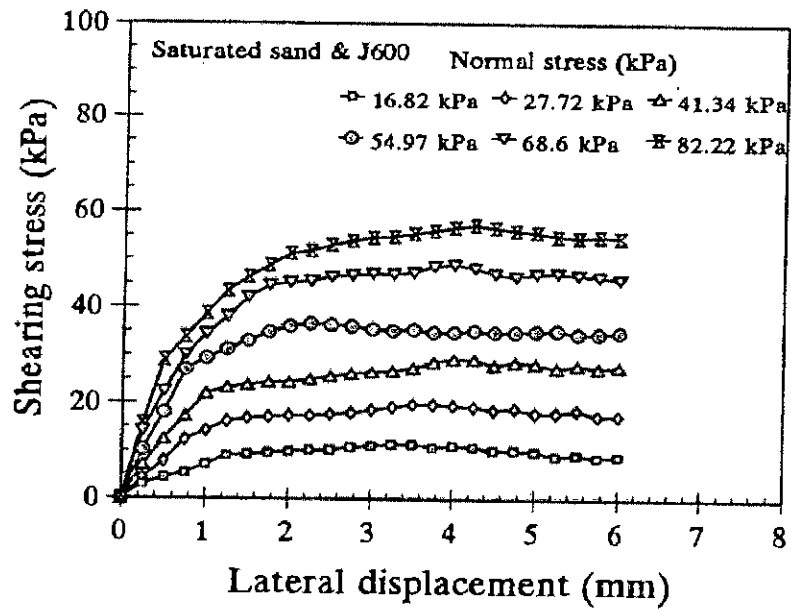


Fig 3.25 Direct shearing test for friction between saturated sand and jute geotextile 600g/m<sup>2</sup> (after Muhammad, 1993)

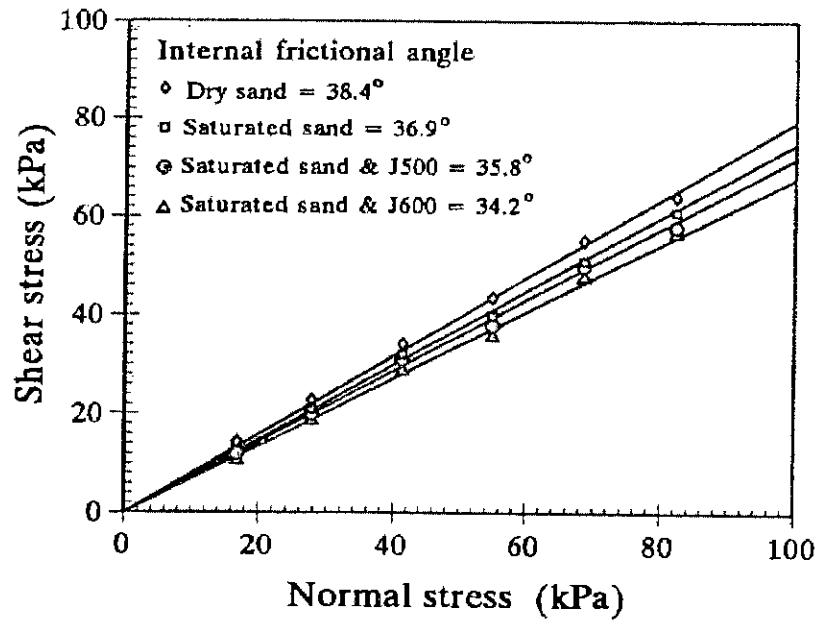


Fig 3.26 Frictional angle for different materials derived from direct shearing tests (after Muhammad, 1993)

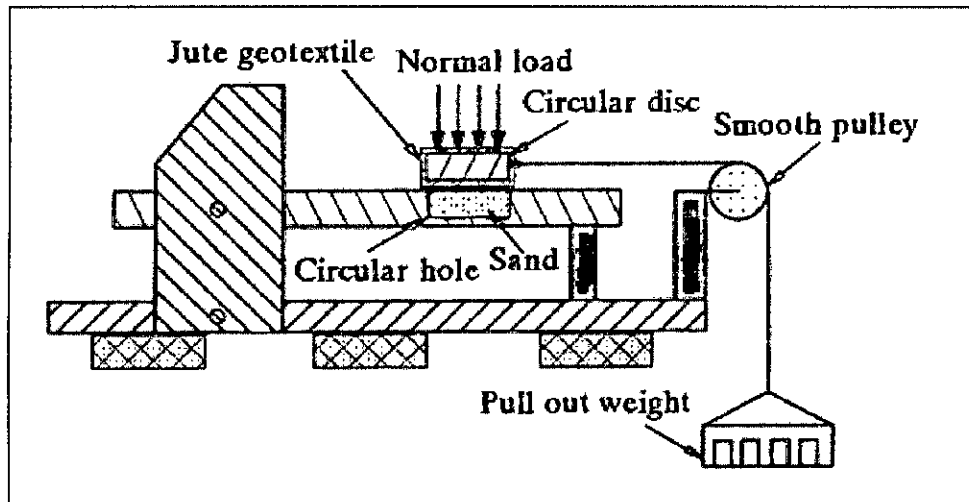


Fig 3.27 Schematic diagram for modified pullout test apparatus (after Muhammand, 1993)

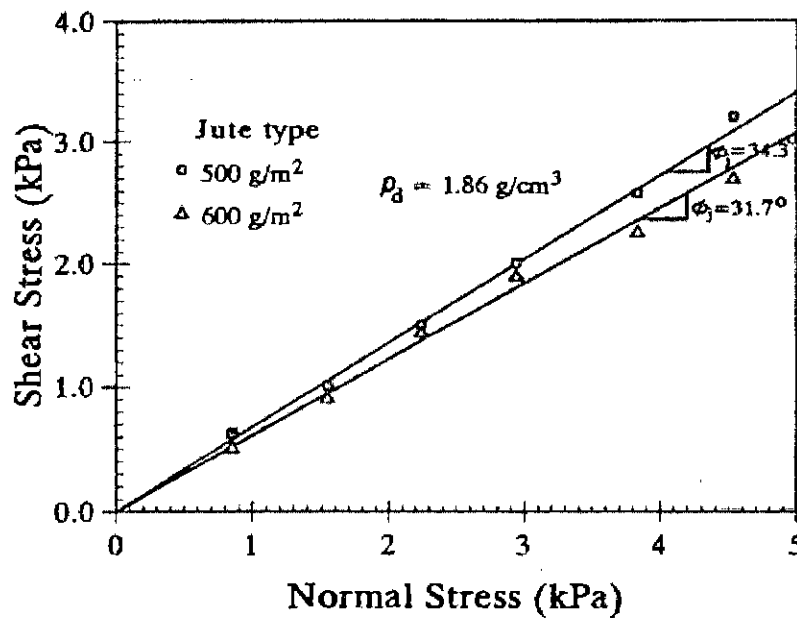


Fig 3.28 Modified pullout test results for interface friction between jute geotextile and wet sand (after Muhammand, 1993)

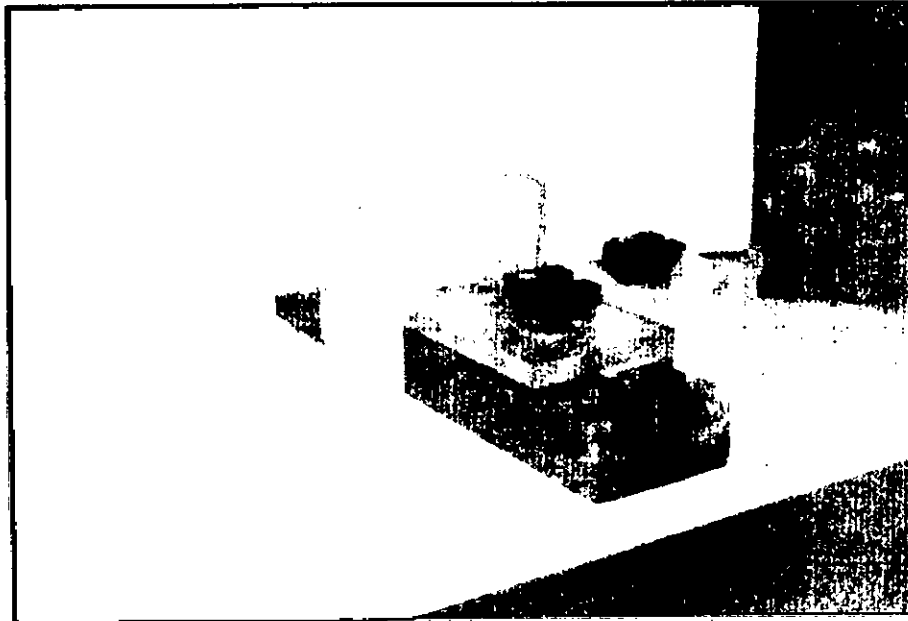


Fig 3.29 Pull out test device (after Muhammand, 1993)

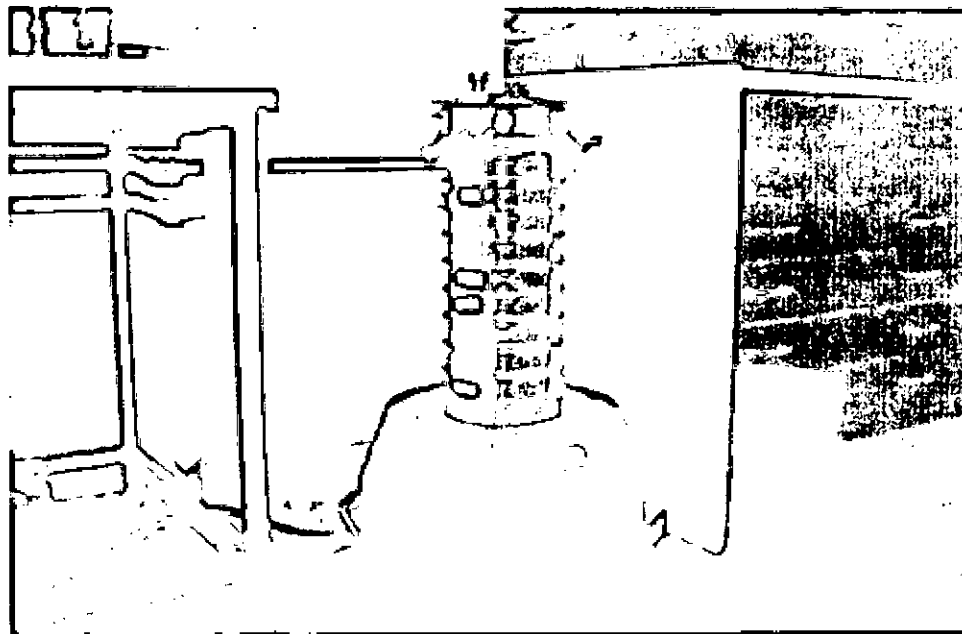


Fig 3.30 Test arrangement of Apparent Opening Size (after Muhammad, 1993)

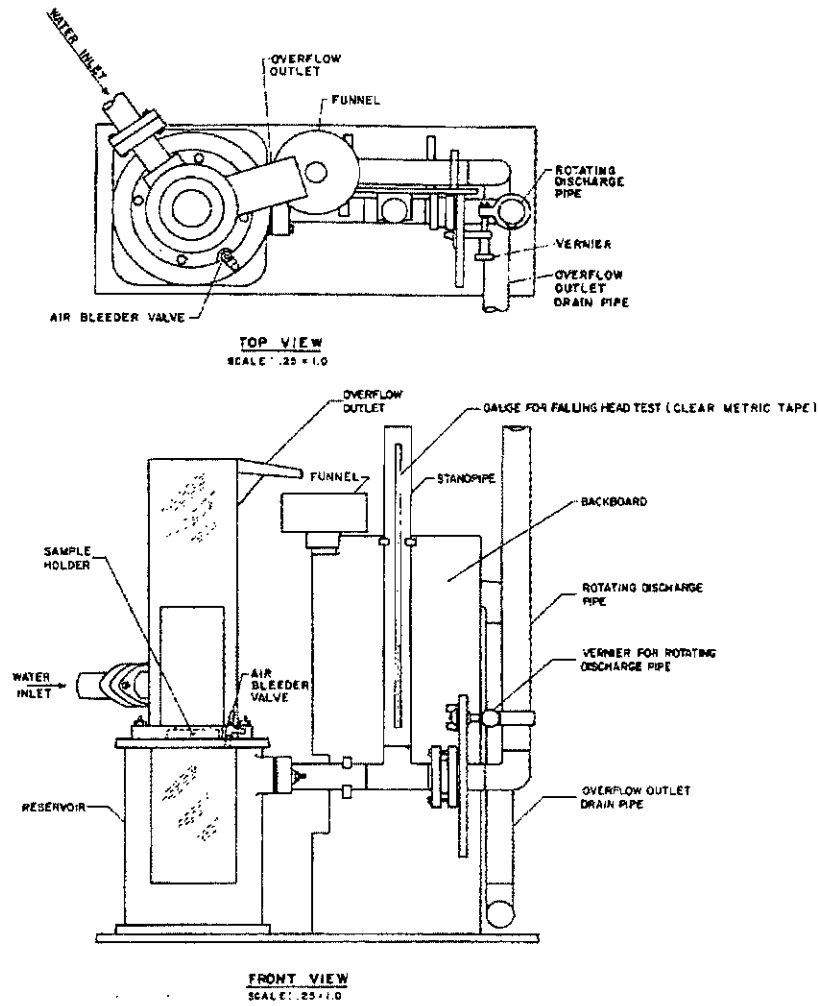


Fig 3.31 Constant and falling head permeability apparatus (after ASTM Book of Standard, 2004)

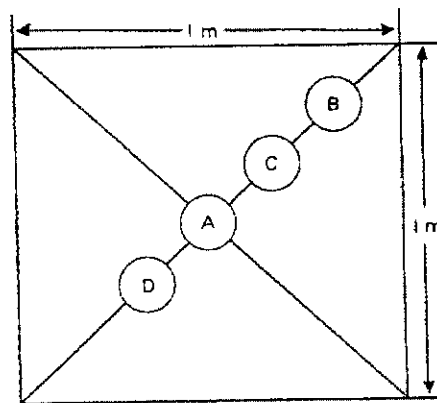


Fig 3.32 Sampling pattern for water permeability of geotextiles by permittivity test (after ASTM Book of Standard, 2004)

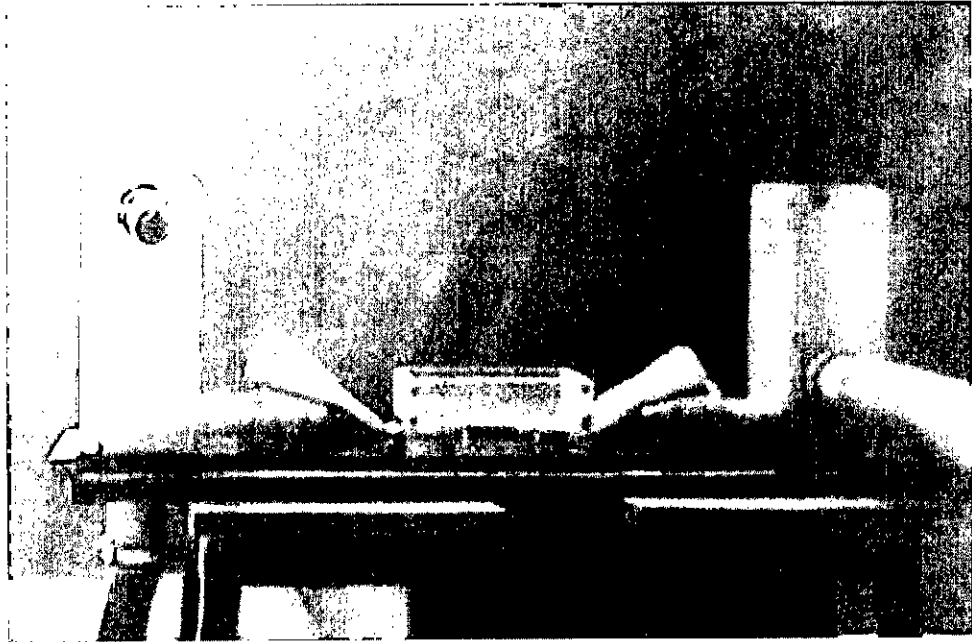


Fig 3.33 Test arrangement of transmissivity

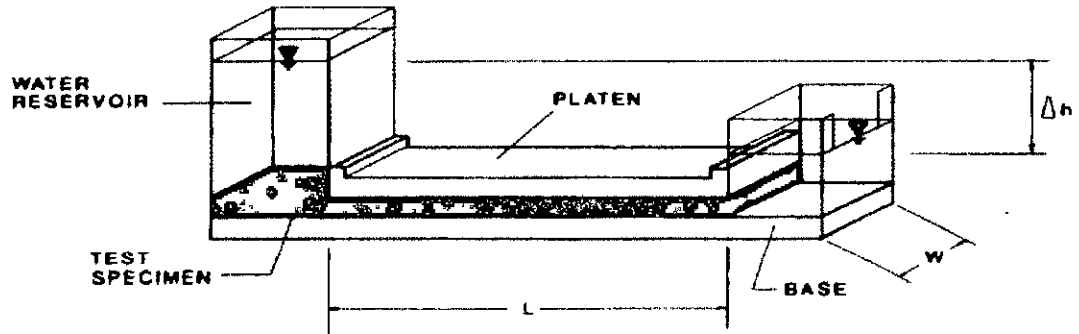


Fig 3.34 Schematic drawing of transmissivity test assembly (after ASTM Book of Standard, 2004)

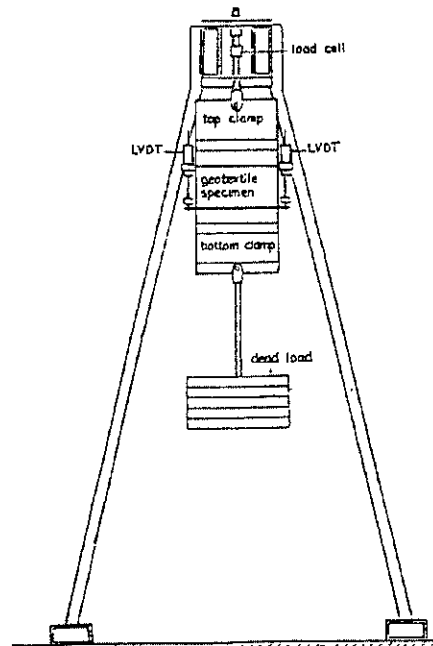


Fig 3.35 Schematic drawing of creep test assembly (after ASTM Book of Standard, 2004)

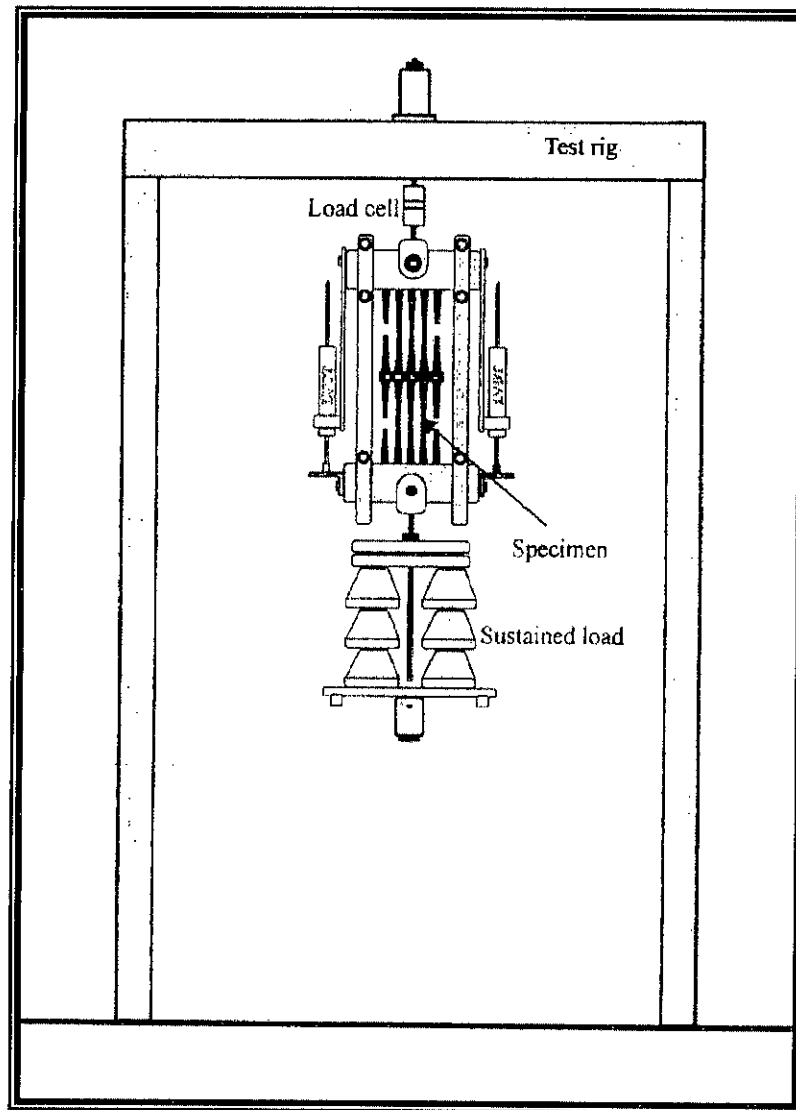


Fig 3.36 Schematic drawing of creep test assembly (after Mahaseth, 2002)

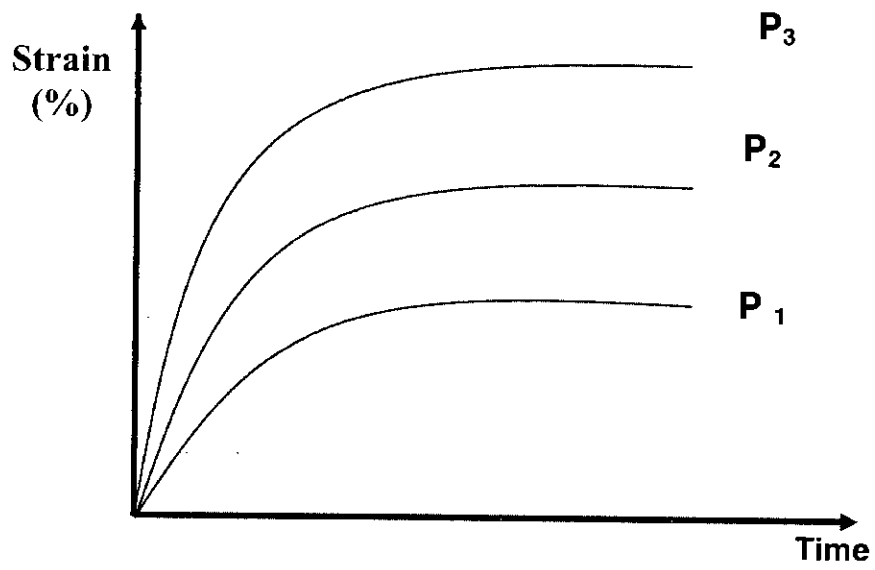


Fig 3.37 Strain versus time plots from sustained load creep tests



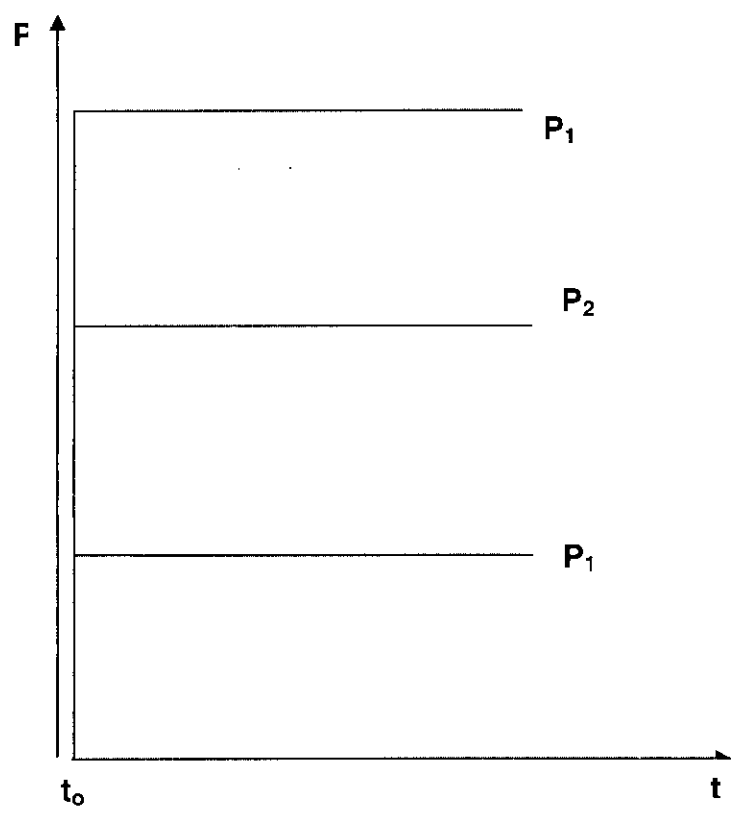
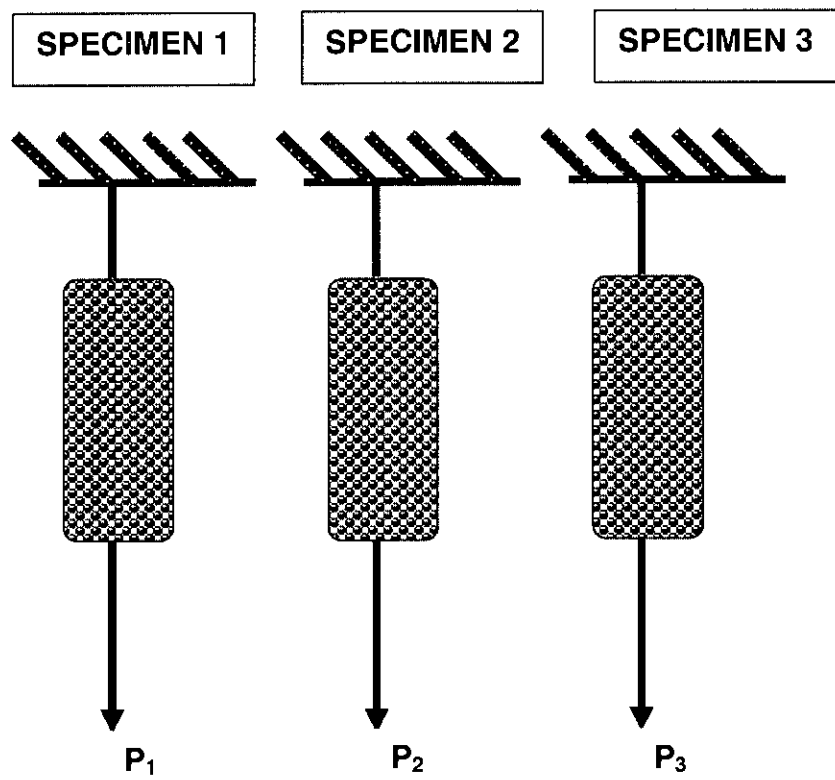


Fig 3.38 Series of sustained loadings versus time for deriving strain envelope for elasto-visco-plastic material

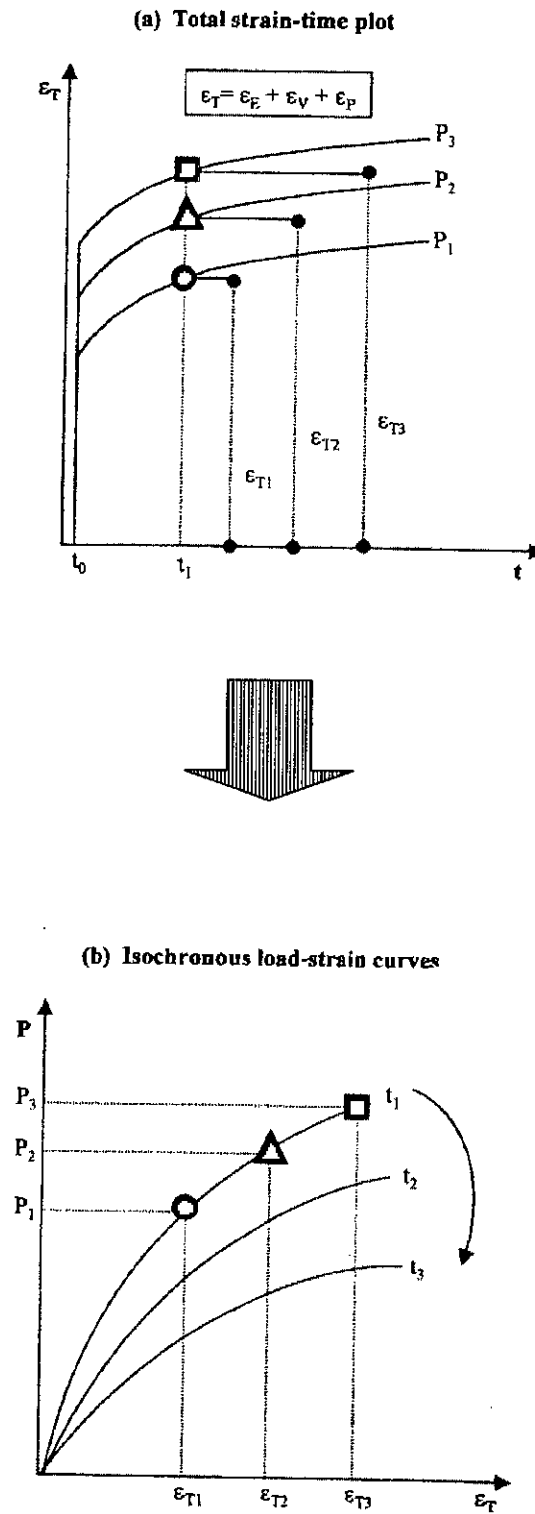
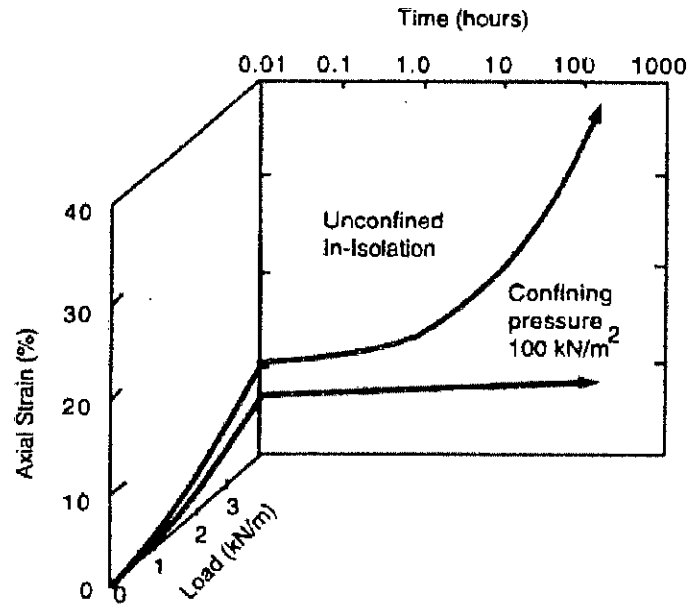
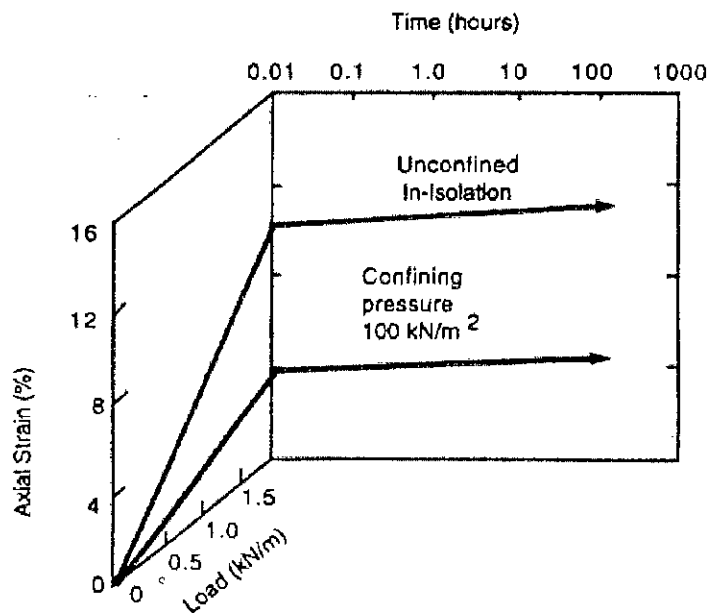


Fig 3.39 Deriving isochronous load-strain curves for elasto-visco-plastic geosynthetics (after Mahaseth, 2002)



(a) Nonwoven Heat Bonded (after Koerner, 1997)



(b) Nonwoven Needle Punched (after Koerner, 1997)

Fig 3.40 Results of confined creep tests on various geotextiles (after McGown et al, 1982, 1986)

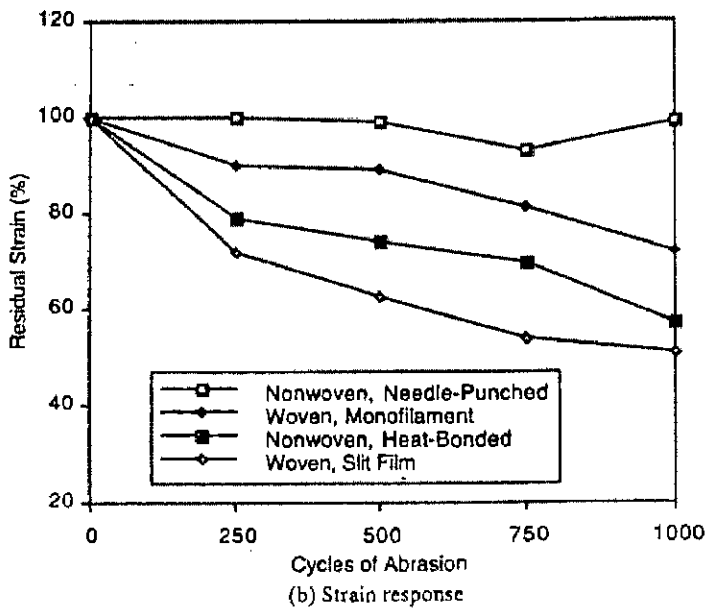
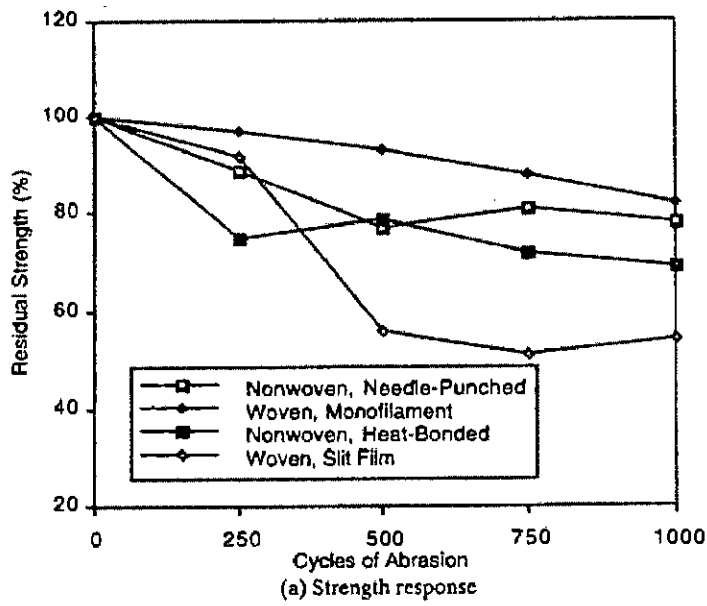
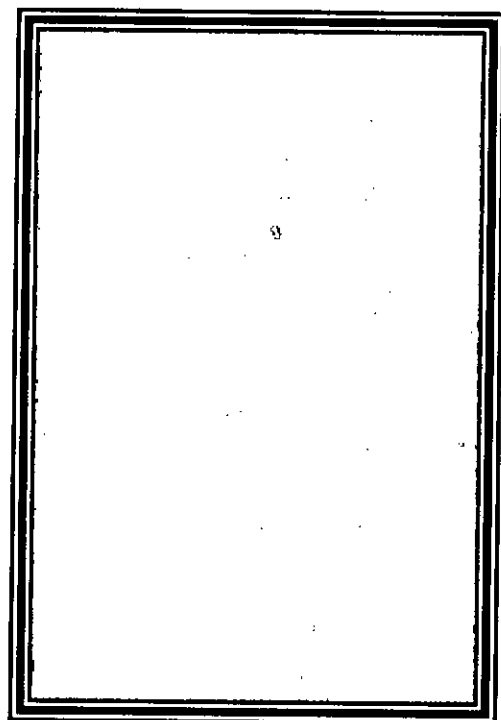
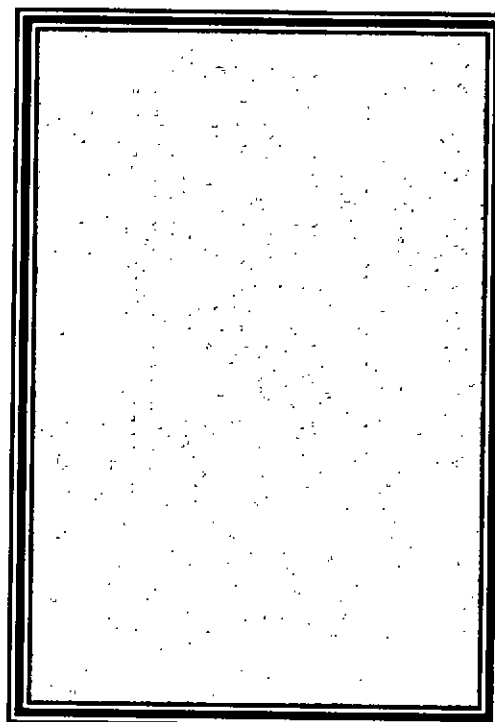


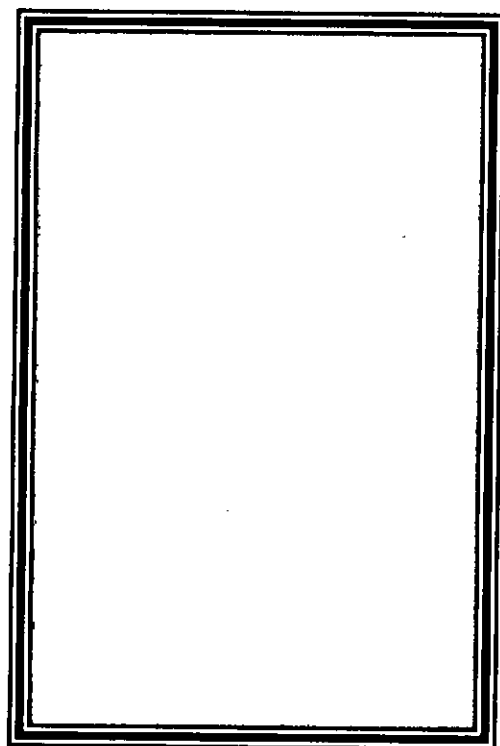
Fig 3.41 Abrasion test results for various geotextiles using the Taber test device model 503 (after Koerner, 1997)



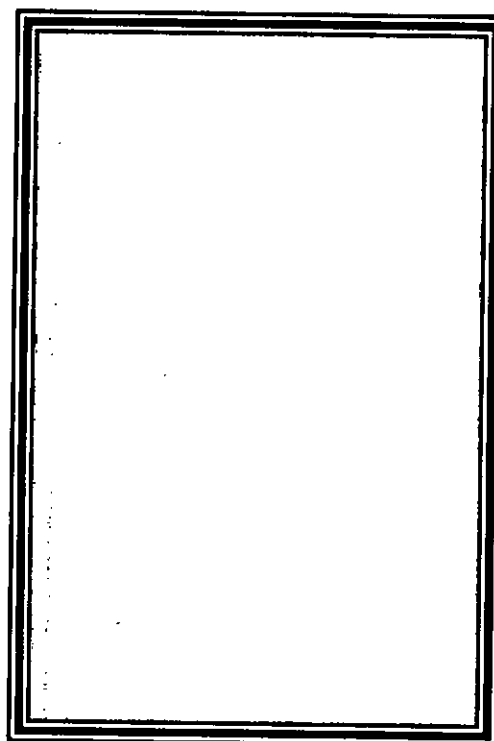
Jute from BJRI



DW Twill from BJMC

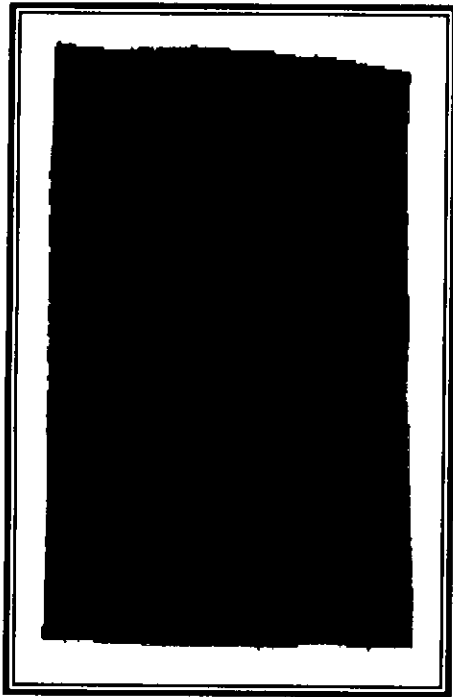


Hessian from BJMC

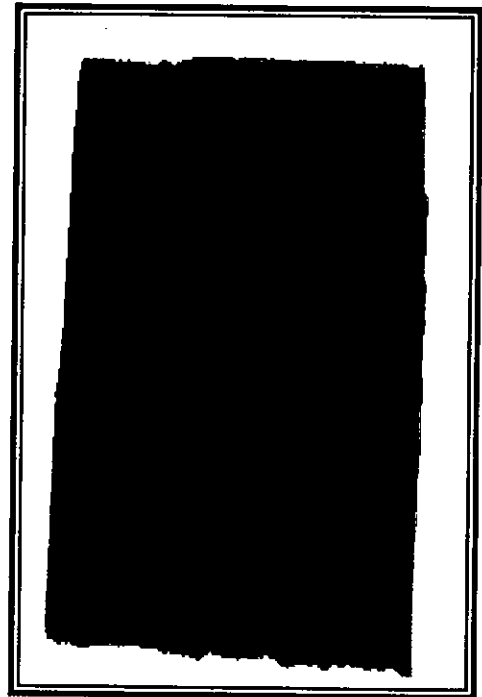


Canvas from BJMC

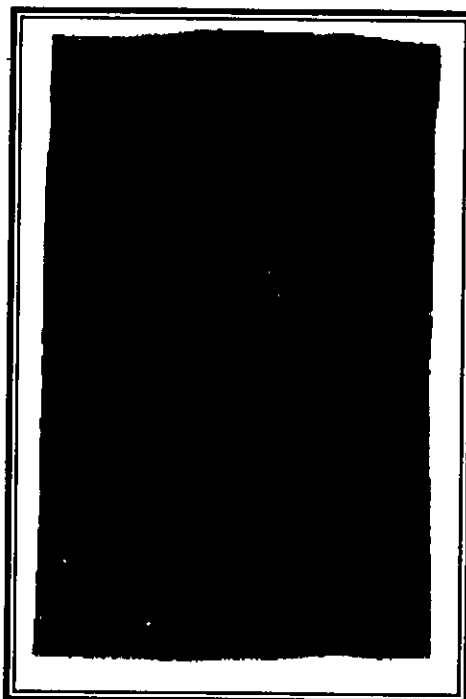
Fig 3.42 Untreated geojute samples selected for tests



Jute collected & treated at BJRI



Canvas collected from BJMC & treated at BJRI



DW Twill collected from BJMC & treated at BJRI

Fig 3.43 Treated geojute samples selected for tests

Handwritten notes in the bottom right corner, including the number '100' and some illegible scribbles.

## **CHAPTER FOUR**

# **EXPERIMENTAL RESULTS AND DISCUSSION**

### **4.1 General**

In Chapter Two a general description on geotextiles, its different types, properties, functions and applications are described elaborately. The laboratory investigation of physical, mechanical, hydraulic and endurance properties of geotextiles are also narrated in Chapter Three as per ASTM and DIN standard. In this Chapter the test results are presented with discussion.

#### **4.1.1 Mass per Unit Area**

To determine the Mass per Unit Area, as per ASTM D 5261-92, five-test specimen each from all seven samples was cut such that they are representative of the entire roll width. The length and width was measured under zero geojute tension. The area of test specimen ranged from 800 cm<sup>2</sup> to 1130 cm<sup>2</sup>. The mass (or weight) was measured to the nearest 0.01% of the total specimen mass. Thereafter the mass per unit area of each of the sample was calculated as per formula given in Chapter Three.

The mass per unit area of untreated samples ranged from 322 g/m<sup>2</sup> to 828 g/m<sup>2</sup>, Jute samples having maximum and Hessian samples having minimum values. It was observed that the densely woven geojutes having more mass per unit area than the porous geojutes. The mass per unit area of treated samples increased considerably compared to the untreated samples ranging from 1218 g/m<sup>2</sup> to 1591 g/m<sup>2</sup>. This increase in mass per unit area was due to the bitumen, which was coated with the samples while it was treated. The results are shown in Fig 4.1.

#### 4.1.2 Nominal Thickness

The thickness of a geojute is the distance between the upper and lower surface when measured under a specified pressure. Thicknesses of the most geojute are likely to vary considerably depending on the magnitude and the duration of pressure applied. The average thickness of a single layer of a geojute may also be obtained by using two or more contiguous layers under pressure that is lower than that using a single layer under the same pressure. The average thickness of the geojute,  $T_{avg}$ , is then calculated from the total thickness  $T_{total}$ , divided by the number of layers tested,  $N$ .

As per ASTM D 5199, test specimens were prepared from laboratory sample in a randomly distributed pattern across the width with no specimen taken nearer than 100 mm (4 in) from the selvage or roll edge. From each unit in the laboratory sample, test specimens were cut such that the edges of the specimens do not extend beyond the edge of the pressor foot by 10 mm (0.39 in) in all directions. Ten specimens were taken for each test. The time after which the dial readings were taken was 5 sec as suggested by ASTM, which was found to be too short for the geojute to reach the equilibrium under applied pressure. The apparent thickness of a geojute decreases with the pressure applied. In the case of geojute, the specimens were placed in between two weights the "presser" plate, upon which the weights are placed, and the "anvil" as shown in Fig 4.2. Strain/dial gauges were placed at 90° top of the presser plate. Initial readings were taken by the strain gauges before placing the jute fabric. Readings were carefully taken again after inserting the jute fabric in between the plates and placing the load increment on the presser plate.



Amongst four untreated samples Jute was found to be the thickest, having a thickness of 2.70 mm and Canvas was found to be the thinnest having thickness of 1.33 mm. The treated samples were found to have higher thicknesses than untreated samples as can be seen in Fig 4.3.

Kabir et al (1994) presented a laboratory study on mechanical properties of Canvas and Twill fibres in order to establish some of their hydraulic and mechanical behavior. Both the samples were manufactured in BJMC mills and are available locally. The thickness of the Canvas was found to be 1.36 mm and Twill 1.82 mm. Same Canvas was selected for this study and the thickness was found to be 1.33 mm. The DW (Double Works) Twill selected for this study mentioned in Table 3.2 is category type 'A' and the Twill tested by Kabir et al (1994) was category type 'B'. The thickness of DW Twill (2.82 mm) is always more than the Twill (1.82 mm) because of its double woven fabrics.

As was discussed earlier that the thickness of jute fabric continues to decrease under pressure for considerable time because of the compressibility. An attempt was taken to study the effect of time on thickness of treated geojute under different pressure. Fig 4.4 indicates that, at the end of five minutes, the plate can be considered to have effectively reached the equilibrium. The variations of thickness for geojutes within first five minutes are shown in Fig 4.5. It is seen that the variation within first five minutes is around 5%. Thus for the thickness tests, the time interval to record readings from strain gauges may be standardized to 5 minutes.

### 4.1.3 Specific Density

According to ASTM definition D 123 "Specific gravity,  $G_s$  is the ratio of the weight in air of a material to the weight of equal volume of water at 4° C "and is expressed by:

$$G_s = \frac{\frac{W_j}{V}}{\frac{W_w}{V}} = \frac{W_j}{W_w}$$

Where  $W_j$  = weight of dry jute of volume  $V$  and  $W_w$  = weight of water of equal volume at  $4^\circ \text{C}$ . To determine the specific density of jute using the volumetric flask the above equation can be rewritten as:

$$G_s = \frac{W_j}{W_{bw} + W_j - W_{bwj}}$$

Where,  $W_{bw}$  = weight of flask + distilled water up to the graduation and  $W_{bwj}$  = weight of flask + geojute + distilled water up to the volumetric graduation of the flask.

For determining absorbency time and absorptive capacity of non-woven fabrics different test methods have been suggested by ASTM D 1117-80. Nevertheless, there is no test method to determine the specific density of geotextile fabrics. A laboratory procedure suggested by Muhammad (1993) was followed in this research work for determining specific density. As per this method, a dry volumetric flask is carefully filled to the graduation mark with distilled and deaired water (Fig 3.5). Care is taken not to reintroduce air into the water by sloshing during the test. With the water level at the graduation, the weight of the flask with the water is recorded. Then the flask is cleaned and dried before weighing a sample of oven-dried jute geojute of about 100 gm to 200 gm. This sample should have been oven-dried overnight to a temperature not exceeding  $70^\circ\text{C}$  with the blower fan on, as jute specimens just as other natural fibers, if overheated may deteriorate in quality or cause ignition. The water is poured in and the weight of the flask with the contents is recorded at regular intervals of about 10 minutes for the first 2 hours and one hour thereafter in order to determine the total weight  $W_{bwj}$ .

The water penetrates into the small pores of the fabric lowering the water level in the flask. To determine the absorption capacity or the specific density within a short period the samples were loosened, untwisted and deaired so that the water can penetrate deep into the fibre pores fast resulting in maximum absorption within about 30 minutes.

Specific density of tested untreated and treated samples is shown in Fig 4.6 and Fig 4.7 respectively. In both cases, it shows the increase of specific density of

samples with soaking time under laboratory condition. After 70-80 hours of soaking all the samples reached their maximum specific density ranged from 0.82 to 1.51 from initial value of 0.43 to 0.95 depending upon the geojute type. It is clear from this test that geojute can easily float up to 2 to 3 hours initially on fresh or salt water due to its low initial specific density, which is advantageous in transporting over the water, and after 4 to 5 hours of soaking in water it can be sunk and placed under water. It is also found that geojute with a lower unit weight ( $\text{g/m}^2$ ) reaches the maximum specific density within a shorter time than that with a higher unit weight. This is may be due to the fibre orientation and configuration of jute. It takes a longer time for water to penetrate deep into the pores of the geojute in the higher unit weight of geojute while it is much faster to penetrate the fibres with lower unit weight.

#### 4.1.4 Wide-Width Tensile Properties

The load-extension behavior of the geojute has been determined by wide width strip uniaxial testing. The equipment used in this test consisted with a tensile testing machine (WOLPERT) with a maximum capacity of 1500 kN shown in Fig 4.8. It has load and elongation recorders and jaws with jagged faces (Fig 4.9) to firmly grip on the specimen to prevent slippage. These special jaws are capable of testing up to 200 mm wide specimens and permit no rotation about the grips. A schematic diagram of the testing machine is also shown in Fig 4.10.

The test specimen for wide-width test was cut 200 mm (8.0 in) wide by 100 mm (8.0 in) long with the length being designated and accurately parallel to the direction for which the tensile strength is being measured. The length of the specimen selected such that it fits the clamps being used. It was kept long enough to extend through the full length of both clamps, as determined for the direction of test. The force range of the testing machine was selected such that break occurs between 10 and 90% of full-scale force. Machine strain is set at a rate  $10 \pm 3\%$ /min.

Three specimens each of all seven samples were tested in machine direction (MD) and cross machine direction (XMD). The outcome plots of Load versus Strain of all the untreated and treated samples are shown in Fig 4.11 through Fig 4.17. The average wide-width tensile strength and elongation observed in all the seven samples

are shown in Fig 4.18 and Fig 4.19. The average strength in untreated samples at MD ranged from 10.32 kN/m to 26.8 kN/m, DW Twill sample being the maximum and Jute sample being the minimum. In XMD, the strength ranged from 10.67 kN/m to 23.9 kN/m. DW Twill samples being the maximum and again Jute samples being the minimum. In case of treated samples in MD, the average strength ranged from 16.25 kN/m to 27.2 kN/m, treated Jute samples being the maximum and treated Canvas samples being the minimum. In XMD, the average strength for treated samples ranged from 18.36 kN/m to 31.58 kN/m, treated DW Twill samples being the maximum and treated Canvas being the minimum.

The wide-width elongations of all the samples are demonstrated in Fig 4.20 and 4.21. The elongation of untreated samples in MD ranged from 6.7% to 13%, DW Twill samples being the maximum and Hessian samples being the minimum. In case of treated samples, the elongation ranged from 10.9% to 21.3%, treated Jute being the maximum and treated Canvas being the minimum. In XMD, the elongation observed in untreated samples ranged from 5% to 8.2%, DW Twill and Hessian samples being the maximum and Canvas samples being the minimum. In case of treated samples, it ranged from 11.3% to 12%, treated Jute being the maximum and treated Canvas samples being the minimum.

All the tests were performed at a strain rate of 10%/min and an aspect ratio of 2 as suggested by ASTM for polymer geotextiles. The Load versus strain show that the maximum tensile strengths develop at the maximum strain and after reaching the maximum value, the tensile force starts dropping to zero once the fibers start to tear apart from its twisted yarn. It was observed in this wide strip test that the tension force keeps on increasing due to reorientation of the fibres until it reaches the strongest fibre configuration. With tearing off some its fibers, the decrease in tension is observed.

The wide-width strength and elongation of geojute is much less than geotextiles. The higher strength and elongation indicates its more ductility and flexibility than geojute.

The failure patterns, elongations and deformed grids for Canvas and Hessian specimens can be seen in Fig 4.22 through Fig 4.25.

#### 4.1.5 Grab Breaking Load and Elongation

The grab tensile test provides an index of the ultimate strength of the specimen at failure. The test results are expressed in units of load (such as pounds) rather than in terms of load per unit width. The test is easy to perform, inexpensive, and quick, taking only minutes to complete. From 40 to 60 specimens can be tested in one hour. As such, it is an excellent index strength test for verifying the quality of products in accordance with manufacturer's specifications, as during construction quality control.

As per ASTM D 4632, the test specimens were cut in rectangular shapes (4 in by 8 in). Specimens were used for grab tests in the machine direction with the longer dimension parallel to the machine direction and the specimens to be used for grab tests in the cross-machine direction with the longer dimension parallel to the cross-machine direction. Ten specimens were tested in each direction. The distance between the clamps at the start of the test was set at 75 mm. The load range of the testing machine was set such that the maximum load occurs between 10 and 90% of full-scale load. Machine was operated at a speed of 300 mm/min.

The constant-rate-of-traverse (CRT) type tensile testing machine (Fig 4.7) was used in this test. The clamps used in this test were conforming to the requirements of specifications D 76. It has all types of gripping surfaces parallel, flat and capable of preventing slipping of the specimen during a test (Fig 4.26 and Fig 4.27). Each clamp have one jaw face measuring 25.4 by 50.8 mm (1 by 2 in), with the longer dimension parallel to the direction of application of the load. The other jaw face of each clamp was larger to its mate.

The average grab breaking strength of untreated samples ranged from 225N to 929N in MD and 248N to 750N in XMD, DW Twill samples having the maximum in both directions. The minimum strength was observed in Hessian and Jute samples in MD and XMD respectively. The results are shown in Fig 4.28 and 4.29. In case of treated samples, the grab breaking strength ranged from 831.6N to 1044N in MD and 668N to 984N in XMD, treated Canvas samples having maximum and treated Jute having minimum in MD. In XMD, treated DW Twill having maximum and treated Canvas having minimum.

The grab breaking elongations of all the samples in MD and XMD are presented in Fig 4.30 and Fig 4.31 respectively. It varied from 19.7% to 38.5% in MD for untreated samples, Jute samples being the maximum and Canvas samples being the minimum. In XMD, the elongations ranged from 17.2% to 29.45%, Jute samples being maximum and Canvas samples being minimum. In case of treated samples in MD, the elongations ranged from 23.6% to 40%, treated Jute being the maximum and treated DW Twill being the minimum. In XMD, the value ranged from 20% to 33.5%, treated Jute being maximum and treated DW Twill being minimum.

The failure patterns, elongations and deformed grids for Canvas and DW Twill before and after the test can be seen from Fig 4.32 through Fig 4.35.

#### 4.1.6 Trapezoid Tearing Strength

This test method is an index test used to measure the force required to continue or propagate a tear in woven or non-woven geotextiles by the trapezoid method. Ten specimens were tested for each machine and cross-machine direction. The rectangular specimen was cut 76.2 by 201.6 mm (3 by 8 in). For the measurement of the tearing strength in the machine (or warp yarns) and cross-machine direction (or filling yarns), the specimens were cut so that the longer dimension parallel to the machine direction and cross machine direction respectively. Each specimen was marked with an isosceles trapezoid template (Fig 3.11). A preliminary cut 15.9 mm (0.625 in) long at the centre of the 25.4 mm (1 in) edge is made. The distances between the clamps were set at 25 mm (1 in). The load range of the testing machine was selected such that the maximum load occurs between 15 and 85% of full scale of load. Machine was set to operate at a speed of 300 mm/min.

Trapezoid tearing strength (TTS) of all the seven samples in MD and XMD is presented in Fig 4.36 and Fig 4.37. The TTS of untreated samples ranged from 137N to 464N in MD, DW Twill samples being the maximum and Canvas samples being the minimum. In XMD, the value ranged from 26N to 153N, DW Twill and Canvas samples again being the maximum and minimum. In case of treated samples, in MD, the strength ranged from 111N to 400N, treated DW Twill and Jute samples having the maximum and the minimum strength respectively. In XMD, the value ranged from

21N to 118N, treated DW Twill samples being the maximum and treated Canvas samples being the minimum. This may be due to the denser and stronger fibre orientation and configuration

The failure patterns, elongations and deformed grids for Canvas and Dw Twill before and after the trapezoid test can be seen from Fig 4.38 through Fig 4.41.

#### 4.1.7 Index Puncture Resistance

Fifteen specimens each on all the seven samples were tested as per ASTM D 4833-88 (Reapproved 1996). The tensile/compression testing machine used for this test was a constant-rate-of extension (CRE) type (Fig 4.9) The clamping arrangement suggested by ASTM shown in Fig 3.13 was adopted in this test. The external diameter of the probe was 100 mm. The diameter of the six holes for securing the ring clamp was 8 mm and equally spaced at a radius of 37 mm. The surfaces of these plates consist of grooves with O-rings. A solid steel rod, with a diameter of 8 mm having a flat end with a  $45^\circ = 0.8$  mm chamfered edge contacting the test specimen's surface was used.

For performing the test, a laboratory sample was taken from a swatch extending the full width of the samples. The test specimen was cut 100 mm X 100 mm to facilitate clamping. The machine speed was set 300 mm/min until the puncture rod completely ruptures the test specimen.

The test results of index puncture resistance are demonstrated in Fig 4.42. Puncture strength of untreated samples ranged from 405N to 840N, DW Twill sample being the maximum and Jute samples being the minimum. In case of treated samples, the value ranged from 205N to 400N, treated Canvas being the maximum and Jute sample being the minimum. The variation in load of individual samples in index puncture resistance test is shown in Fig 4.43.

#### 4.1.8 CBR Puncture Resistance

The CBR puncture resistance tests of all the seven samples were performed. Six specimens were taken for each type of samples. A conventional soil-testing CBR plunger and mold were used in this test as shown in Fig 3.14 and Fig 3.15. The penetrating steel rod is 50 mm in diameter and the samples were firmly clamped in an empty mold with a 150 mm inside diameter. The machine speed was set at 300 mm/min.

The outcome test results are shown in Fig 4.44. The average CBR resistance values for untreated samples ranged from 1560N to 4480N, DW Twill samples being the maximum and Jute samples being the minimum. In case of treated samples, the value ranged from 1470N to 3740N, treated Jute samples having the maximum and treated Canvas samples having the minimum values. The variation in load of individual samples in CBR puncture resistance test is shown in Fig 4.45.

#### 4.1.9 Burst Strength Test

As per ASTM D 3786-79, for the determination of the burst strength ten specimens were taken for each type of samples. The samples were circles of 5 in (125 mm) in diameter. The machine, which was used, conforms the requirement of ASTM standards (Fig 3.16). In this test, an inflatable rubber membrane was used to distort the samples into the shape of a hemisphere of 30 mm diameter. The diaphragm was expanded by hydraulic pressure to the point of specimen rupture.

The outcome of the burst test results of treated and untreated samples are presented in Fig 4.46 and Fig 4.47 respectively. The bursting strength of untreated sample ranged from 1245 kPa to 2360 kPa, Canvas samples having the maximum value and Jute samples having the minimum value. In case of treated sample, the value ranged from 1560 kPa to 2530 kPa, treated DW Twill samples having the maximum and treated Jute samples having the minimum.



#### 4.1.10 Apparent Opening Size (AOS)

Apparent Opening Size (AOS),  $O_{95}$  is a property of geotextile, which indicates the approximate largest particle that would effectively pass through the geotextile. To perform the test as per ASTM D 4751-87, a full width swatch 1 m (1 yd) long from the end of each roll of fabrics is taken in the lot sample, after first discarding a minimum of 1 m (1 yd) of fabric from the very outside of the roll. Five specimens from each swatch in the laboratory sample were cut to fit the appropriate sieve pan. The specimens were cut from a single swatch spaced along a diagonal line on the swatch.

As per the ASTM sieving method, a geojute specimen was placed in a sieve frame (Fig 4.48). The sample was secured in such a way that it is taut, without wrinkles or bulges. Care was taken so that the sample was not stretched or deformed such that it changes or distorts the openings in the fabric. Then 50 gms of standard sand fractions were placed on the centre of the geojute surface, started with the smallest diameter glass beads that would be tested. A mechanical sieve Shaker shaken the geojute and frame laterally for 5 minutes. It imparted lateral and vertical motion to sieve, causing the particles thereon to bounce and turn to present different orientations to the sieving surface. By placing, the sand fractions still on the surface of the specimen in a pan and weighed. The glass beads that pass through the specimen were also weighed and recorded. The process was repeated by using the next larger bead size fractions until the weight of beads passing through the specimen is 5% or less. The procedure was repeated on a new specimen of the same type of geojute with other various sizes of sand fractions until its equivalent or apparent opening size is determined.

To determine the AOS of all the untreated samples plotting method was adopted. The plotting was done on the percentage of beads passing the specimen versus the bead size for each of the bead sizes used for each specimen. For each specimen, the values of Percent Passing (Ordinate) vs Bead Size, mm (Abcissa) on semi-log graph was plotted. A straight line is drawn connecting the two data points representing the bead sizes, which are immediately on either side of the 5% passing ordinate. The particle size in mm (abscissa) at the intersection of the straight line

plotted and the 5% passing ordinate is the AOS of the specimen in mm, i.e., the theoretical bead size that would result in exactly 5% passing the specimen.

The AOS of all the untreated samples are presented in Fig 4.49 through Fig 4.52. AOS of Jute, Canvas, DW Twill and Hessian are 0.28, 0.075, 0.8 and 1.0 mm respectively. The AOS of treated samples could not be performed with sand fractions because of the bitumen that coated on it. The result obtained from this study conforms to the results of Kabir et. al. (1994) where the AOS of Canvas and Twill was found to be 0.06 mm and 0.6 mm.

#### 4.1.11 Water Permeability and Permittivity

For the determination of the permittivity as per ASTM D 4431-98, the device shown in Fig 4.53 was used. Constant head method was followed, as per the standard written around the constant head test at a head of 50 mm. Due attention was given in the important test consideration for this test i.e. the preconditioning of the fabric, temperature and the use of de-aired water.

In order to obtain a representative value of permittivity, a specimen of 1-m<sup>2</sup> (1-yd<sup>2</sup>) was taken. As per Fig 3.32 four specimens, A, B, C, and D were selected. The diameters of the cut specimen were considered as 73 mm (2.87 in) so that it fits the testing apparatus. The specimen was conditioned by soaking in a closed container of deaired water, at room conditions, for a period of 2 hour. As per the procedure described in ASTM, a head of 50 mm (2 in) of water was maintained on the geojute sample throughout the test. The quantity of flow was measured for 15 minutes time. Five readings were taken per specimen and average value of permittivity was determined for the specimen. After the first specimen has been tested under a 50 mm head, using the same specimen, subsequently at 10, 20, 30, 40, 60 and 70 mm head readings were taken to determine the region of laminar flow.

The water permeability results of all seven samples as determined are presented in Fig 4.54. The permittivity of untreated samples ranged from 0.03 s<sup>-1</sup> to 1.19 s<sup>-1</sup>, Hessian samples having maximum due to the most porous fibre orientation and Canvas sample having minimum values. In case of treated samples, the value

ranged from  $0.0 \text{ s}^{-1}$  to  $0.06 \text{ s}^{-1}$ , treated DW Twill samples having maximum value and treated Canvas sample having zero value. By construction, Canvas is a densely woven fabric and after treatment, its all pores were filled with bitumen, which did not allow any water to pass through it.

#### 4.1.12 In-plane Flow Rate per Unit Width and Hydraulic Transmissivity

Though a number of test devices are configured to determine the transmissivity of geotextile, where liquid (usually water) flows in the plane of the geotextile (of dimensions  $L \times W \times t$ ) in a parallel flow trajectory; a device conforms the requirement of ASTM D 4716 and ISO/DIS 12958 was used for this study (Fig 3.33 and Fig 3.34).

The flow rate per unit width was determined by measuring the quantity of water that passed through a test specimen in 15 minutes time under a specific normal stress and a specific hydraulic gradient. The applied normal compressive stresses were selected at 10 kPa, 15 kPa, 20 kPa, 25 kPa and 30kPa. Different hydraulic gradient were selected for different sample. The hydraulic gradients were 0.87 for Jute, 0.97 for Canvas and DW Twill, 1.15 for Hessian, 0.65 for Treated Jute, 0.67 for treated Canvas and treated DW Twill.

Three specimens were removed from each laboratory sample, which were spaced along a diagonal extending across the swatch. Specimens were cut such that the longer dimension was parallel to the geojute direction to be tested. The specimen width and length was kept as 100 mm and 165 mm respectively.

The flow rate per unit width ( $\text{m}^3/\text{s}\cdot\text{m}$ ) versus normal compressive stress and hydraulic transmissivity ( $\text{m}^2/\text{s}$ ) versus normal compressive stress is presented in Fig 4.55 and Fig 4.56 respectively. As can be seen from these fig that the flow rate per unit width and hydraulic transmissivity decreases exponentially with the increase of normal stress. It may also be noted that the increase in transmissivity with increasing mass per unit area.

Koerner (1997) reported hydraulic transmissivity of geotextiles reaches constant value after approximately 85 kPa (Fig 4.57). The tested jute samples show also same behavior. Because beyond such load the yarn structure is sufficiently tight and dense to hold the load but still convey liquid to some extent. It may also be noted Jute sample show maximum flow rate/unit width and hydraulic transmissivity. Initially the samples have a greater difference in both flow rate and hydraulic transmissivity. As flow continues after 15-kPa stress the difference between samples are reduced.

Six nonwoven jute based geotextiles consisting of varying proportions of jute and polypropylene fibres were evaluated for their engineering properties by ASTM/BIS standards for geotextiles and related products by Rao et al (1994). Both normal and in-plane permeabilities were determined for all the fabrics type. As can be seen from Fig 4.58 and Fig 4.59, both the coefficient of normal permeability and coefficient of in-plane permeability follow a decreasing trend with increase in normal stress. Again the normal and in-plane permeabilities of the fabrics were increasing with thickness of the fabric. Thus, the thicker fabrics have excellent filtration and drainage characteristics.

#### **4.1.13 Unconfined Tension Creep Behaviour**

Unconfined creep test on treated and untreated Canvas samples was performed as per ASTM D 5262-97. The load for creep test was selected from the tensile strength determined from wide-width tensile test. Considering the maximum tensile strength as 100%, creep test stresses at 10%, 20%, 30%, and 40% were planned to evaluate. Stresses were applied for 1,000 hours and readings were taken at progressively longer time increments from the beginning of the test e.g. 1, 2, 5, 10 and 30 minutes; then 1, 2, 5, 10, 30, 100, 200, 500 and 1000 hours.

The preparation of sample is an important factor for successful completion of creep test on geojute samples. In addition to ASTM D 5262-97, the sample preparation and test procedure presented by Kabir (1988) was also followed in this study. Each specimen was cut 200 mm (8 in) wide by 300 mm (12 in) long, with the length dimension being designated and accurately parallel to the direction for which

the creep behavior is being measured. Centrally, two parallel lines were drawn near the centre of each specimen length and separated by 100 mm (4 in). These lines are extended to the full width of the specimen, and are exactly perpendicular to the length of the specimen. On the both ends, each 100mm (4 in) sample was made hardened by repeated application of Solvent cement so that it does not extend or specimen integrity is not affected while the load is being hung (Fig 4.60 and 4.61). The clamps for hanging the sample was as wide as the specimen, with appropriate clamping power capable of preventing slippage or damage to the specimen. The clamps and clamping technique designed to minimize eccentric loading of the specimen. Prior to the application of load, the centering of the specimen was done. A creep test arrangement is shown in Fig 4.62.

The maximum tensile strength for untreated Canvas determined from wide-width tensile was 24 kN/m. The stresses selected for this test were 2.4 kN/m, 4.8 kN/m, 7.2 kN/m and 9.6 kN/m. The tests for all the samples were performed successfully up to 1,000 hours except for 9.6 kN/m load. This sample ruptured on 34<sup>th</sup> day at the end of 816 hours. After removing the loads completing 1000 hours, the recoverable strain was measured. The elongation or percent strain versus time is plotted for each stress increment. As can be seen from Fig 4.63 that the material is less susceptible to creep, even less than polyester geosynthetics. Kabir (1994) conducted a study on mechanical properties of some jute-based fabrics and fibre drains and reported Canvas fabrics is susceptibility to creep (Fig 4.64), even less than polyester geosynthetics, which show a good agreement with the tested data. It may also be seen from Fig 4.63 that Canvas behaves like an elasto-plastic material i.e. the material behaves partly like elastic and partly like a plastic material upon subjection to loading. Upon application of load the material acquires an instantaneous elastic strain followed by development of a plastic strain component with time under sustained load. After removal of the sustained load, there is an elastic component of the strain was found to recover fully. The plastic strain component was found not to recover at all even long time after the removal of load. It may be appreciated that most of the geotextiles, on the other hand, behave like an elasto-visco-plastic material.

Based on the data presented in Fig 4.63, a plot of isochronous curves is developed (Fig 4.65), following the procedure described in Chapter Two. Isochronous

curves are the plots of load versus strain at the same temperature from different loading tests. The curves are plotted for 1, 10, 100 and 1000 hrs. From this diagram, the strain corresponding to load and vice-versa within the range of test data may be found out. The isochronous load versus strain diagrams presented by Kabir (1994) is shown in Fig 4.66.

The maximum tensile strength for treated Canvas determined from wide-width tensile was 27.5 kN/m. The stresses selected for this test were 2.7 kN/m, 5.5 kN/m, 8.3 kN/m and 10.8 kN/m. The test for 2.7 kN/m only could be performed successfully up to 1,000 hours and loads were removed properly. The sample hung for the test of 5.5 kN/m ruptured on 23<sup>rd</sup> day at the end of 552 hours. The sample hung for the test of 8.3 kN/m load ruptured just after 55 minutes. The test for the load 10.8 kN/m did not performed since the previous test sample ruptured within very short time. The elongation or percent strain versus time is plotted for each stress increment. As can be seen from Fig 4.67 that the untreated Canvas also less susceptible to creep. The untreated and treated creep samples before and after test is presented in Fig 4.68 through 4.71.

## 4.2 Comparison with Available Geotextile Data

In order to suggest geojute as potential substitute or competitive candidate material in the applications where geotextiles have already been successfully used, an attempt has been taken to compare the available geotextile test data with tested untreated and treated geojute data in this research. In this connection, test data of twenty geotextiles which were tested in BUET geotechnical laboratory has been collected and plotted. The comparisons are shown in Fig 4.72 through Fig 4.78. A zoning is shown on all graphs so that the clusters of plotted data can easily be seen. This zoning is not based on statistical analysis. At the end a summary in tabular form is presented in terms of comparative properties of synthetic geotextile & geojute in Table 4.1.

#### 4.2.1 Mass per Unit Area

The mass per unit area of the geotextiles remain within the range of 240 g/m<sup>2</sup> to 640 g/m<sup>2</sup>. Most of the geotextile mass remain 400 g/m<sup>2</sup>. The untreated geojutes mass per unit area ranged from 322.40 g/m<sup>2</sup> to 828.06 g/m<sup>2</sup>. The mass per unit area of treated geojute ranged from 1218.2 g/m<sup>2</sup> to 1590.7 g/m<sup>2</sup>. The mass per unit area of untreated geojute falls within the range of geotextiles. After treatment the mass per unit area of treated geojute increases proportionately (Fig 4.72).

#### 4.2.2 Thickness

The thicknesses of the geotextiles vary largely. It ranges from 2 mm to around 4.5 mm. The thickness of the untreated and treated geojute varied from 1.33 mm to 2.42 mm and 2.52 mm to 3.62 mm respectively. The thickness of the locally produced geotextiles varies from 1.5 mm to 4 mm so that the user can choose as per their requirement (Fig 4.73).

#### 4.2.3 CBR Puncture Strength

The CBR puncture resistances of geotextiles vary between 2660N to 5450N. This wide variation may be due to variation in thickness and mass per unit area. The CBR puncture resistances of untreated jute vary between 1566N to 4492N. The treated CBR puncture resistances vary widely 1471N to 3736N (Fig 4.74).

#### 4.2.4 Grab Tensile Strength

The grab tensile strength of geotextiles varies between 1163N to 2590N in MD and 780N to 1880N in XMD. The average grab breaking strength of untreated geojutes varies between 225N to 929N in MD and 248N to 750N in XMD. In case of treated jute, the grab breaking strength ranged from 831.6N to 1044N in MD and 668N to 984N in XMD (Fig 3.75). The grab breaking strength of untreated geojute is quite low compared to synthetic geotextiles. Due to treatment the strength of geojute increased significantly in both the directions (Fig 4.75).

#### 4.2.5 Grab Tensile Elongation

The grab tensile elongation of geotextiles varies between 64% to 140% in MD and 61% to 122% in XMD. The grab elongation of untreated geojutes varies between 19.7% to 35.5% in MD and 17.2% to 29.5% in XMD. In case of treated samples in MD, the elongations ranged from 23.6% to 40%. In XMD, the value ranged from 20% to 33.5%. The grab elongation of untreated and treated geojute do not vary largely. Being synthetic material geotextiles are susceptible to large elongation. Thus the variation in elongation between geojute and geotextile is too high (Fig 4.76).

#### 4.2.6 Wide-width Tensile Strength

The wide-width tensile strength of geotextiles varies between 18 kN/m to 48 kN/m in MD and 15 kN/m to 31 kN/m in XMD. The average strength in untreated geojute at MD ranged from 10.3 kN/m to 23.9 kN/m and at XMD from 10.7 kN/m to 26.8 kN/m. In case of treated samples in MD, the average strength ranged from 16.3 kN/m to 27.2 kN/m. In XMD, the average strength for treated geojute ranged from 18.4 kN/m to 31.58 kN/m. Canvas and DW Twill having wide-width strength closure to the lower range of geotextiles. Jute and Hessian may not be suitable considering wide-width strength. The treated geojute value shows inconsistent result (Fig 4.77).

#### 4.2.7 Wide-width Elongation

The wide-width elongations of the geotextiles ranged from 28% to 120% in MD and 53% to 100% in XMD. The elongation of untreated geojute ranged from 6.7% to 12.3% in MD and 5% to 8.2% in XMD. In case of treated samples, the elongation ranged from 10.9% to 21.3% in MD and 11.3% to 12% in XMD. In wide-width tensile test geotextile again show a large elongation than geojute (Fig 4.78).



**Table: 4.1: Comparative Properties of Synthetic Geotextile and Geojute**

Ser No	Name of observations	Effect on synthetic Geotextile	Effect of Jute Geotextile
1	Biodegradability	Nonbiodegradable	Designed biodegradable.
2	Photo degradability	Not Photodegradable	Photodegradable
3	Ionic Property	Normally nonionic	Anionic
4	Metal content	Mercury, lead, cadmium, copper, nickel, cobalt, zinc, Arsenic etc.	None
5	Stabilizer/sensitizer filler/pigment.	Present	Absent
6	Warming effect	Soil temperature	No effect
7	Leaching effect	pH changes from 4.5-8.5	-
8	Compatible	Normally not compatible	Compatible
9	Biomass	Negative effect	Non-slippery
10	Stacking effect	Slippery	Non-slippery
11	On Burning	Toxic gas evolves	Only CO evolves.
12	Effect on water	Pollution on leaching	No pollution
13	Effect on fish/microbes/eggs etc.	Harmful	Harmless
14	Effect on plant	Harmful	Helpful
15	Effect on biological pathway	Possibility of creating disturbance in biological pathway	No disturbance
16	Effect on agricultural activity.	Increase insect growth by increasing soil temperature.	No effect.
17	Prone to rat	Yes	Modified
18	Extensibility	High extensible	Low extensible
19	Shape and size	Any dimension	Any dimension

Ser No	Name of observations	Effect on synthetic Geotextile	Effect of Jute Geotextile
20	Fabrication	Wove, nonwoven and composite	Woven, nonwoven and composite
21	Expected design life	Non possible (if possible, creates other problems)	Possible
22	Application technology	Special technology and costly.	Simple and indigenous.
23	Full scale model study in Bangladesh	was not done	Done
24.	Origin	Foreign Local	Local
25	Cost	More	Less
26	Availability	Imported	Local and easy
27	Foreign exchange	Yes	No.

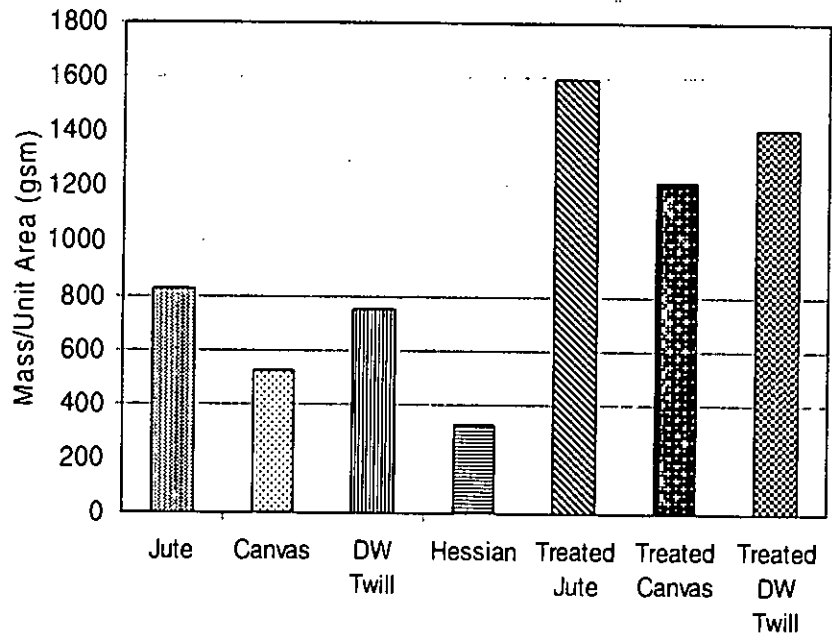


Fig 4.1 Mass per unit area of tested samples

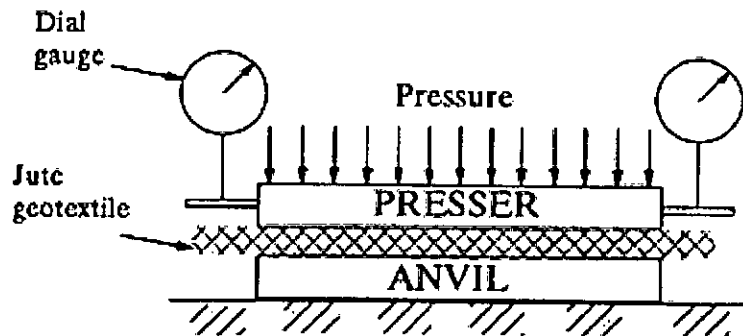


Fig 4.2 Schematic arrangement for measurement of equivalent single layer thickness

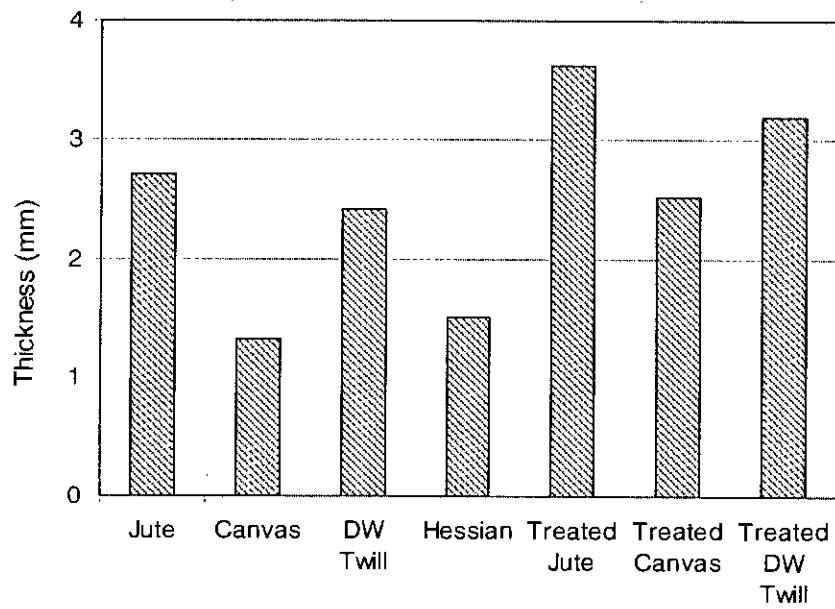
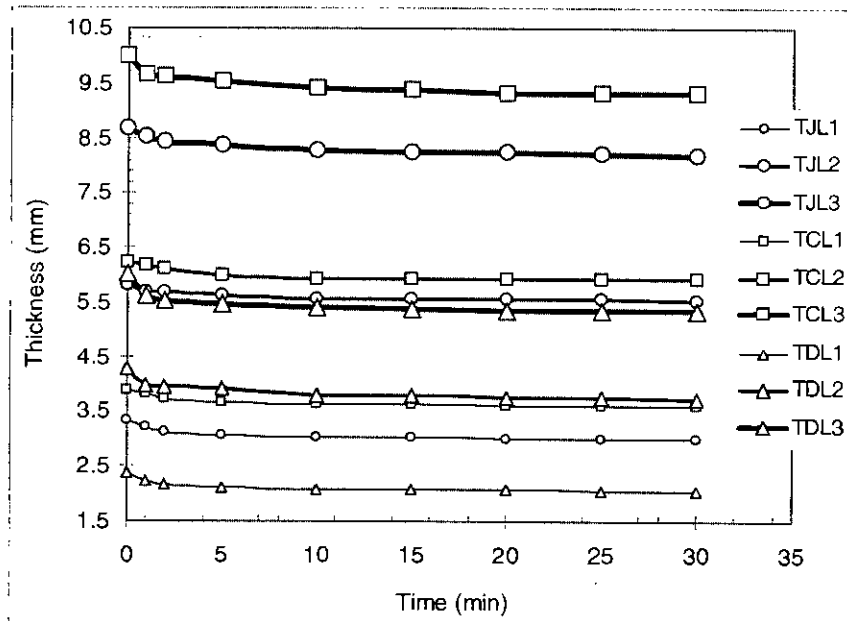


Fig 4.3 Nominal thickness of tested samples



TJL1: Treated Jute Layer 1. TCL1: Treated Canvas Layer 1. TDL1: Treated DW Twill Layer 1

Fig 4.4 Variation of thickness of treated geojute with time

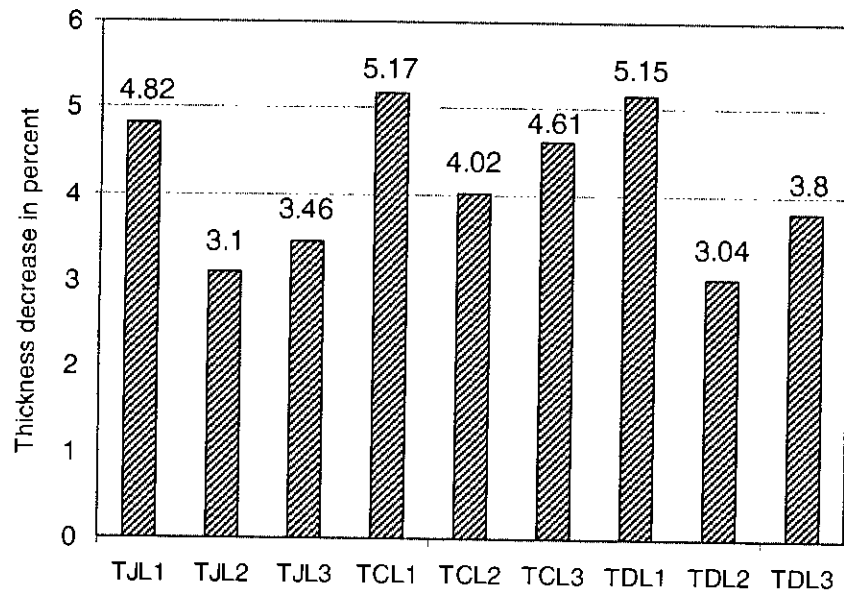


Fig 4.5 Variation of thickness in percentage within first five minutes of geojute

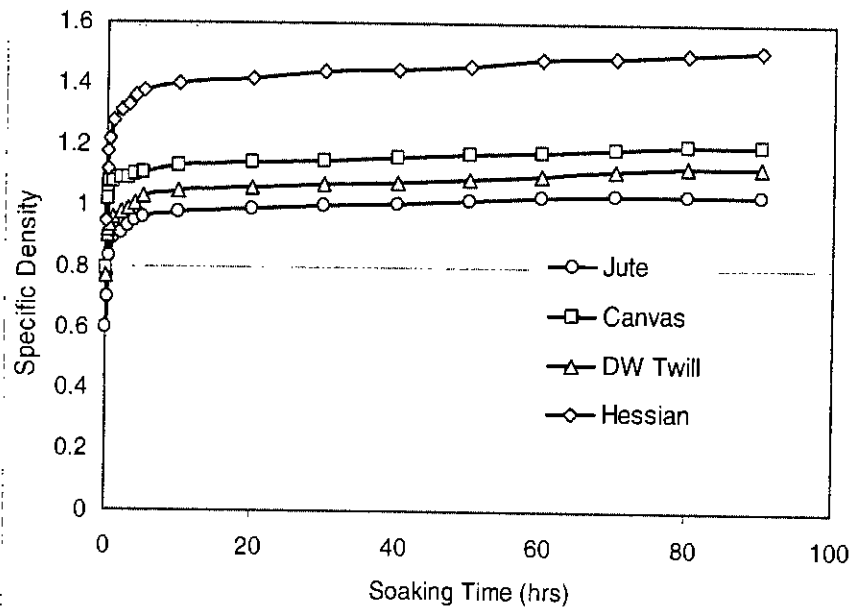


Fig 4.6 Variation of specific density with time for untreated geojute

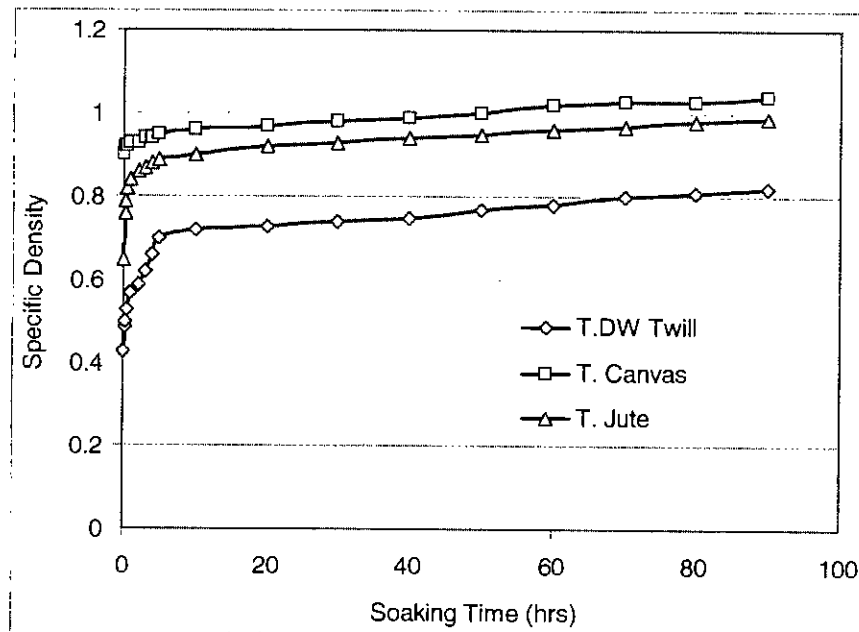


Fig 4.7 Variation of specific density with time for treated geojute

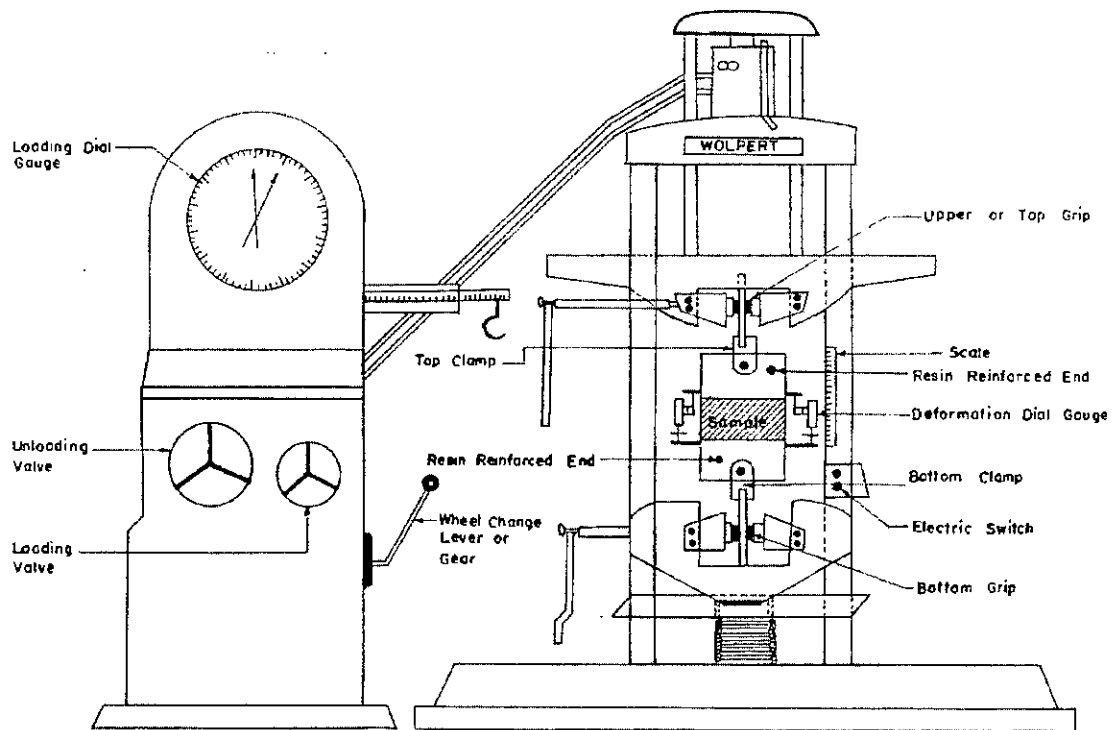


Fig 4.8 Repeated loading universal testing machine

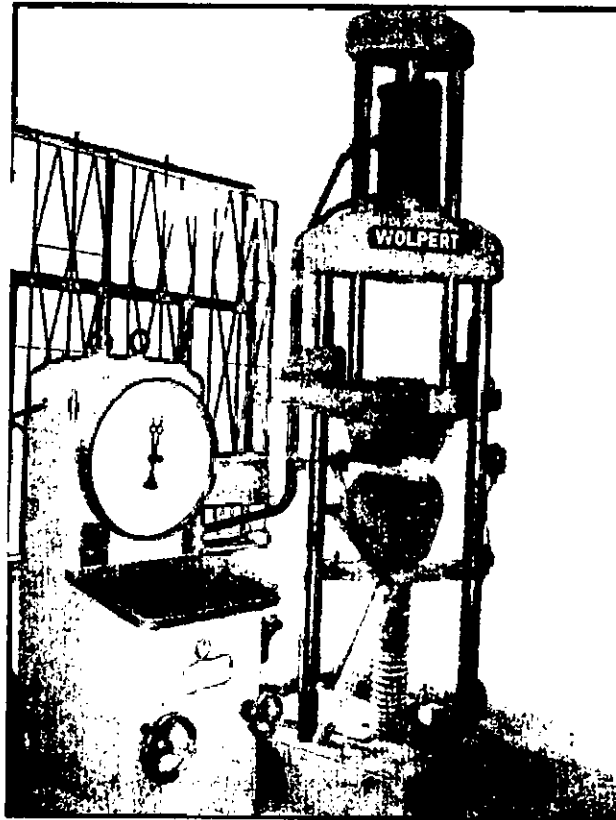


Fig 4.9 Wide-width strip tensile test using WOLPERT machine

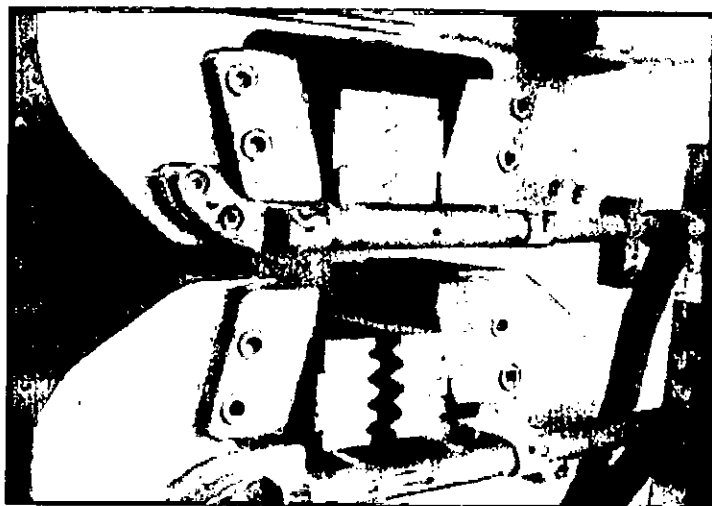


Fig 4.10 Grip and jaws of wide-width strip tensile machine

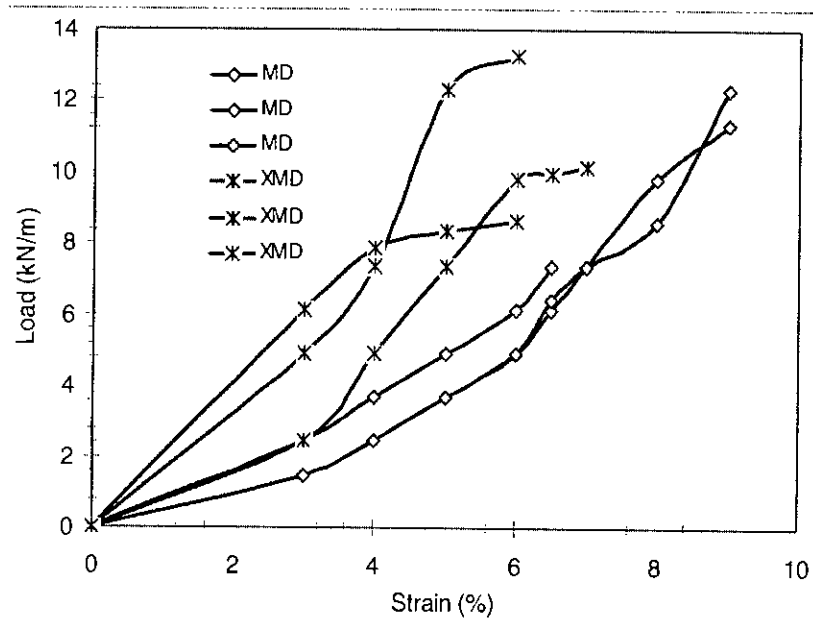


Fig 4.11 Load versus strain for untreated Jute

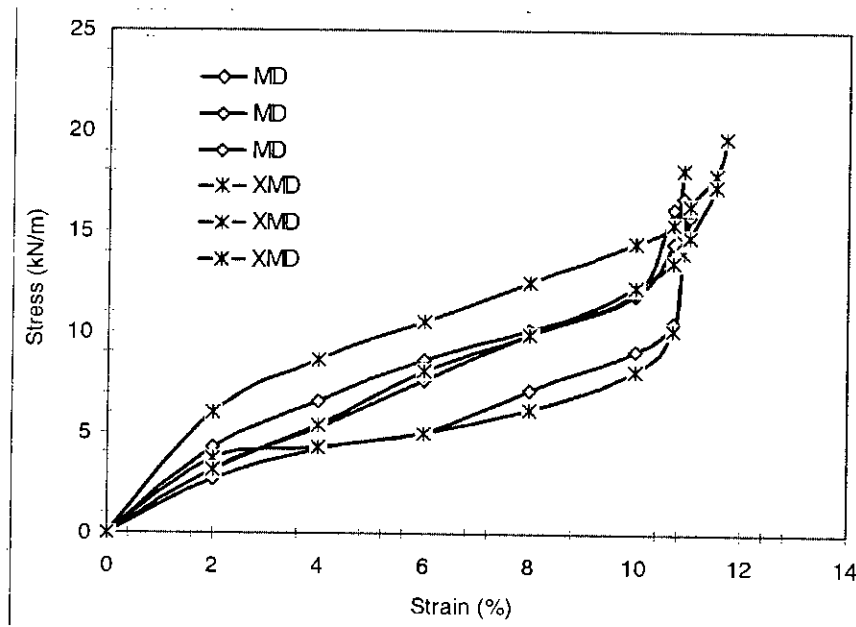


Fig 4.12 Load versus strain for treated Jute



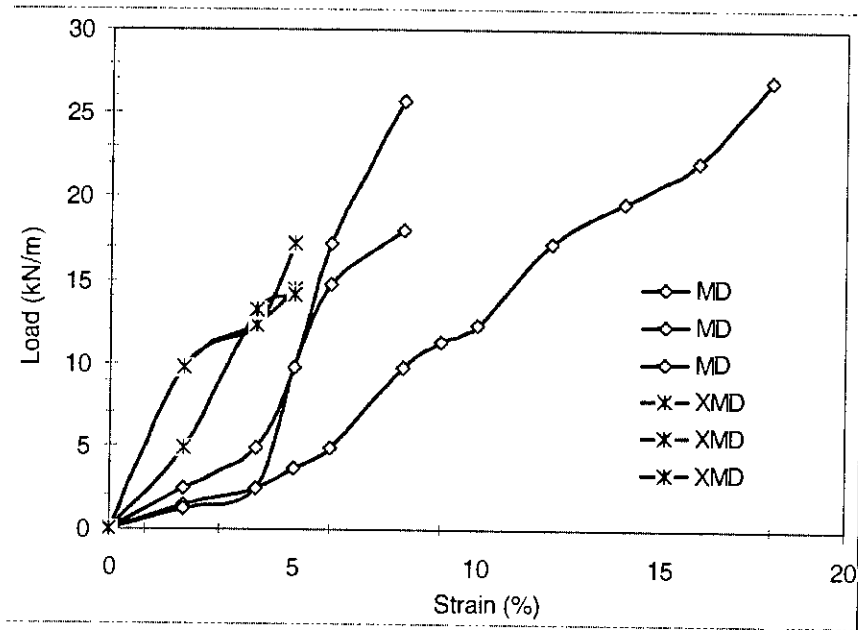


Fig 4.13 Load versus strain for untreated Canvas

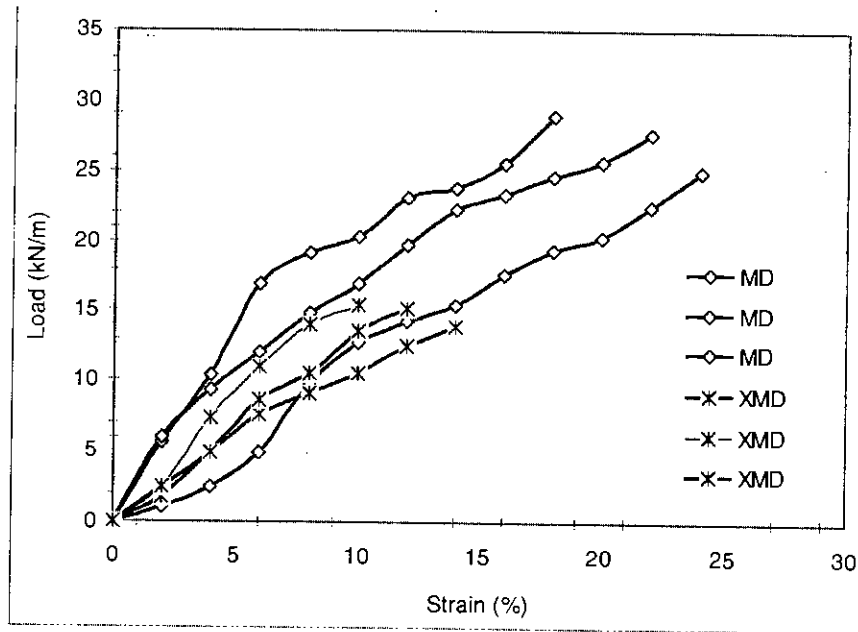


Fig 4.14 Load versus strain for treated Canvas

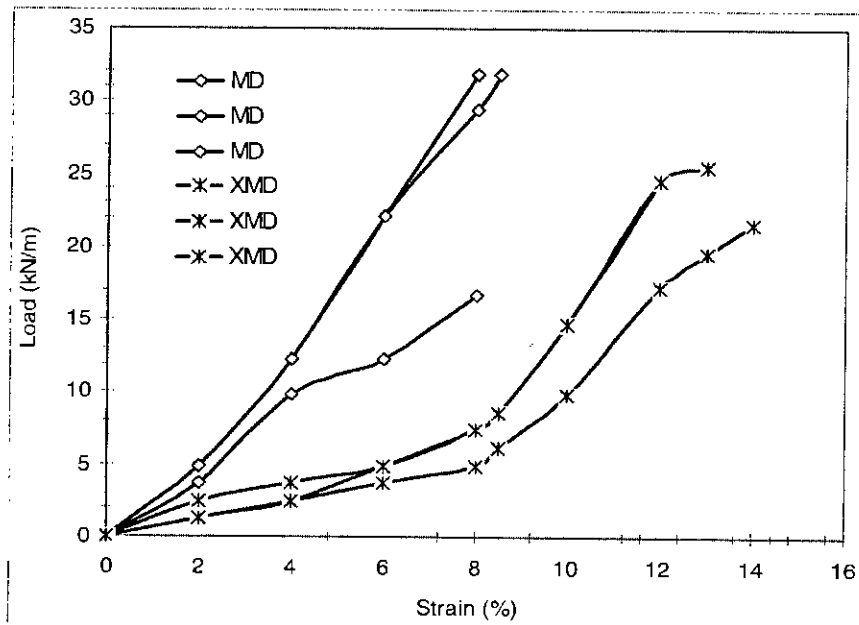


Fig 4.15 Load versus strain for untreated DW Twill

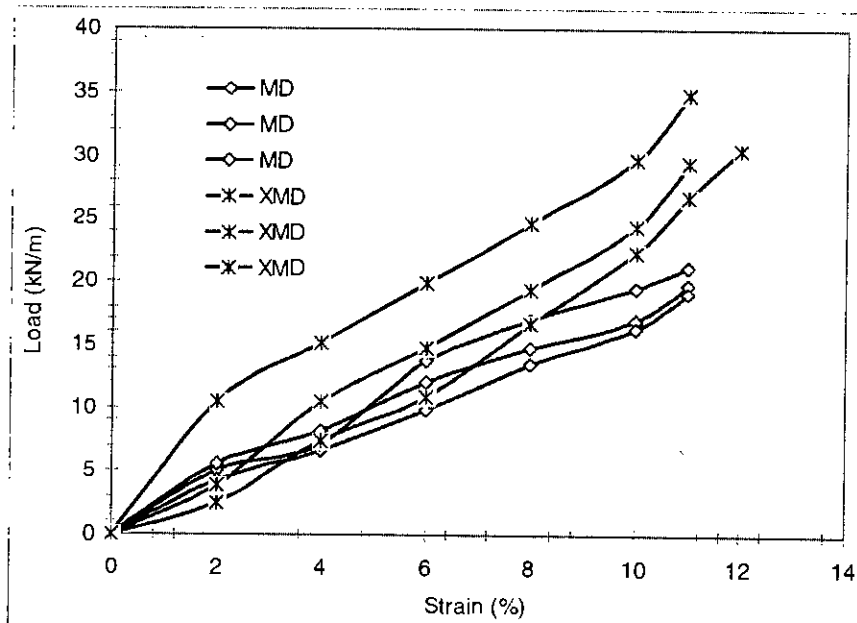


Fig 4.16 Load versus strain for treated DW Twill

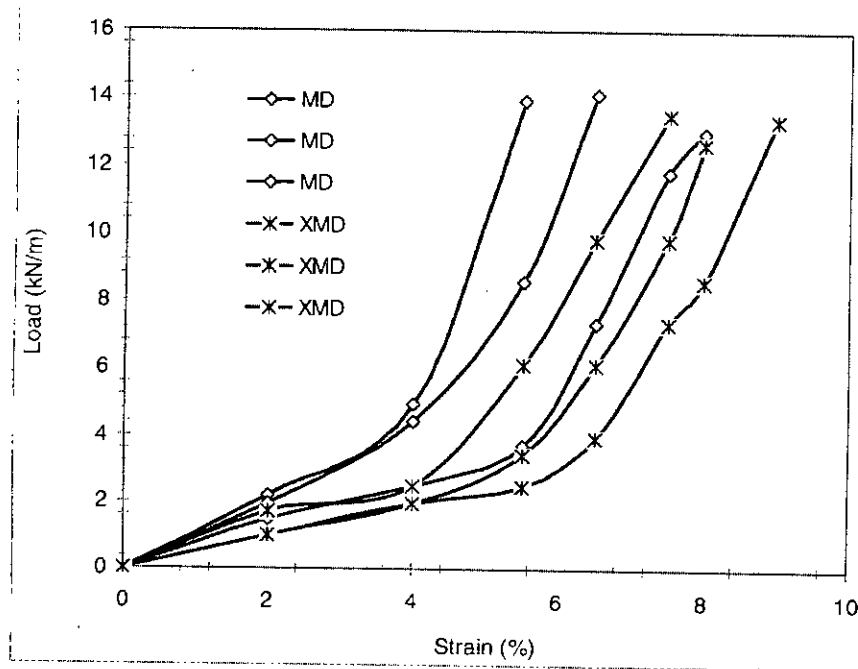
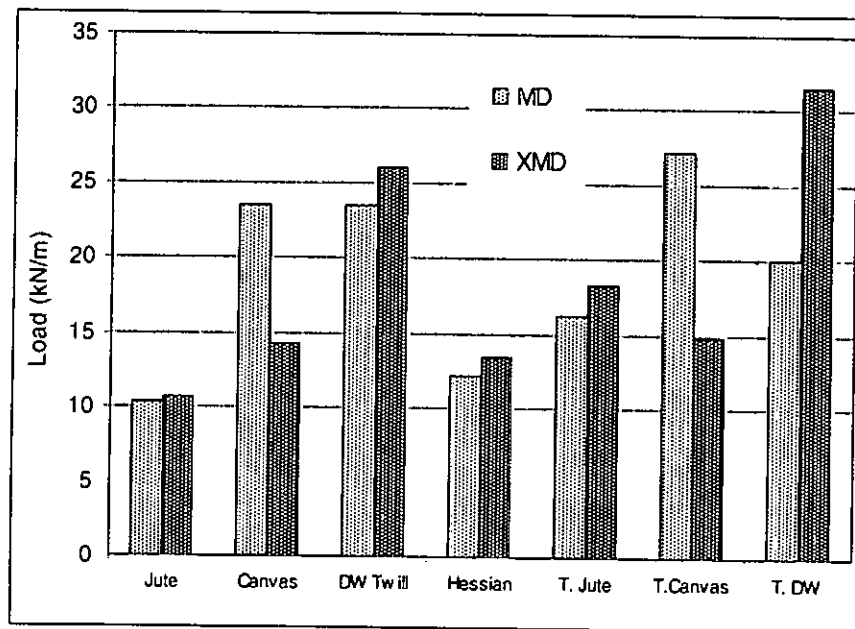
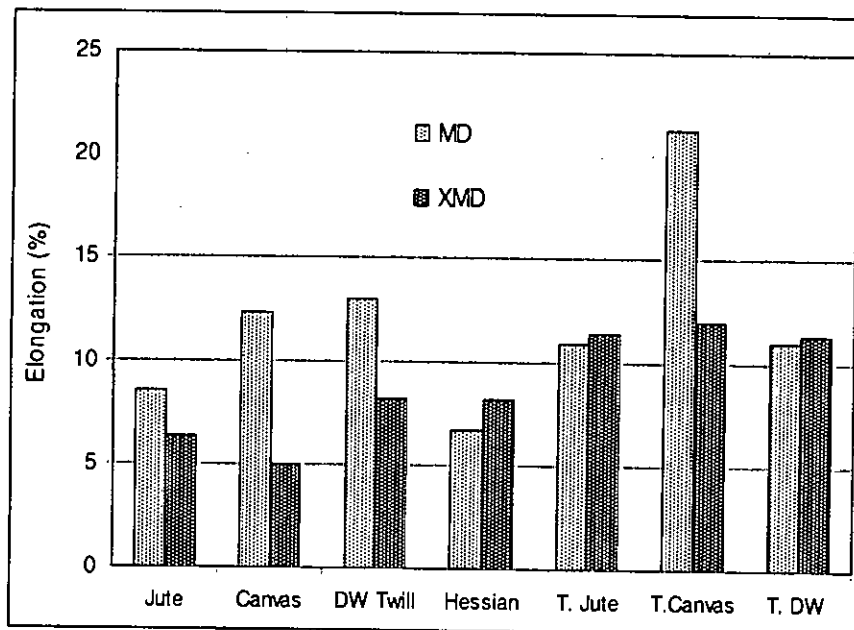


Fig 4.17 Load versus strain for untreated Hessian



T. Jute: Treated Jute. T. Canvas: Treated Canvas. T. DW. Treated DW Twill

Fig 4.18 Average wide-width tensile strength of tested samples



T. Jute: Treated Jute. T. Canvas: Treated Canvas. T. DW. Treated DW Twill

Fig 4.19 Average wide-width tensile elongation of tested samples

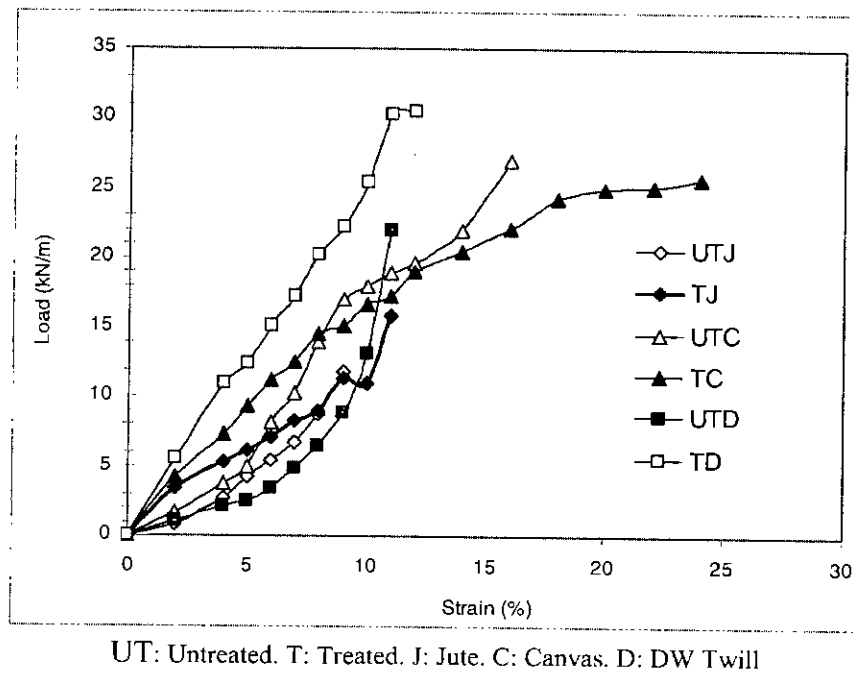


Fig 4.20 Average wide-width elongation of tested samples in MD

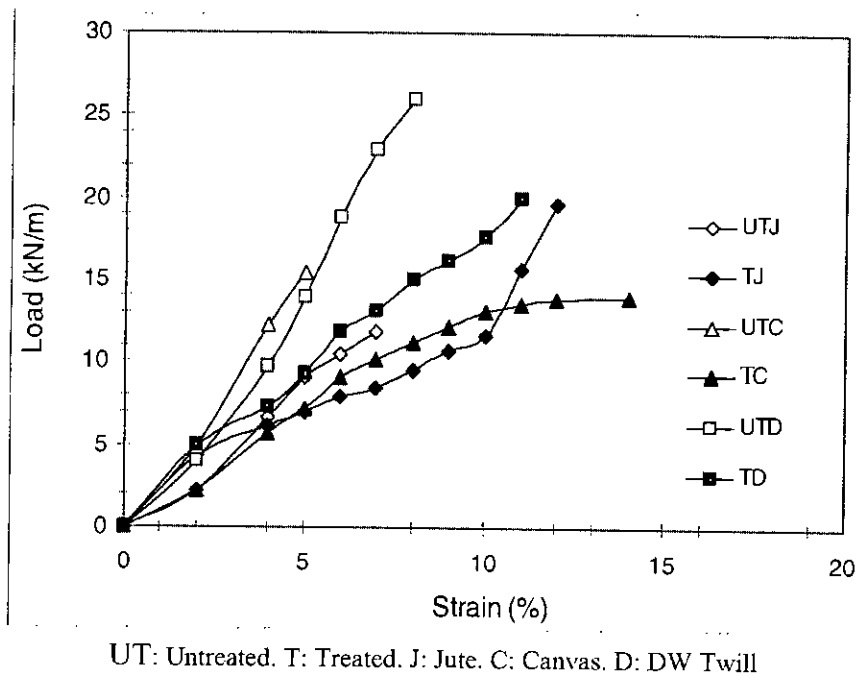


Fig 4.21 Average wide-width elongation of tested samples in XMD

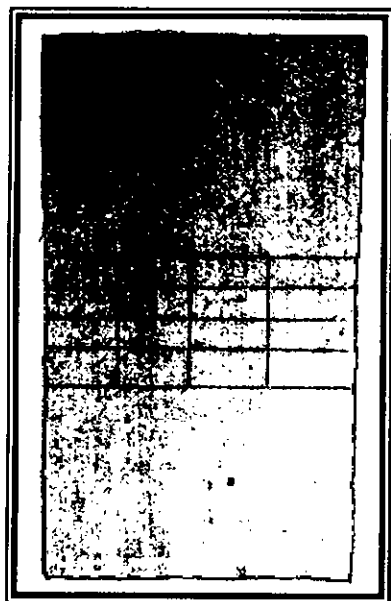


Fig 4.22 Canvas before wide-width test



Fig 4.23 Canvas after wide-width test

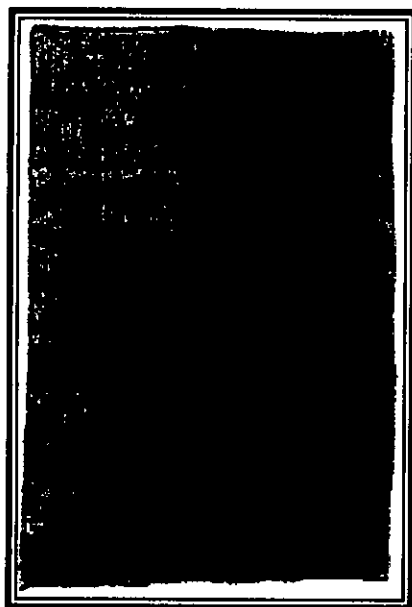


Fig 4.24 Hessian before wide-width test

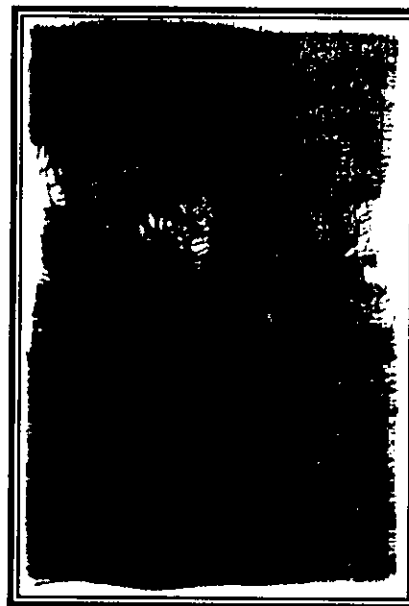


Fig 4.25 Hessian after wide-width test

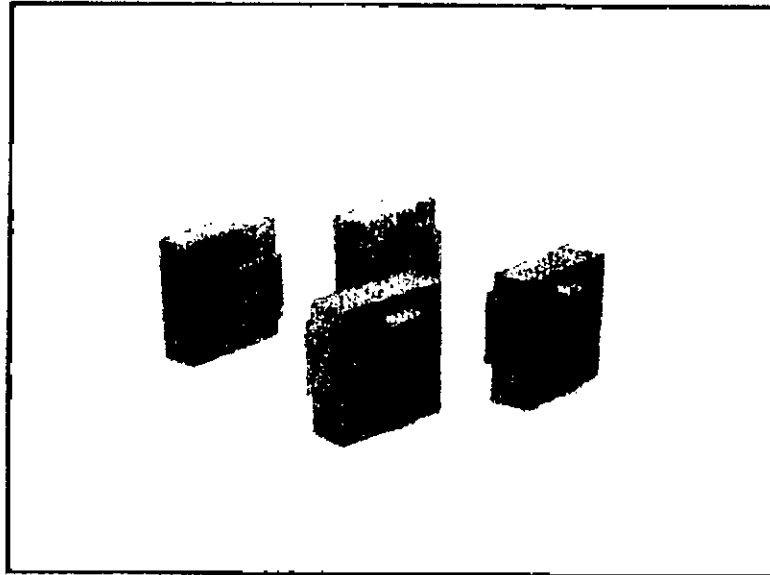


Fig 4.26 Clamps of grab breaking test

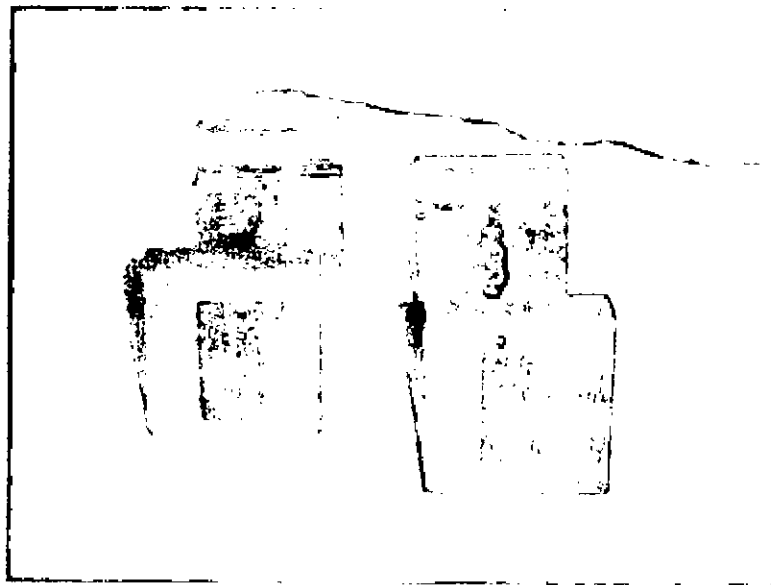


Fig 4.27 Clamps of grab breaking test

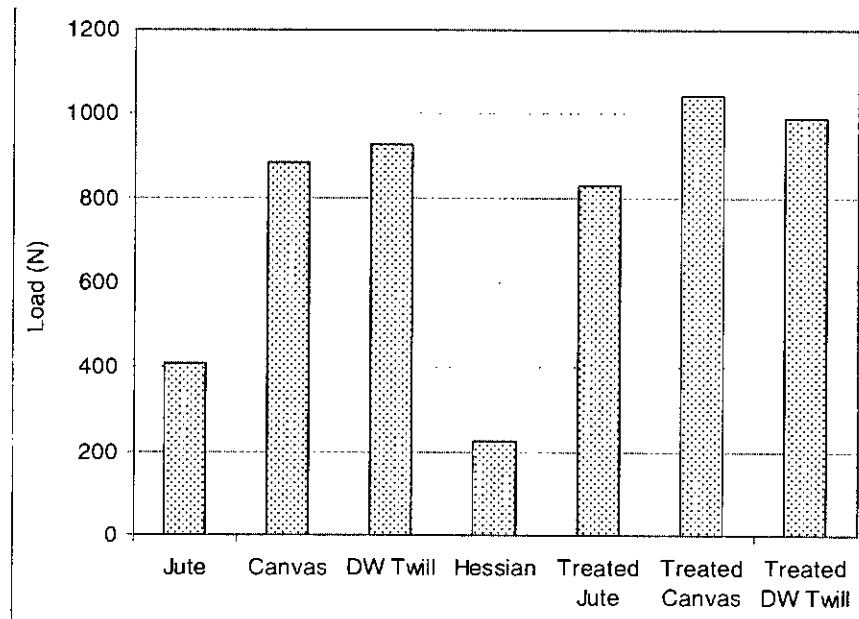


Fig 4.28 Grab breaking load of samples in MD

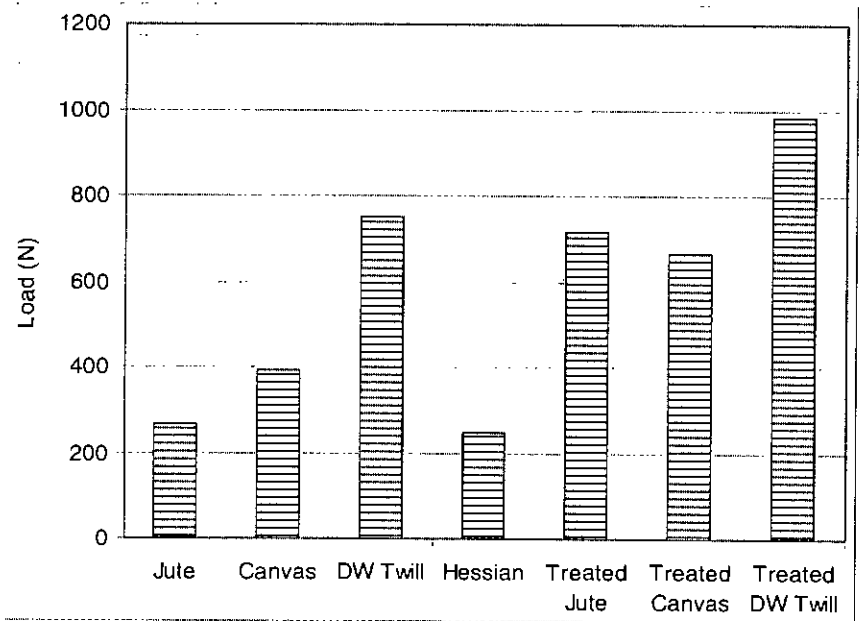


Fig 4.29 Grab breaking load of samples in XMD



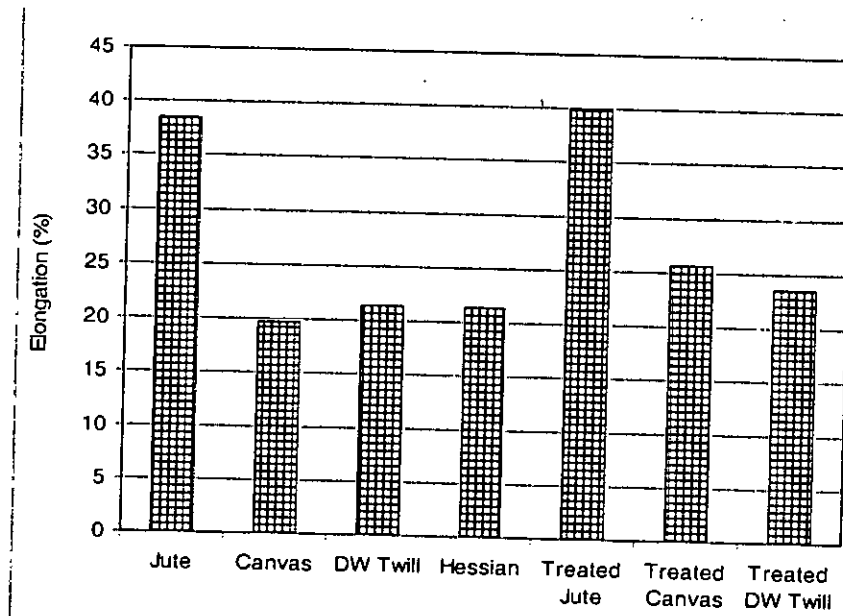


Fig 4.30 Grab breaking elongations of samples in MD

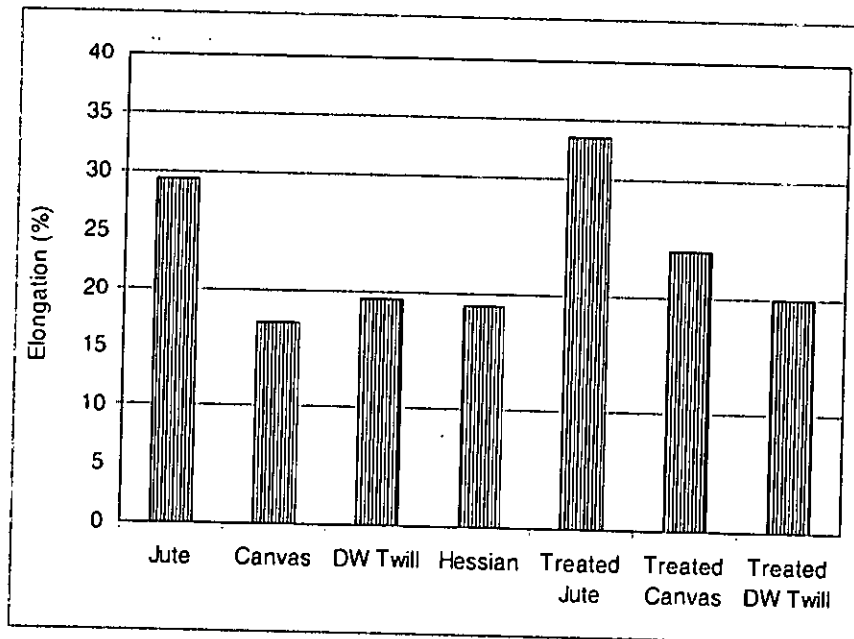


Fig 4.31 Grab breaking elongations of samples in XMD

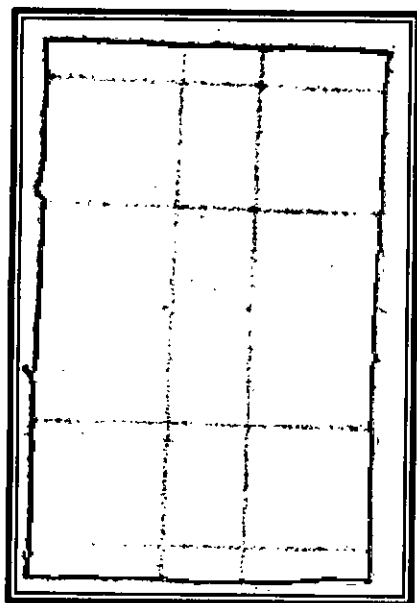


Fig 4.32 Canvas before grab test

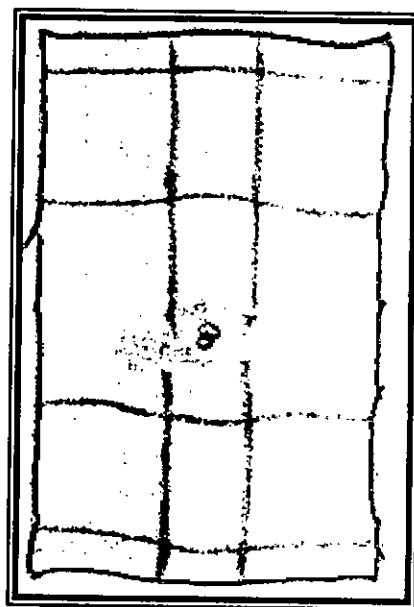


Fig 4.33 Canvas after grab test

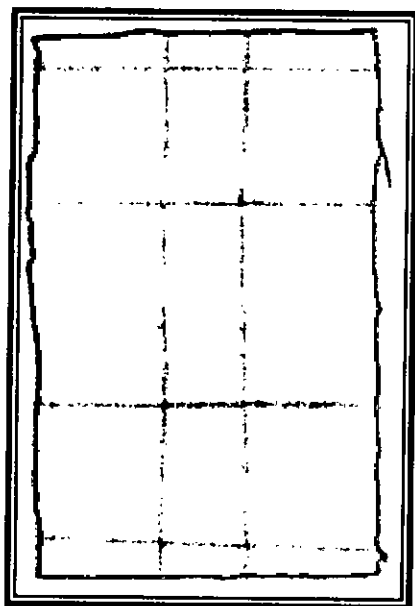


Fig 4.34 Hessian before grab test

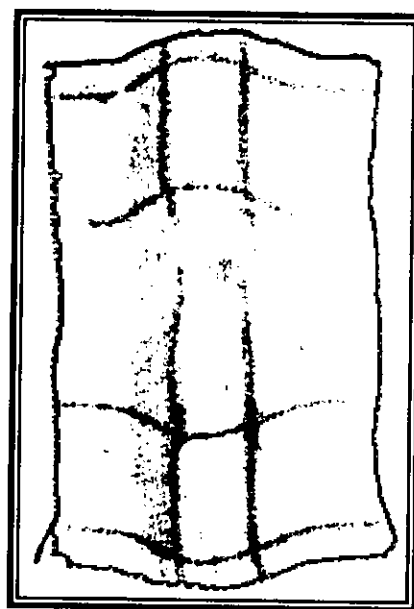


Fig 4.35 Hessian after grab test

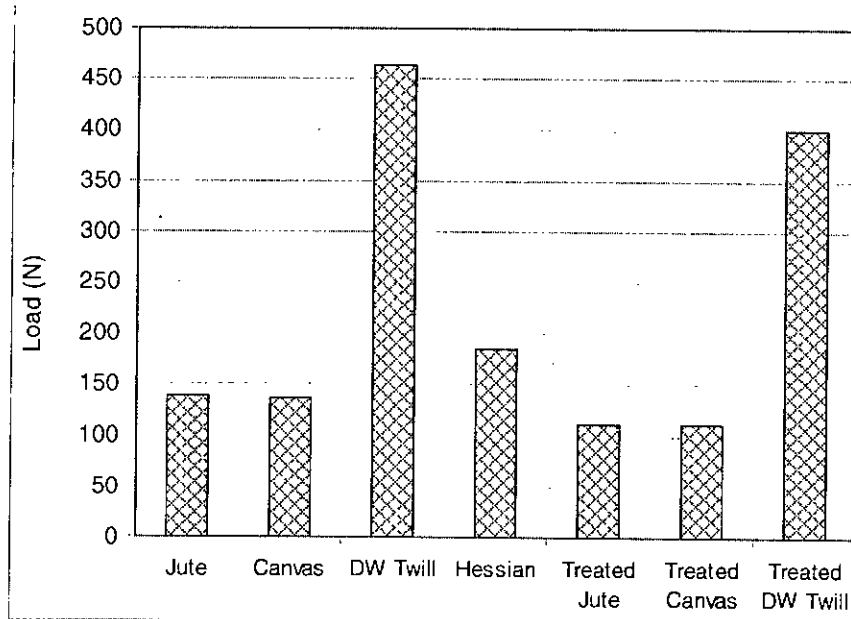


Fig 4.36 Trapezoid tearing strength of samples in MD

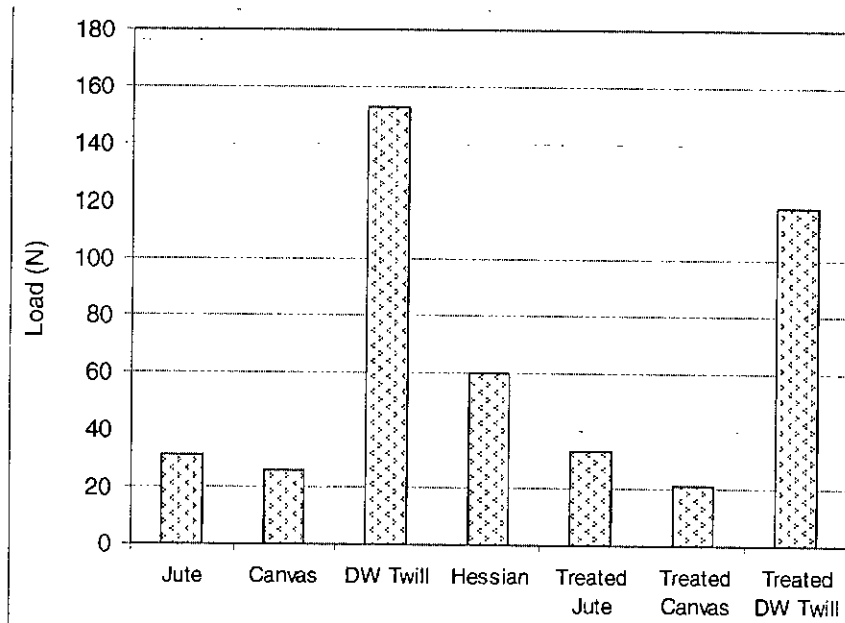


Fig 4.37 Trapezoid tearing strength of samples in XMD

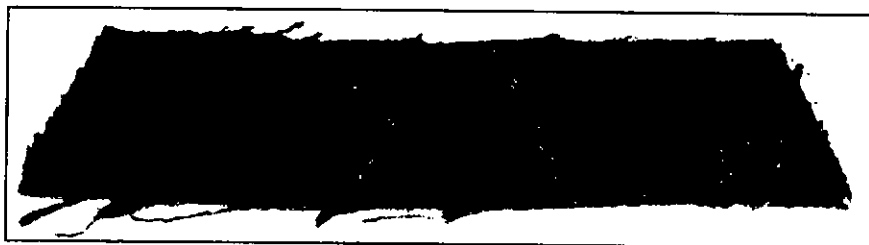


Fig 4.38 DW Twill sample before Trapezoid test

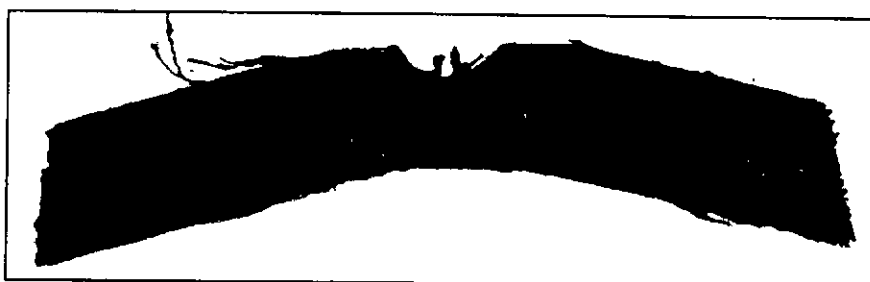


Fig 4.39 DW Twill sample after trapezoid test

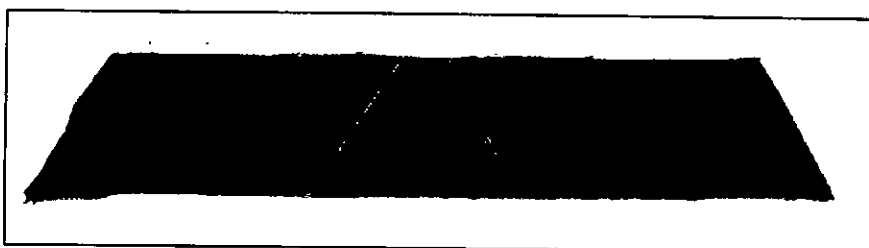


Fig 4.40 Canvas sample before trapezoid test

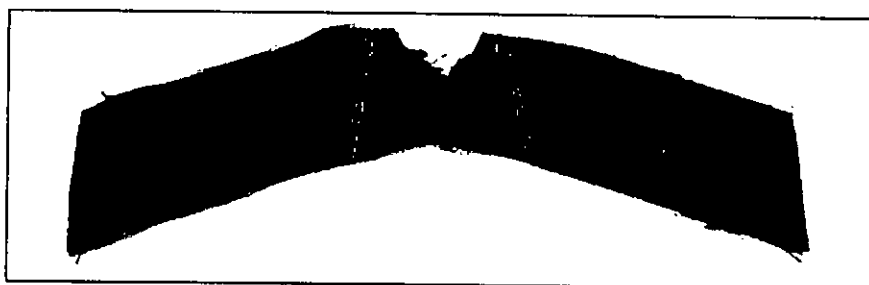


Fig 4.41 Canvas sample after trapezoid test

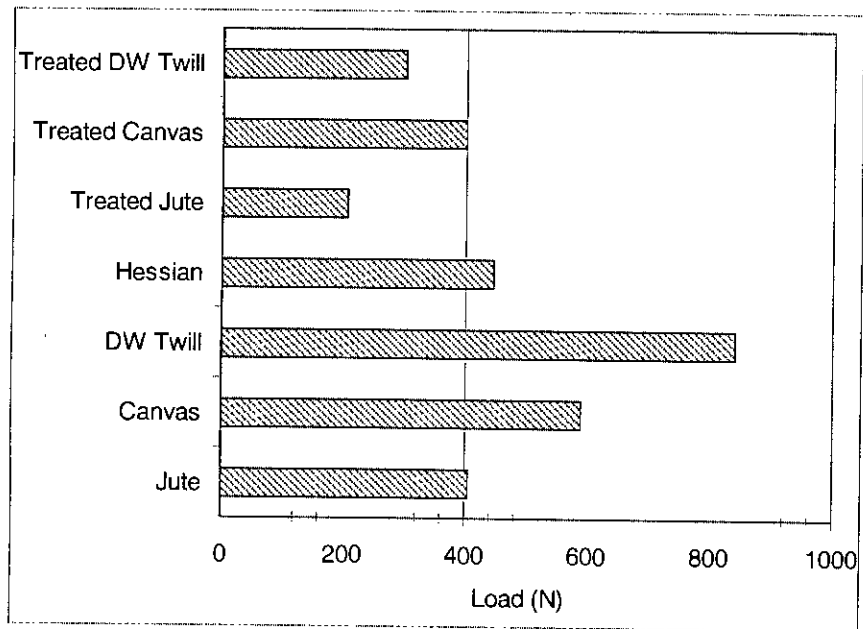
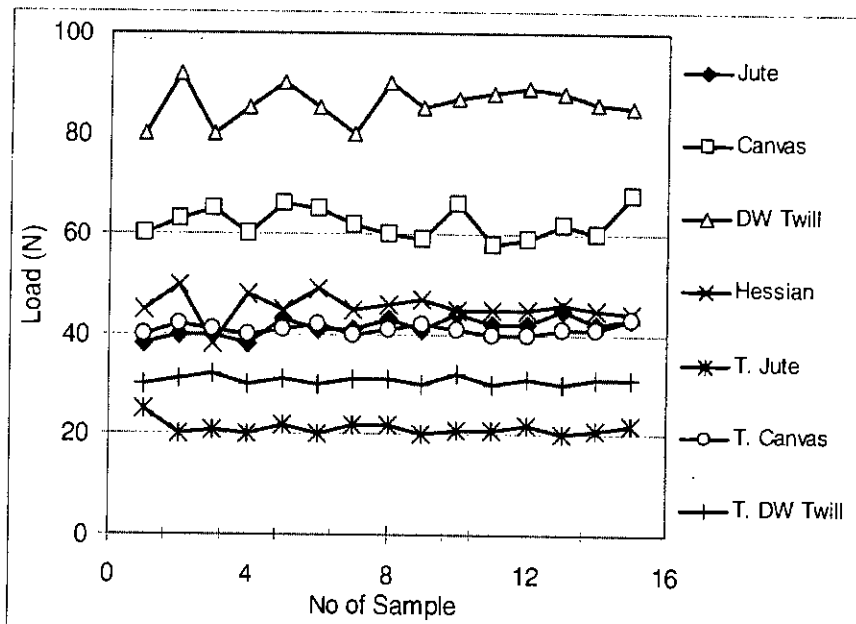


Fig 4.42 Index punctures strength of tested geojute



T: Treated

Fig 4.43 Variation in load of individual sample in index puncture test

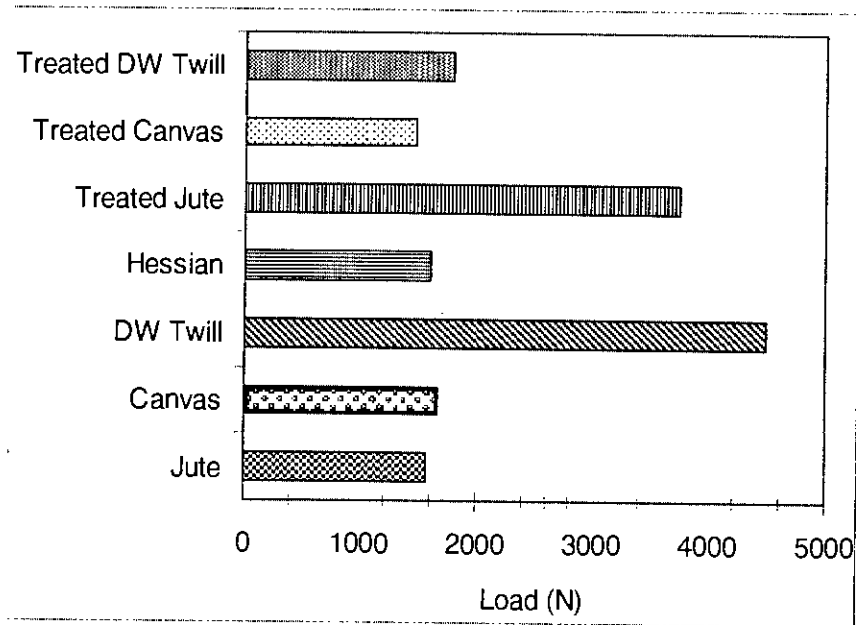


Fig 4.44 CBR strength of samples

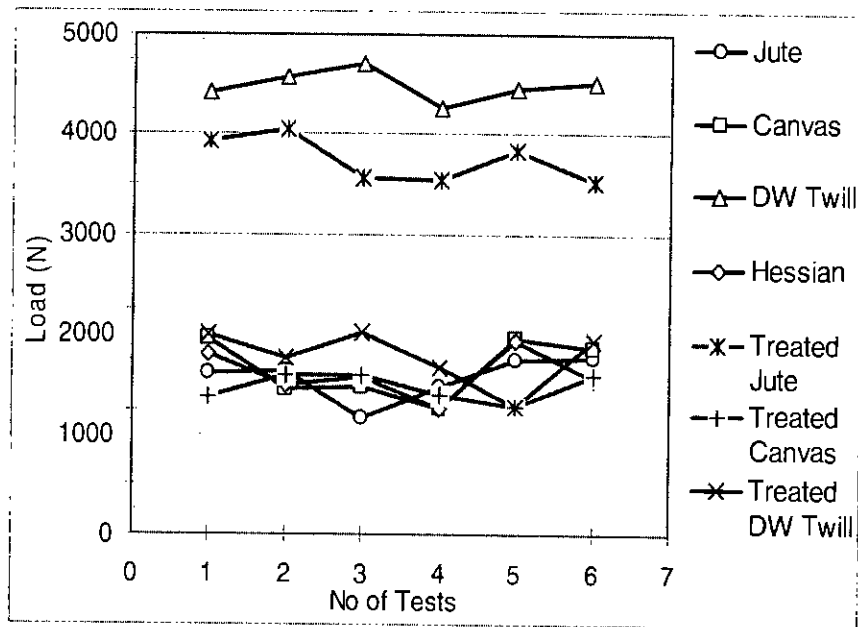


Fig 4.45 Variation in load of individual sample in CBR puncture test

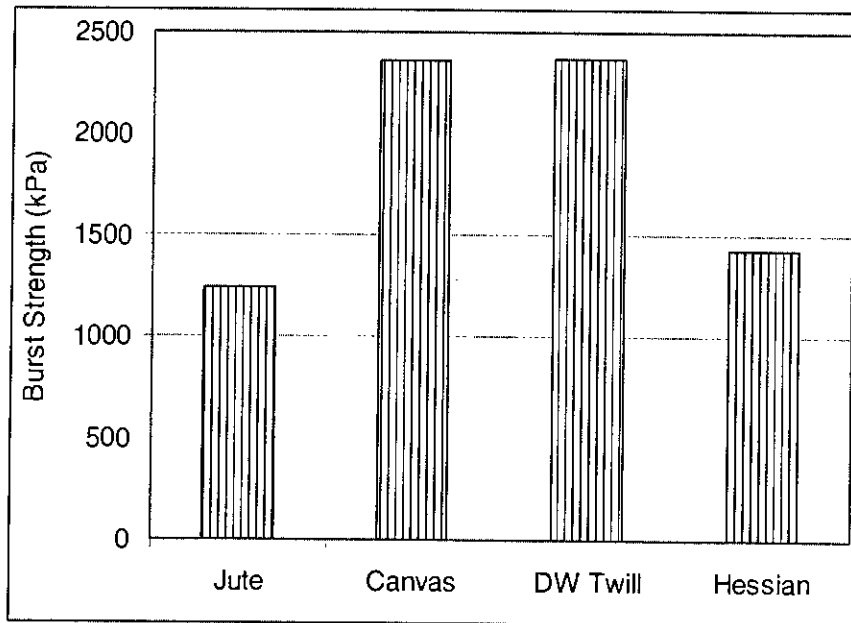


Fig 4.46 Burst strength of untreated samples

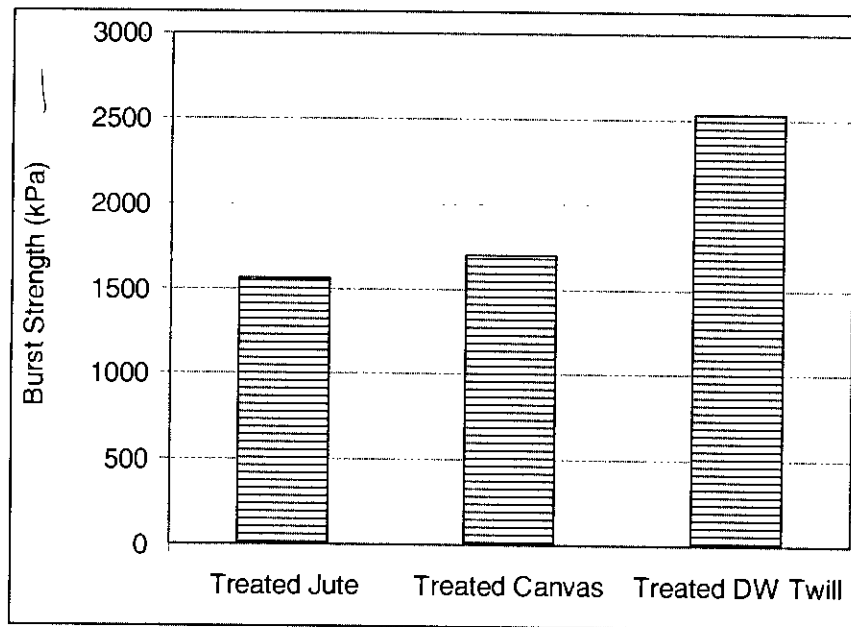


Fig 4.47 Burst strength of treated samples

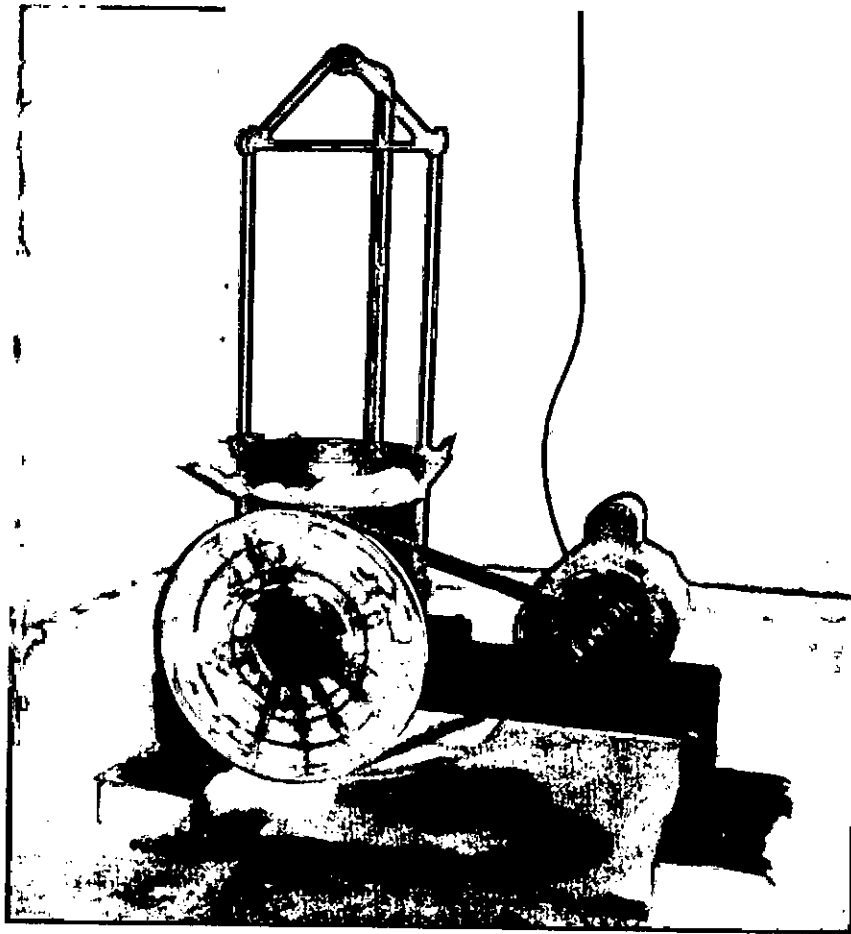


Fig 4.48 Sieve analysis machine



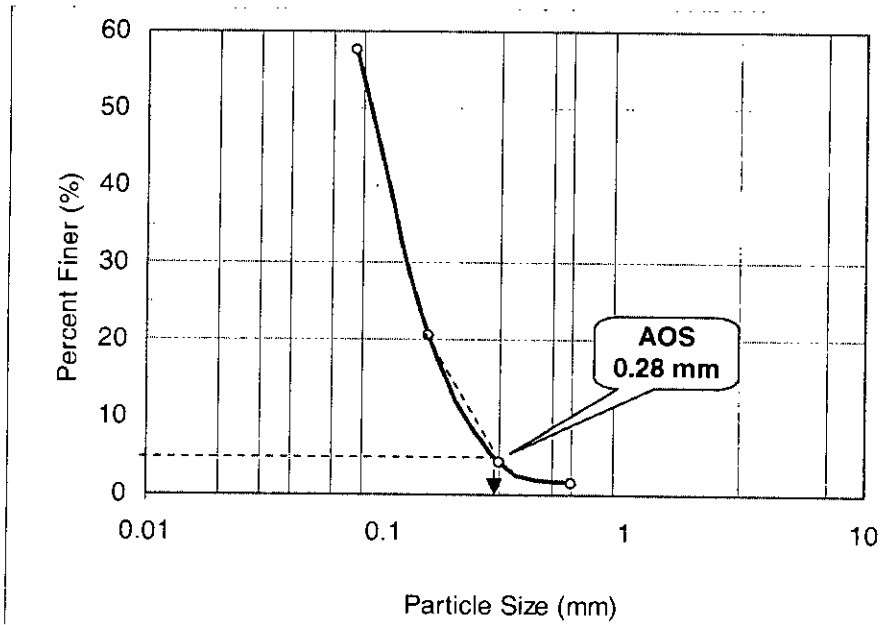


Fig 4.49 Apparent opening size plot of Jute

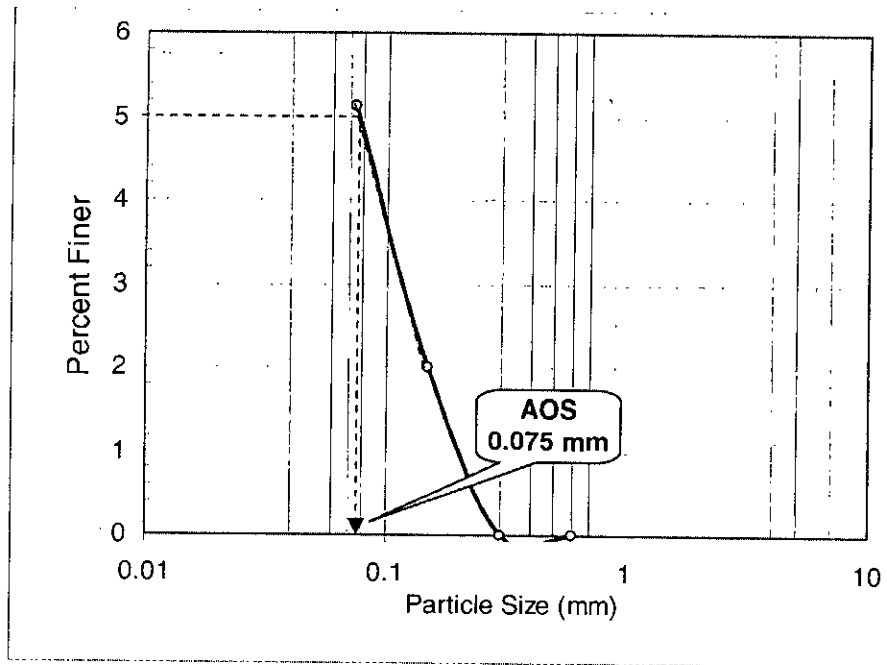


Fig 4.50 Apparent opening size plot of Canvas

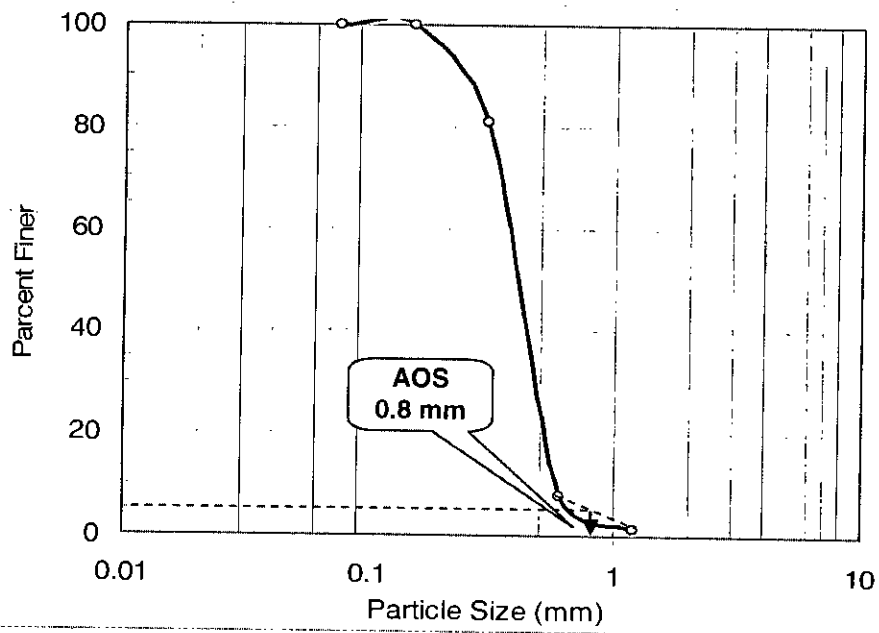


Fig 4.51 Apparent opening size plot of DW Twill

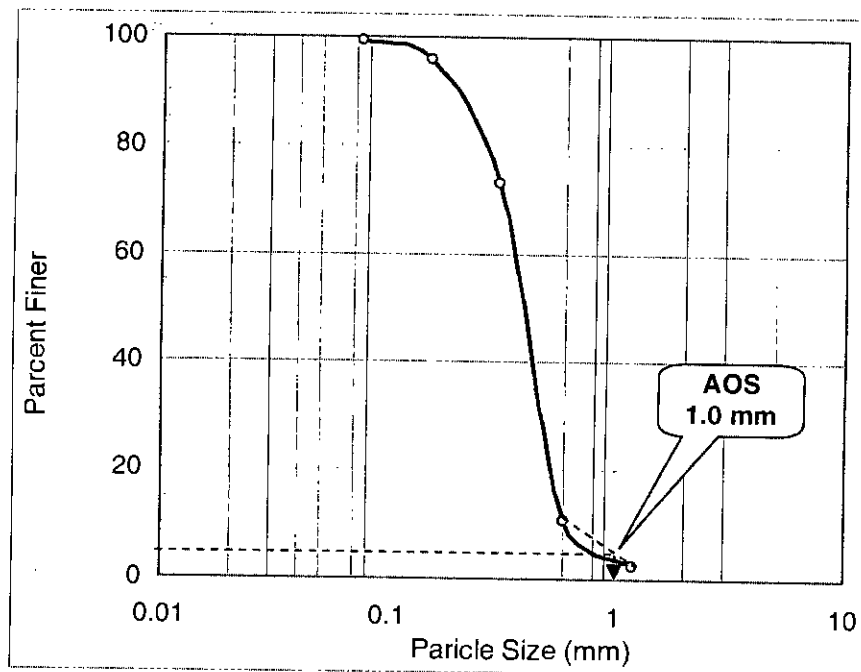


Fig 4.52 Apparent opening size plot of Hessian



Fig 4.53 Test arrangement of Permittivity

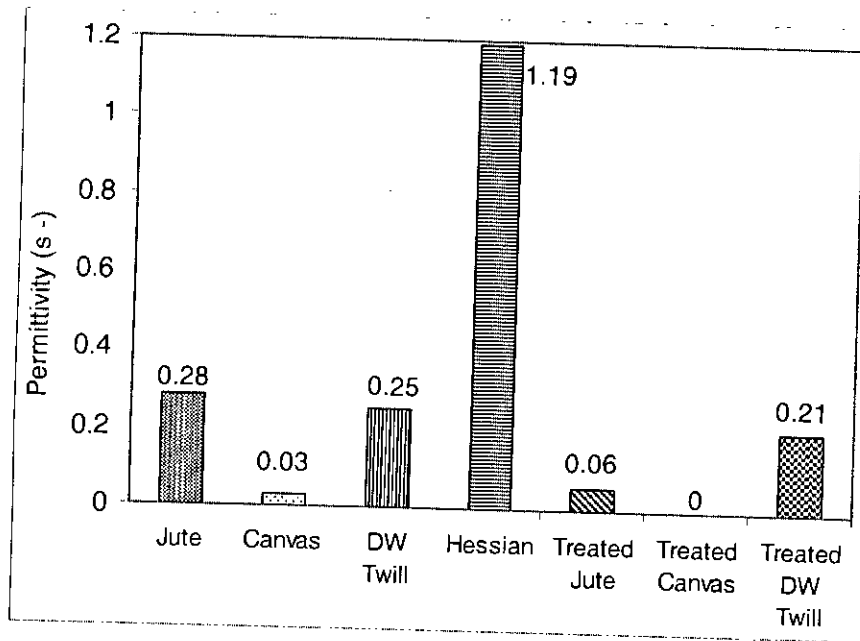


Fig 4.54 Permittivity results of samples

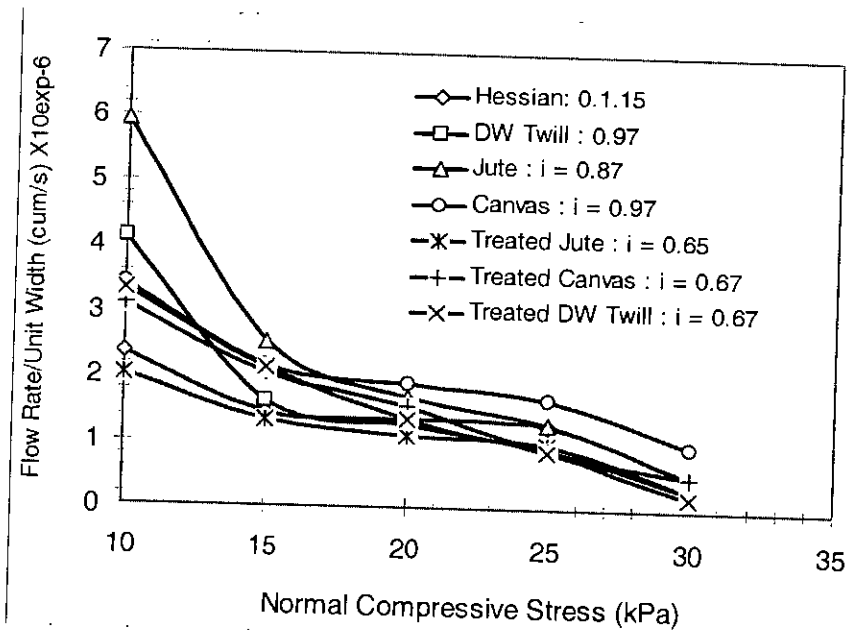


Fig 4.55 Flow rate per unit width versus normal compressive stress of samples

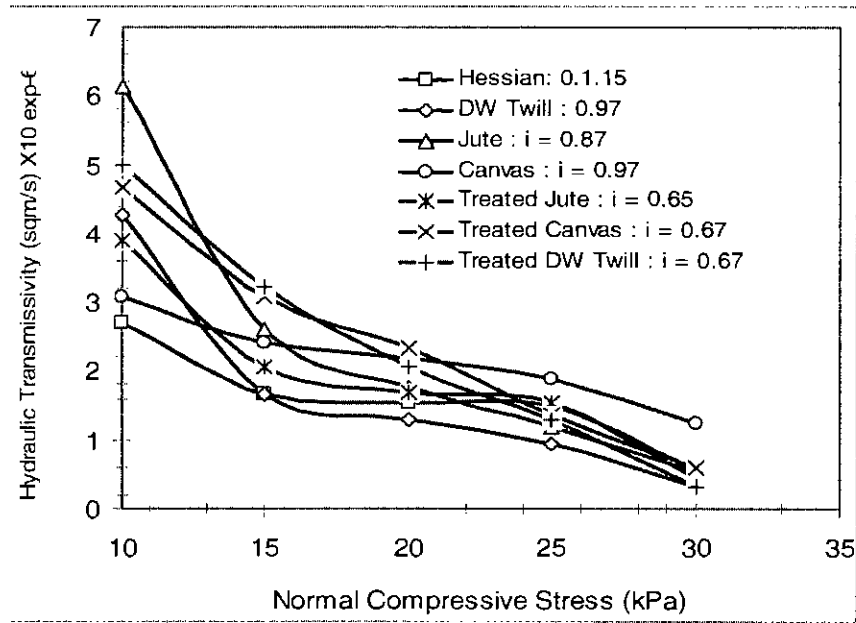


Fig 4.56 Hydraulic transmissivity versus normal compressive stress of samples

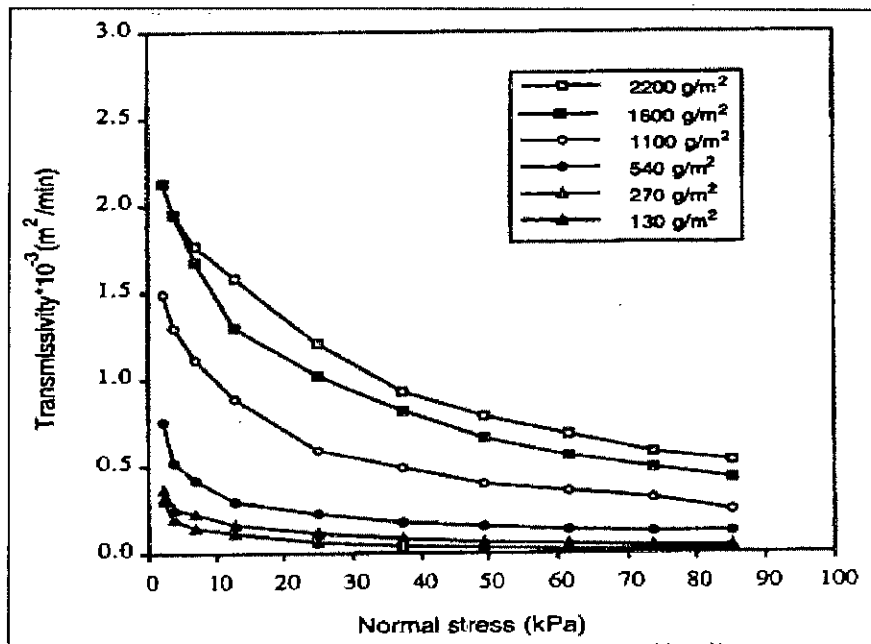


Fig 4.57 Transmissivity test results for different mass per unit area of nonwoven needle-punched geotextile (after Koerner, 1997)

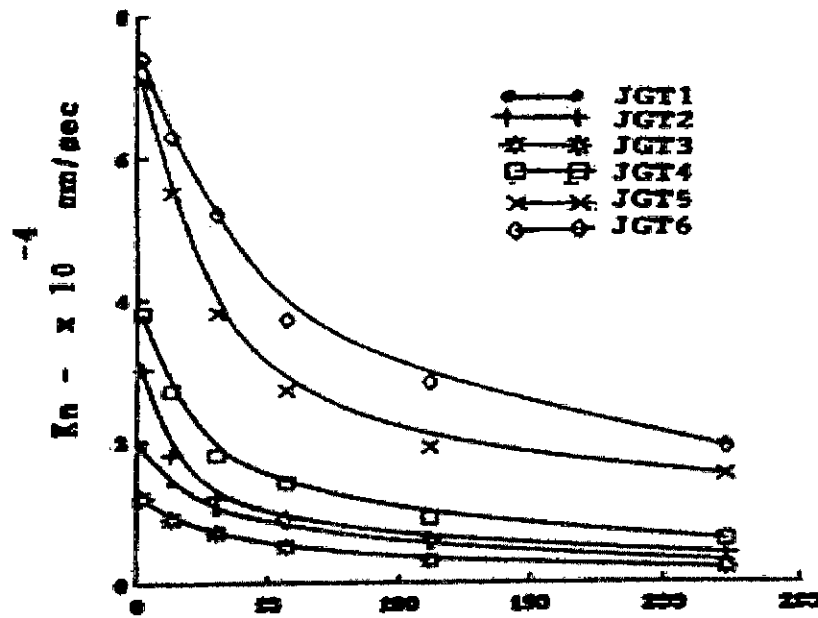


Fig 4.58 Co-efficient of normal permeability versus normal stress (after Rao et al, 1994)

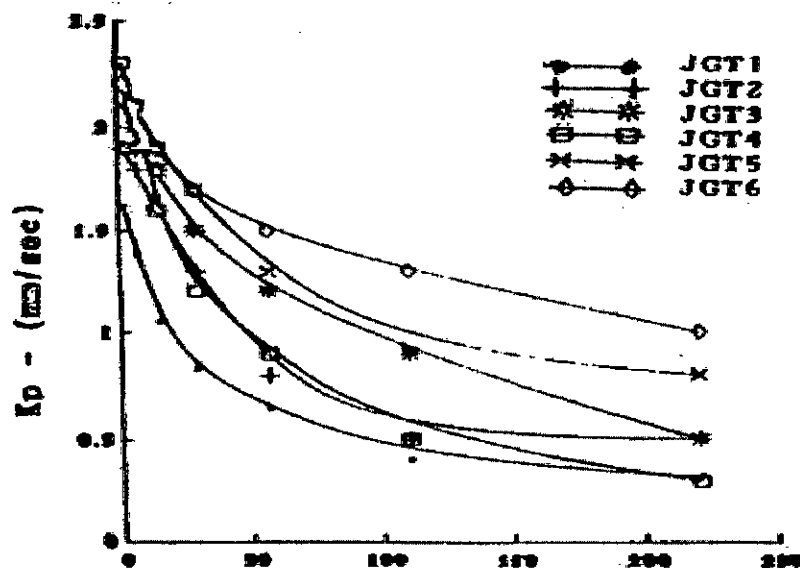


Fig 4.59 Co-efficient of in-plane permeability versus normal stress (after Rao et al, 1994)

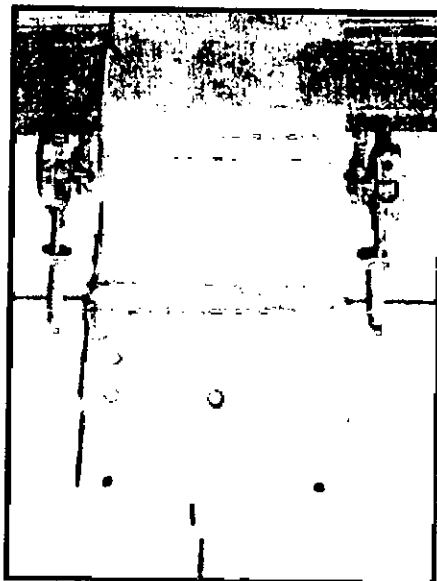


Fig 4.60 Untreated Canvas sample ready for test

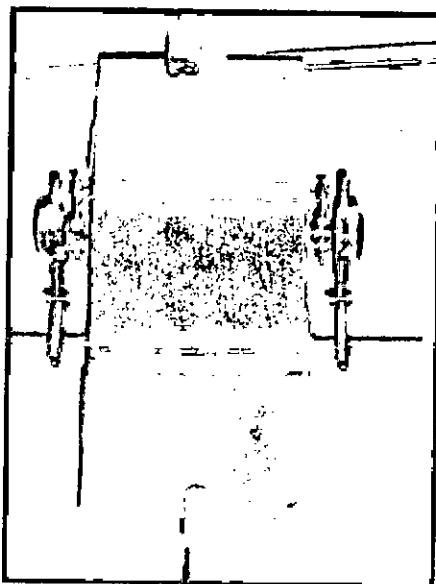


Fig 4.61 Treated Canvas sample ready for test



Fig 4.62 Creep test on progress



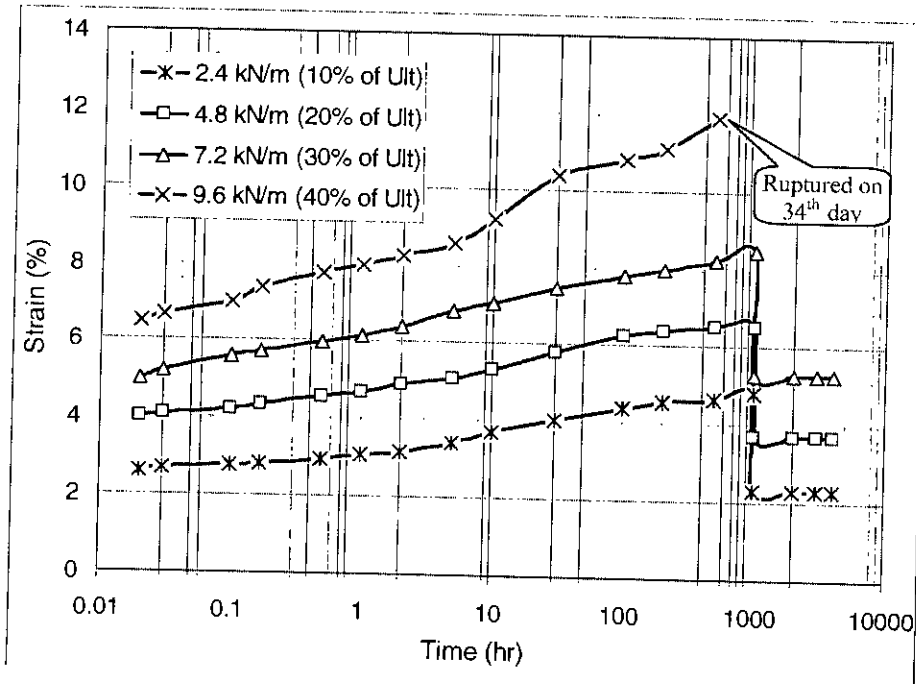


Fig 4.63 Creep test results of untreated Canvas sample

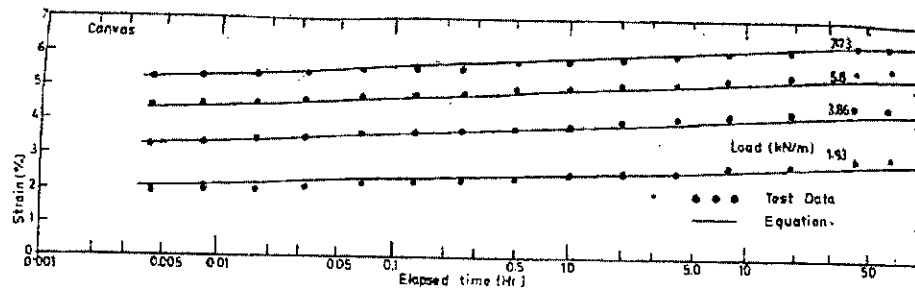


Fig 4.64 Creep strain versus log time plots for Canvas (after Kabir, 1994)

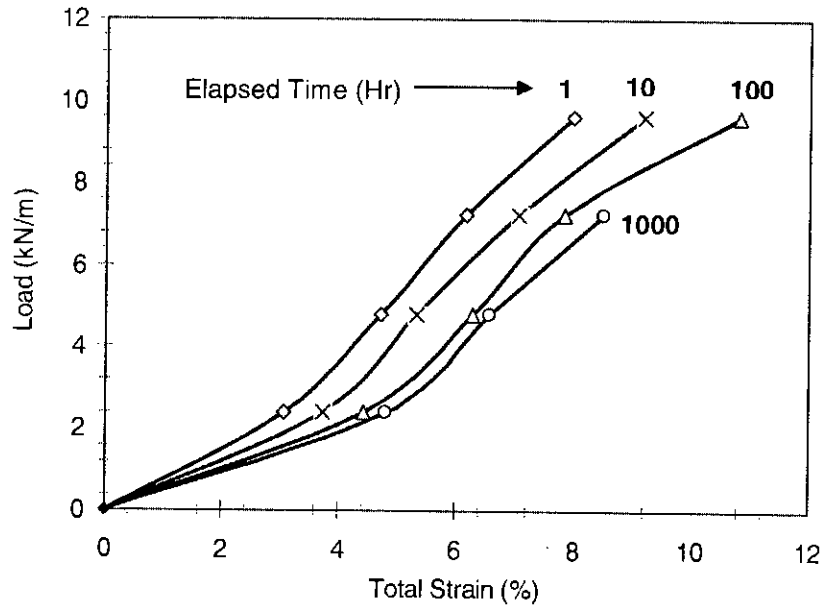


Fig 4.65 Isochronous load versus strain diagrams for untreated Canvas

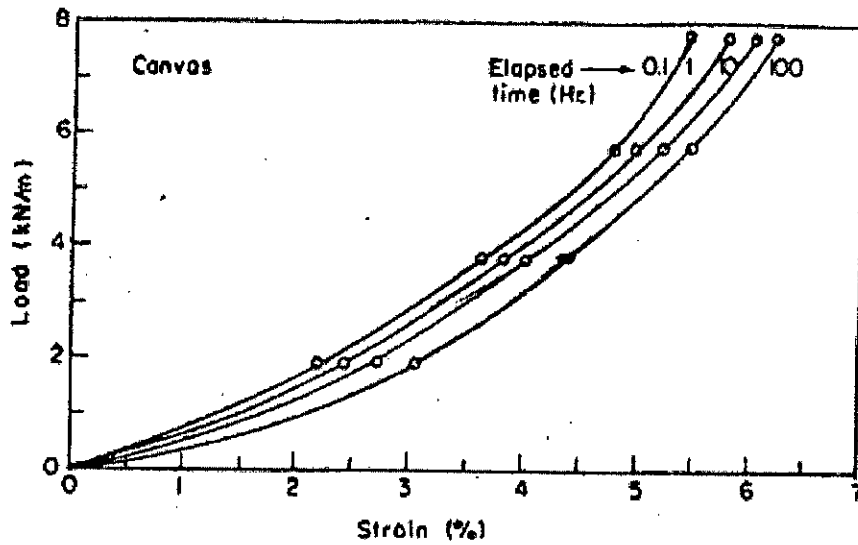


Fig 4.66 Isochronous load versus strain diagrams for Canvas (after Kabir, 1994)

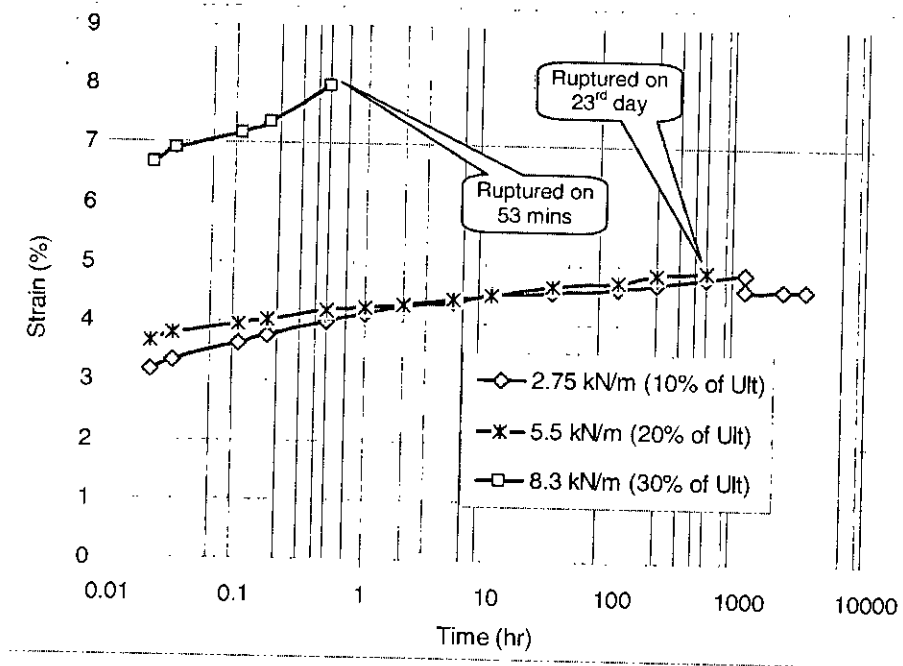


Fig 4.67 Creep test results of treated Canvas sample

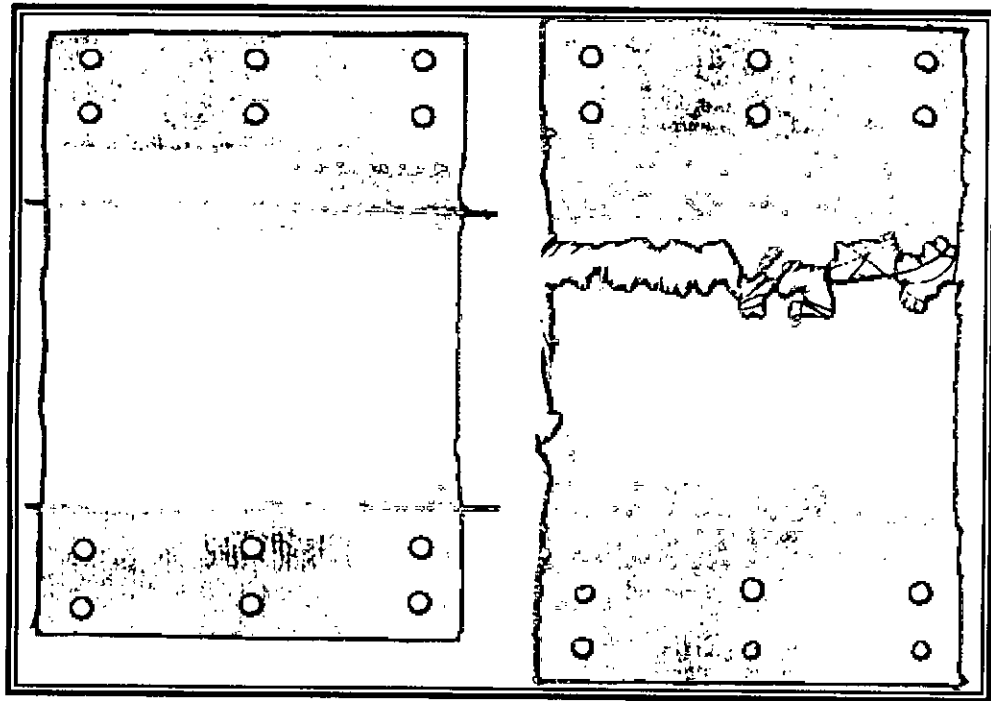


Fig 4.68 Canvas before Creep test

Fig 4.69 Ruptured Canvas on 34<sup>th</sup> day at 40% of ultimate load

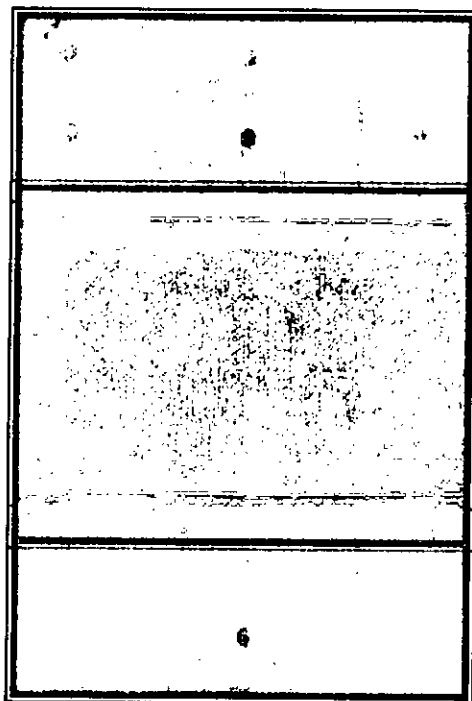


Fig 4.70 Treated Canvas before Creep test



Fig 4.71 Ruptured treated Canvas on 23rd Day at 20% of ultimate load

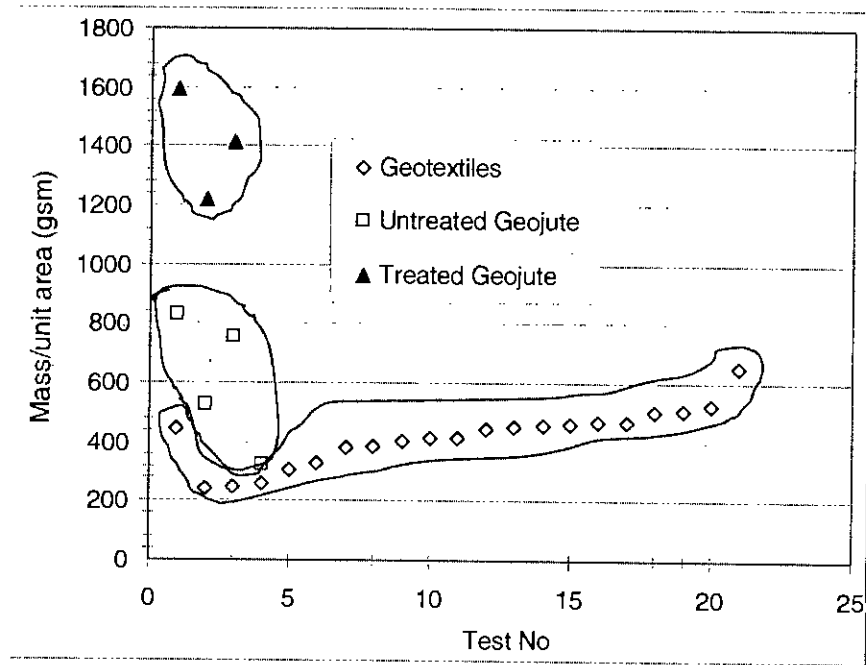


Fig 4.72 Mass per unit area of geotextiles, untreated and treated geojute

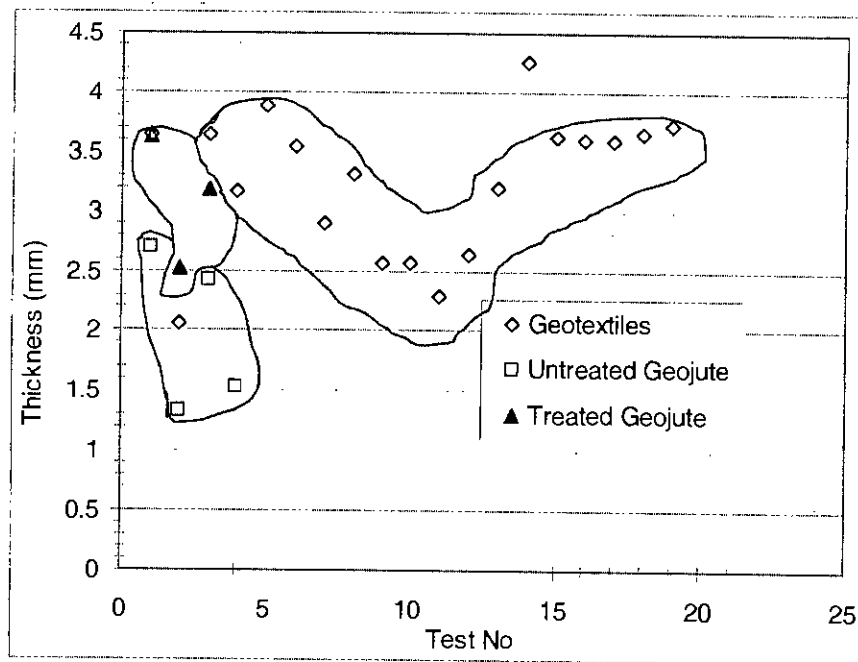


Fig 4.73 Thickness of geotextiles, untreated and treated geojute

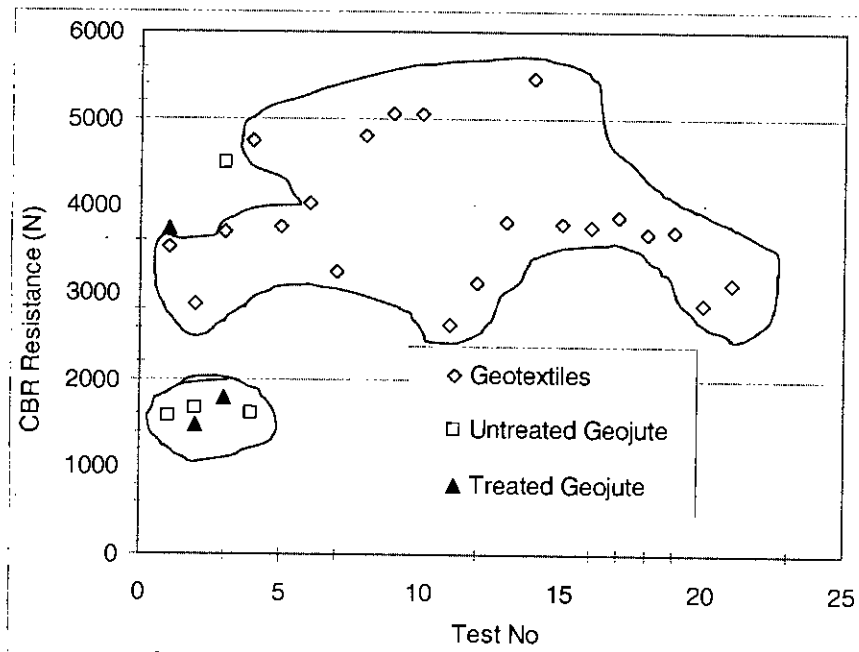


Fig 4.74 CBR puncture resistance of geotextiles, untreated and treated geojute

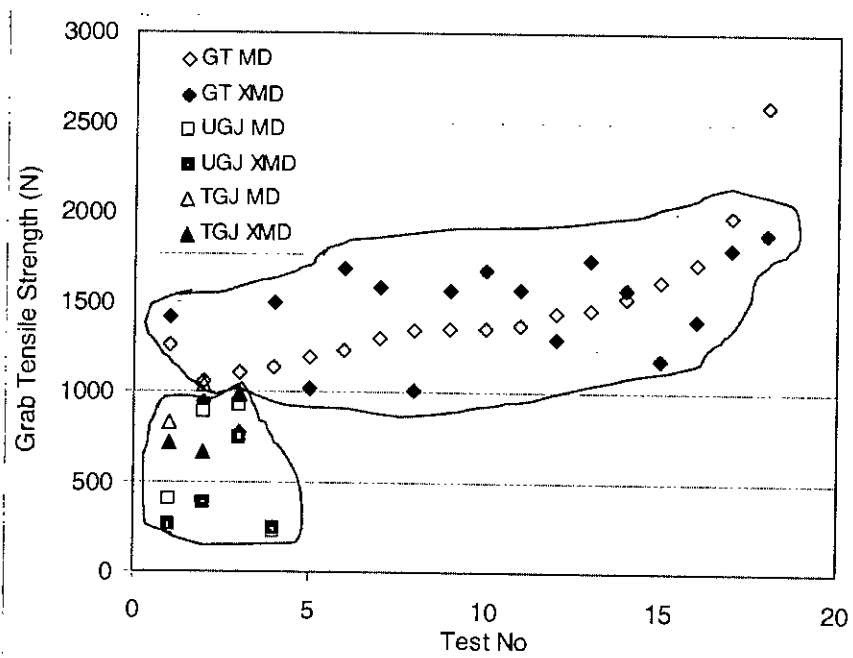


Fig 4.75 Grab tensile strength of geotextiles, untreated and treated geojute

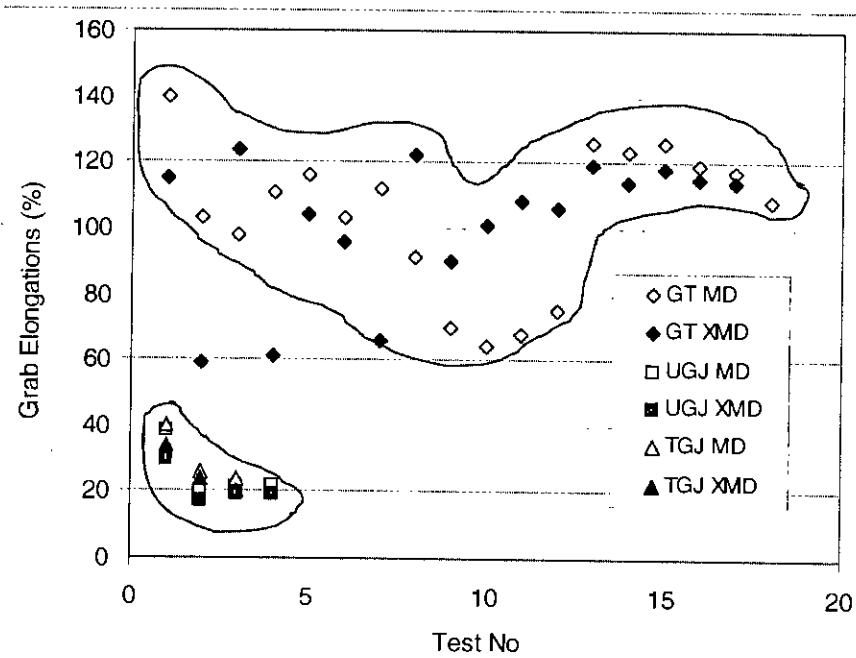


Fig 4.76 Grab tensile elongation of geotextiles, untreated and treated geojute

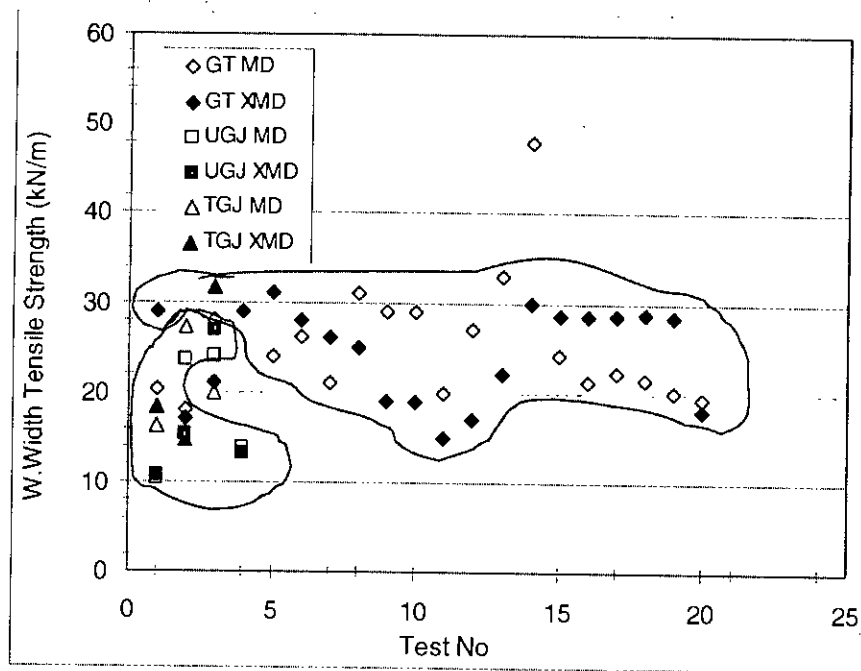


Fig 4.77 Wide-width tensile strength of geotextiles, untreated and treated geojute

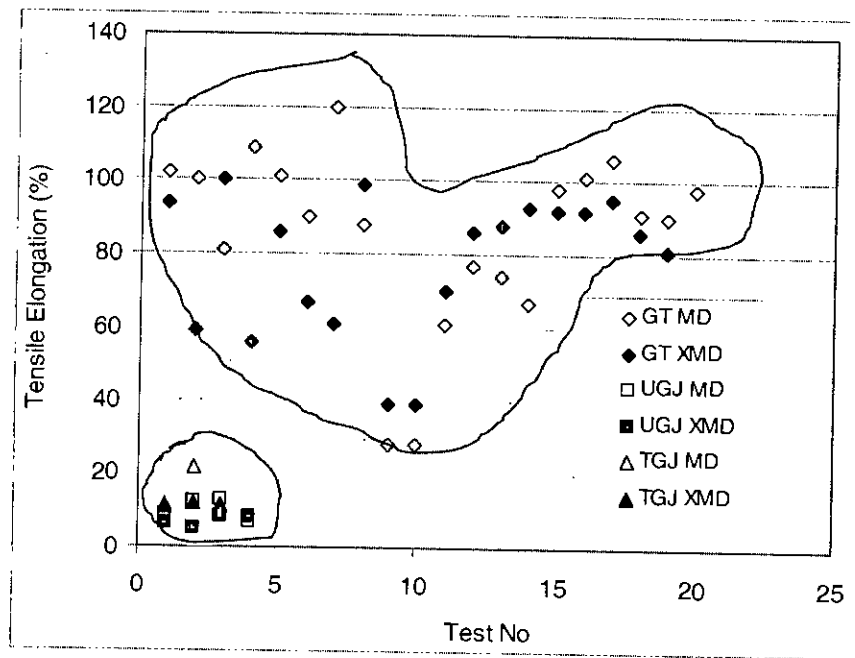


Fig 4.78 Wide-width elongation of geotextiles, untreated and treated geojute



## **CHAPTER FIVE**

# **DESIGNING WITH GEOJUTE AND TECHNICAL ASSESSMENT**

### **5.1 General**

It is already mentioned in Chapter Two that since no standard test methods for determining engineering properties or design methods for geojute are available to date, the methods for determining the test and the design commonly employed for geotextiles might be adopted. In this direction, Muhammad (1993), Rao et al (1994), Kabir et al (1994) attempted to evaluate the different properties of geojute and jute geotextile. Due to the wide range of applications and variety of available geojute having different properties, the selection of a particular design method or design philosophy is a critical decision. In view of these, four design examples for reinforcement, separation, drainage and filtration functions have been presented using the procedures outlined by Koerner (1997) for geotextile applications based on the test results of this study.

### **5.2 Design Methods**

To a designer many possible design methods or combinations of methods are available. However, as Koerner (1997) describes the ultimate decision for a particular application usually takes one of three directions: design-by-cost-and-availability, design-by-specification, and design-by-function.

### 5.2.1 Design-by-Cost-and-Availability

This method is quite simple. Available funds are divided by the area to be covered and a maximum available unit price that can be allocated for the geojute is calculated. The geojute with the best properties is then selected within this unit price limit and according to its availability. Intuition plays a critical role in the selection process. The method is obviously weak technically but is one that is still sometimes practiced.

### 5.2.2 Design-by-Specification

This method is very common and is used almost exclusively when dealing with public agencies. In this method, several application categories are listed in association with various physical, mechanical and/or hydraulic properties. Different agencies have very different perspectives as to what properties are important and as to their method of obtaining the numeric values.

### 5.2.3 Design by Function

This method consists of assessing the primary function that the geojute will serve and then calculating the required numerical value of a particular property for that function. Dividing this value into the candidate geojute's allowable property value gives a factor of safety (FS).

$$FS = \frac{\text{allowable (test) property}}{\text{required (design) property}}$$

where,

Allowable property = a numeric value based on a laboratory test that models  
the actual situation

Required property = a numeric value obtained from a design method that  
models the actual situation, and

FS = factor of safety against unknown loads and/or uncertainties in the  
analytic or testing process; sometimes called a global factor of safety

If the factor of safety is sufficiently greater than 1.0, the candidate geojute is acceptable. The above process can be repeated for a number of available geojute, and if others are acceptable then the final choice becomes one of availability and least cost.

### 5.3 Allowable versus Ultimate Geotextile Properties

Test properties represent idealized conditions and the results when used directly in design, results in upper-bound values. In the design-by-function concept, the factor of safety was formulated around an allowable test value. Thus, most laboratory test values cannot generally be used directly; they must be suitably modified for the in situ conditions. This could be done directly in the test procedure, for example, by conducting a completely simulated performance test; but in most cases this simply is not possible. Simulating installation damage, performing long-term creep testing, using site-specific liquids, reproducing in situ pore-water stresses, providing complete stress state modeling, and so on, are generally not feasible. To account for such differences between the laboratory measured test value and the desired performance value, two approaches are suggested by Koerner (1997) are:

- Use an extremely high factor of safety at the end of a problem.
- Use reduction factors on the laboratory-generated test value to make it into a site-specific allowable value.

Koerner (1997) used the second alternative. By doing this, the usual value of the factor of safety is used in the final analysis. These approaches refer to the general laboratory-obtained value as an *ultimate* value and to modify it by reduction factors to an *allowable* value. In designing with geojute, the methods applied for geotextile will be followed.

$$T_{\text{allow}} = T_{\text{ult}} \left( \frac{1}{RF_{ID} \times RF_{CR} \times RF_{CD} \times RF_{BD}} \right)$$

$$T_{\text{allow}} = T_{\text{ult}} \left( \frac{1}{\text{II RF}} \right)$$

### 5.3.1 Strength-Related Problems

For problems dealing separation and reinforcement, the formulation of the allowable values takes the following form. Typical values for reduction factors are given in Table 5.1. These values, however, must be tempered by the site-specific considerations. If the laboratory test includes the mechanism listed, it appears in the equation as a value of 1.0.

**Table 5.1 Recommended Reduction Factor Values for Use in Strength-Related Problems**

Application Area	Range of Reduction Factors			
	Installation Damage	Creep*	Chemical Degradation	Biological Degradation
Separation	1.1 to 2.5	1.5 to 2.5	1.0 to 1.5	1.0 to 1.2
Cushioning	1.1 to 2.0	1.2 to 1.5	1.0 to 2.0	1.0 to 1.2
Unpaved roads	1.1 to 2.0	1.5 to 2.5	1.0 to 1.5	1.0 to 1.2
Walls	1.1 to 2.0	2.0 to 4.0	1.0 to 1.5	1.0 to 1.3
Embankments	1.1 to 2.0	2.0 to 3.5	1.0 to 1.5	1.0 to 1.3
Bearing capacity	1.1 to 2.0	2.0 to 4.0	1.0 to 1.5	1.0 to 1.3
Slope stabilization	1.1 to 1.5	2.0 to 3.0	1.0 to 1.5	1.0 to 1.3
Pavement overlays	1.1 to 1.5	1.0 to 2.0	1.0 to 1.5	1.0 to 1.1
Railroads (filter/sep.)	1.1 to 3.0	1.0 to 1.5	1.5 to 2.0	1.0 to 1.2
Flexible forms	1.1 to 1.5	1.5 to 3.0	1.0 to 1.5	1.0 to 1.1
Silt fences	1.1 to 1.5	1.5 to 2.5	1.0 to 1.5	1.0 to 1.1

Where

$T_{allow}$  = allowable tensile strength,

$T_{ult}$  = ultimate tensile strength,

$RF_D$  = reduction factor for installation damage,

$RF_{CR}$  = reduction factor for creep.  $RF_{CD}$  = reduction factor for chemical degradation,

$RF_{BD}$  = reduction factor for biological degradation, and

IIRF = value of cumulative reduction factors.

### 5.3.2 Flow-Related Problems

For filtration and drainage applications problems dealing with flow through or within a geojute, such as, the formulation of the allowable values takes the following form. Typical values for reduction factors are given in Table 5.2. It may be noted that these values must be tempered by the site-specific conditions. If the laboratory test includes the mechanism listed, it appears in the equation as a value of 1.0.

$$q_{\text{allow}} = q_{\text{ult}} \left[ \frac{1}{RF_{SCB} \times RF_{CR} \times RF_{IN} \times RF_{CC} \times RF_{BC}} \right]$$

$$q_{\text{allow}} = T_{\text{ult}} \left( \frac{1}{\text{IIRF}} \right)$$

where

$q_{\text{allow}}$  = allowable flow rate,

$q_{\text{ult}}$  = ultimate flow rate,

$RF_{SCB}$  = reduction factor for soil clogging and blinding,

$RF_{CR}$  = reduction factor for creep reduction of void space,

$RF_{IN}$  = reduction factor for adjacent materials intruding into geojute's void space,

$RF_{CC}$  = reduction factor for chemical clogging,

$RF_{BC}$  = reduction factor for biological clogging, and

IIRF = value of cumulative reduction factors.

**Table 5.2 Recommended Reduction Factor Values for Use in Flow-Related Problems**

Application Area	Range of Reduction Factors				
	Soil Clogging and Blinding	Creep Reduction of Voids	Intrusion into Voids	Chemical Clogging	Biological Clogging
Retaining wall filters	2.0 to 4.0	1.5 to 2.0	1.0 to 1.2	1.0 to 1.2	1.0 to 1.3
Underdrain filters	5.0 to 10	1.0 to 1.5	1.0 to 1.2	1.2 to 1.5	2.0 to 4.0
Erosion-control filters	2.0 to 10	1.0 to 1.5	1.0 to 1.2	1.0 to 1.2	2.0 to 4.0
Landfill filters	5.0 to 10	1.5 to 2.0	1.0 to 1.2	1.2 to 1.5	5.0 to 10
Gravity drainage	2.0 to 4.0	2.0 to 3.0	1.0 to 1.2	1.2 to 1.5	1.2 to 1.5
Pressure drainage	2.0 to 3.0	2.0 to 3.0	1.0 to 1.2	1.1 to 1.3	1.1 to 1.3

## 5.4 Designing for Separation

### 5.4.1 General

In the application of separation function, the geojute is normally placed on the soil subgrade. Thereafter stone is placed, spread and compacted on top of it. The subsequent deformations are very localized and occur around each individual stone particle. A number of scenarios can be developed showing which geojute properties are required for a given situation. In this section, one such condition is discussed.

### 5.4.2 Problem

Given a 700 kPa truck-tire inflation pressure on a stone-base course consisting of 50 mm maximum-size stone with a geojute beneath it, calculate (a) the required grab tensile stress on the geojute, and (b) the factor of safety for untreated Jute (produced in BJRI) whose grab strength at 33% is 348 N with cumulative reduction factors of 2.5 and  $f(\epsilon) = 0.52$ .

### 5.4.3 Solution

(a) Using an empirical relationship that  $d_v = 0.33 d_a$  and  $f(\epsilon) = 0.52$ , the required grab tensile strength is as follows.

$$\begin{aligned} T_{\text{reqd}} &= p' (d_v)^2 (0.52) \\ &= p' (0.33 d_a)^2 (0.52) \\ &= 0.057 p' d_a^2 \\ &= 0.057 (700) (1000) (0.050)^2 \\ &= 100 \text{ N} \end{aligned}$$

(b) The factor of safety for a 348 N grab tensile geojute at 33% strain with cumulative reduction factors of 2.5 is as follows.

$$\begin{aligned} FS &= T_{\text{allow}} / T_{\text{reqd}} \\ &= (348/2.5) / 100 \\ &= 1.39 \end{aligned}$$

which is acceptable

## 5.5 Designing for Soil Reinforcement

### 5.5.1 General

This section discusses the uses of geojute in the primary function of reinforcement. This type of soil reinforcement raises a unique set of applications, whereby the geojute in layers and the interspersed soil form a system rather than acting as discrete material elements. Koerner (1997) reported two different approaches to the design of geotextile walls: that used by Broms (1978) and that used by the US Forest Service, Steward et al and Whitcomd (1979). The latter method was followed in this section. This method follows the work that Lee et al (1973) did on reinforced earth with metallic strips and was originally adapted to geotextile walls by Bell et al (1975). The design progresses in parts, as follows:

- Internal stability is first addressed to determine geojute spacing, geojute length and overlap distance.
- External stability against overturning, sliding and foundation failure is investigated and the internal design is verified or modified accordingly.
- Miscellaneous considerations, including wall-facing details, are addressed.

### 5.5.2 Problem 1: Geojute Reinforced Walls

Design a 6-m-high wrap-around type of geojute wall that is to carry a storage area of equivalent dead load of 10 kPa. The wall is to be backfilled with a granular soil (SP) having the properties of  $\gamma = 18 \text{ kN/m}^3$ ,  $\phi = 36^\circ$ , and  $c_a = 0$ . A DW Twill with warp (machine) direction ultimate wide-width tensile strength of 25 kN/m and friction angle with granular soil of  $\delta = 24^\circ$  (since no test of DW Twill related to  $\delta$  is carried out, the usual value applied for geotextile, i.e.  $2/3 \phi$  is taken) is intended to be used in its construction. The orientation of the geojute is perpendicular to the wall face and the edges are to be overlapped or sewn to handle the weft (cross machine) direction. A factor of safety of 1.4 is to be used along with site-specific reduction factors.

### 5.5.3 Solution

#### 5.5.3.1 Internal Stability

Determine the horizontal pressure as a function of the depth  $z$  in order to calculate the spacing of the individual layers, i.e., the  $S_v$  value.

$$\begin{aligned}
 K_a &= \tan^2 (45 - \theta/2) \\
 &= \tan^2 (45 - 36/2) \\
 &= 0.26 \\
 \sigma_h &= \sigma_{hs} + \sigma_{hq} \\
 &= K_a \gamma z + K_a q \\
 &= (0.26) (18) (z) + (0.26) (10) \\
 &= 4.68z + 2.60
 \end{aligned}$$



and the allowable geojute strength with the following reduction factors:

$$\begin{aligned}
 T_{\text{allow}} &= T_{\text{ult}} \left( \frac{1}{RF_{ID} \times RF_{CR} \times RF_{CD} \times RF_{BD}} \right) \\
 &= 25 \left( \frac{1}{1.2 \times 2.5 \times 1.15 \times 1.1} \right) \\
 &= 25 / 3.79 \\
 &= 6.6 \text{ kN/m}
 \end{aligned}$$

Now using the following equation under for varying depths, calculate the geojute layer spacing.

### Geojute Spacing

At  $z = 6$  m:

$$\begin{aligned}
 S_v &= \frac{T_{\text{allow}}}{\sigma_h (\text{FS})} \\
 &= \frac{T_{\text{allow}}}{[4.68 (z) + 2.60] 1.4} \\
 &= \frac{6.6}{[4.68 (6.0) + 2.60] 1.4}
 \end{aligned}$$

$$S_v = 0.1537 \text{ m} \quad \text{use } 0.15 \text{ m}$$

By trial and error, see if the spacing can be opened up to 0.30 m at  $z = 2.7$  m.

$$S_v = \frac{6.6}{[4.68 (2.7) + 2.60] 1.4}$$

$$S_v = 0.31 \text{ m} \quad \text{use } 0.30 \text{ m}$$

By trial and error, see if the spacing can be opened up to 0.40 m at  $z = 1.2$  m.

$$S_v = \frac{6.6}{[4.68 (1.2) + 2.6] 1.4}$$

$$S_v = 0.57 \text{ m} \quad \text{use } 0.4 \text{ m}$$

Thus, the layers and their spacing are as shown in Fig 5.1. At this point there is a Mechanically Stabilize Earth (MSE) mass, actually a geosynthetically stabilized earth mass, which is self-standing within itself.

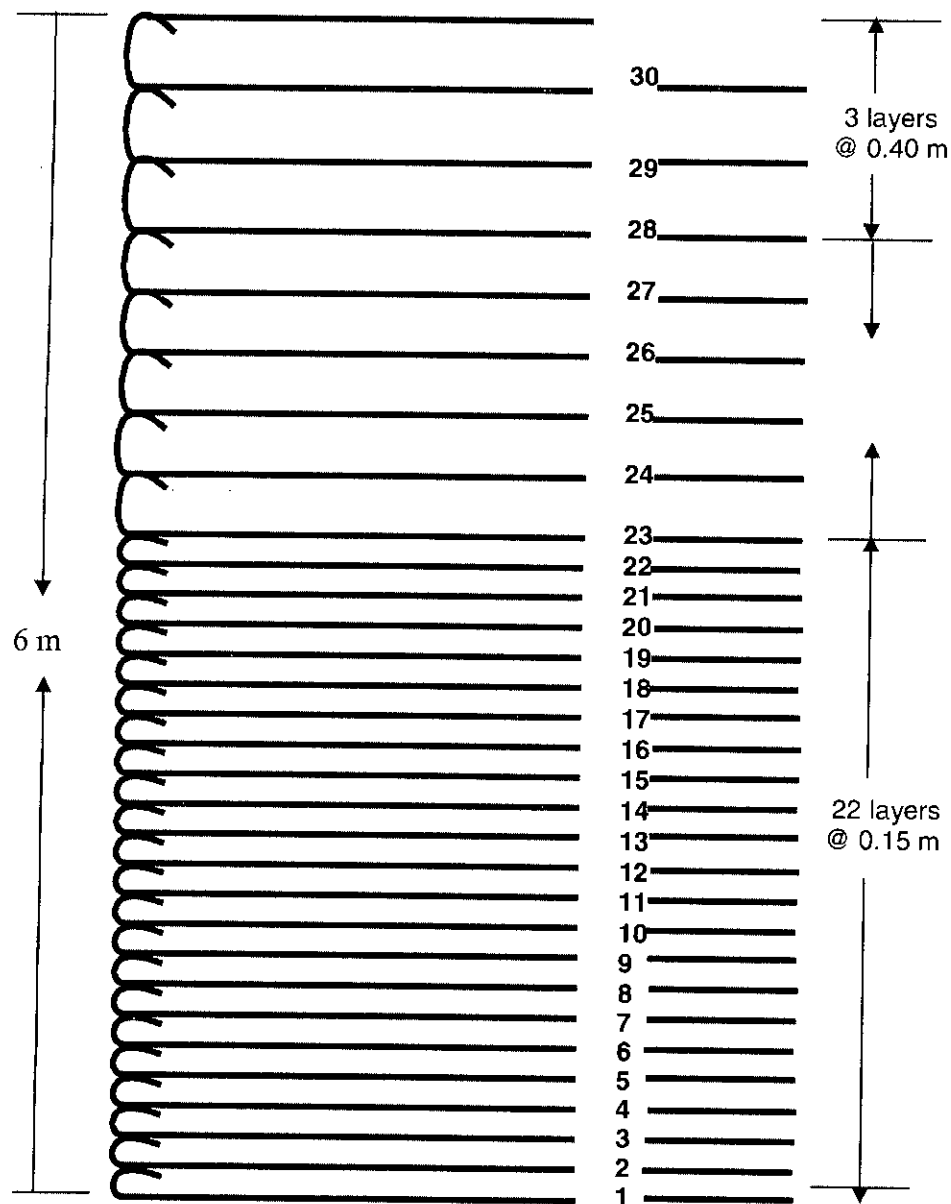


Fig 5.1 Geojute reinforcement layout for retaining wall

Due to the critical nature of some MSE walls, a serviceability criterion can be imposed, limiting the possible outward deflection of the wall to some acceptable value, for example, 20 mm. This is done utilizing the wide-width stress-versus strain response of the reinforcement at the design (allowable) stress in the reinforcement. This latter value includes both reduction factors and the factor of safety.

### Geojute length (L)

$L_c$  with  $\delta = 24^\circ$  and  $c_d = 0$ . Note that  $L_R$  uses a Rankine failure plane and is calculated from the following equation;

$$\begin{aligned} L_c &= [S_v \sigma_h (FS)] / [2(c + \gamma z \tan \delta)] \\ &= [S_v (4.68z + 2.60)1.4] / [2(0 + 18z \tan 24^\circ)] \\ &= [S_v (6.55z + 3.64)] / 16.0z \quad \text{and} \end{aligned}$$

$$L_R = (H - z) \tan (45 - 36/2)$$

$$L_R = (6.0 - z) (0.509)$$

It may be noted that the calculated  $L_c$  values are very small (this is typically the case with geojute walls) and the minimum value of 1.0 m should be used. When this is added to  $L_R$  for the total length, it should be rounded up to an even number of meters. In addition, the important consideration of total geojute width must be addressed. Three situations can be envisioned.

**Case 1.** If the geojute rolls are wide enough they can be deployed parallel to the wall and the weft or cross machine direction is the important property insofar as its wide-width strength is concerned. While this is possible for the lower fabric layers, it is not for the uppermost, since, for example,  $4.0 + 0.40 + 1.0 = 5.40$  m, which is wider than current commercially available geojutes.

**Case 2.** Alternatively, two adjacent rolls of fabric can be used parallel to the wall, but a sewn seam, or large overlap, must be used for the uppermost fabric layers. If sewn seams are used, an appropriate partial factor of safety must be used.

**Case 3.** The fabric layers can be deployed perpendicular to the wall, thereby utilizing their warp or machine direction wide-width strength in the major principal stress directions. This is the case posed in this example. This requires sewn seams or

overlaps in the opposite direction. However, in this (the minor principal stress) direction the required forces are significantly lower, for example, 35 to 50% of the major principal stress direction.

**Table 5.3 Geojute Length and Spacing**

Layer No	Depth, z (m)	Spacing, $S_v$ (m)	$L_e$ (m)	$L_e$ min (m)	$L_R$ (m)	$L_{calc}$ (m)	$L_{spec}$ (m)
30	0.40	0.40	0.39	1.0	2.85	3.85	Use 4.0
29	0.80	0.40	0.28	1.0	2.65	3.65	
28	1.20	0.40	0.24	1.0	2.44	3.44	
27	1.50	0.30	0.17	1.0	2.29	3.29	Use 3.5
26	1.80	0.30	0.16	1.0	2.14	3.14	
25	2.10	0.30	0.16	1.0	1.99	2.99	
24	2.40	0.30	0.15	1.0	1.83	2.83	
23	2.70	0.30	0.15	1.0	1.68	2.68	
22	2.85	0.15	0.07	1.0	1.60	2.60	Use 3.0
21	3.00	0.15	0.07	1.0	1.53	2.53	
20	3.15	0.15	0.07	1.0	1.45	2.45	
19	3.30	0.15	0.07	1.0	1.37	2.37	
18	3.45	0.15	0.07	1.0	1.30	2.30	
17	3.60	0.15	0.07	1.0	1.22	2.22	
16	3.75	0.15	0.07	1.0	1.15	2.15	
15	3.90	0.15	0.07	1.0	1.07	2.07	
14	4.05	0.15	0.07	1.0	0.99	1.99	Use 2.0
13	4.20	0.15	0.07	1.0	0.92	1.92	
12	4.35	0.15	0.07	1.0	0.84	1.84	
11	4.50	0.15	0.07	1.0	0.76	1.76	
10	4.65	0.15	0.07	1.0	0.69	1.69	
9	4.80	0.15	0.07	1.0	0.61	1.61	
8	4.95	0.15	0.07	1.0	0.53	1.53	
7	5.10	0.15	0.07	1.0	0.46	1.46	
6	5.25	0.15	0.07	1.0	0.38	1.38	
5	5.40	0.15	0.07	1.0	0.31	1.31	
4	5.55	0.15	0.07	1.0	0.23	1.23	
3	5.70	0.15	0.07	1.0	0.15	1.15	
2	5.85	0.15	0.07	1.0	0.08	1.08	
1	6.00	0.15	0.07	1.0	0.00	1.00	

### Geojute Overlap Length

Overlap length  $L_0$ , to see if it is less than the 1.0m recommended value using the following Eq.

$$\begin{aligned} L_0 &= [S_v \sigma_h (FS)] / [4(C_a + \gamma z \tan \delta)] \\ &= S_v [\{4.68(z) + 2.60\} 1.4] / 4[0 + (18) z \tan 24^\circ] \end{aligned}$$

Which is maximum at the upper layer at  $z = 0.40$  m,

$$\begin{aligned} L_0 &= 0.40[\{4.68(0.40) + 2.60\} 1.4] / 4[0 + (18) (0.40) \tan 24^\circ] \\ &= 0.195 \text{ m} \end{aligned}$$

OK use 1.0 m

### 5.5.3.2 External Stability

Standard geotechnical engineering concepts are used to analyze over turning, sliding and bearing capacity.

#### Check for Over Turning

$$\begin{aligned} K_a &= \tan^2 (45 - \theta/2) \\ &= \tan^2 (45 - 34/2) \\ &= 0.28 \end{aligned}$$

$$\begin{aligned} Pa &= 0.5 \gamma H^2 K_a \\ &= 0.5 (18) (6)^2 (0.28) \\ &= 90.7 \text{ kN/m} \end{aligned}$$

$$Pa \cos 34 = 75.2 \text{ kN/m}$$

$$Pa \sin 34 = 50.7 \text{ kN/m}$$

Now for overturning, moments are taken about the toe of the wall to generate a factor of safety value.

$$\begin{aligned} FS_{OT} &= \frac{\sum \text{resisting moments}}{\sum \text{driving moments}} \\ &= [w_1 x_1 + w_2 x_2 + w_3 x_3 + Pa \sin \delta (4)] / [Pa \cos \delta (2)] \end{aligned}$$

$$= [(6)(2)(18)(1) + (3.9)(1)(18)(2.5) + (1.8)(1)(18)(3.5) + (50.7)(4)] / (75.2)(2)$$

$$= 4.7 > 2.0 \quad \text{which is acceptable}$$

This value calculated factor of safety is very typical of walls of this type. Even further, overturning is not a likely failure mechanism since this is a very flexible MSE system that cannot support bending stresses.

### Check for Sliding

For sliding, horizontal forces at the bottom of the wall are summed to calculate another factor of safety:

$$FS_s = \frac{\sum \text{resisting moments}}{\text{driving moments}}$$

$$= [c_a + (w_1 + w_2 + w_3 + Pa \sin \delta) / 2 \tan \delta]^2 / Pa \cos \delta$$

$$= [16 + (216 + 70.2 + 32.4 + 50.7) / 2 \tan 14.2] / 75.2$$

$$FS_s = 1.7 > 1.5 \quad \text{acceptable (but barely)}$$

### Check for Foundation Failure

Finally, check for a foundation failure using shallow-foundation bearing capacity theory

$$P_{ult} = cN_c + qN_q + 0.5\gamma BN_\gamma$$

$$= (20)(10.98) + 0 + 0.5(18.5)(2)(2.65)$$

$$= 269 \text{ kN/m}^2$$

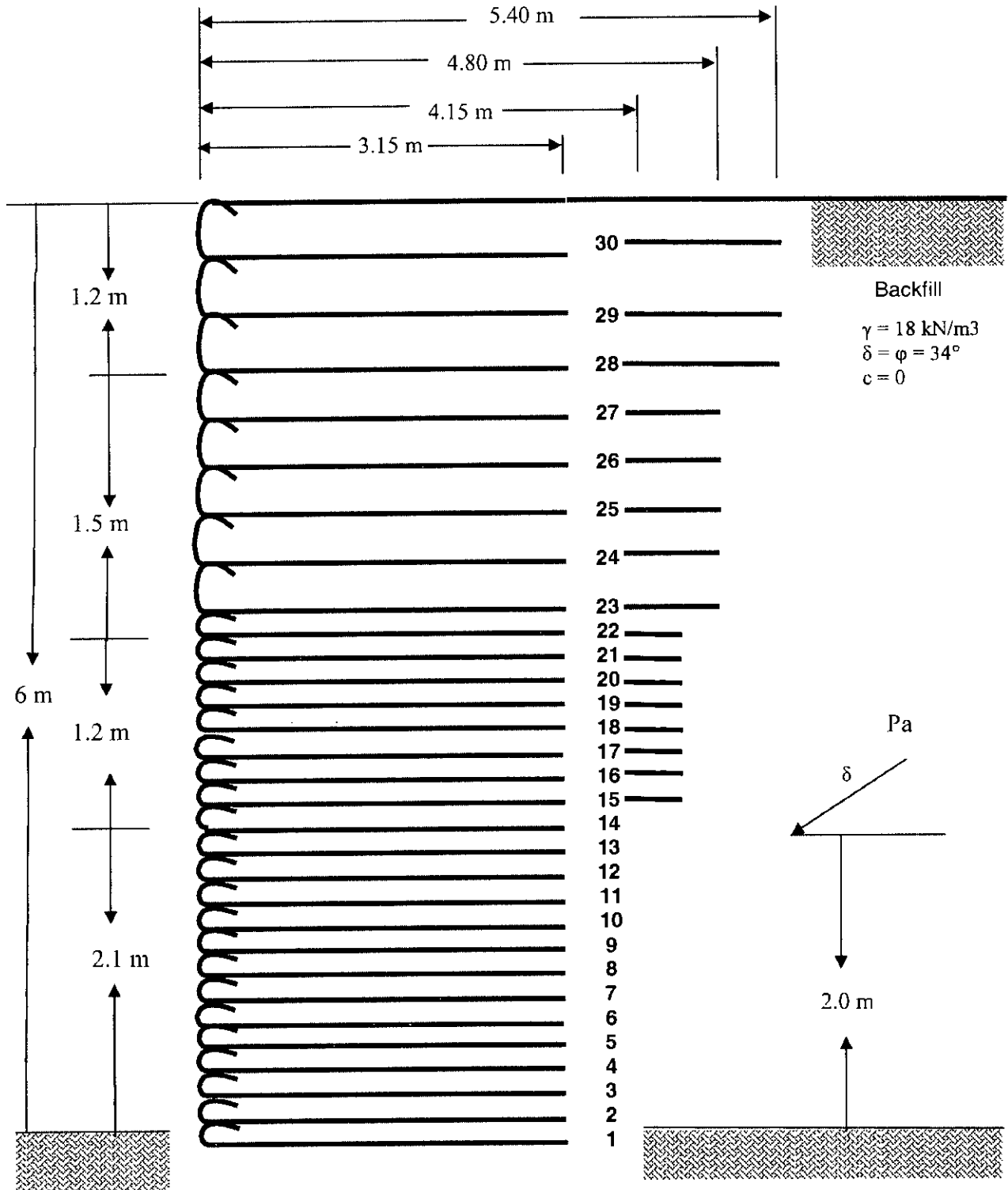
$$P_{act} = (18)(6) + (10)$$

$$= 118 \text{ kN/m}^2$$

$$FS_{BC} = P_{ult} / P_{act} = 269 / 118$$

$$= 2.3 > 2.0 \text{ which is acceptable}$$

The internal design is now complete and the total arrangement is shown below.



**Foundation soil**

- $\gamma = 18.5 \text{ kN/m}^3$
- $\phi = 15^\circ$
- $\delta = 0.95 \phi = 14.2^\circ$
- $c = 20 \text{ kN/m}^2$
- $c = 0.80c = 16 \text{ kN/m}$

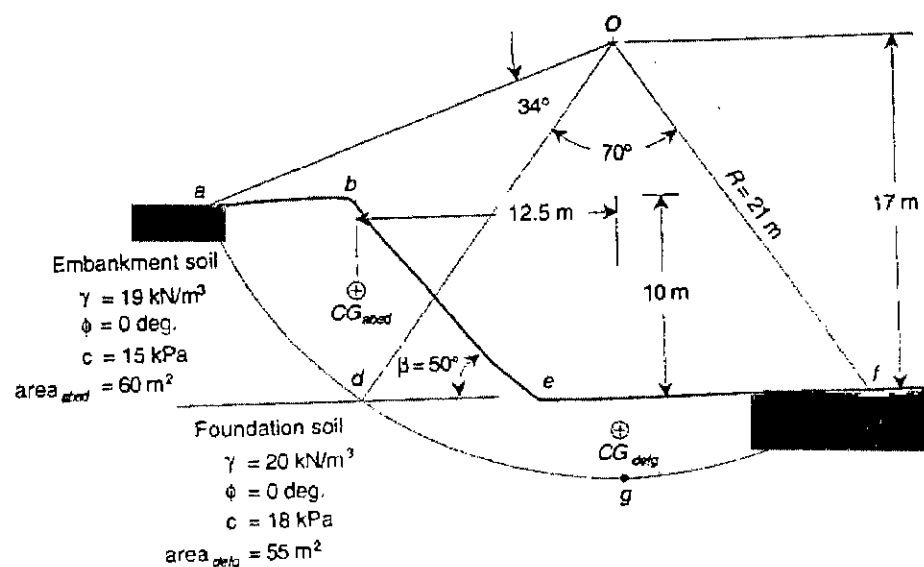
It uses thirty layers of fabric (the lowest twenty-two at 0.15 m spacing; the middle five at 0.30 m spacing; the upper three at 0.40 m spacing). Considering the fabric lengths, it is divided into four layers. From layer 1 to layer 14: 3.15 m ( $2+0.15+1$ ). From layer 15 to layer 22: 4.15 m ( $3+0.15+1$ ). From layer 23 to layer 27: 4.8 m ( $3.5+0.30+1$ ). From layer 28 to layer 30: 5.40 m ( $4+0.4+1$ ). The detail length and spacing are shown in Table 5.3.

### 5.5.4 Problem 2: Geotextile Reinforced Embankment

#### 5.5.4.1 Part I

For the 10m high,  $50^\circ$  angle slope shown on Fig below, which consists of a silty clay embankment ( $\gamma = 19 \text{ kN/m}^3$ ,  $\phi = 0^\circ$ ,  $c = 15 \text{ kPa}$ , area =  $60 \text{ m}^2$ , centre of gravity as indicated) on a silty clay foundation ( $\gamma = 20 \text{ kN/m}^3$ ,  $\phi = 0^\circ$ ,  $c = 18 \text{ kPa}$ , area =  $55 \text{ m}^2$ , center of gravity as indicated) determine:

- The factor of safety with no geojute reinforcement
- The factor of safety with DW Twill of ultimate tensile strength 25 kN/m at MD placed along the surface between the foundation soil and the embankment soil
- The factor of safety with ten layers of the same DW Twill placed at 1 m intervals from the foundation interface to the top of the embankment. Assume that sufficient anchorage behind the slip circle shown is available to mobilize full geojute strength.





### 5.5.4.2 Solution

The following computational data are needed in all parts of the problem:

$$W_{abcd} = 60 * 19 = 1140 \text{ kN/m}$$

$$W_{defg} = 55 * 20 = 1100 \text{ kN/m}$$

$$L_{ad} = 2 * 21 * \pi (34/360) = 12.5 \text{ m}$$

$$L_{df} = 2 * 21 * \pi (70/360) = 25.7 \text{ m}$$

- (a) Slope as shown (with no geojute reinforcement)

$$FS = \sum \frac{\text{resisting moments}}{\text{driving moments}}$$

$$FS = \sum \frac{(c_e L_{ad} + c_f L_{df})R}{W_{abcd} (12.5) + W_{defg} (0)}$$

$$= \frac{[15 * 12.5 + 18 * 25.7] 21}{1140 * 12.5 + 0}$$

$$= 0.96 \quad \text{not acceptable: failure is indicated}$$

- (b) Slope with a geojute along surface ed with sufficient anchorage beyond point d:

$$FS = (13650 + 25 * 17) \div 14250$$

$$= 0.99 \quad \text{not acceptable: failure is indicated}$$

- (c) Slope with ten layers at 1 m interval from surface ed upward, all of which have sufficient anchorage behind the strip surface:

$$FS = [13650 + 25(17 + 16 + 15 + 14 + \dots + 9 + 8)] \div 14250$$

$$= 1.18 \quad \text{not acceptable:}$$

**Note:** If we double the layers, i.e. twenty layers at 0.50 m intervals from surface ed upwards then,

$$FS = [13650 + 25(17 + 16.5 + 16 + \dots + 8 + 7.5)] \div 14250$$

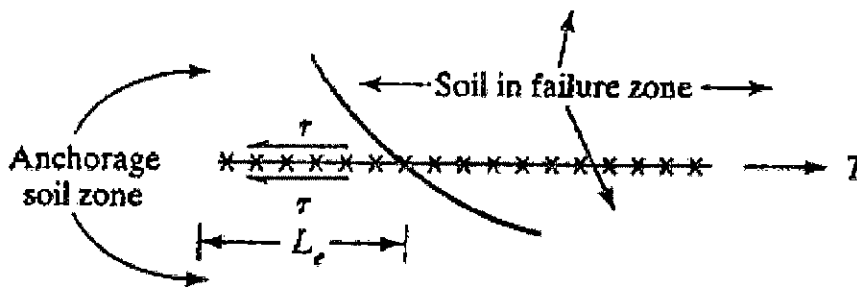
$$= 1.39 \quad \text{acceptable: barely}$$

### 5.5.4.3 Part II

For the slope in Part I, (a) determine how much embedment (or anchorage length) is required behind the potential slip circle in order to mobilize the allowable tensile strength of the geojute. Assume that the transfer efficiency of the geojute to the shear strength of the soil is 0.80 and base the calculation on a FS = 1.5, (b) determine the total length of the geojute, using 8.0 m as the maximum distance from the slope face to the failure plane.

### 5.5.4.4 Solution

From the fig below it appears that the concentration decreases rapidly as the embedment length increases and that separate mobilized and fixed portions of the geojute exist.



For this example however, a linear distribution will be assumed over a continuous displaced length, since it results in a conservative length. Taking force summation in the x-direction results in the following equation:

$$2\tau EL_c = T_{\text{allow}} (\text{FS})$$

$$2(15)(0.8) L_e = 25(1.5)$$

$$L_e = 1.56 \text{ m}$$

which is the required embedment length beyond the potential slip circle for sufficient anchorage of each geojute.

(b) The total length of each geojute layer will be  $1.56 + 8.0 = 9.56$  m and total length of required geojute in the whole embankment will be  $9.56 \text{ m} \times 20 = 191.2$  m.

## 5.6 Designing for Filtration

### 5.6.1 General

When liquid flows across the plane of the geojute, the geojute acts and is designed as a filter. In Chapter two a number of applications were presented in which geojute are used adjacent to soil for the purpose of allowing liquid to pass through them while retaining the soil on the upstream side. Generally, the situations represent liquid moving in one direction only, but in some cases reversing the flow was mentioned by Koerner(1997), for example, in tidal areas. Koerner (1997) describes the situations involving flow conditions on a worst-case scenario basis. The designs to follow cover most of the commonly encountered situations. The specific designs to be treated are the following:

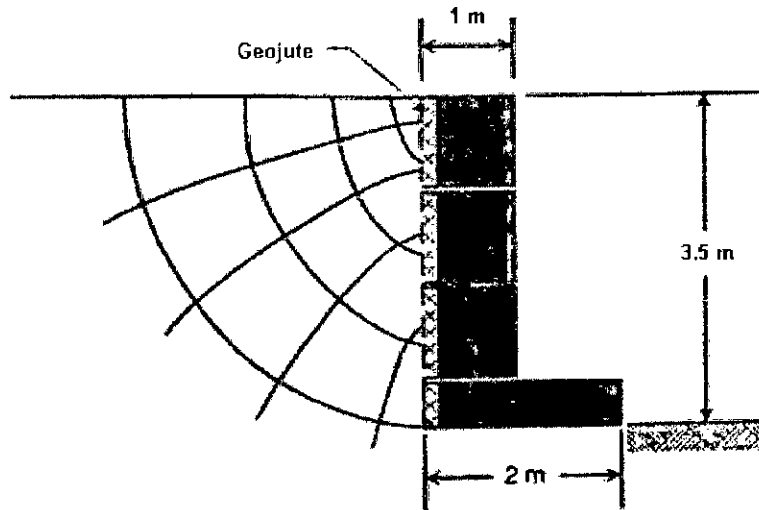
- Geojute filters behind retaining walls
- Geojute filters wrapped around underdrains
- Geojute filters used beneath erosion control structures
- Geojute filters used as silt fences

In this chapter, design method on geojute filters behind retaining walls is shown only.

### 5.6.2 Problem

Given a 3.5 m high gabion wall consisting of three 1 X 1 X 3 m long baskets sitting on a 0.5 x 2 x 3 m long mattress as shown below, the backfill soil is a medium-dense silty sand of  $d_{10} = 0.03$  mm,  $C_u = 2.5$ ,  $k = 0.0075$  m/s, and  $D_R = 70\%$ . Check the adequacy of four candidate geojutes whose laboratory test properties are given below. Use the cumulative reduction factors as 15.0, in order to adjust the ultimate laboratory-obtained permittivity value to an allowable field-oriented value.

No	Geojute Type	Permittivity ( $s^{-1}$ )	AOS (mm)
1	Jute	0.28	0.28
2	Canvas	0.03	0.075
3	DW Twill	0.25	0.8
4	Hessian	1.19	1.0



### 5.6.3 Solution

The design is in two stages, with the first being a determination of the flow factor of safety of the geojute; the second being a consideration of the AOS.

(a) The first is done by calculating the required permittivity,  $\psi$ , which is  $\psi = k/t$ .

(1) Calculate the actual flow rate using a flow net.

$$\begin{aligned} q &= kh (F/N) \\ &= (0.0075) (3.5) (4/5) \\ &= 0.021 \text{ m}^2/\text{s} \end{aligned}$$

(2) Calculate the required permittivity.

$$\begin{aligned} q &= kiA \\ &= k(\Delta h/t) A \\ k/t &= q/(\Delta h A) \\ \psi_{reqd} &= 0.021/(3.5 \times 3.5 \times 1) = 1.71 \times 10^{-3} \text{ s}^{-1} \end{aligned}$$

(3) Check against the allowable permittivity of the candidate geojute

**Jute:**

$$\Psi_{ult} = 0.28 \text{ s}^{-1}$$

$$\Psi_{allow} = \Psi_{ult} \left( \frac{1}{RF_{SCB} \times RF_{CR} \times RF_{IN} \times RF_{CC} \times RF_{BC}} \right)$$

$$= 0.28/15.0$$

$$= 0.019 \text{ s}^{-1}$$

$$FS = \Psi_{\text{allow}} / \Psi_{\text{reqd}}$$

$$= 0.019 / 0.00171$$

$$= 10.9 \quad \text{acceptable}$$

**Canvas:**

$$\Psi_{\text{ult}} = 0.03 \text{ s}^{-1}$$

$$\Psi_{\text{allow}} = 0.03 / 15.0$$

$$= 2 \times 10^{-3} \text{ s}^{-1}$$

$$FS = \Psi_{\text{allow}} / \Psi_{\text{reqd}}$$

$$= 2 \times 10^{-3} / 0.00171$$

$$= 1.17 \quad \text{not acceptable}$$

**DW Twill:**

$$\Psi_{\text{ult}} = 0.25 \text{ s}^{-1}$$

$$\Psi_{\text{allow}} = 0.25 / 15.0$$

$$= 0.017 \text{ s}^{-1}$$

$$FS = \Psi_{\text{allow}} / \Psi_{\text{reqd}}$$

$$= 0.017 / 0.00171$$

$$= 9.94 \quad \text{acceptable}$$

**Hessian:**

$$\Psi_{\text{ult}} = 1.19 \text{ s}^{-1}$$

$$\Psi_{\text{allow}} = 1.19 / 15.0$$

$$= 0.08 \text{ s}^{-1}$$

$$FS = \Psi_{\text{allow}} / \Psi_{\text{reqd}}$$

$$= 0.08 / 0.00171 = 47 \quad \text{acceptable}$$

The above shows that many commercially available geojute can easily handle the required flow.

(b) The second part of the design relates to the geojute's opening size, to prevent excessive soil loss. The four candidate geojutes have AOS values of 0.28, 0.075, 0.8 and 1.0 respectively.

(1) The appropriate criterion for opening size must first be selected. Since this is a noncritical situation, Carroll's criterion will be used. This calls for the following relation:

$$O_{95} < 2.5 d_{85}$$

Since  $d_{10} = 0.03$  mm and  $C_u = 2.5$ , and an approximate value of  $d_{85} = 0.15$  mm.

(Note, that the  $d_{85}$  value should be obtained directly by sieving the upstream soil)

$$\begin{aligned} O_{95} &< 2.5(0.15) \\ &< 0.375 \text{ mm} \end{aligned}$$

(2) Check against the candidate geojutes AOS values:

Jute:	AOS = 0.28 mm < 0.375 mm	acceptable with FS = 1.34
Canvas:	AOS = 0.075 mm < 0.375 mm	not acceptable with FS = 5.0
DW Twill:	AOS = 0.8 mm < 0.375 mm	not acceptable with FS = 0.46
Hessian:	AOS = 1.0 mm > 0.375 mm	not acceptable with FS = 0.375

Thus, Canvas is too densely packed fabric, will not allow required flow through the fabric itself. Again, DW Twill and Hessian are too open and will experience excessive soil loss based upon this soil-retention criterion. Only Jute is acceptable. The technical decision as to which of these geojute to use will be based on the site-specific concern as to which mechanism (permeability or soil retention) is more important. The nontechnical, but important, final decision is based on cost and availability.

## 5.7 Designing for Drainage

### 5.7.1 General

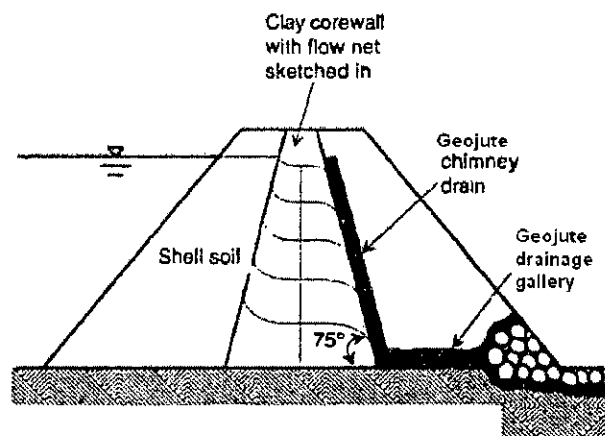
Drainage refers to planar flow within the structure of the geojute. For the flow capability of geojute, there are mainly two general categories: gravity flow and pressure flow. Some of the applications in each category may be listed below:

Gravity drainage: Chimney drains and drainage galleries in earth and earth/rock dams, pore water dissipaters behind retaining walls, flow interceptors (as in fin drains) beneath a geomembrane-lined reservoir for water drainage or gas conveyance.

Pressure drainage: As vertical drains for rapid soil consolidation, within the soil backfill of reinforced earth walls, within earth embankments and dams, beneath surcharge fills. In this chapter, an example is shown on gravity drainage system.

### 5.7.2 Problem I: Gravity Drainage

Given a 5 m high-zoned earth dam for use as an irrigation reservoir, the dam has a cross section as shown below. A geojute is being considered as a chimney drain and drainage gallery. The geojute under consideration is Jute (manufactured in BJRI) having  $\theta = 3.68 \times 10^{-4} \text{ m}^2/\text{min}$  at 10 kPa. Use cumulative reduction factors of 3.0 to convert this to  $\theta_{\text{allow}}$ . What factor of safety does this geojute have for flow seeping through the core wall, which is a clayey silt of permeability  $1 \times 10^{-7} \text{ m/s}$ ?



### 5.7.3 Solution

In stages, the solution is as follows:

(a) Calculate the maximum seepage coming through the clay core wall that the geojute must carry. The use of a flow net (as shown in the sketch) gives

$$\begin{aligned} q &= kh (F/N) \\ &= (1 \times 10^{-7}) (5) (5/2) \\ &= 1.25 \times 10^{-6} \text{ m}^2/\text{s} \\ &= 7.5 \times 10^{-5} \text{ m}^2/\text{min} \end{aligned}$$

(b) Calculate the gradient of flow in the geojute

$$\begin{aligned} i &= \sin 75^\circ \\ &= 0.97 \end{aligned}$$

(c) Calculate the required transmissivity  $\theta_{\text{reqd}}$  using Darcy's Formula

$$\begin{aligned} q &= kiA \\ &= ki (t \times W) \\ &= (kt) (i \times W) \\ kt &= q/(i \times W) \\ \theta_{\text{reqd}} &= (7.5 \times 10^{-5}) / (0.97 \times 1.00) \\ &= 7.73 \times 10^{-5} \text{ m}^2/\text{min} \end{aligned}$$

(d) Determine the global factor of safety:

$$\begin{aligned} \text{FS} &= \theta_{\text{allow}} / \theta_{\text{reqd}} \\ &= (\theta_{\text{ult}} / \text{II RF}_p) / \theta_{\text{reqd}} \\ &= \{(3.68 \times 10^{-4}) / 3.0\} / (7.73 \times 10^{-5}) \\ &= 1.6 \end{aligned}$$

Due to the critical nature of this application, this FS value is too low and a minimum value of 5.0 is recommended. Two options present themselves: one is to use multiple layers of Jute (to increase  $\theta_{\text{allow}}$ ) in the lower part of the chimney drain and in the drainage gallery (the upper part of the chimney drain could still use one layer); the



other is to use the  $FS = 5.0$  and back-calculate the necessary Jute's transmissivity. This latter suggestion is illustrated as follows.

$$\begin{aligned}\theta_{\text{allow}} &= \theta_{\text{reqd}} \times FS \\ &= (7.73 \times 10^{-5}) \times 5.0 \\ \theta_{\text{allow}} &= 3.87 \times 10^{-4} \text{ m}^2/\text{min}\end{aligned}$$

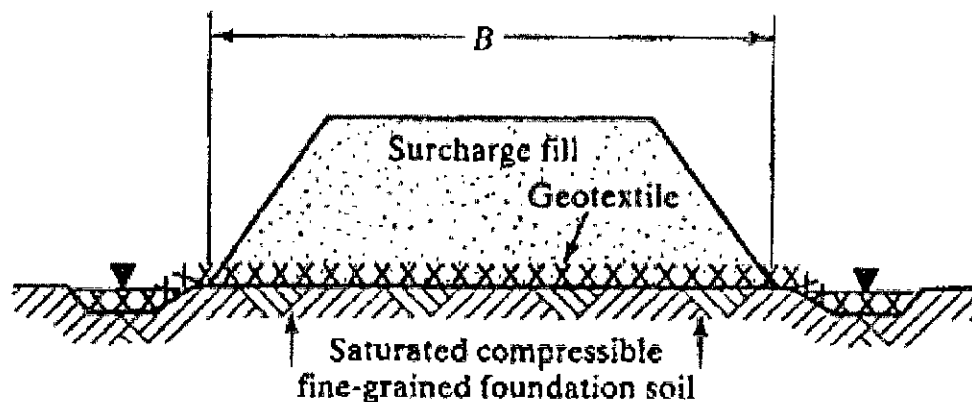
This, in turn, requires a Jute to have an ultimate (or as-manufactured) transmissivity considerably in excess of  $\theta_{\text{allow}}$ . If the cumulative reduction factor is 3.0

$$\begin{aligned}\theta_{\text{allow}} &= (3.87 \times 10^{-4}) \times 3.0 \\ &= 11.6 \times 10^{-4} \text{ m}^2/\text{min}\end{aligned}$$

This is possible only by selecting an extremely thick nonwoven needle-punched geotextile. Alternatively, geonets or geocomposites can be considered.

#### 5.7.4 Problem II: Pressure Drainage

Given a variable-width surcharge fill placed in 10 days (14,400 min) on a foundation soil of  $1 \times 10^{-9}$  m/s permeability and  $4.6 \times 10^{-6}$  m<sup>2</sup>/min coefficient of consolidation, as shown below: (a) determine the required Jute (produced in BJRI) transmissivity as a function of base width of the surcharge fill and graph the result; (b) using a ultimate geotextile transmissivity of  $0.37 \times 10^{-3}$  m<sup>2</sup>/min and cumulative reduction factors of 5.0, find the maximum width of surcharge that can be used under these conditions.

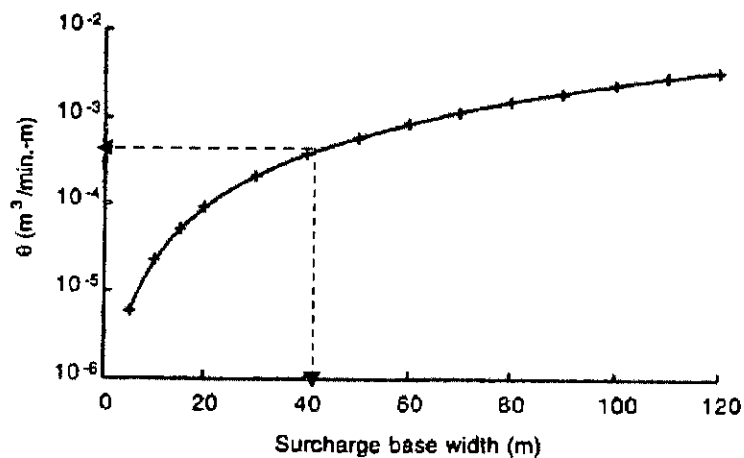


### 5.7.5 Solution

- (a) To determine the graph of B versus  $\theta$

$$\begin{aligned}\theta_{reqd} &= k_p t = (B^2 k_s) / (c_v T)^{1/2} \\ &= [(1 \times 10^{-9}) (60) B^2] / [(4.6 \times 10^{-6}) (0.0144 \times 10^6)]^{1/2} \\ &= 2.33 \times 10^{-7} B^2 \text{ where B is in m}\end{aligned}$$

when different values of B are plotted, the following curve results:



- (b) Using the above graph.

$$\begin{aligned}\theta_{ult} &= 0.00075 \text{ m}^2/\text{min} \\ \theta_{allow} &= \theta_{ult} / \text{IIRF}_p \\ &= 0.00075 / 5.0 \\ &= 0.00015 \text{ m}^2/\text{min}\end{aligned}$$

and from the chart the value is as follows:

$$B_{\max} = 43 \text{ m}$$

## 5.8 Economic Aspects

### 5.8.1 General

Economic aspects consist of analyzing plans, proposals or projects to find their comparative advantages and disadvantages and of getting down the results in a logical framework. Thus, the essence of economic aspects is the assessment of the relative merits of different courses of action, to assist the process of decision-making

(Lichfield et al. 1975). Economic evaluation is closely related with economic aspects which is concerned with the effects on the economy i.e., whether the plan or the proposal is financially viable. The qualitative answers obtained by testing the plans need to be translated into monetary terms to easily assess the comparative merits and demerits of the plans. It is, therefore, very common to express the evaluations in economic terms. The idea is to use of money as a measure of effectiveness of the several plans and to provide a common yardstick. In many situations, it is possible to assign a monetary value to the impact of the plan but there are many more where it is not possible, at the present stage of knowledge, to translate the impact in real money terms. In spite of this drawback, it is convenient to evaluate to the plans in economic terms and this practice has become common.

### **5.8.2 Need and Considerations for Economic Evaluation**

For a given set of goals and proposals, it is possible to formulate a number of alternatives. The cost of these plans may vary and so the benefits that are likely to accrue from them. Economic analysis has found a ready application in problems concerned with the evaluation of all sorts of plans. Although a full-fledged economic evaluation is not within the limit of this study, a small economic aspect is presented here.

### **5.8.3 Comparative Costs of Geojute and Geotextiles**

In making a proper economic assessment or evaluation, a number of inputs are required. Such as, material cost, labor cost etc. Again, these inputs vary place to place. In this study, an attempt has been made to assess the comparative cost of untreated and treated geojute (Table 5.4). The updated to date rates are collected from BJRI, BJMC and local market. The costs are shown in terms of per sq. ft. Fig 5.2 show the comparative costs of the tested untreated geojute. A cost comparison between different types of geotextiles is shown in Table 5.5. Geotextiles manufactured in country are cheaper than foreign ones. No woven geotextiles are produced in the country and prices of foreign made woven geotextiles are around 10% more than nonwoven ones. The manufacturer quoted the price only in C&F Chittagong. While

calculating unit price local taxes are included. The comparative costs of treated geojute with geotextiles are shown in Fig 5.3. Cost comparison between tested geojute and nonwoven geotextile (locally produced), geojute and nonwoven geotextile (foreign produced), geojute and woven geotextile (foreign produced) are shown in Table 5.6, Table 5.7 and Table 5.8 respectively.

Table 5.9 lists the mills that produce the tested geojute with their location. Jute is produced in BJRI loom. It is mainly produced for research purpose not for commercial sale. However, if ordered it can be produced in all the jute mills of BJMC. DW Twill and Hessian are produced in all the mills of BJMC and extensively used in the country mainly for packaging purpose. Canvas being very thickly woven fabric cannot be produced in all the jute mills of BJMC except the mills listed in the table.

**Table 5.4 Cost Comparisons between Geojutes**

Parameters	Jute	Canvas	DW Twill	Hessian
Length (inch)	3600	3600	3600	3600
Breadth (inch)	40	37	28.5	40
Price/100 yds (\$)	-	40.75	20.89	21.00
Service Charge (%)	-	7.5	7.5	7.5
Price/sft (Tk)	1.62	2.77	1.84	1.32
Treatment cost/sft (Tk)	0.35	0.30	0.35	0.41
Total cost/sft (Tk)	1.97	3.07	2.19	1.73

(Source: Marketing Division, BJMC)

**Table 5.5 Cost of Woven and Nonwoven Geotextiles**

Thickness (mm)	Cost/sft (Tk)		
	Nonwoven (locally produced)	Nonwoven (Foreign) (including tax)	Woven (Foreign) (including tax)
1.5	4.65	5.55	6.11
2.0	5.11	7.09	7.80
2.5	5.40	8.31	9.14
3.0	6.50	11.19	12.30
3.5	7.43	13.25	14.58
4.0	8.36	17.36	19.10
Average	6.25	10.46	11.51

**Table 5.6 Cost Comparison between Tested Geojute and Nonwoven Geotextile (locally produced)**

	Untreated		Treated	
	Higher price in percentage (%)	Higher price by times	Higher price in percentage (%)	Higher price by times
Jute	74	3.9	68	3.2
Canvas	56	2.3	51	2.0
DW Twill	71	3.4	65	2.8
Hessian	79	4.7	72	3.6

**Table 5.7 Price Comparison between Tested Geojute and Nonwoven Geotextile (foreign produced)**

	Untreated		Treated	
	Higher price in percentage (%)	Higher price by times	Higher price in percentage (%)	Higher price by times
Jute	84.5	6.46	81.2	5.3
Canvas	73.5	3.8	70.7	3.4
DW Twill	82.4	5.7	79.0	7.8
Hessian	87.4	7.9	83.5	6.0

**Table 5.8 Price Comparison between Tested Geojute and Nonwoven Geotextile (foreign produced)**

	Untreated		Treated	
	Higher price in percentage (%)	Higher price by times	Higher price in percentage (%)	Higher price by times
Jute	85.9	7.1	82.9	5.8
Canvas	75.9	4.2	73.3	3.7
DW Twill	84.0	6.3	81.0	5.3
Hessian	88.5	8.7	85.0	6.7

**Table 5.9 Sources of Geojutes**

Name of Product	Name of Mills	Address
Jute	Bangladesh Jute Research Institute	Manikmiah Avenue, Dhaka
Canvas	Latif Bawany Jute Mills Ltd	Demra, Dhaka
	Karim Jute Mills Ltd	Demra, Dhaka
	Bangladesh Jute Mills Ltd	Ghorasal, Narshingdi
	Hafiz Jute Mills Ltd.	Bashbaria, Chittagong
DW Twill	All the jute mills of BJMC	-
Hessian	All the jute mills of BJMC	-

(Source: Marketing Division, BJMC)

The costing of different jute products developed by BJRI in 1997 by blending jute with hydrophobic fiber like coir or by modification with bitumen, latex and wax resinous materials with the collaboration of BJMC and other governmental and non-governmental organizations are listed in Table 5.10.

**Table 5.10: Summary of Cost of Jute Blended with Different Materials at BJRI**

Type	Composition	Possible Durability	Wt./Unit (gm)	Cost Tk/yd <sup>2</sup>
Woven Jute in different structure	Jute	2-6 month	220-800	8-18
Woven Jute in different structure	Jute, Coir	5-12 month	220-800	12-32
Woven Jute but treated composite	Jute Bitumen Carbon	6-48 Month	Var. Wt.	12-35
Non woven	Jute blanket	6-18 month	800	65
Woven with different construction	Jute latex	5-20 year	≥ 800	20-40
Non woven	Jute Blanket + Latex	5-20 year	≥ 800	80

(Source: Directorate of Technology, BJRI)

## 5.9 Economic Benefit of Using Geojute in Different Applications

### 5.9.1 Separation

The design procedure for separation function by utilizing grab strength is illustrated in Sec 5.4. It is seen that the untreated Jute (produced in BJRI) can be used in this function for short term applications. If this material is used instead of nonwoven geotextile (locally produced) than 74% cost may be saved (Table 5.6).

### 5.9.2 Reinforced Wall

This design example has been presented using the procedure for geotextile outlined by Koerner (1997). Except the wide-width tensile strength of geotextile and geojute all the data's related to this design were same as shown in Koerner and this study. The wide-width tensile strength of geotextile was 50 kN/m. For this reinforced wall, total amount of geotextile required 41 m. While in this design example the wide-width tensile strength of DW Twill was 25 kN/m. Total amount of DW Twill will be required as calculated in this wall is 81.5m. Keeping all parameters same the

variation is only in amount of geojute. Considering price difference it is seen that the local manufactured geotextile is around four times costlier than DW Twill (Table 5.6). If DW Twill is used it will require double the amount (81.5 m) of geotextile, even though 50% cost will be saved since geotextile is four times costlier than DW Twill.

### 5.9.3 Reinforced Embankment

DW Twill was tried in designing reinforced embankment in Sec 5.5.4. For this particular design example total length of DW Twill and geotextile will be required is 191.2 m and 105.5 m. Though required amount of DW Twill is almost double than geotextile, if it is used instead of nonwoven geotextile (locally produced) than 46% cost will be saved (Table 5.6).

### 5.9.4 Filtration

In designing for filtration, it was found that Jute (produced in BJRI) was acceptable with FS 1.34. Geojute or geotextile which ever is used, total 10.5 m<sup>2</sup> will be required. If untreated Jute is used instead of nonwoven geotextile (locally produced) than 74% cost will be saved. Though considering high FS (5.0) Canvas was not accepted, even with this FS if it is used instead of nonwoven geotextile (locally produced) than 56% cost will be saved (Table 5.6)

### 5.9.5 Drainage

Two design examples in the application of geojute for drainage function have been illustrated in Sec 5.7. Jute (produced in BJRI) was tried in gravity drainage design. It is seen that with the given situation illustrated in this Sec Jute may not be suitable for the application in drainage function. On the other hand in pressure drainage function Jute (produced in BJRI) was also tried. It was found quite suitable and if it is used instead of nonwoven geotextile (locally produced) than 74% cost will be saved.



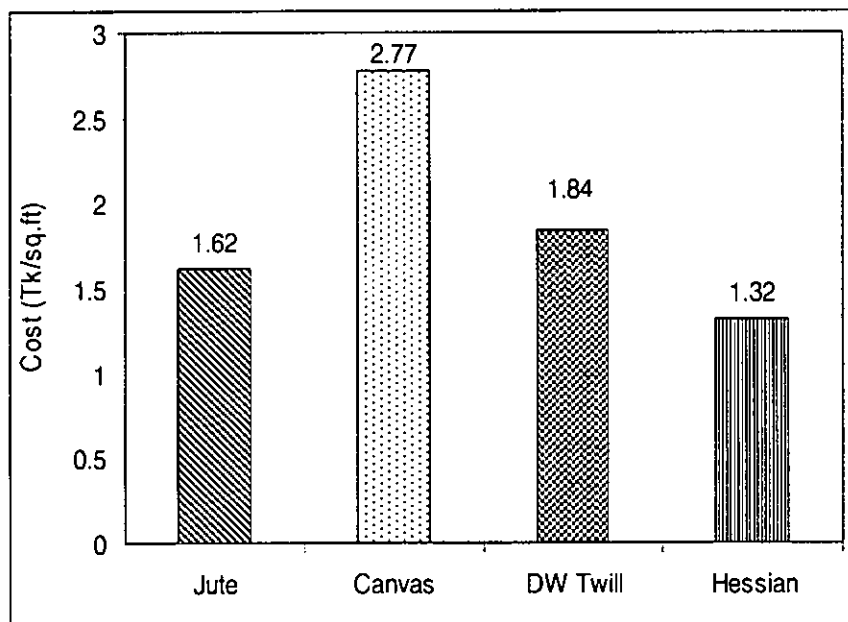


Fig 5.2 Comparative costs of the tested untreated geojute

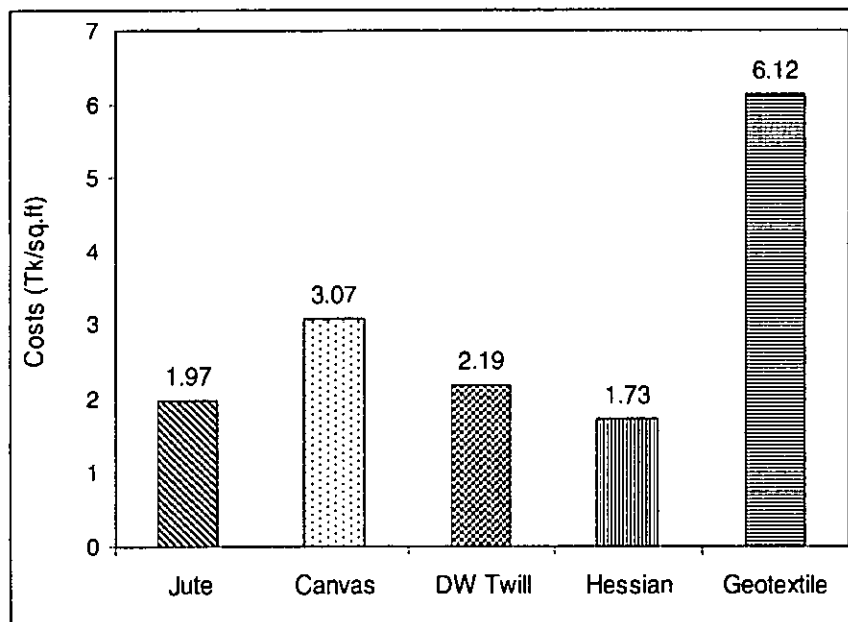


Fig 5.3 Comparative costs of treated geojute with geotextiles

## ***CHAPTER SIX***

### ***CONCLUSIONS AND RECOMMENDATIONS***

#### **6.1 General**

The feasibility study of using geojute as an alternative of geotextile in civil engineering application is the main concern of this study. Four types of untreated samples were selected. Three of these were treated and same sets of tests were performed on both treated and untreated samples to compare the results. Total thirteen tests were performed on each of the samples. The application areas and test methods have been discussed elaborately in Chapter Two. The laboratory investigations and experimental results with discussions were presented in Chapter Three and Chapter Four respectively. Based on these test results some design procedures have been presented in Chapter Five.

## **6.2 Conclusions on Experimental Results**

### **6.2.1 Mass per Unit Area**

Test method for mass per unit area is used basically to determine if the geotextile material meets specifications for mass per unit area and for quality control to determine specimen conformance. It was observed that the densely woven geojutes having more mass per unit area than the porous geojutes. The mass per unit area of treated samples increased considerably compared to the untreated samples. This increase in mass per unit area was due to the bitumen, which was coated with the samples while it was treated. The mass per unit area of nonwoven geotextile falls in the range of tested geojute.

### **6.2.2 Thickness**

Average thickness of a stack of woven geojute depends on the number of layers and the pressure applied on the geojute. Total thickness for any number of layers can be calculated under any applied load. Pressure applied on the jute sheet in the field should be simulated in the laboratory under pressure plates. Equivalent thickness for fewer numbers of layers as used in the field will be higher than that used in the laboratory test due to variation and uniformity of the effective load developed on the geojute by the soil material. It is observed that the geojute having more mass per unit area is thicker than the geojute having less mass per unit area thinner and porous. The thickness of nonwoven geotextiles varies from 1.5 mm to 4 mm.

### **6.2.3 Specific Density**

Specific density of geojute depends on the water absorption capacity of its fibers. It was found that geojute with a lower unit weight ( $\text{g/m}^2$ ) reaches the maximum specific density within a shorter time than that with a higher unit weight. It was also clear from this test that geojute can easily float up to 2 to 3 hours initially on fresh or salt water due to its low initial specific gravity, which is advantageous in transporting over the water, and after 4 to 5 hours of soaking in water it can be sunk and placed under water. There is a significant increase in specific density for low dense geojute

which demonstrates that the water penetrates deep into the fibre pores because of its large openings and loose orientation of the fibers in the weaving.

#### **6.2.4 Wide-width Tensile Test**

The wide-width tensile strength of geojute depends on types of strands, style of woven, weight per unit area and fiber quality. Strength does not depend on length or width of geojute. It is clear from the tensile properties determined by this test that the geojute materials are strong enough for use in the soil reinforcement scheme. The tearing strains as obtained from wide-width test, when the fibers start tearing apart from the strands. For DW Twill it was found to be around 13% in XMD whereas the maximum strain, though it could not be measured, was much more than that. Therefore geojute can sustain a considerable amount of strain in different geotechnical field applications before complete failure.

#### **6.2.5 Grab Tensile and elongation**

The grab tensile test provides an index of the ultimate strength of the specimen at failure. The test is easy to perform, inexpensive, and quick, taking only minutes to complete. As such, it is an excellent index strength test for verifying the quality of products in accordance with manufacturer's specifications. The average grab strength and elongation of geojutes were found to be 513 N and 23% respectively and average grab strength and elongation of nonwoven geotextiles are 1430 N and 102% respectively. It is clear from this test that the grab strength and elongation of geojute material are quite less than that of nonwoven geotextiles.

#### **6.2.6 Trapezoid Tearing strength**

Trapezoid tearing test is an important test because during installation geotextiles are subjected to tearing stresses. The tearing stress of geojute also depends on style of woven, weight per unit area and fiber quality. DW Twill was found to be the best among four untreated geojute materials considering tearing strength (464 N). The tearing strength of nonwoven geotextiles ranged from 90 N -1300 N.

### **6.2.7 Index and CBR Puncture**

Geotextiles resistance to objects such as stones and stumps under quasi-static conditions is quite good. The index puncture resistance of DW Twill was found to be 840N and is the best among four untreated material. The typical ranges of nonwoven geotextiles are between 45N– 450N. DW Twill is also strong enough considering the CBR puncture resistance

### **6.2.8 Burst Resistance**

The determination of the burst resistance of geotextile by Mullen burst test is still quite good analogous to field situation. DW Twill show best possible resistance against burst strength among four untreated materials.

### **6.2.9 Apparent Opening Size (AOS)**

The method to determine AOS of geotextile using sand fraction is simple and quick procedure. AOS of the tested geotextiles are sufficient to retain fine to medium sand particles as defined by Unified Soil Classification System (USCS).

### **6.2.10 Permittivity**

The determination of cross-plane permeability as defined by Permittivity is an important indicator of the quantity of water that can pass through a geotextile material in an isolated condition. The water permeability results of four untreated samples indicated Hessian as the most porous material and Canvas as the most impermeable material. After treatment, the permittivity of Canvas decreased to zero. This may be due to filling of pores of fibres with bitumen, which ultimately did not allow any water to pass through. In this permittivity test, the specimens were tested under zero normal stress which may not always be the situation encountered in the field. To make the test more performance-oriented, permittivity test under load should be performed.

### **6.2.11 Transmissivity**

The flow rate per unit width ( $m^3/s-m$ ) and hydraulic transmissivity ( $m^2/s$ ) follow a decreasing trend with the increase of normal stress and subsequently reach to constant values. Most of the geotextiles reach in this constant value after approximately 85 kPa. The tested jute samples also show the same behavior. Because beyond such load the yarn structure is sufficiently tight and dense to hold the load but still convey liquid to some extent. It is noted that the increase in transmissivity is with increasing mass per unit area and thickness of the fabrics. Thus, the thicker materials are best suited to convey water in the drainage function, but these are subjected to relatively high compression under load.

### **6.2.12 Unconfined Creep Behavior**

The unconfined tension creep test of Canvas samples were performed in untreated and treated condition. Creep behavior of Canvas fabrics revealed that the material is less susceptible to creep, even less than polyester geosynthetics. The tested Canvas in untreated condition could sustain its 30% of maximum wide-width tensile load. After treatment, it could sustain only its 10% of wide-width tensile load. It may also be seen that Canvas behaves like an elasto-plastic material i.e. the material behaves partly like elastic and partly like a plastic material upon subjection to loading.

## **6.3 Conclusions on Designing with Geojute**

### **6.3.1 Separation**

In the application of separation function, a number of scenarios can be developed showing which geojute properties are required for a given situation. The properties are burst resistance, grab tensile strength, puncture resistance and impact or tear resistance. These are described in detail in Chapter Two. The design procedure by utilizing grab strength is illustrated in Chapter Five. It is seen that the untreated Jute (produced in BJRI) may be used in separation function for short term applications. If

Jute is used instead of nonwoven geotextile (locally produced) than 74% cost may be saved.

### 6.3.2 Reinforcement

One design method illustrated in the primary function of reinforcement utilizing wide-width tensile strength data of DW Twill following the procedure of Koerner. Since it was out of scope of this thesis, the data which were used by Koerner related to soil parameters, soil and geotextile friction etc were adopted in this study. It seems DW Twill is quite satisfactory to be applied in reinforcement function for short term. As per design procedure both internal and external stability were checked properly. DW Twill has fulfilled all the necessities required to be applied as reinforcement material. Since DW Twill possess almost half wide-width tensile strength than geotextile, in design method the vertical spacing of geojute was double than geotextile. If DW Twill is used it will require double the amount of geotextile, even though 50% cost will be saved since geotextile is four times costlier than DW Twill. After treatment DW Twill may be used for longer term.

DW Twill was also tried in designing reinforced embankment. It was found suitable to be used in reinforced embankment. In cost comparison it is seen that if it is used instead of nonwoven geotextile (locally produced) than 46% cost will be saved.

### 6.3.3 Filtration

In the application of filtration function, all the four geojutes were checked using laboratory test properties obtained from this study. The design procedure is based on two stages. The first stage is done by calculating the required permittivity. It is seen that Jute, DW Twill and Hessian can be used as filtration material behind flexible wall systems consisting gabion wall to allow the backfill soil to be retained in its position. The second part of the design relates to the geojute's opening size, so as to prevent excessive soil loss. After checking Jute (produced in BJRI) was found acceptable with FS 1.34. DW Twill and Hessian are too open and will experience excessive soil loss based upon this soil-retention criterion. It is seen that if untreated Jute is used instead of nonwoven geotextile (locally produced) than 74% cost will be

saved. Though considering high FS (5.0) Canvas was not accepted, even with this FS if it is used instead of nonwoven geotextile (locally produced) than 56% cost will be saved.

The technical decision as to which of these geojute to use will be based on the site-specific concern as to which mechanism (permeability or soil retention) is more important. The nontechnical, but important, final decision is based on cost and availability.

#### **6.3.4 Drainage**

Two design examples in the application of geojute for drainage function have been presented. Jute (produced in BJRI) was checked in the application as a chimney drain and drainage gallery in a 5 m zoned earth dam for use as an irrigation reservoir. This type of application is critical in nature and requires a minimum FS value of 5.0. After checking, it was found that Jute may not be suitable for the application in drainage function in the situation depicted in that example. On the other hand in pressure drainage function Jute (produced in BJRI) was also tried. It was found quite suitable and if it is used instead of nonwoven geotextile (locally produced) than 74% cost will be saved.



### RECOMMENDATIONS FOR FUTURE RESEARCH

- a. Sensitivity of geojute materials to rate of strain in short term tensile testings require to be evaluated.
- b. In designing with geojute, it is necessary to know the soil-geojute interaction behavior. Determination of such soil-geojute interaction behavior in proper technical and feasible way, therefore, requires attention.
- c. Creep behavior is an important phenomenon and need to be evaluated properly. Further study related to creep behavior in future with modeling can be undertaken.
- d. Full scale model test may be performed in order to assess the overall performance of geojute as a potential alternative to geotextiles.

**REFERENCES**

- Abdullah, A.B.M., (1999). "A hand book on Geotextiles Particularly Natural Geotextiles from Jute and other Vegetable Fibres", Bangladesh Jute Research Institute, Dhaka, pp. 33-87.
- Ahmed, A. U. (1994), "Analysis and Design of Geosynthetics Reinforced Unpaved Roads on Clay Subgrades", M.Sc Engineering Thesis, Bangladesh University of Engineering and Technology, Dhaka.
- Alim, A. (1978). A Hand Book of Bangladesh Jute Associated Printers Limited, Dhaka.
- Andrawes, K. Z., McGown, A. and Kabir, M. H. (1984), "Uniaxial Strength Testing of woven and Nonwoven Geotextiles". Geotextiles and Geomembranes, Vol 1, pp. 41-56.
- ASTM D 3786 – 79 Standard Test Method for Hydraulic Bursting Strength of Knitted Goods and Nonwoven Fabrics-Diaphragm Bursting Strength Tester Method
- ASTM D 4439-98 Standard Terminologies for Geosynthetics
- ASTM D 4491-96 Standard Test Methods for Water Permeability of Geotextiles by Permittivity
- ASTM D 4533-91 Standard Test Method for Trapezoid Tearing Strength of Geotextiles

- ASTM D 4595-86 (Reapproved 1994) Standard Test Method for Tensile Properties of Geotextiles by the Wide-Width Strip Method
- ASTM D 4632-91 Standard Test Method for Grab Breaking Load and Elongation of Geotextiles
- ASTM D 4716-95 Test Method for determining the (In-plane) Flow Rate per Unit Width and Hydraulic Transmissivity of a Geosynthetic Using a Constant Head
- ASTM D 4751-95 Standard Test Method for Determining Apparent Opening Size of a Geotextile
- ASTM D 4833-88 (Reapproved 1996) Standard Test Method for Index Puncture Resistance of Geotextiles, Geomembranes and Related Products
- ASTM D 4884-96 Standard Test Method for Strength of Sewn or Thermally Bonded Seams of Geotextiles
- ASTM D 5199-98 Standard Test Method for Measuring the Nominal Thickness of Geotextiles and Geomembranes
- ASTM D 5261-92 Standard Test Method for Measuring Mass per Unit Area of Geotextiles
- ASTM D 5262-97 Standard Test Method for Evaluating Unconfined Tension Creep Behavior of Geosynthetics
- ASTM D 792-98 Standard Test Method for Density and Specific Gravity (Relative Density) of Plastics by Displacement
- Barrett, R. J., "Use of Plastic Filters in Coastal Structures", Proc. 16<sup>th</sup> Intl. Conf. Coastal Engineering, pp. 1048-1067.
- Bell, J.R., Stilley, A. R., and Vandre, B., (1975), "Fabric Retained Earth Walls," Proc. 13th Eng. Geol. Soils Eng. Symp., Moscow, ID: Idaho DOT, pp. 46-57.
- Broms, B. B., (1978), "Design of Fabric Reinforced Retaining Structures," Proc. Symp. Earth Reinforcement, Pittsburgh, PA: ASCE, pp. 282-303.

- Calhoun, C. C. (1972), "*Development of Design Criteria and Acceptance Specification for Plastic Filter Cloth*", US Army Corps of Engineers, Waterways Experiment Station, Vicksburg, MS.
- Carroll, R. G., Jr., (1983), Geotextile Filter Criteria, Engineering Fabrics in Transportation Construction, TRR 916, TBR, Washington, DC. pp. 46-53.
- Das M Braja (1990), Principles of Foundation Engineering, 2<sup>nd</sup> Edition, PWS-KENT Publishing House, Boston.
- Dembicki, E. and Jermolowicz, P., (1991), "*Soil Geotextile Interaction*", Geotextiles and Geomembranes, Vol. 10, pp. 249-268.
- den Hoedt, G., and Mouw, K. A. G., "The Application of High strength Woven Fabrics in hydraulic Engineering Construction", Proceeding 7<sup>th</sup> International Congr. Koninklyke Vlaamse Ingenieursvereniging, Vol. 2 Rotterdam: V. Z. W. pp. 11-19.
- Desai, N. B., Shah, H. N., Shah, L. M., Pandya, H. P., (1988), "*Creep Behavior of Indigenous Geosynthetics Material*", Proc. of the First Indian Geotextiles Conference on Reinforced Soil and Geotextiles, Bombay, India, 1988.
- Dewar, S., "*The Oldest Roads in Britain*", The Countryman, Vol. 59, No. 3, 1962, pp. 547-555.
- Girard, H., Fischer, S. and Alonso, E. (1990), "*Problems of Friction Posed by the Use of Geomembranes on Dam Slopes---Examples and Measurement*", Geotextiles and Geomembranes, Vol. 9, pp. 129-143.
- Giroud, J. P., (1981). "Designing with *Geotextiles*", Mater Const. (Paris), Vol. 14, No. 82, pp. 257-272.
- Giroud, J. P., (1984). "*Geotextiles and Geomembranes*", Geotextiles and Geomembranes, Vol. 1, pp.5-40.
- Giroud, J. P., Arman, A. and Bell, J. R. (1985). "*Geotextiles in Geotechnical Engineering Practice and Research*", Geotextiles and Geomembranes, Vol. 2, pp.179-242.

- Giroud, J.P. (1982), "*Filter Criteria for Geotextiles*", Proc. 2<sup>nd</sup> International Conference on Geotextiles, Las Vegas, U.S.A., Vol. 1, pp. 103-108.
- Grech T., (1995), "*Study of Marketing of Jute Geotextiles of ABC Mill Adamjee Jute Mills, Narayanganj*", Report submitted to Ministry of Jute.
- Haliburton, T. A., and Wood, P. D., (1992), "*Evaluation of U.S. Army Corps of Engineers Gradient Ratio Test for Geotextile Performance*," Proc. 2d Intl. Conf. on Geotextiles, St. Paul, MN: IFAI, pp. 97-101.
- Haliburton, T. A., Fowler, J., Langman, J. P., (1980), "Design and Construction of a Fabric Reinforced Test Section at Pinto Pass, Mobile, Alabama", Trans Res. Record #79, Washington, D.C.
- Heerten, I. G., (1983), *Geotextile Application in Geotechnical Engineering*, Indian Geotechnical Conference, Madras, India, Vol II, pp. 37-53.
- Indian Jute Industries' Research Association, (2004), "*Jute Geotextiles*", [www.worldjute.com](http://www.worldjute.com)
- Ingold, T. S., (1982), "*Some Observations on the Laboratory Measurement of Soil-Geotextile Bond*", Geotechnical Testing Journal, Vol. 5, No 3-4, pp. 57-67.
- John, N. W. M. (1987). *Geotextiles*, Blackie and Sons Ltd., London, pp. 347.
- Jute Manufactures Development Council, (2004), "*GeoJute\_\_Jute for the Future*", [www.jmdcindia.com](http://www.jmdcindia.com)
- Kabir, M. H., Zakaria M., Zoynul, M. A. and Nuruzzaman, A.S.M. (1998), "*Use of Jute Fabrics as Soil Filter*", First Indian Geotextile Conference on Reinforced Soil and Geotextiles, Bombay, India, Vol 1, pp. G35-G40.
- Kabir, M. H., Zakaria, Zoynul, M. A. and Saha, G. P (1998), "*Jute Fabric Reinforced Unpaved Road Design*", First Indian Geotextile Conference, Bombay, India, Vol 1, pp. G9-G14.
- Kabir, M.H., Ahmed K.U., Hossain, S.S., (1994), "*Mechanical Properties of Some Jute Fabrics and Fibre Drains*", Fifth International Conference on Geotextiles, Geomembranes and Related Products, Singapore, pp. 861-866.

- Karunaratne, G.P., Tan, S. A. and Muhammad, N. (1992), "*Geotechnical Properties of Jute Geotextiles*", Proc. of Earth Reinforcement Practice.
- Khan, M.A.A., Rao, G.V., Sarma, G.V.N., (1994) "*Durability of Jute Geotextile*", Fifth International Conference on Geotextiles, Geomembrane and Related Products, Singapore, 5-9 September 1994, pp. 857-860.
- Koerner, G. R. and Koerner, R. M., (1990), "*The Installation Survivability of Geotextiles and Geogrids*", Proc 4<sup>th</sup> IGS Conference on Geotextiles, Geomembranes and Related Products, Rotterdam: A A Balkema, pp. 597-774.
- Koerner, R. M. (1997), Designing with Geosynthetics, 4<sup>th</sup> Edition, Prentice Hall Inc., New Jersey.
- Koerner, R. M., and Welsh, J. P. (1980) "Construction and Geotechnical Engineering Using Synthetic Fabrics", New York: John Wiley and Sons.
- Koerner, R. M., Monteleone, M. J., Schmidt, R. K., and Roethe, A. T., (1986) "*Puncture and Impact Resistances of geosynthetics*", Proc. 3<sup>rd</sup> International Conference geotextiles, Vienna: Austrian Engineering Society, pp. 695-700.
- Kokkalis, A. and Papacharisis, N., (1989), "*A Simple Laboratory Method of Estimating the In-soil Behavior of Geotextiles*", Geotextiles and Geomembranes, Vol. 8, pp. 147-157.
- Koutsourais, M. M., Sprague, C. J. and Pucetas, R.C. (1991), "*Interfacial Friction Study of Cap and Liner Components for Landfill Design*", Geotextiles and Geomembranes, Vol. 10, pp. 531-548.
- Kozlowski, R, (1996), "*Bast Fibrous Plants as a Source of Raw Materials for Diversified Areas of Application*", Proc. 3rd Annual Conference, American Kenaf Society, Texas, USA.
- Lee et al (1987), "*Layered Clay Sand Scheme Reclamation*", Journal of Geotechnical Engineering, ASCE, Vol. 113, pp. 984-95.
- Lee et al (1989), "*Performance of Fibre Drain in Consolidation of Soft soils*", Proc. 12<sup>th</sup> International Conference on SMFE, Rio De Janeiro, Brazil.

- Lee, K. L., Adams, B. D., and Vagneron, J. M. J., (1973), "*Reinforced Earth Retaining Walls*," J. Soil Mech. Foundation. Eng. Div., Vol. 99, No. SM10, pp. 745-764.
- Leshchinsky, D. and Fowler, J. (1990). "*Laboratory Measurement of load-Elongation Relationship of High-Strength Geotextiles, Geotextiles and Geomembranes*", Vol. 9, pp. 145-164.
- Lichfield B. H., Henry, G. (1975), Economic Aspects and Analysis of Projects, 2<sup>nd</sup> Edition, Prentice Hall Inc., New Jersey.
- Liu, A., (2004) "*Jute an Environmentally Friendly Product*", Proc International Commodity Organization in Transition, United Nation Conference on Trade and Development, pp. 24-76.
- Liu, Aimin (2004), "*Jute – An Environmentally Friendly Product*", written for International Commodity Organization in Transition, published by United Nation Conference on Trade and Development
- Lydick, L. D. and and Zagorski, G. A. (1991), "*Interface Friction of Geonets: A Literature Survey*", Geotextiles and Geomembranes, Vol. 10, pp. 549-558.
- Mahaseth, B., (2002) "*Isothermal Response of Geosynthetics to Different Loading Regimes*", M.Sc. Thesis, Department of Civil Engineering, Bangladesh University of Engineering and Technology.
- Mandal, J.N. and Murti, M. V. R. (1990), "*Potential for Use of Natural Fibres in Geotechnical Engineering*", Fourth International Conference on Geotextiles, Geomembranes and Related Products, Hague.
- McGown, A., Andrawes, K. Z. and Kabir, M. H. (1982), "*Load-Extension Testing of Geotextiles Confined in-soil*", Proc. of the 2<sup>nd</sup> International Conference on Geotextiles, Las Vegas, Vol. III, pp. 793-798.
- McGown, A., Andrawes, K. Z., and Kabir, M. H., (1982) "*The Load Extension Testing of Geotextiles Confined in Soil*", Proc. 2nd International Conference on Geotextiles, Vienna: Austrian Engineering Society, pp. 707-712.

- McGown, A., Andrawes, K. Z., and Murry, R. T., (1986) "*The Load-Strain-Time-Temperature Behaviour of Geotextiles and Geogrids*," Proc. 3<sup>rd</sup> International Conference on Geotextiles, IFAI, pp. 793-796.
- Moritz, K. and Murray, H. (1982). "*Comparison between Different Tensile Tests and the Plunger Test (CBR Test)*", Proc. of the 2<sup>nd</sup> International Conference on Geotextiles, Las Vegas, Vol. III, pp. 757-718.
- Muhammad N., (1993), "*Use of Jute Geotextile in Layered Clay-Sand Reclamation Scheme*", M.Sc. Thesis, Department of Civil Engineering, National University of Singapore, Singapore.
- Myles, B. and Carswell, I.G. (1986). "*Tensile Testing of Geotextiles*", Proc. of the 3<sup>rd</sup> International Conference on Geotextiles, Vienna, Vol. III, pp. 713-718.
- National Academy of Engineering (1970), Scour at Bridge Waterways, NCHRP publisher, 5, Highway research Board, Washinton, D.C.
- NAVFAC, DM – 7.2, Bureau of Yards and Docks, US Navy, Apr, 1992
- Newby, J. E., "*Southern Pacific Transportation Co. Utilization of Geotextiles in Railroad Subgrade*," Proceeding 2<sup>nd</sup> International Conference on Geotextiles, St. Paul, MN: IFAI, 1982, pp. 467-472.
- Ognik, H. J. M. (1975), "*Investigations on the Hydraulic Characteristics of Synthetic Fabrics*", Publication no 146, Waterloopkunding Laboratorium Delft Hydraulics Laboratory.
- Prodhan, Z.H., (1994), "*Integrated Jute Geotextile Reinforced Earth Structures Design*", Lead Paper presented on Regional Seminar on New Application of Jute, Jointly organized by IJO, UNIDO and ICS.
- Prodhan, Z.H., (2001), "*Adaptive Research of Jute Geotextile in the Field of Civil Engineering Particularly in the Rural Roads for Pilot Scale Application*", Project Paper on slope protection work at Pakulla-Lauhati road in Delduar Upazilla under Tangail district.



- Raise, Y., Koerner, R. M., and Lord, A. E., Jr., (1987), "*Filtration Properties of Geotextiles under Long Term Testing*," Proc. ASCE/PennDOT Conf. Advances in Geotechnical Eng., Harris-burg, PA: PennDOT, pp. 1-13.
- Ramaswamy, S. D. and Aziz, M. A. (1989), "*Jute Geotextiles for Roads*", First International Workshop on Geotextiles, Nov 22-29, Bangalore, India.
- Ranganathan, S. R., Quayyum, Z., (1993) New Horizons for Jute, National Information Centre for Textile and Allied Subjects (NICTAS), Ahmedabad, India.
- Rankilor, P.R. (1981). Membranes in Ground Engineering, John Wiley and Sons, Ltd.
- Rao, A. S. (2003), "*Jute Geotextile Application in Kakinada Port Area*" Proc. of the National Seminar of Jute Geotextile and Innovative Jute Products, New Delhi, India, 25-26 Aug.
- Rao, J.P., Viswanadham, B.V.S. & Yadav, (1994) O.P., "*Jute Based Geotextiles & Their Evaluation for Civil Engineering Applications*", Fifth International Conference on Geotextiles, Geomembrane and Related Products, Singapore, 5-9 September 1994, pp. 853-856.
- Slim, W.J. (1955), Defeat into Victory, War Memories, World War II.
- Steward, J E., Williamson, R., and Mohny. J., (1977), "*Earth Reinforcement in Guidelines for Use of Fabrics in Construction and Maintenance of Low Volume Roads*", U.S. Forest Service. Portland, OR.
- Talukder, M. K., Majumdar, A. K., Debanath, C. R. , Majumdar, A., (1998), "*A Study of Jute and Polypropylene Needle Punched Nonwoven Fabrics for Geotextiles*", First Indian Geotextiles Conference on Reinforced Soil and Geotextiles, Bombay, India, 8-9 December, 1988, pp. G3-G7.
- Thomson, J. C., "*The role of Natural Fibres in Geotextile Engineering*", First Indian Geotextile Conference on Reinforced Soil and Geotextiles, Bombay, India, Vol 1, pp. G25-G29.

- U.S. Departments of the Army and the Air force (1995), "*Engineering Use of Geotextiles*", Technical Manual, Army TM 5-818-8 & Air Force Afjman 32-1030.
- Welsh, J. P., (1977), "*PennDOT Uses a New Method for Solving Scour Problems beneath Bridge Piers*", Highway Focus, Vol. 9, No 1, pp. 11-19.
- Whitcomb, W., and Bell, J. R., (1979), "*Analysis Techniques for Low Reinforced Soil Retaining Walls*," Proc. 17th Eng. Geol. Soils Eng. Symp., 'Moscow, ID: Idaho DOT, pp. 35-62.
- Williams, N. D., and Abouzakhm. M. A., (1989), "*Evaluation of Geotextile/Soil Filtration Characteristics Using the Hydraulic Conductivity Ratio Analysis*," Journal Geotextiles and Geomembranes, Vol. 8, No. 1, pp. 1-26.
- Yamauchi, T. (1992). "*Historical Review of Geotextiles for Reinforcement of Earth Works in Asia*", Proc. of the International Symposium on Earth Reinforcement Practice, Fukuoka, Kyushu, Special & Keynote Lectures, pp. 1-15.

## Typical Ranges of Properties for Currently Available Geotextiles

Physical Properties		
1	Specific Gravity	0.09-1.7
2	Mass per unit area	135-1000 g/m <sup>2</sup>
3	Thickness	0.25-7.5 mm
4	Stiffness	nil to 25,000 mg-cm
Mechanical Properties		
5	Compressibility	nil to high
6	Tensile strength (grab)	0.45-4.5 KN
7	Tensile strength (wide width)	9 - 180 KN/m
8	Confined tensile strength 18-180 KN/m	18 - 180 KN/m
9	Seam Strength	50 - 100% of tensile
10	Cyclic fatigue strength	50 - 100% of tensile
11	Burst strength	350 - 5200 KPa
12	Tear strength	90 - 1300 N
13	Impact strength	14 - 200 J
14	Puncture strength	45 - 450 N
15	Friction behavior	60 - 100 % of soil friction
16	Pullout behavior	50 - 100 % of geotextile strength
Hydraulic Properties		
17	Porosity (nonwoven)	50 - 90 %
18	Percent open area (woven)	nil to 36%
19	Apparent opening area (sieve size)	2.0 to 0.075 mm ( # 10 to # 200)
20	Permittivity	0.02 - 2.2 s <sup>-1</sup>
21	Permittivity under load	0.01 to 3.0 s <sup>-1</sup>
22	Transmissivity	0.01 to 2.0X10 <sup>-3</sup> m <sup>2</sup> /min
23	Soil retention : turbidity curtains	m.b.e.
24	Soil retention : silt fences	m.b.e.
Endurance Properties		
25	Installation damage	0 - 70% of fabric strength
26	Creep response	g.n.p. if < 40% strength is being used
27	Confined creep response	g.n.p. if < 50% strength is being used
28	Stress relaxation	g.n.p. if < 40% strength is being used
29	Abrasion	50 - 100% of geotextile strength
30	Long term clogging	m.b.e. for critical condition
31	Gradient ratio clogging	m.b.e. for critical condition
32	Hydraulic conductivity ratio	0.4 - 0.8 appear to be acceptable
Degradation Properties		
33	Temperature Degradation	high temperature accelerates degradation
34	Oxidative Degradation	m.b.e. for long service lifetimes
35	Hydrolysis Degradation	m.b.e. for long service lifetimes
36	Chemical Degradation	g.n.p. unless aggressive chemicals
37	Radioactive Degradation	g.n.p.
38	Biological Degradation	g.n.p.

Abbreviations: m.b.c. must be evaluated g.n.p. generally no problem (after Koerner, 1997)

**The ASTM & DIN Standards for Determining Design Parameters**

ser	No	ASTM Test	Design Parameters
1	D 5261	Standard Test Method for Measuring Mass per Unit Area of Geotextiles	Physical Properties
2	D 5199	Standard Test Method for Measuring the Nominal Thickness of Geosynthetics	Physical Properties
3	D 792	Standard Test Method for Density and Specific Gravity of Plastics by Displacement	Physical Properties
4	D 4595	Standard Test Method for Tensile Properties of Geotextiles by the Wide-Width Strip	Tensile Strength for Separation Tensile Strength for Reinforcement
5	D 4632	Standard Test Method for Grab Breaking Load and Elongation of Geotextiles	Tensile Strength
6	D 4533	Standard Test Method for Trapezoid Tearing Strength of Geotextiles	Tear Strength for Reinforcement
7	D 4491	Standard Test Methods for Water Permeability of Geotextiles by Permittivity	Permittivity for Separation
8	D 4716	Test Method for Determining the (In-plane) Flow Rate per Unit Width and Hydraulic Transmissivity	Transmissivity for Separation
9	D 5262	Standard Test Method for Evaluating Unconfined Tension Creep Behavior of Geosynthetics	Long term tensile strength
10	D 3786	Test Method for Hydraulic Burst Strength	Burst Test Pressure for Separation
11	D 4751	Standard Test Method for Determining Apparent Opening Size of a Geotextile	AOS & EOS for Separation
12	DIN 54307	Standard Test Method for CBR Puncture Resistance of Geotextiles	Puncture Resistance for Separation

Name of the Test: Wide-Width Tensile Test

Name of the sample: Jute

Date of Test: 11 Oct 2004

Machine Speed: 10 + 3% /min

No of Specimen in each Direction: 6

Specimen Size: 8"X8"

Temperature: 27° C

Elongation (mm)	Load (kgf)					
	MD			XMD		
	S 1	S 2	S 3	S 1	S 2	S 3
0	0	0	0	0	0	0
3	50	20	40	50	100	125
4	70	50	50	100	150	160
5	100	75	77	150	250	170
6	125	100	100	200	270	176
6.5	150	125	123	203	-	-
7	-	150	150	207	-	-
8	-	175	200	-	-	-
9	-	230	230	-	-	-
10	-	-	250	-	-	-
Avg. Load (kgf)	210			218		
Avg. Elongation (mm)	8.5			6.3		

Name of the Test: Wide-Width Tensile Test

Name of the sample: Canvas

Date of Test: 11 Oct 2004

Machine Speed: 10 + 3% /min

No of Specimen in each Direction: 6

Specimen Size: 8"X8"

Temperature: 27° C

Elongation (mm)	Load (kgf)					
	MD			XMD		
	S 1	S 2	S 3	S 1	S 2	S 3
0	0	0	0	0	0	0
2	30	25	50	100	100	100
4	50	50	100	250	250	270
5	75	150	136	294	350	289
6	100	200	200	-	-	-
8	200	300	350	-	-	-
9	230	366	422	-	-	-
10	250	-	524	-	-	-
12	350	-	-	-	-	-
14	400	-	-	-	-	-
16	450	-	-	-	-	-
18	550	-	-	-	-	-
Avg. Load (kgf)	480			311		
Avg. Elongation (mm)	12.3			5.0		

Name of the Test: Wide-Width Strip Tensile Test

Name of the sample: DW Twill

Date of Test: 11 Oct 2004

Machine Speed: 10 + 3% /min

No of Specimen in each Direction: 6

Specimen Size: 8"X8"

Temperature: 27° C

Elongation (mm)	Load (kgf)					
	MD			XMD		
	S 1	S 2	S 3	S 1	S 2	S 3
0	0	0	0	0	0	0
2	75	100	100	25	25	50
4	200	250	250	50	50	75
6	250	450	450	100	75	100
8	340	650	600	150	100	150
8.5			650	175	125	175
10	-	-	-	300	200	300
12	-	-	-	500	350	500
13	-	-	-	-	400	520
14	-	-	-	-	440	-
Avg. Load (kgf)	546.7			486.7		
Avg. Elongation (mm)	8.2 mm			13.0		

Name of the Test: Wide-Width Strip Tensile Test

Name of the sample: Hessian

Date of Test: 11 Oct 2004

Machine Speed: 10 + 3% /min

No of Specimen in each Direction: 6

Specimen Size: 8"X8"

Temperature: 27° C

Elongation (mm)	Load (kgf)					
	MD			XMD		
	S 1	S 2	S 3	S 1	S 2	S 3
0	0	0	0	0	0	0
2	45	40	30	35	20	20
4	100	90	50	50	40	40
5.5	284	175	75	125	70	50
6.5	-	288	150	200	125	80
7.5	-	-	240	276	200	150
8	-	-	264	-	258	175
9	-	-	-	-	-	272
Avg. Load (kgf)	278.7			268.7		
Avg. Elongation (mm)	6.7			8.2		



Name of the Test: Wide-Width Strip Tensile Test

Name of the sample: Treated Jute

Date of Test: 10 Dec 2004

Machine Speed: 10 + 3% /min

No of Specimen in each Direction: 6

Specimen Size: 8"X8"

Temperature: 27° C

Elongation (mm)	Load (kgf)					
	MD			XMD		
	S 1	S 2	S 3	S 1	S 2	S 3
0	0	0	0	0	0	0
2	50	20	40	50	100	125
4	70	50	50	100	150	160
6	100	75	77	150	250	170
8	125	100	100	200	270	176
10	150	125	123	203	-	-
10.7	-	150	150	207	-	-
10.9	-	175	200	-	-	-
11	-	230	230	-	-	-
11.5	-	-	250	-	-	-
11.7	-	-	-	402	-	-
Avg. Load (kgf)	331.33			374.67		
Avg. Elongation (mm)	10.9			11.4		

Name of the Test: Wide-Width Strip Tensile Test

Name of the sample: Treated Canvas

Date of Test: 10 Dec 2004

Machine Speed: 10 + 3% /min

No of Specimen in each Direction: 6

Specimen Size: 8"X8"

Temperature: 27° C

Elongation (mm)	Load (kgf)					
	MD			XMD		
	S 1	S 2	S 3	S 1	S 2	S 3
0	0	0	0	0	0	0
2	22	114	122	35	50	50
4	50	212	190	100	150	100
6	100	345	245	155	223	176
8	200	390	301	185	285	215
10	260	415	345	215	314	275
12	290	470	402	255	-	310
14	315	485	455	284	-	-
16	360	520	475	-	-	-
18	395	590	501	-	-	-
20	415	-	524	-	-	-
22	460	-	564	-	-	-
24	510	-		-	-	-
Avg. Load (kgf)	555			303		
Avg. Elongation (mm)	21.3			12.0		

Name of the Test: Wide-Width Strip Tensile Test

Name of the sample: Treated DW Twill

Date of Test: 10 Dec 2004

Machine Speed: 10 + 3% /min

No of Specimen in each Direction: 6

Specimen Size: 8"X8"

Temperature: 27° C

Elongation (mm)	Load (kgf)					
	MD			XMD		
	S 1	S 2	S 3	S 1	S 2	S 3
0	0	0	0	0	0	0
2	102	114	88	212	50	79
4	145	165	135	307	150	212
6	280	245	201	405	220	301
8	345	301	275	502	340	395
10	398	345	333	605	455	498
11	431	403	389	710	545	600
12	-	-	-	-	622	-
Avg. Load (kgf)	408			644		
Avg. Elongation (mm)	11.0			11.3		

Name of the Test: Specific Gravity

Sample: Jute

Flask No: 1

$$\text{Formula: } G_s = \frac{W_j}{W_{bw} + W_j - W_{bwj}}$$

$W_j$  = Weight of dry Jute = 30.0 gm

$W_{bw}$  = Weight of Flask + distilled water up to graduation = 663.3 gm

$W_{bwj}$  = Weight of Flask + Jute + distilled water up to graduation

ser	Time (min)	$W_{bwj}$ (gm)	$G_s$	ser	Time (hr)	$W_{bwj}$ (gm)	$G_s$
1	0	643.6	0.60	19	1.0	629.89	0.89
2	1	644.42	0.61	20	2.0	630.63	0.91
3	2	645.21	0.62	21	3.0	661.34	0.93
4	3	645.98	0.63	22	4.0	662.02	0.95
5	4	646.73	0.64	23	5.0	669.32	0.96
6	5	647.45	0.65	24	10.0	662.99	0.98
7	6	648.15	0.66	25	20.0	663.30	0.99
8	7	648.82	0.67	26	30.0	633.3	1.00
9	8	649.48	0.68	27	40.0	663.9	1.01
10	9	650.12	0.69	28	50.0	664.19	1.02
11	10	650.74	0.70	29	60.0	664.47	1.03
12	12	651.93	0.72	30	70.0	664.75	1.04
13	14	652.5	0.73	31	80.0	664.75	1.04
14	16	653.6	0.75	32	90.0	664.75	1.04
15	18	654.13	0.76	33			
16	20	657.4	0.77	34			
17	25	656.1	0.80	35			
18	30	654.64	0.83	36			

Name of the Test: Specific Gravity

Sample: Canvas                      Flask No: 2

$$\text{Formula: } G_s = \frac{W_j}{W_{bw} + W_j - W_{bwj}}$$

$W_j$  = Weight of dry Jute = 26.1 gm

$W_{bw}$  = Weight of Flask + distilled water up to graduation = 691.6 gm

$W_{bwj}$  = Weight of Flask + Jute+ distilled water up to graduation

ser	Time (min)	$W_{bwj}$ (gm)	$G_s$	Ser	Time (hr)	$W_{bwj}$ (gm)	$G_s$
1	0	684.66	0.79	19	1.0	993.53	1.08
2	1	685.87	0.82	20	2.0	693.76	1.09
3	2	686.63	0.84	21	3.0	693.76	1.09
4	3	687.35	0.86	22	4.0	693.97	1.10
5	4	688.04	0.88	23	5.0	694.19	1.11
6	5	688.7	0.90	24	10.0	694.60	1.13
7	6	689.33	0.92	25	20.0	694.80	1.14
8	7	689.93	0.94	26	30.0	695.00	1.15
9	8	690.79	0.97	27	40.0	695.2	1.16
10	9	691.34	0.99	28	50.0	695.40	1.17
11	10	692.11	1.02	29	60.0	695.58	1.18
12	12	692.36	1.03	30	70.0	695.77	1.19
13	14	692.60	1.04	31	80.0	695.95	1.20
14	16	692.60	1.04	32	90.0	695.95	1.20
15	18	692.84	1.05	33			
16	20	693.10	1.06	34			
17	25	693.31	1.07	35			
18	30	693.50	1.08	36			

Name of the Test: Specific Gravity

Sample: DW Twill

Flask No: 3

$$\text{Formula: } G_s = \frac{W_j}{W_{bw} + W_j - W_{bwj}}$$

$W_j$  = Weight of dry Jute = 30.7 gm

$W_{bw}$  = Weight of Flask + distilled water up to graduation = 643.7 gm

$W_{bwj}$  = Weight of Flask + Jute+ distilled water up to graduation

ser	Time (min)	$W_{bwj}$ (gm)	$G_s$	Ser	Time (hr)	$W_{bwj}$ (gm)	$G_s$
1	0	634.53	0.77	19	1.0	653.06	0.96
2	1	678.84	0.79	20	2.0	686.37	0.98
3	2	679.33	0.80	21	3.0	686.69	0.99
4	3	679.80	0.81	22	4.0	687.30	1.01
5	4	980.26	0.82	23	5.0	687.89	1.03
6	5	680.71	0.83	24	10.0	688.46	1.05
7	6	681.15	0.84	25	20.0	688.74	1.06
8	7	682.00	0.86	26	30.0	689.00	1.07
9	8	682.81	0.88	27	40.0	689.27	1.08
10	9	683.21	0.89	28	50.0	689.53	1.09
11	10	683.59	0.90	29	60.0	689.79	1.1
12	12	683.59	0.90	30	70.0	690.29	1.12
13	14	683.96	0.91	31	80.0	690.53	1.13
14	16	683.96	0.91	32	90.0	690.53	1.13
15	18	683.96	0.91	33			
16	20	684.33	0.92	34			
17	25	684.69	0.93	35			
18	30	685.04	0.94	36			

Name of the Test: Specific Gravity

Sample: Hessian                      Flask No: 4

$$\text{Formula: } G_s = \frac{W_j}{W_{bw} + W_j - W_{bwj}}$$

 $W_j$  = Weight of dry Jute = 26.6 gm $W_{bw}$  = Weight of Flask + distilled water up to graduation = 676.8 gm $W_{bwj}$  = Weight of Flask + Jute+ distilled water up to graduation

ser	Time (min)	$W_{bwj}$ (gm)	$G_s$	ser	Time (hr)	$W_{bwj}$ (gm)	$G_s$
1	0	675.4	0.95	19	1.0	682.27	1.28
2	1	675.98	0.97	20	2.0	683.09	1.31
3	2	676.53	0.99	21	3.0	683.40	1.33
4	3	676.80	1.00	22	4.0	683.84	1.36
5	4	677.32	1.02	23	5.0	684.12	1.38
6	5	677.82	1.04	24	10.0	684.40	1.4
7	6	678.54	1.07	25	20.0	980.10	1.42
8	7	691.69	1.09	26	30.0	684.93	1.44
9	8	679.22	1.10	27	40.0	685.06	1.45
10	9	679.44	1.11	28	50.0	685.18	1.46
11	10	679.65	1.12	29	60.0	685.43	1.48
12	12	680.06	1.14	30	70.0	685.55	1.49
13	14	680.46	1.16	31	80.0	685.67	1.50
14	16	680.66	1.17	32	90.0	685.78	1.51
15	18	680.66	1.17	33			
16	20	680.86	1.18	34			
17	25	681.23	1.20	35			
18	30	681.60	1.22	36			

Name of the Test: Specific Gravity

Sample: Treated Jute

Flask No: 5

$$\text{Formula: } G_s = \frac{W_j}{W_{bw} + W_j - W_{bwj}}$$

W<sub>j</sub> = Weight of dry Jute = 60.8 gmW<sub>bw</sub> = Weight of Flask + distilled water up to graduation = 1293.3 gmW<sub>bwj</sub> = Weight of Flask + Jute+ distilled water up to graduation

ser	Time (min)	W <sub>bwj</sub> (gm)	G <sub>s</sub>	ser	Time (hr)	W <sub>bwj</sub> (gm)	G <sub>s</sub>
1	0	1260.56	0.65	19	1.0	1281.72	0.84
2	1	1263.35	0.67	20	2.0	1283.40	0.86
3	2	1264.69	0.68	21	3.0	1284.21	0.87
4	3	1265.98	0.69	22	4.0	1285.00	0.88
5	4	1267.24	0.70	23	5.0	1285.79	0.89
6	5	1268.47	0.71	24	10.0	1286.54	0.90
7	6	1269.66	0.72	25	20.0	1288.01	0.92
8	7	1270.81	0.73	26	30.0	1288.72	0.93
9	8	1271.94	0.74	27	40.0	1289.42	0.94
10	9	1273.03	0.75	28	50.0	1290.10	0.95
11	10	1274.10	0.76	29	60.0	1290.77	0.96
12	12	1275.14	0.77	30	70.0	1291.42	0.97
13	14	1275.14	0.77	31	80.0	1292.06	0.98
14	16	1276.15	0.78	32	90.0	1292.69	0.99
15	18	1276.15	0.78	33			
16	20	1277.14	0.79	34			
17	25	1279.04	0.81	35			
18	30	1279.95	0.82	36			



Name of the Test: Specific Gravity

Sample: Treated Canvas

Flask No: 6

$$\text{Formula: } G_s = \frac{W_j}{W_{bw} + W_j - W_{bwj}}$$

W<sub>j</sub> = Weight of dry Jute = 61.7 gmW<sub>bw</sub> = Weight of Flask + distilled water up to graduation = 1292.1 gmW<sub>bwj</sub> = Weight of Flask + Jute+ distilled water up to graduation

ser	Time (min)	W <sub>bwj</sub> (gm)	G <sub>s</sub>	ser	Time (hr)	W <sub>bwj</sub> (gm)	G <sub>s</sub>
1	0	1285.2	0.90	19	1.0	1287.3	0.93
2	1	1286.2	0.91	20	2.0	1287.7	0.93
3	2	1286.3	0.91	21	3.0	1288.0	0.94
4	3	1286.4	0.92	22	4.0	1288.3	0.94
5	4	1286.5	0.92	23	5.0	1288.7	0.95
6	5	1286.5	0.92	24	10.0	1289.5	0.96
7	6	1286.5	0.92	25	20.0	1290.19	0.97
8	7	1286.6	0.92	26	30.0	1290.84	0.98
9	8	1286.6	0.92	27	40.0	1291.48	0.99
10	9	1286.6	0.92	28	50.0	1292.1	1.0
11	10	1286.7	0.92	29	60.0	1293.31	1.02
12	12	1286.7	0.92	30	70.0	1293.90	1.03
13	14	1286.7	0.92	31	80.0	1293.90	1.03
14	16	1286.8	0.92	32	90.0	1294.47	1.04
15	18	1286.8	0.92	33			
16	20	1286.9	0.92	34			
17	25	1286.9	0.92	35			
18	30	1287.0	0.92	36			

Name of the Test: Specific Gravity

Sample: Treated DW Twill

Flask No: 7

$$\text{Formula: } G_s = \frac{W_j}{W_{bw} + W_j - W_{bwj}}$$

W<sub>j</sub> = Weight of dry Jute = 58.7 gmW<sub>bw</sub> = Weight of Flask + distilled water up to graduation = 1241.4 gmW<sub>bwj</sub> = Weight of Flask + Jute + distilled water up to graduation

ser	Time (min)	W <sub>bwj</sub> (gm)	G <sub>s</sub>	Ser	Time (hr)	W <sub>bwj</sub> (gm)	G <sub>s</sub>
1	0	1165.0	0.43	19	1.0	1197.18	0.57
2	1	1169.0	0.45	20	2.0	1200.61	0.59
3	2	1171.4	0.46	21	3.0	1205.42	0.62
4	3	1172.5	0.46	22	4.0	1211.16	0.66
5	4	1173.4	0.46	23	5.0	1216.24	0.70
6	5	1175.0	0.47	24	10.0	1218.57	0.72
7	6	1175.7	0.47	25	20.0	1219.69	0.73
8	7	1176.5	0.47	26	30.0	1220.78	0.74
9	8	1177.2	0.48	27	40.0	1221.83	0.75
10	9	1178.5	0.48	28	50.0	1223.87	0.77
11	10	1179.3	0.49	29	60.0	1224.84	0.78
12	12	1179.8	0.49	30	70.0	1226.73	0.80
13	14	1180.3	0.49	31	80.0	1227.63	0.81
14	16	1181.2	0.49	32	90.0	1228.51	0.82
15	18	1182.3	0.50	33			
16	20	1183.2	0.50	34			
17	25	1187.2	0.52	35			
18	30	1190.1	0.53	36			

Name of the Test: Grab Breaking Load and Elongation

Machine Speed:  $300 \pm 10$  mm/min

No of Samples in each Direction: 10

Specimen Size: 4"X8" (Jaw 1"X3")

ser	Load (kgf)	Elongation (mm)	Load (kgf)	Elongation (mm)
	<b>Jute</b>			
	MD		XMD	
1	40	34	30	21
2	45	26	15	26
3	40	24	30	24
4	39	25	29	21
5	44	26	28	25
6	47	30	25	21
7	44	31	30	22
8	40	32	29	20
9	39	25	30	21
10	40	26	25	20
Avg	41.8	28.9	27.1	22.1
N	410	38.5%	266	29.5%
ser	<b>Canvas</b>			
	MD		XMD	
	1	92	14	37
2	90	16	43	11
3	92	14	44	11
4	91	15	40	12
5	90	14	42	14
6	92	16	45	15
7	90	15	44	12
8	83	14	42	14
9	92	15	43	12
10	90	15	40	13
Avg	90.2	14.8	40	12.9
N	885	19.7%	392	17.2%

ser	Load (kgf)	Elongation (mm)	Load (kgf)	Elongation (mm)
	<b>DW Twill</b>			
	MD		XMD	
1	70	16	74	12
2	95	16	80	17
3	90	17	70	13
4	90	15	80	15
5	89	16	75	12
6	95	17	78	15
7	96	16	79	16
8	94	16	78	14
9	92	15	75	15
10	96	16	76	16
Avg	94.7	16	76.5	14.5
N	929	21.3%	750	19.3%
ser	<b>Hessian</b>			
	MD		XMD	
	1	2	3	4
1	30	21	28	21
2	16	15	24	11
3	16	12	23	11
4	25	15	25	15
5	19	14	24	12
6	22	15	26	14
7	23	15	25	15
8	25	16	26	16
9	29	20	27	15
10	24	18	25	12
Avg	22.9	16.1	25.3	14.2
N	225	21.5%	248	19%

U  
R

ser	Load (kgf)	Elongation (mm)	Load (kgf)	Elongation (mm)
	<b>Treated Jute</b>			
	MD		XMD	
1	82	29	77	29
2	100	32	68	24
3	77	33	71	23
4	89	30	75	23
5	85	29	78	24
6	83	30	74	25
7	75	31	75	26
8	80	28	75	23
9	88	29	69	28
10	89	30	70	26
Avg	84.8	30.1	73.2	25.1
N	831.6	40%	718	33.5%
ser	<b>Treated Canvas</b>			
	MD		XMD	
	Load (kgf)	Elongation (mm)	Load (kgf)	Elongation (mm)
1	89	17	65	19
2	114	21	75	18
3	121	21	60	17
4	115	20	66	18
5	114	21	65	19
6	110	18	68	18
7	99	19	69	18
8	98	20	70	17
9	101	18	71	18
10	104	18	72	19
Avg	106.5	19.3	68.1	18.1
N	1044	25.7%	668	24%

ser	Load (kgf)	Elongation (mm)	Load (kgf)	Elongation (mm)
	<b>Treated DW Twill</b>			
	MD		XMD	
1	126	22	90	15
2	112	20	78	14
3	92	18	122	15
4	98	15	120	16
5	96	16	114	14
6	98	17	95	15
7	97	18	97	15
8	98	17	96	14
9	96	15	95	15
10	96	19	96	16
Avg	100.9	17.7	100.3	14.9
N	990	23.6%	984	20%

Name of the Test: In-plane Flow Rate per Unit Width and Hydraulic Transmissivity

Sample Dimension: 16.5 cm X 10 cm

Temperature: 25° C

Collection Time: 15 minutes

S e r	Normal Stress (KPa)	Load (Kg)	Q <sub>t</sub> (ml)				Flow Rate q <sub>w</sub> (m <sup>3</sup> /s-m)	Hy. Trans θ (m <sup>2</sup> /s)
			1	2	3	AVG		
Sample : Hessian								
Head : 14.4 cm			DOT: 12 Oct 2004				i= 1.15	
1	10.0	16.825	230	210	200	213	2.37X10 <sup>-6</sup>	2.71 X10 <sup>-6</sup>
2	15.0	25.239	140	130	120	130	1.44X10 <sup>-6</sup>	1.66X10 <sup>-6</sup>
3	20.0	33.650	125	120	120	122	1.36X10 <sup>-6</sup>	1.55X10 <sup>-6</sup>
4	25.0	42.060	124	115	110	116	1.29X10 <sup>-6</sup>	1.48X10 <sup>-6</sup>
5	30.0	50.480	51	42	39	44	0.49X10 <sup>-6</sup>	0.56X10 <sup>-6</sup>
Sample : DW Twill								
Head : 16.0 cm			DOT: 12 Oct 2004				i= 0.97	
1	10.0	16.825	390	360	370	373	4.14X10 <sup>-6</sup>	4.27 X10 <sup>-6</sup>
2	15.0	25.239	150	145	140	145	1.61X10 <sup>-6</sup>	1.66 X10 <sup>-6</sup>
3	20.0	33.650	120	115	110	115	1.28X10 <sup>-6</sup>	1.28 X10 <sup>-6</sup>
4	25.0	42.060	90	90	69	83	0.92X10 <sup>-6</sup>	0.95 X10 <sup>-6</sup>
5	30.0	50.480	35	23	20	26	0.29X10 <sup>-6</sup>	0.33X10 <sup>-6</sup>
Sample : Jute								
Head : 16.0 cm			DOT: 12 Oct 2004				i= 0.87	
1	10.0	16.825	605	520	480	535	5.94X10 <sup>-6</sup>	6.13X10 <sup>-6</sup>
2	15.0	25.239	250	225	210	228	2.53X10 <sup>-6</sup>	2.61 X10 <sup>-6</sup>
3	20.0	33.650	160	155	150	155	1.72X10 <sup>-6</sup>	1.77 X10 <sup>-6</sup>
4	25.0	42.060	107	105	104	105	1.16X10 <sup>-6</sup>	1.2 X10 <sup>-6</sup>
5	30.0	50.480	51	46	43	47	0.52X10 <sup>-6</sup>	0.54X10 <sup>-6</sup>

Se r	Normal Stress (KPa)	Load (Kg)	Q <sub>t</sub> (ml)				Flow Rate q <sub>w</sub> (m <sup>3</sup> /s-m)	Hy. Trans θ (m <sup>2</sup> /s)
			1	2	3	AVG		
Sample : Canvas Head : 19.0 cm      DOT: 12 Oct 2004      i= 0.97								
1	10.0	16.825	275	210	165	217	3.41X10 <sup>-6</sup>	3.09 X10 <sup>-6</sup>
2	15.0	25.239	175	165	160	167	2.15X10 <sup>-6</sup>	2.42X10 <sup>-6</sup>
3	20.0	33.650	140	135	133	136	1.91X10 <sup>-6</sup>	2.18X10 <sup>-6</sup>
4	25.0	42.060	70	60	50	60	1.67X10 <sup>-6</sup>	1.88X10 <sup>-6</sup>
5	30.0	50.480	12	16	15	14	0.96X10 <sup>-6</sup>	1.25X10 <sup>-6</sup>
Sample : Treated Jute Head : 10.8 cm      DOT: 2 Nov 2004      i= 0.65								
1	10.0	16.825	185	180	182	182	2.02X10 <sup>-6</sup>	3.89X10 <sup>-6</sup>
2	15.0	25.239	120	121	122	121	1.34X10 <sup>-6</sup>	2.05X10 <sup>-6</sup>
3	20.0	33.650	100	101	100	100	1.11X10 <sup>-6</sup>	1.7X10 <sup>-6</sup>
4	25.0	42.060	89	90	89	90	1.0X10 <sup>-6</sup>	1.53X10 <sup>-6</sup>
5	30.0	50.480	26	25	27	26	0.29X10 <sup>-6</sup>	0.44X10 <sup>-6</sup>
Sample : Treated Canvas Head : 11 cm      DOT: Nov 2004      i= 0.67								
1	10.0	16.825	285	280	275	280	3.11 X10 <sup>-6</sup>	4.67X10 <sup>-6</sup>
2	15.0	25.239	187	185	183	185	2.05 X10 <sup>-6</sup>	3.08X10 <sup>-6</sup>
3	20.0	33.650	145	140	135	140	1.56 X10 <sup>-6</sup>	2.34X10 <sup>-6</sup>
4	25.0	42.060	84	82	80	82	0.91 X10 <sup>-6</sup>	1.36X10 <sup>-6</sup>
5	30.0	50.480	48	46	44	46	0.51 X10 <sup>-6</sup>	0.59X10 <sup>-6</sup>
Sample : Treated DW Twill Head : 11.0 cm      DOT: Nov 2004      i= 0.67								
1	10.0	16.825	305	295	297	299	3.32X10 <sup>-6</sup>	4.98X10 <sup>-6</sup>
2	15.0	25.239	205	190	185	193	2.14X10 <sup>-6</sup>	3.22X10 <sup>-6</sup>
3	20.0	33.650	125	122	121	123	1.37X10 <sup>-6</sup>	2.05X10 <sup>-6</sup>
4	25.0	42.060	80	75	78	78	0.87X10 <sup>-6</sup>	1.3X10 <sup>-6</sup>
5	30.0	50.480	21	19	18	19	0.21X10 <sup>-6</sup>	0.32X10 <sup>-6</sup>



Name of the Test: Water Permeability &amp; Permittivity

Sample: Jute

Quantity of Flow:  $7000 \text{ ml} = 7 \times 10^6 \text{ mm}^3$ 

Ser	Head (mm)	Time (min-sec)						V=Q/AT (mm/sec)	$\Psi = QR_i / hAt (s^{-1})$
		1	2	3	4	5	avg		
Sample # 1      Dia: 100 mm									
1	10	2-46	2-45	2-47	2-48	2-45	2-46	5.37	
2	20	1-45	1-46	1-45	1-45	1-45	1-45	8.49	
3	30	1-27	1-26	1-24	1-27	1-25	1-26	10.36	
4	40	1-13	1-14	1-13	1-14	1-14	1-14	12.04	
5	50	1-02	1-03	1-02	1-02	1-02	1-02	14.38	0.26
6	60	0-55	0-56	0-55	0-57	0-55	0-56	15.92	
7	70	0-49	0-48	0-48	0-47	0-46	0-47	18.96	
Sample # 2      Dia: 118 mm									
1	10	1-49	1-48	1-49	1-47	1-48	1-48	5.93	
2	20	1-18	1-17	1-18	1-19	1-20	1-18	8.21	
3	30	0-55	0-57	0-55	0-56	0-57	0-56	11.43	
4	40	0-46	0-48	0-47	0-48	0-47	0-47	13.62	
5	50	0-37	0-36	0-38	0-37	0-37	0-37	17.30	0.31
6	60	0-33	0-34	0-34	0-33	0-34	0-34	18.82	
7	70	0-30	0-29	0-29	0-30	0-29	0-30	21.33	
Sample # 3      Dia: 103 mm									
1	10	3-18	3-20	3-19	3-20	3-19	3-19	4.22	
2	20	2-15	2-14	2-14	2-15	2-13	2-14	6.27	
3	30	1-35	1-34	1-35	1-32	1-33	1-34	8.94	
4	40	1-13	1-14	1-13	1-13	1-13	1-13	11.51	
5	50	1-02	1-02	1-03	1-03	1-02	1-02	13.55	0.24
6	60	0-52	0-53	0-52	0-52	0-53	0-53	15.85	
7	70	0-42	0-42	0-42	0-42	0-41	0-42	20.00	
Sample # 4      Dia: 104 mm									
1	10	2-55	2-56	2-55	2-55	2-56	2-55	4.71	
2	20	2-01	2-02	2-0	2-0	2-01	2-01	6.81	
3	30	1-07	1-08	1-07	1-07	1-08	1-07	12.30	
4	40	0-55	0-56	0-55	0-56	0-55	0-55	14.98	
5	50	0-47	0-46	0-47	0-47	0-46	0-47	17.53	0.31
6	60	0-36	0-35	0-36	0-36	0-35	0-36	22.89	
7	70	0-32	0-31	0-32	0-32	0-31	0-32	25.75	

Avg  $\Psi = 0.28 \text{ s}^{-1}$ 

Name of the Test: Water Permeability &amp; Permittivity

Sample: Canvas

Quantity of Flow:  $7000 \text{ ml} = 7 \times 10^6 \text{ mm}^3$ 

Ser	Head (mm)	Time (min-sec)						V=Q/AT (mm/sec)	$\Psi=QR/hAt (s^{-1})$
		1	2	3	4	5	avg		
Sample # 1      Dia: 104 mm									
1	10	10	22-2	22-3	22-0	22-3	22-3	22-2	0.62
2	20	20	19-47	19-45	19-37	1-40	19-45	19-43	0.70
3	30	30	17-20	17-26	17-21	17-24	17-26	17-23	0.79
4	40	40	11-21	11-15	11-25	11-30	11-21	11-22	1.21
5	50	50	9-35	9-26	9-29	9-30	9-36	9-31	1.44
6	60	60	7-05	7-07	7-11	7-10	7-10	7-08	1.93
7	70	70	5-54	5-50	5-49	5-46	5-50	5-50	2.35
Sample # 2      Dia: 118 mm									
1	10	22-48	22-45	22-46	22-45	22-45	22-46	0.48	
2	20	14-10	14-12	14-15	14-12	14-14	14-13	0.54	
3	30	9-58	9-55	9-55	9-56	9-56	9-56	0.61	
4	40	8-46	8-45	8-46	8-45	8-46	8-46	0.94	
5	50	7-24	7-25	7-26	7-25	7-25	7-26	1.12	0.026
6	60	5-27	5-26	5-25	5-26	5-26	5-26	1.50	
7	70	4-53	4-55	4-54	4-54	4-55	4-56	1.83	
Sample # 3      Dia: 104 mm									
1	10	22-26	22-25	22-25	22-26	22-25	22-26	0.61	
2	20	18-15	18-16	18-15	18-19	18-17	18-18	0.75	
3	30	11-31	11-30	11-29	11-29	11-30	11-30	1.19	
4	40	7-55	7-56	7-55	7-55	7-56	7-56	1.73	
5	50	8-23	8-25	8-25	8-24	8-25	8-25	1.63	0.029
6	60	7-58	7-55	7-58	7-56	7-55	7-56	1.73	
7	70	6-45	6-46	6-46	6-55	6-56	6-56	1.98	
Sample # 4      Dia: 104 mm									
1	10	22-58	22-59	22-58	22-56	22-57	22-58	0.60	
2	20	19-15	19-18	19-18	19-18	19-18	19-17	0.71	
3	30	12-12	12-14	12-14	12-14	12-15	12-14	1.12	
4	40	10-11	10-14	10-15	10-14	10-12	10-13	1.34	
5	50	8-55	8-56	8-56	8-56	8-55	8-56	1.54	0.027
6	60	7-55	7-56	7-58	7-55	7-55	7-56	1.73	
7	70	6-18	6-15	6-15	6-14	6-18	6-17	2.19	

Avg  $\Psi = 0.027 \text{ s}^{-1}$

Name of the Test: Water Permeability &amp; Permittivity

Sample: DW Twill

Quantity of Flow:  $7000 \text{ ml} = 7 \times 10^6 \text{ mm}^3$ 

Ser	Head (mm)	Time (min-sec)						V=Q/AT (mm/sec)	$\Psi = QR/hAt (s^{-1})$
		1	2	3	4	5	avg		
Sample # 1      Dia: 104 mm									
1	10	3-45	3-47	3-46	3-47	3-48	3-47	3.63	
2	20	2-52	2-53	2-54	2-53	2-53	2-53	4.76	
3	30	1-35	1-35	1-36	1-36	1-36	1-36	8.58	
4	40	1-15	1-16	1-15	1-15	1-16	1-16	10.84	
5	50	1-05	1-04	1-05	1-05	1-05	1-05	12.68	0.23
6	60	0-58	0-57	0-58	0-57	0-58	0-58	14.21	
7	70	0-48	0-47	0-48	0-48	0-48	0-48	17.16	
Sample # 2      Dia: 104 mm									
1	10	3-04	3-05	3-05	3-05	3-04	3-04	4.48	
2	20	1-50	1-51	1-52	1-50	1-53	1-52	7.36	
3	30	1-12	1-13	1-12	1-12	1-12	1-13	11.29	
4	40	1-04	1-03	1-04	1-04	1-03	1-04	12.88	
5	50	0-59	0-58	0-58	0-57	0-58	0-58	14.21	0.26
6	60	0-50	0-51	0-50	0-51	0-50	0-50	16.48	
7	70	0-41	0-40	0-41	0-41	0-40	0-41	20.10	
Sample # 3      Dia: 104 mm									
1	10	3-33	3-30	3-2	3-33	3-30	3-32	3.89	
2	20	2-45	2-44	2-44	2-45	2-44	2-45	4.99	
3	30	1-45	1-46	1-45	1-44	1-45	1-46	7.77	
4	40	1-14	1-15	1-16	1-15	1-15	1-16	10.84	
5	50	0-58	0-55	0-57	0-57	0-58	0-56	14.71	0.27
6	60	0-48	0-47	0-47	0-48	0-47	0-47	17.53	
7	70	0-41	0-40	0-40	0-41	0-40	0-41	20.10	
Sample # 4      Dia: 104 mm									
1	10	3-29	3-28	3-28	3-29	3-28	3-29	3.94	
2	20	2-50	2-51	2-50	2-51	2-51	2-51	4.82	
3	30	1-55	1-50	1-52	1-52	1-53	1-53	7.29	
4	40	1-14	1-15	1-14	1-15	1-14	1-15	10.99	
5	50	1-08	1-09	1-08	1-09	1-09	1-09	11.94	0.22
6	60	0-55	0-56	0-57	0-58	0-58	0-57	14.46	
7	70	0-45	0-45	0-44	0-45	0-45	0-45	18.31	

Avg  $\Psi = 0.25 \text{ s}^{-1}$

Name of the Test: Water Permeability &amp; Permittivity

Sample: Hessian

Quantity of Flow:  $7000 \text{ ml} = 7 \times 10^6 \text{ mm}^3$ 

Ser	Head (mm)	Time (min-sec)						V=Q/AT (mm/sec)	$\Psi=QR/hAt (s^{-1})$
		1	2	3	4	5	avg		
Sample # 1      Dia: 100 mm									
1	10	0-45	0-46	0-45	0-45	0-46	0-45	19.81	
2	20	0-31	0-31	0-30	0-31	0-31	0-31	28.75	
3	30	0-21	0-21	0-20	0-21	0-21	0-21	42.44	
4	40	0-18	0-18	0-19	0-18	0-17	0-18	49.52	
5	50	0-14	0-14	0-15	0-14	0-15	0-14	63.66	1.16
6	60	0-13	0-13	0-13	0-13	0-13	0-13	68.56	
7	70	0-12	0-12	0-12	0-12	0-12	0-12	74.27	
Sample # 2      Dia: 118 mm									
1	10	0-35	0-36	0-35	0-36	0-36	0-36	17.78	
2	20	0-19	0-18	0-19	0-19	0-19	0-19	33.69	
3	30	0-17	0-17	0-18	0-18	0-16	0-17	37.65	
4	40	0-15	0-15	0-14	0-16	0-15	0-15	42.67	
5	50	0-11	0-11	0-10	0-12	0-11	0-11	58.19	1.06
6	60	0-10	0-10	0-10	0-10	0-10	0-10	64.01	
7	70	0-08	0-08	0-08	0-08	0-08	0-08	80.01	
Sample # 3      Dia: 103 mm									
1	10	0-40	0-40	0-41	0-39	0-40	0-40	21.00	
2	20	0-29	0-29	0-28	0-29	0-30	0-29	28.97	
3	30	0-20	0-20	0-19	0-20	0-20	0-20	42.00	
4	40	0-18	0-18	0-17	0-18	0-18	0-18	46.67	
5	50	0-12	0-12	0-11	0-12	0-12	0-12	70.00	1.27
6	60	0-10	0-10	0-11	0-10	0-10	0-10	84.01	
7	70	0-08	0-08	0-08	0-08	0-08	0-08	105.01	
Sample # 4      Dia: 104 mm									
1	10	0-47	0-47	0-46	0-47	0-04	0-47	17.53	
2	20	0-32	0-32	0-31	0-31	0-32	0-32	25.75	
3	30	0-22	0-22	0-21	0-22	0-22	0-22	37.45	
4	40	0-17	0-17	0-17	0-17	0-16	0-17	48.47	
5	50	0-12	0-12	0-12	0-13	0-11	0-12	68.67	1.25
6	60	0-10	0-10	0-10	0-10	0-10	0-10	82.4	
7	70	0-08	0-08	0-08	0-08	0-08	0-08	103	

Avg  $\Psi = 1.19 \text{ s}^{-1}$

Name of the Test: Water Permeability &amp; Permittivity

Sample: Treated Jute

Quantity of Flow:  $7000 \text{ ml} = 7 \times 10^6 \text{ mm}^3$ 

Ser	Head (mm)	Time (min-sec)						V=Q/AT (mm/sec)	$\Psi=QR/hAt (s^{-1})$
		1	2	3	4	5	avg		
Sample # 1      Dia: 100 mm									
1	10	19-11	19-20	19-22	19-12	19-15	19-16	0.84	
2	20	15-15	15-14	15-15	15-20	15-25	15-18	0.90	
3	30	11-50	11-55	11-45	11-40	11-45	11-47	1.17	
4	40	8-25	8-26	8-40	8-30	8-50	8-34	1.60	
5	50	4-6	4-8	4-10	4-5	4-6	4-7	3.34	0.07
6	60	3-40	3-45	3-40	3-44	3-40	3-42	3.71	
7	70	3-18	3-20	3-20	3-15	3-18	3-18	4.16	
Sample # 2      Dia: 118 mm									
1	10	18-12	18-15	18-22	18-10	18-20	18-16	0.76	
2	20	16-25	16-20	16-25	16-25	16-30	16-25	0.84	
3	30	12-36	12-40	12-45	12-30	12-30	12-36	1.09	
4	40	10-14	10-15	10-20	10-25	10-14	10-17	1.35	
5	50	4-25	4-30	4-25	4-25	4-30	4-27	3.09	0.06
6	60	3-30	3-32	3-35	3-35	3-30	3-32	3.89	
7	70	3-10	3-12	3-15	3-14	3-12	3-13	4.27	
Sample # 3      Dia: 103 mm									
1	10	20-25	20-25	20-24	20-23	20-25	20-24	0.67	
2	20	17-20	17-21	17-25	17-25	17-20	17-22	0.79	
3	30	13-10	13-15	13-20	13-25	13-22	13-18	1.03	
4	40	11-15	11-20	11-12	11-20	11-20	11-17	1.22	
5	50	4-35	4-30	4-35	4-25	4-25	4-30	3.05	0.06
6	60	3-45	3-45	3-45	3-35	3-40	3-42	3.71	
7	70	3-30	3-32	3-30	3-28	3-29	3-30	8.86	
Sample # 4      Dia: 104 mm									
1	10	19-20	19-22	19-25	19-25	19-25	19-23	0.71	
2	20	17-45	17-46	17-25	17-40	17-30	17-62	0.76	
3	30	14-25	14-30	14-25	14-45	14-48	14-35	0.94	
4	40	9-45	9-48	9-50	9-55	9-55	9-51	1.39	
5	50	4-12	4-15	4-12	4-15	4-15	4-14	3.24	0.06
6	60	3-45	3-45	3-46	3-45	3-48	3-46	3.65	
7	70	3-20	3-22	3-21	3-25	3-25	3-23	4.06	

Avg  $\Psi = 0.06 \text{ s}^{-1}$

Name of the Test: Water Permeability & Permittivity

Sample: Treated Canvas

Quantity of Flow: 7000 ml=7X10<sup>6</sup> mm<sup>3</sup>

Ser	Head (mm)	Time (min-sec)						V=Q/AT (mm/sec)	Ψ=QR <sub>i</sub> /hAt (s <sup>-1</sup> )
		1	2	3	4	5	avg		
		Sample # 1						Dia: 100 mm	
1	10	No Flow							
2	20								
3	30								
4	40								
5	50								
6	60								
7	70								
		Sample # 2						Dia: 104 mm	
1	10	No Flow							
2	20								
3	30								
4	40								
5	50								
6	60								
7	70								
		Sample # 3						Dia: 104 mm	
1	10	No Flow							
2	20								
3	30								
4	40								
5	50								
6	60								
7	70								
		Sample # 4						Dia: 104 mm	
1	10	No Flow							
2	20								
3	30								
4	40								
5	50								
6	60								
7	70								

Name of the Test: Water Permeability &amp; Permittivity

Sample: Treated DW Twill

Quantity of Flow:  $7000 \text{ ml} = 7 \times 10^6 \text{ mm}^3$ 

Ser	Head (mm)	Time (min-sec)						V=Q/AT (mm/sec)	$\Psi=QR/hAt (s^{-1})$
		1	2	3	4	5	avg		
Sample # 1      Dia: 104 mm									
1	10	4-35	4-36	4-30	4-35	4-36	4-34	3.00	
2	20	3-30	3-35	3-36	3-34	3-36	3-34	3.85	
3	30	2-40	2-40	2-35	2-30	2-35	2-36	5.28	
4	40	1-55	1-50	1-55	1-53	1-52	1-53	7.29	
5	50	1-23	1-25	1-20	1-22	1-23	1-23	9.93	0.20
6	60	1-15	1-14	1-16	1-15	1-15	1-15	10.99	
7	70	1-05	1-06	1-05	1-06	1-06	1-06	12.49	
Sample # 2      Dia: 104mm									
1	10	4-32	4-33	4-35	4-30	4-35	4-33	3.02	
2	20	3-40	3-45	3-40	3-44	3-45	3-43	3.70	
3	30	2-50	2-55	2-50	2-55	2-50	2-52	4.79	
4	40	2-00	2-01	1-58	1-59	2-02	2-00	6.87	
5	50	1-03	1-04	1-03	1-04	1-03	1-03	13.08	0.26
6	60	0-58	0-59	0-58	0-58	0-59	0-58	14.21	
7	70	0-52	0-50	0-52	0-53	0-52	0-52	15.85	
Sample # 3      Dia: 104 mm									
1	10	4-40	4-42	4-40	4-42	4-40	4-41	2.93	
2	20	3-35	3-36	3-35	3-35	3-35	3-35	3.83	
3	30	2-45	2-44	2-45	2-45	2-44	2-45	4.99	
4	40	2-05	2-04	2-03	2-00	2-08	2-04	6.65	
5	50	1-20	1-15	1-14	1-16	1-18	1-17	10.70	0.21
6	60	1-05	1-06	1-05	1-04	1-05	1-05	12.68	
7	70	0-55	0-56	0-58	0-55	0-55	0-56	14.71	
Sample # 4      Dia: 104 mm									
1	10	4-40	4-44	4-42	4-45	4-44	4-43	2.91	
2	20	3-45	3-44	3-45	3-45	3-44	3-45	3.66	
3	30	2-55	2-56	2-55	2-50	2-50	2-53	4.76	
4	40	2-10	2-11	2-15	2-20	2-10	2-13	6.20	
5	50	1-34	1-33	1-33	1-33	1-30	1-33	8.86	0.18
6	60	1-20	1-22	1-20	1-22	1-22	1-21	10.17	
7	70	1-05	1-06	1-04	1-04	1-05	1-05	12.68	

Avg  $\Psi = 0.21 \text{ s}^{-1}$

Name of the Test: CBR Puncture Resistance

Machine Speed: 300 +10 mm

No of Specimen: 6

Sample	Jute	Canvas	DW Twill	Hessian	Treated Jute	Treated Canvas	Treated DW Twill
Load (kgf)							
1	164	200	450	184	400	140	205
2	166	148	466	152	413	163	181
3	120	150	480	160	363	162	206
4	150	128	435	128	361	143	171
5	178	200	455	198	391	131	131
6	180	190	460	158	360	162	199
Total (kgf)	958	1016	2746	980	2288	901	1093
Avg (kgf)	159.66	169.33	457.68	163.33	381.33	150.2	182.2
Avg (N)	1566	1661	4488	1602	3740	1473	1787



Name of the Test: Index Puncture Resistance

Machine Speed: 300 +10 mm

No of Specimen: 15

ser	Jute	Canvas	DW Twill	Hessian	Treated Jute	Treated Canvas	Treated DW Twill
Load (kgf)							
1	38	45	80	45	25	30	40
2	40	50	92	50	20	31	42
3	40	45	80	38	19	30	41
4	38	48	85	48	25	31	40
5	43	50	90	45	24	30	42
6	41	49	85	49	22	31	41
7	41	50	80	45	26	32	42
8	43	49	90	46	21	31	40
9	41	45	85	47	22	31	41
10	44	44	87	45	23	31	41
11	42	48	88	45	24	30	42
12	42	45	89	45	21	31	41
13	45	47	88	46	22	30	40
14	42	47	86	45	22	32	42
15	43	45	85	44	23	31	41
Total (kgf)	623	707	1290	683	319	615	473
Avg (kgf)	41.53	47.13	86	45.53	21.27	41	31.53
Avg (N)	407.3	462.2	843.4	446.5	208.6	402	309.2
Calibrated (N)	2551	2880	5256	2782	1300	2505	1927

Name of the Test: Apparent Opening Size

Weight of Sand Fraction Taken: 50 gm

No of Specimen: 5

Duration of Shaking: 5 mins

Sieve No	Sieve Opening	Tests						% Finer
		1	2	3	4	5	Avg	
Jute								
16-30	1.19-0.6	0.0	2.6	0.0	0.0	1.2	0.76	1.52
30-50	0.6-0.3	1.5	4.4	0.8	0.6	3.1	2.08	4.16
50-100	0.3-0.15	11.5	19.6	3.8	4.8	11.3	10.2	20.4
100-200	0.15-0.074	44.5	26.6	23.5	20.0	29.5	28.82	57.64
Canvas								
16-30	1.19-0.6	0.0	0.0	0.0	0.0	0.0	0.0	0.0
30-50	0.6-0.3	0.0	0.0	0.0	0.0	0.0	0.0	0.0
50-100	0.3-0.15	0.0	1.0	1.3	1.1	1.6	1.0	2.0
100-200	0.15-0.074	0.0	3.8	2.5	2.8	3.0	2.42	4.84
DW Twill								
8-16	2.38-1.19	1.5	1.4	1.3	0.6	1.2	1.2	2.4
16-30	1.19-0.6	4.6	9.7	3.3	4.5	4.3	5.28	10.56
30-50	0.6-0.3	45.3	35.9	33.7	36.1	31.2	36.44	72.88
50-100	0.3-0.15	49.6	49.8	49.8	44.5	45.6	47.86	95.72
100-200	0.15-0.074	49.9	49.0	49.6	49.8	49.6	49.58	99.16
Hessian								
8-16	2.38-1.19	1.1	0.0	1.3	0.6	0.3	0.66	1.32
16-30	1.19-0.6	3.3	3.7	4.3	4.2	3.8	3.86	7.72
30-50	0.6-0.3	35	40	38	47.5	42.1	40.52	81.04
50-100	0.3-0.15	50	50	50	50	50	50	100
100-200	0.15-0.074	50	50	50	50	50	50	100

Name of the Test: Burst Strength Test

No of Specimen: 10

ser	Jute	Canvas	DW Twill	Hessian	Treated Jute	Treated Canvas	Treated DW Twill
Load (kPa)							
1	1240	2401	2380	1456	1566	1698	2540
2	1245	2354	2356	1432	1581	1685	2542
3	1250	2369	2388	1410	1540	1690	2545
4	1250	2356	2398	1425	1586	1685	2525
5	1240	2358	2355	1412	1536	1705	2538
6	1234	2350	2366	1423	1523	1706	2512
7	1256	2362	2360	1425	1585	1705	2516
8	1240	2386	2385	1405	1570	1701	2540
9	1256	2310	2388	1420	1546	1698	2502
10	1239	2354	2354	1412	1567	1697	2540
Total (kPa)	12450	23600	23730	14220	15600	16970	25300
Avg (kgf)	1245	2360	2373	1422	1560	1697	2530

Name of the Test: Trapezoid Tearing Strength

Date of Test: 13 Oct

Machine Speed: 300 + 10 mm/min

Ser	Jute		Canvas		DW Twill		Hessian	
	MD	XMD	MD	XMD	MD	XMD	MD	XMD
1	18	3	24	2	55	15	22	6
2	13	4	15	3	55	18	21	7
3	14	5	12	2	40	16	22	5
4	15	2	12	3	44	15	23	6
5	13	3	14	4	51	16	21	7
6	12	4	13	3	45	14	22	6
7	11	2	13	2	45	15	12	5
8	20	3	14	3	46	16	12	6
9	14	4	12	2	47	15	22	6
10	11	2	11	2	45	16	12	7
Avg (kgf)	14.1	3.2	14	2.6	47.3	15.6	18.9	6.1
Avg (N)	197	31	137	26	464	153	185	60
Ser	Treated Jute		Treated Canvas		Treated DW Twill			
	MD	XMD	MD	XMD	MD	XMD		
1	15	5	16	2	45	11		
2	10	4	12	2	40	12		
3	10	4	10	2	35	12		
4	12	3	10	3	40	11		
5	10	4	12	3	45	12		
6	11	2	11	1	40	12		
7	11	4	12	2	42	15		
8	15	3	10	3	40	11		
9	10	2	11	1	40	12		
10	9	3	10	2	41	12		
Avg (kgf)	11.3	3.4	11.4	2.1	40.8	12.0		
Avg (N)	111	33	112	21	400	118		

Name of the Test: Unconfined Tension Creep Behavior

Name of the Sample: Canvas

Load: 48 kg (10% of 480 kg)

2.4 kN/m

Strain,  $\epsilon = (\Delta L \times 100) / L_g$

Here,  $L_g = 4.00$  in

Ser	Date & Time	Elapsed Time	Dial Reading			$\Delta L$ (in)	$\Delta \epsilon$ (%)	$\epsilon$ (%)
			W	E	Avg			
1	30 Oct 04 1000 Hrs	0 Min	140	270				
2		1 Min	230	150	105.0	0.1050	2.6250	2.6250
3		2 Min	233	147	3.0	0.0030	0.0750	2.7000
4		6 Min	236	145	2.5	0.0025	0.0625	2.7625
5		10 Min	239	142	3.0	0.0030	0.0750	2.8375
6		30 Min	242	138	3.5	0.0035	0.0875	2.9250
7		1 Hr	250	135	5.5	0.0055	0.1375	3.0625
8		2 Hr	255	130	4.0	0.0040	0.1000	3.1625
9		5 Hr	260	127	10.0	0.0100	0.2500	3.4125
10		10 Hr	268	115	12.0	0.0120	0.3000	3.7125
11		30 Hr	280	103	13.5	0.0135	0.3375	4.0500
12		100 Hr	295	89	14.5	0.0145	0.3625	4.4125
13		200 Hr	300	83	5.5	0.0055	0.1375	4.5500
14		500 Hr	305	79	4.5	0.0045	0.1125	4.6625
15	11 Dec 04 1000 Hrs	1000 Hr	311	85	6.0	0.0060	0.1500	4.8125
16	11 Dec 04 1000 Hrs	1000 Hr	208	184	101	0.1010	2.5250	2.2875

Name of the Test: Unconfined Tension Creep Behavior

Name of the Sample: Canvas

Load: 96 kg (20% of 480 kg)

4.8 kN/m

Strain,  $\epsilon = (\Delta L \times 100) / L_g$

Here,  $L_g = 4.00$  in

Ser	Date & Time	Elapsed Time	Dial Reading			$\Delta L$ (in)	$\Delta \epsilon$ (%)	$\epsilon$ (%)
			W	E	Avg			
1	30 Oct 04 1100 Hrs	0 Min	308	235				
2		1 Min	112	110	160.5	0.1605	4.0125	4.0125
3		2 Min	110	105	3.5	0.0035	0.0875	4.1000
4		6 Min	104	98	5.5	0.0055	0.1375	4.2375
5		10 Min	100	94	4.0	0.004	0.1000	4.3375
6		30 Min	92	85	8.5	0.0085	0.2125	4.5500
7		1 Hr	85	79	6.5	0.0065	0.1625	4.7125
8		2 Hr	76	72	8.0	0.0080	0.2	4.9125
9		5 Hr	69	64	7.5	0.0075	0.1875	5.1000
10		10 Hr	60	55	9.0	0.0090	0.225	5.3250
11		30 Hr	40	37	19.0	0.0190	0.475	5.8000
12		100 Hr	20	20	18.5	0.0185	0.4625	6.2625
13		200 Hr	15	15	5.0	0.0050	0.125	6.3875
14		500 Hr	08	09	6.5	0.0065	0.1625	6.5500
15	11 Dec 04 1100 Hrs	1000 Hr	08	09	0.0	0.0000	0.0000	6.5500
16	11 Dec 04 1100 Hrs	1000 Hr	124	121	114	0.1140	2.8500	3.7000

Name of the Test: Unconfined Tension Creep Behavior

Name of the Sample: Canvas

Load: 144 kg (30% of 480 kg)

7.2 kN/m

Strain,  $\epsilon = (\Delta L \times 100) / L_g$

Here,  $L_g = 4.00$  in

Ser	Date & Time	Elapsed Time	Dial Reading			$\Delta L$ (in)	$\Delta \epsilon$ (%)	$\epsilon$ (%)
			W	E	Avg			
1	27 Nov 04 1106 Hrs	0 Min	606	293				
2		1 Min	800	498	199.5	0.1995	4.9875	4.9875
3		2 Min	809	505	8.0	0.0080	0.2000	5.1875
4		6 Min	823	521	15.5	0.0155	0.3875	5.5750
5		10 Min	828	526	5.0	0.0050	0.1250	5.7000
6		30 Min	838	538	11.0	0.0110	0.2750	5.9750
7		1 Hr	844	546	7.0	0.0070	0.1750	6.1500
8		2 Hr	855	556	10.5	0.0105	0.2625	6.4125
9		5 Hr	871	573	16.5	0.0165	0.4125	6.8250
10		10 Hr	880	583	9.5	0.0095	0.2375	7.0625
11		30 Hr	895	599	15.5	0.0155	0.3875	7.4500
12		100 Hr	910	614	15.0	0.0150	0.3750	7.8250
13		200 Hr	915	620	5.5	0.0055	0.1375	7.9625
14		500 Hr	926	630	10.5	0.0105	0.2625	8.2250
15	7 Jan 05 1106 Hrs	1000 Hr	939	640	11.5	0.0115	0.2875	8.5125
16	7 Jan 05 1106 Hrs	1000 Hr	807	516	128	0.1280	3.2	5.3125

Name of the Test: Unconfined Tension Creep Behavior

Name of the Sample: Canvas

Load: 192 kg (40% of 480 kg)

9.6 kN/m

Strain,  $\epsilon = (\Delta L \times 100) / L_g$

Here,  $L_g = 4.00$  in

Ser	Date & Time	Elapsed Time	Dial Reading			$\Delta L$ (in)	$\Delta \epsilon$ (%)	$\epsilon$ (%)
			W	E	Avg			
1	05 Oct 04 1112 Hrs	0 Min	79.0	150.0				
2		1 Min	342.0	405.0	259.0	0.2590	6.475	6.475
3		2 Min	349.0	413.0	7.5	0.0075	0.1875	6.6625
4		6 Min	360.0	430.0	14.0	0.0140	0.3500	7.0125
5		10 Min	372.0	448.0	15.0	0.0150	0.3750	7.3875
6		30 Min	384.0	465.0	14.5	0.0145	0.3625	7.7500
7		1 Hr	391.0	476.0	9.0	0.0090	0.2250	7.9750
8		2 Hr	397.5	489.1	10.0	0.0100	0.2500	8.2250
9		5 Hr	410.0	505.5	14.5	0.0145	0.3625	8.5875
10		10 Hr	432.0	533.0	24.75	0.0248	0.6200	9.2075
11		30 Hr	482.0	577.0	47.0	0.0470	1.1750	10.3825
12		100 Hr	501.0	593.0	17.5	0.0175	0.4375	10.8200
13		200 Hr	515.0	600.0	10.5	0.0105	0.2625	11.0825
14		500 Hr	552.0	630.0	33.5	0.0335	0.8375	11.9200
15	14 Nov 04 1112 Hrs	1000 Hr	Ruptured on 41st					
16	05 Oct 04 1112 Hrs	0 Min	79.0	150.0				



Name of the Test: Unconfined Tension Creep Behavior

Name of the Sample: Treated Canvas

Load: 55 kg (10% of 555 kg)

2.75 kN/m

Strain,  $\epsilon = (\Delta L \times 100) / L_g$

Here,  $L_g = 4.00$  in

Ser	Date & Time	Elapsed Time	Dial Reading			$\Delta L$ (in)	$\Delta \epsilon$ (%)	$\epsilon$ (%)
			W	E	Avg			
1	18 Dec 04 1255 Hrs	0 Min	745	212				
2		1 Min	630	350	126.5	0.1265	3.1625	3.1625
3		2 Min	625	358	6.5	0.0065	0.1625	3.3250
4		6 Min	612	369	12.0	0.012	0.3000	3.6250
5		10 Min	607	374	5.0	0.005	0.1250	3.7500
6		30 Min	596	384	10.5	0.0105	0.2625	4.0125
7		1 Hr	590	388	5.0	0.005	0.01250	4.1375
8		2 Hr	584	392	5.0	0.025	0.1250	4.2625
9		5 Hr	580	396	4.0	0.004	0.1000	4.3625
10		10 Hr	576	401	4.5	0.0045	0.1125	4.4750
11		30 Hr	573	404	3.0	0.003	0.0750	4.5500
12		100 Hr	570	407	3.0	0.003	0.0750	4.6250
13		200 Hr	567	411	3.5	0.0035	0.0875	4.7125
14		500 Hr	564	415	3.5	0.0035	0.0875	4.8000
15	29 Jan 05 1000 Hrs	1000 Hr	560	419	4.0	0.004	0.1000	4.9000
16	7 Feb 05 1100 Hrs	1000 Hr	549	407	11.5	0.0115	0.2875	4.6125

Name of the Test: Unconfined Tension Creep Behavior

Name of the Sample: Treated Canvas

Load: 110 kg (20% of 555 kg)

5.5 kN/m

Strain,  $\epsilon = (\Delta L \times 100) / L_g$

Here,  $L_g = 4.00$  in

Ser	Date & Time	Elapsed Time	Dial Reading			$\Delta L$ (in)	$\Delta \epsilon$ (%)	$\epsilon$ (%)	
			W	E	Avg				
1	28 Nov 04 1005 Hrs	0 Min	455	506					
2		1 Min	601	360	146.0	0.146	3.6500	3.6500	
3		2 Min	606	365	5.0	0.005	0.1250	3.7750	
4		6 Min	613	354	6.5	0.0065	0.1625	3.9375	
5		10 Min	617	350	4.0	0.004	0.1000	4.0375	
6		30 Min	624	345	6.0	0.006	0.1500	4.1875	
7		1 Hr	626	342	2.5	0.0025	0.0625	4.2500	
8		2 Hr	628	341	1.5	0.0015	0.0375	4.2875	
9		5 Hr	633	336	5.0	0.005	0.1250	4.4125	
10		10 Hr	635	334	2.0	0.002	0.0500	4.4625	
11		30 Hr	637	332	2.0	0.002	0.0500	4.5125	
12		100 Hr	638	329	1.5	0.0015	0.0375	4.5500	
13		200 Hr	641	329	1.5	0.0015	0.0375	4.5875	
14		500 Hr	656	329	7.5	0.0075	0.1875	4.7750	
15	08 Jan 05 1000 Hrs	1000 Hr	Ruptured on 20 Dec 04 after 552 Hrs (23 rd days)						

Name of the Test: Unconfined Tension Creep Behavior

Name of the Sample: Treated Canvas

Load: 165 kg (30% of 555 kg)

8.3 kN/m

Strain,  $\epsilon = (\Delta L \times 100) / L_g$

Here,  $L_g = 4.00$  in

Ser	Date & Time	Elapsed Time	Dial Reading			$\Delta L$ (in)	$\Delta \epsilon$ (%)	$\epsilon$ (%)
			W	E	Avg			
1	5 Dec 05 1000 Hrs	0 Min	899	831				
2		1 Min	648	550	266	0.266	6.65	6.65
3		2 Min	637	541	10	0.01	0.25	6.9
4		6 Min	626	530	11	0.011	0.275	7.175
5		10 Min	615	527	7	0.007	0.175	7.35
6		30 Min	574	518	25	0.025	0.625	7.975
7		1 Hr	Ruptured at 57 mins					

Name of the Test: Mass per Unit Area

No of Samples: 6

Sample	Length (cm)	Width (cm)	Area (cm <sup>2</sup> )	Mass (gm)	m (gsm)	m avg
Jute						
1	36.20	31.00	1122.20	93.1	829.62	828.06
2	34.30	30.73	1054.04	86.4	819.7	
3	33.50	31.50	1055.25	84.0	796.02	
4	36.07	31.43	1133.68	97.3	858.27	
5	34.50	30.97	1068.47	89.4	836.71	
Canvas						
1	31.07	30.20	938.31	49.8	530.74	523.09
2	33.20	30.87	1024.88	49.3	481.03	
3	30.53	32.40	989.17	54.3	548.95	
4	33.13	30.53	1011.46	53.8	531.90	
5	28.07	27.87	782.31	40.9	522.81	
DW Twill						
1	37.00	33.00	1221.00	91.7	751.02	755.46
2	30.30	35.07	1062.62	82.6	777.32	
3	30.70	35.07	1076.65	81.8	759.76	
4	34.37	32.57	1119.43	84.5	754.85	
5	30.60	34.80	1064.88	78.2	734.36	
Hessian						
1	28.77	28.63	823.69	25.1	307.73	322.40
2	28.70	27.93	801.59	25.9	323.11	
3	27.87	28.37	788.72	25.4	322.04	
4	29.13	27.90	812.73	26.3	323.60	
5	28.00	28.53	798.84	26.8	335.49	

Sample	Length (cm)	Width (cm)	Area (cm <sup>2</sup> )	Mass (gm)	m (gsm)	m avg
Treated Jute						
1	163.0	72.0	11736.0	1866.85	1590.7	1590.7
2	161.0	71.5	11511.5	1831.13	1590.4	
3	162.0	72.5	11745.0	1868.28	1591.0	
4	163.0	71.5	11654.5	1853.88	1590.7	
5	161.0	72.5	11672.5	1856.74	1590.7	
Treated Canvas						
1	312.0	96.0	29952	3648.5	1218.12	1218.2
2	313.0	96.0	30048	3660.1	1218.16	
3	312.0	95.5	29796	3629.6	1218.20	
4	312.5	95.0	29796	3629.6	1218.20	
5	312.0	96.0	29952	3648.5	1218.12	
Treated DW Twill						
1	190.0	73	13870	1958.7	1412.20	1412.2
2	191.0	72	13752	1941.1	1411.50	
3	189.0	73	13797	1948.9	1412.55	
4	190.0	73	13870	1958.7	1412.20	
5	191.0	72	13752	1941.1	1411.50	

Name of the Test: Nominal Thickness

Pressure Applied: 2 kPa

No of Specimen: 10

Time for taking reading: 5 sec

Dial Division: 1 div = 0.01 mm

Sample	Jute	Canvas	DW Twill	Hessian	Treated Jute	Treated Canvas	Treated DW Twill
Dial Reading (div)							
1	256.5	133.5	242.6	147.5	369.5	252.1	319.5
2	247.5	132.6	242.8	156.5	359.5	253.1	322.5
3	217.5	133.2	242.8	148.5	344.5	251.3	326.5
4	207.5	132.8	242.6	157.5	349.5	253.1	305.5
5	234.5	133.6	242.5	146.5	349.5	252.1	317.5
6	245	133.2	242.7	157.5	398.5	252.4	319.9
7	234.5	133.6	242.5	146.5	344.5	254.2	317.5
8	217.5	133.8	242.6	148.5	398.5	250.1	318.8
9	272.5	133.5	242.8	156.5	349.5	249.5	314.5
10	272.5	134.2	242.5	156.5	344.5	248.5	317.5
Total	2405.5	1334	2426.4	1522	3608	2516.4	3179.7
Thickness (mm)	<b>2.40</b>	<b>1.33</b>	<b>2.42</b>	<b>1.52</b>	<b>3.62</b>	<b>2.52</b>	<b>3.18</b>

